
# The selective oxidation of cyclohexane via the *in-situ* utilisation of $H_2O_2$

Thesis submitted in accordance with the requirement of Cardiff University for the degree of Doctor of Philosophy

**Caitlin Crombie**

School of Chemistry

Cardiff University

2020

## Abstract.

Three primary reactions have been investigated within this thesis using heterogeneous catalysis; the direct synthesis of hydrogen peroxide, the oxidation of cyclohexane and the oxidation of benzyl alcohol both via the *in-situ* production of $H_2O_2$.

The direct synthesis of $H_2O_2$ from molecular $H_2$ and $O_2$ provides a promising alternative to the anthraquinone process currently industrially implemented. Within the literature many additives, halides and acids, have been utilized to increase $H_2O_2$ selectivity be reducing the degradation of $H_2O_2$ to form $H_2O$. Currently Pd based catalysts are the most advanced showing high activity towards $H_2O_2$ synthesis. The alloying of Pd with other metals, especially Au, has then shown increases in activity and selectivity due to electronic and geometric enhancements. In this thesis, a combination of preparation methods and catalyst supports have been investigated as has the alloying of Pd with a range of non-noble metals under ambient temperatures, with obvious financial advantages.

The oxidation of cyclohexane via the *in-situ* production of $H_2O_2$ has been investigated. The conditions normally explored for the aerobic oxidation of cyclohexane are high temperatures which are costly and unsuitable for $H_2O_2$ synthesis and encourages $H_2O$ formation. Hence the use of $H_2O_2$ for cyclohexane oxidation allows for better activity at lower temperatures, but the use of commercial $H_2O_2$ comes with the added drawbacks of the anthraquinone process. The use of $H_2O_2$ generated *in-situ* would be advantageous by avoiding the transport and handling of concentrated solutions of $H_2O_2$. This work explored a variety of reaction conditions to discover the possibility of the oxidation of cyclohexane via the *in-situ* production of $H_2O_2$ under milder conditions than those utilized for the aerobic oxidation. Investigation then continued into catalyst design to increase oxidation product yield.

The oxidation of benzyl alcohol via the *in-situ* production of $H_2O_2$ has already been explored in the literature and hence its feasibility had already been demonstrated. In this thesis catalysts design was implemented, focusing on Fenton's metal, Fe, in combination with Pd due to the known radical mechanism of benzyl alcohol oxidation. Electron Paramagnetic Resonance studies have been utilized to investigate the reaction mechanism and to distinguish the activity differences observed between catalysts.

## Acknowledgements.

First and fore most I would like to thank Professor Graham Hutching for providing me with this amazing opportunity four years ago. Thank you for all your help and guidance throughout my PhD, your input has been invaluable.

I would also like to acknowledge and thank Haldor Topsoe for their contribution into this research, especially Martin Skov Skjøth-Rasmussen whose industrial expertise and input was extremely helpful.

I would like to give a massive thank you to Dr Rich Lewis whose supervision and input I would not have survived without. Thank you for all your help not only in meetings and in the lab but especially with the writing of this thesis and the numerous emails of questions that you answered swiftly. Thanks also to Dr Greg Shaw and Dr Jennifer Edwards for your helpful input in group meetings. Thank you to Dr Dave Morgan and Dr Tom Davies for all their help in conducting and analysis XPS and TEM data. Thanks to Xi Lui at Shanghai Jiao Tong University for the running and interpretation of HAADF-STEM imaging. Thank you to Rebekah Taylor and Dr Andrea Folli for the running, interpretation, and their expertise in EPR. Thank you to all the Staff in the Chemistry department and especially to Steve Morris and Lee Wescombe in the workshop for mending many broken autoclaves throughout my time.

Thank you to all of those in the CCI that filled the offices and labs and made the CCI a wonderful place to spend the last four years. Thanks especially to all those in 'Team $H_2O_2$' and those who worked in 0.90 in a windowless dark basement lab you all brought a little bit of sunshine. An extra special thank you to my partner in the Haldor Topsoe project, Dávid, whose friendship and support I wouldn't have survived without. Thank you to all my friends both in Cardiff and at home who have supported to me and listen to me ramble on. To Todd, thank you! Thank you for your support and thank you mostly for surviving and supporting me to the end under the oddest of circumstances that 2020 has brought us.

My biggest and heartfelt thanks go to my parents and my family who without them I wouldn't be here today. To my parent for always supporting me and encouraging me to go on, no thanks will ever be enough, you truly are amazing.

## Publications associated with this thesis.

C. M. Crombie, R. J. Lewis, D. Kovačič, D. J. Morgan, T. E. Davies, J. K. Edwards, M. S. Skjøth-Rasmussen & G. J. Hutchings. The Influence of Reaction Conditions on the Oxidation of Cyclohexane via the In-Situ Production of $H_2O_2$. *Catal. Lett*., 2021, **151**, 164–171.

C. M. Crombie, R. J. Lewis, D. Kovačič, D. J. Morgan, T. J. A. Slater, T. E. Davies, J. K. Edwards, M. S. Skjøth-Rasmussen & G. J. Hutchings. The Selective Oxidation of Cyclohexane via In-situ $H_2O_2$ Production Over Supported Pd-based Catalysts. *Catal Lett.*, 2021.

C. M. Crombie, R. J. Lewis, R. L. Taylor, D. J. Morgan, T. E. Davies, A. Folli, D. M. Murphy, J. K. Edwards, J. Qi, H. Jiang, C. J. Kiely, X. Liu, M. S. Skjøth-Rasmussen and G. J. Hutchings. Enhanced Selective Oxidation of Benzyl Alcohol via In Situ $H_2O_2$ Production over Supported Pd-Based Catalysts. *ACS Catal*., 2021, **11**, 2701–2714.

# Table of Contents.

# 1 Introduction.

## 1.1 Catalysis; definition and concept.

Catalysis is the phenomenon of materials which increase the rate of a reaction or process without being directly consumed in the reaction itself.[1] They lower the activation energy, $E_a$, by providing an alternative pathway for the reaction to occur by, Figure 1.1, and hence increase the rate of reaction according to the Arrhenius equation, Equation 1.1, without changing the overall standard Gibbs free energy change in the reaction.[2]

$$k = Ae^{\frac{-E_a}{RT}} \qquad \textit{Equation 1.1}$$

*Where; k is rate of reaction, A is the pre-exponential factor, $E_a$ is the activation energy, R is the universal gas constant and T is temperature.*

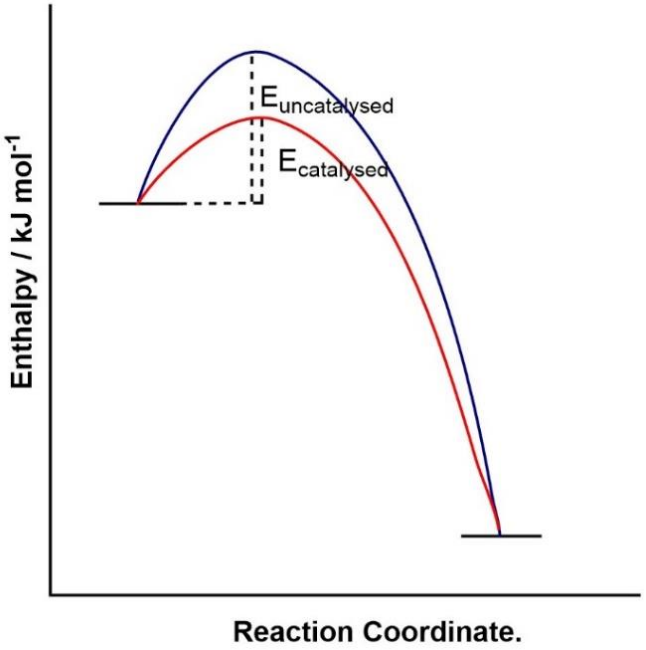


***Figure 1.1.*** *A generic reaction coordinate showing the difference in activation enthalpy of a non-catalysed (blue) and catalysed (red) reaction.[2]*

Most famously a more advanced definition of catalyst came from Ostwald at the end of the 19th century. He defined catalysis in terms of physical chemistry and added that a catalyst accelerates a reaction exclusive of affecting the position of the equilibrium and thermodynamics.[3] This work was also recognised as the basis for his Nobel Prize for Chemistry awarded in 1909.[4]

Catalysts have widespread use in many industrial applications, and many depend on these to not only reduce costs, by reducing energy consumption, but often also to provide more selective reactions. It is believed that around 90 % of all chemicals and

materials produced industrially, encounter a catalyst at least once in their production cycle.[1]

There is constant research and development to improve the selectivity, efficiency and lifetime of catalysts to improve the economics and operability of industrial procedures. Recent advances are targeted towards green chemistry where the aim is to keep energy consumption and the environmental impact of processes to a minimum.[5] Catalysis is one of the key 12 principles of green chemistry. As the global population and economy has increased as has the demand of industrially efficient processes. With increasing industrial demand, a decrease in natural resources and obvious changes in global climate have been observed. As such scientific and industrial research has begun to focus on the use of green chemistry practices. These principles focus on using renewable and more benign reactants and solvents, decreasing waste, and increasing the atom efficiency of reactions.[6] The use of catalytic amounts of material compared to stoichiometric show obvious advantages. If catalysis can also be implemented to increase the reaction selectivity and increase energy efficiency by working under milder conditions then even more green principles can be met.[6]

### 1.1.1 Biocatalysis.

Biocatalysis uses natural, living systems as catalysts and this usually involves enzymes which can catalyses organic transformations.[7] Enzymes can catalyse a number of transformations such as glucose isomerase which catalyses the isomerisation of glucose to fructose or succinate dehydrogenase which catalyses the dehydrogenation of succinate to fumerate.[7]

Enzymes are normally substrate specific which although can be a drawback due to their use in a limited number of reactions it also leads to incredibly high reaction selectivity. Enzymes can distinguish between different enantiotropic atoms, faces and groups of a molecule and hence can catalyse an enantioselective reaction by producing predominately one stereoisomer of the product, leading to enantiomeric excesses (e.e) greater than 99 %.[7]

Enzymes often operate under mild conditions (5 – 50 °C) in aqueous conditions and deactivate or denature in harsher conditions. Again, this can be both an advantage and disadvantage of biocatalysis. In terms of green chemistry there is a move towards less energy intensive processes with reduced waste, using benign water solvents under

ambient conditions with high selectivities towards the desired product. Certainly, many biocatalysts can be put into this class. However this does restrict the conditions at which biocatalysts can be employed and it does show their limited stability.[7]

Biocatalysis can be used in a variety of applications industrially, mostly in chemical production which can be applied to the fine chemical industry, basic chemicals and the pharmaceutical and medicinal sectors where the production of enantiomerically pure compounds is imperative. They can also be employed into analytical and diagnostic procedures again most importantly in the medical sector.[7]

### 1.1.2 Homogeneous catalysis.

Homogeneous catalysis typically involves the reactants and catalyst in the same phase. This happens most frequently when both catalyst and reactants are in the liquid phase.[8]

Most homogenous catalysts currently consist of inorganic organometallic molecules or transition metal complexes.[9] Transition metal complexes employ an ionic metal centre with various organic ligands coordinated upon it. These can be very tuneable catalysts with the ligands varying the selectivity of the reaction. They are often single site catalysts with the reactants becoming part of the metal complex sphere during the course of the reaction which can lead to high selectivity. However, the major drawback to homogeneous catalysis is the difficult recovery and separation of the catalyst from the reaction medium. Recovery can be expensive or if avoided can lead to metal contaminated reactant streams.[8]

### 1.1.3 Heterogeneous catalysis.

Heterogeneous catalysis occurs when the reactants and catalyst are in different phases; here the catalysis occurs at the boundary between the two phases.[1,2,10] Solid catalysts and gaseous or liquid phase reagents are most common, in which the catalysis occurs at the surface of the solid catalyst, thus the structure of the surface plays a very important role in the catalytic performance.[1,10] The surface is where the bulk structure ceases, and thus the surface atoms are in unsaturated environments with potential 'free' bonds. These can interact with the reagents which can adsorb onto the surface for catalysis to take place. The adsorption of the reactant species is often thermodynamically favoured, which can be the driving force of the catalysed reaction.[11]

There are several mechanisms of bimolecular reactions on solid surfaces depending on the adsorption of the reactants. When both reactants are adsorbed onto the surface and both react while on the surface is a Langmuir-Hinshelwood mechanism, Figure 1.2.[12] When one molecule is absorbed onto the surface and reacts with a molecule in the gas or liquid phase surrounding the surface is an Eley-Rideal mechanism.[13] Another mechanism which utilises lattice components of the catalyst surface that end up in the reaction products via absorbed intermediates is describes as a Mars Van Krevelen mechanism. This involves redox properties of the catalyst surface and is often observed as lattice oxygen species which are then incorporated into the product material and the oxygen vacancies replenished by molecular $O_2$.[14]

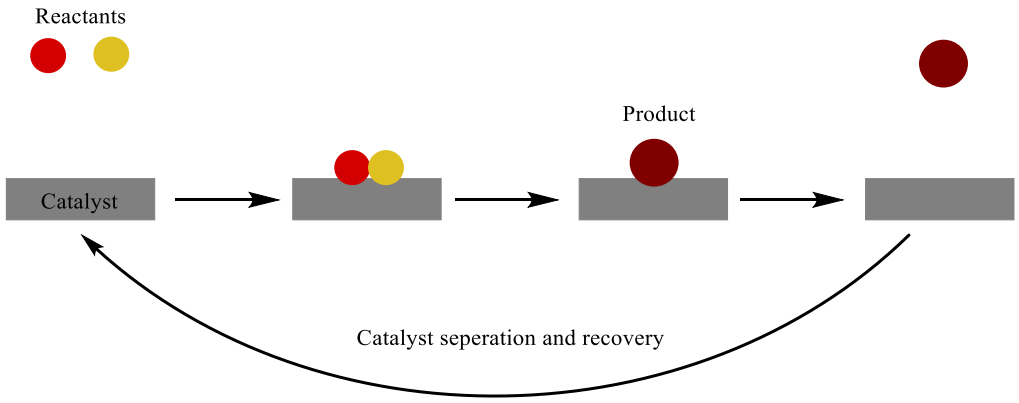


***Figure 1.2*** *A generic reaction scheme for the interaction between a solid catalyst and reactants in a heterogeneous reaction, via a Langmuir-Hinshelwood mechanism.[12]*

### 1.1.3.1 Nanoparticle catalysis.

Nanoparticles are loosely defined as particles with a diameter in the range of 1 to 100 nm. Nanoparticles have potential applications in a wide range of areas, including catalysis and electro catalysis, fuel cells, materials and coatings and optical electronics, and are considered as at the forefront of controlled catalyst synthesis.[15]

When no diffusion limitations are in place the catalytic reaction rate should be proportional to the surface area of the active sites of the catalyst.[10] Hence from this it can be rationalised that the smaller the catalyst particle or the greater the dispersion of the active sites of the catalyst the greater the activity. One way to produce small disperse nanoparticle is to produce colloidal solutions of metal nanoparticles which are quasi-homogenous catalysts. However, these solutions of often reduced metal can be unstable due to the oxidation of the metal and/or the coalescence of particles.[16] Hence supported nanoparticle catalyst are common for the advantages of reducing

sintering of the metal particles and positive enhancements from metal-support interactions as well as obvious advantages with recoverability of the catalyst.[1,10]

The main stages of preparing a supported nanoparticle catalyst are illustrated in Scheme 1.1.

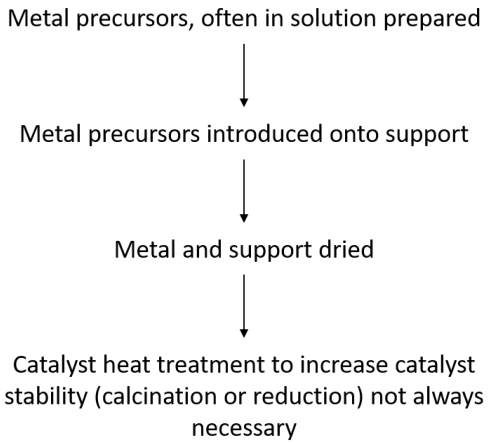


***Scheme 1.1.*** *The generic formulation of supported metal catalysts.*

This is a great way to stabilise small nanoparticles and increase surface area of the catalysts by the use of high surface area supports which can increase particle dispersion.

## 1.2 Hydrogen Peroxide ($H_2O_2$).

The discovery and initial production of $H_2O_2$ can be attributed to Louis Jacques Thenard back in 1818 when he reacted barium chloride with nitric acid.[17] He then improved his system by the addition of hydrochloric acid and then sulphuric acid to precipitate the barium sulphate by-product, Scheme 1.2.[18]

$$BaO_2 + HCl \rightarrow BaCl_2 + H_2O_2$$

$$BaCl_2 + H_2SO_4 \rightarrow BaSO_4 + 2HCl$$

$$BaO_2 + H_2SO_4 \rightarrow BaSO_4 + H_2O_2$$

***Scheme 1.2.*** *Route utilised by L.J Thenard for producing $H_2O_2$.*

$H_2O_2$ is an increasingly desired commodity chemical. It has several industrially relevant uses with the largest being in the paper and pulp bleaching, and water treatment industries. Other uses include, but are not exclusive to, removal of toxic compounds and pollutants, disinfectants and chemical transformations and production.[19]

$H_2O_2$ is considered an efficient and green oxidant due to its high active oxygen content, compared to other common oxidants, and producing only $H_2O$ as the by-product, as displayed in Table 1.1.[20]

***Table 1.1*** *Common industrial oxidants and their active oxygen content.*[20]

| Oxidant | Active oxygen content (% w/w) | By product |
|---|---|---|
| $H_2O_2$ | 47.1 | $H_2O$ |
| t-BuOOH | 17.8 | t-BuOH |
| $HNO_3$ | 25.0 | $NO_x$, $N_2O$, $N_2$ |
| $N_2O$ | 36.4 | $N_2$ |
| NaClO | 21.6 | NaCl |

Some extent of its oxidative transformations is within the polymer industry. Here it can be used for the epoxidation of propylene to propylene oxide and the oxidation of cyclohexanone to its corresponding oxime, which lead to production polyurethane and ε-caprolactam respectively.[20]

### 1.2.1 The anthraquinone autoxidation process.

Industrially $H_2O_2$ is produced by the anthraquinone (AO) process, as it has been since it was patented in the 1940's by IG Farben Industrie Corporation.[21] The AO process proceeds via the hydrogenation of a substituted anthraquinone to hydrogenised anthraquinone and its subsequent oxidation back to the quinone, as shown in Scheme 1.3.[20]

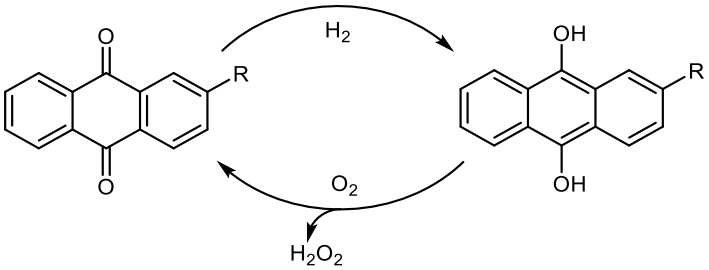


***Scheme 1.3.*** *Reaction scheme for the anthraquinone process.*

Although this process avoids the potentially dangerous contact of both $H_2$ and $O_2$ gases it is an arduous process which produces concentrations of $H_2O_2$ of around 30 wt. % after successive catalytic cycles. This solution then needs to be distilled to a more concentrated solution before transportation and distribution which comes with its own safety issues. Solutions are then diluted again for desired purpose.[20,22,23] Concentrated solutions of $H_2O_2$ can be explosive once it starts to decompose and as it is a strong oxidiser it will accelerate burning if involved in a fire. This shows the serious safety concerns associated with both the transportation and storage of concentrated $H_2O_2$. To

avoid the decomposition of commercial $H_2O_2$ additional acid or halide stabilisers are often implemented.[18] Although this can have advantages with the storage and stabilisation of $H_2O_2$ when it comes to the use of $H_2O_2$, especially in catalysis, these stabilisers can interact with the reaction. Especially in the case of halide and inorganic additives which are potential catalyst poisons.[24]

This system has been refined and adapted over the years to produce high efficiency and selectivity toward $H_2O_2$. However, the anthraquinone molecule can decompose and hydrogenate under the conditions and this leads to the continual addition of anthraquinone throughout $H_2O_2$ production decreasing the efficiency of the process.[20] Hence from these limitations of the AO process research has focussed on other methods to form $H_2O_2$.

The fuel cell approach uses electrochemistry to produce $H_2O_2$ via a three-phase system with the gases, electrolyte and electrodes. Here an alkaline solution of $H_2O_2$ is produced via oxidation of $H_2$ gas to $H^+$ ions at the anode which pass into the electrolyte where gaseous $O_2$ is reduced at the cathode.[25]

Supercritical-$CO_2$ is used as a solvent, above its critical temperature and pressure, 31.1 °C and 73.75 bar, to increase solubility and mass transfer of gases within catalytic systems.[26] This can lead to high concentrations of both $H_2$ and $O_2$ leading to greater rates of reactions and easy recovery of $H_2O_2$ by extraction into water and the evaporation of $CO_2$ into the gas phase above the critical conditions.[27]

The plasma method uses a dielectric barrier charge to turn the gaseous $H_2$ and $O_2$ mixtures to plasma mixtures. Within the plasma the reactants are turned into radicals, via collisions with free electrons, which then react to form $H_2O_2$.[28]

The direct synthesis of $H_2O_2$ using a variety of metal catalysts has been extensively studied with assorted homogeneous[23,27] and heterogeneous catalysts.[33-90] It is the heterogeneous studies that are the focus of the background of this project.

## 1.3 The direct synthesis of $H_2O_2$.

While the AO process shows the in direct reaction of $H_2$ and $O_2$ other approaches have looked at the direct combination of $H_2$ and $O_2$.[30-90] This direct synthesis potentially provides a 100 % atomic efficient reaction with no need for an anthraquinone intermediate. However, gas mixtures of $H_2$ and $O_2$ are explosive and hence care must

be taken to work outside these explosive regions (5 – 95%) which can limit $H_2O_2$ production.[29]

The original patent for the synthesis of $H_2O_2$ via a direct route was published in 1914 by Henkel and Weber,[30] but commercialisation of the process is still a challenge. The main problem associated with the process is the inherently low catalytic selectivity of $H_2O_2$. The selectivity of $H_2O_2$ synthesis is often dramatically reduced due to two possible degradation pathways, Scheme 1.4. The degradation produces water either from the decomposition or hydrogenation, which is thermodynamically more favourable, of $H_2O_2$. The gas mixtures, $H_2$ and $O_2$, can also directly react, by combustion, to produce the water by-product which again is more thermodynamically more favourable compared to $H_2O_2$ synthesis.[20]

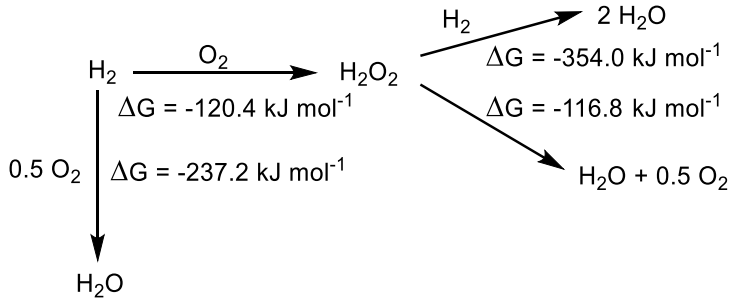


***Scheme 1.4.*** *Reaction scheme for the direct synthesis of $H_2O_2$, production of by products and degradation pathways.*[20]

#### 1.3.1.1 Direct Synthesis of $H_2O_2$ using supported metal catalysts.

Since the initial patents in 1914 Pd has known to catalyse the liquid-phase direct synthesis of $H_2O_2$.[30] Hence much research to the present date has focused on Pd-based catalysts.

Lunsford and co-workers have shown the colloidal Pd can catalyse the synthesis of $H_2O_2$.[31–33] They investigated a solution of $PdCl_2$ and solid $Pd/SiO_2$ catalysts but found in the presence of HCl that dissolution of $Pd/SiO_2$ occurred to form $PdCl_4^{2-}$. They observed this $PdCl_4^{2-}$ was the active Pd species in both the homo and heterogeneous catalysts, Figure 1.3.[33] These Pd catalysts showed a linear increase in $H_2O_2$ production with increasing time up to 5 hours showing limited $H_2O_2$ degradation.[31–33]

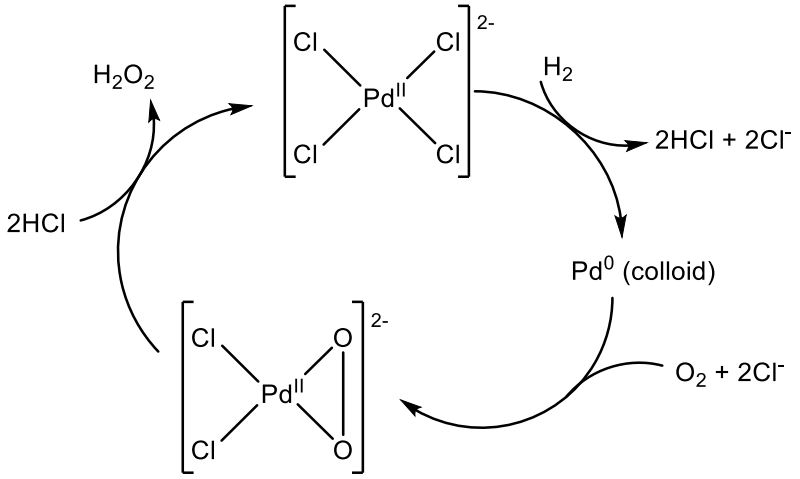


***Figure 1.3.*** *Catalytic cycle of the formation of $H_2O_2$ from $PdCl_4^{2-}$ Recreated from Reference 31, Copyright © 2004 Elsevier Inc..*[31]

Although these colloidal Pd have shown high activity industrially homogeneous catalysts are not ideal due to the need to stabilise colloidal Pd and to recover for successive uses. Hence research has focussed on supported Pd catalysts. Pd catalysts have shown to provide high $H_2O_2$ synthesis activity but there has always been a problem with the selectivity of the reaction due to the subsequent $H_2O_2$ degradation activity of the catalyst.[20,34] Hence catalytic research has focussed on increasing $H_2O_2$ synthesis activity while maintaining high selectivity to $H_2O_2$.

#### 1.3.1.1.1 Catalyst active site and reaction mechanism.

Though it is generally agreed that different active sites are present for both the synthesis and decomposition of $H_2O_2$ it is still debated what the exact nature of these sites are.

From isotope labelling experiments of $O_2$ conducted by Dissanayake and Lunsford it has been concluded that the initial step of reaction is the addition of $O_2$ onto the catalyst surface to produce an adsorbed oxygen intermediate, $O_2$*, Figure 1.4. It is then imperative for this O-O bond to remain intact for the formation of $H_2O_2$. Cleavage of the O-O bond is irreversible and will lead to the by-product $H_2O$.[33]

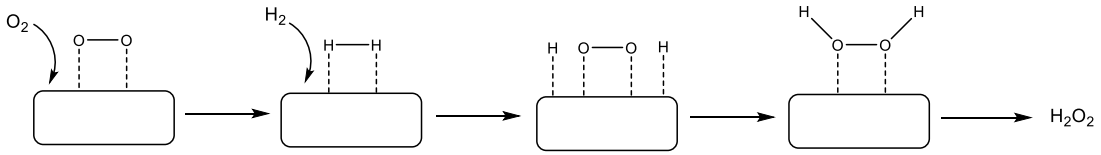


***Figure 1.4.*** *A proposed schematic for the formation of $H_2O_2$ on a catalyst surface.*[33]

Hence synthesising a catalyst with the highest selectivity requires actives sites which can bind to $O_2$ but without excess back donation of electron density into the $2\pi^*$

orbitals in the absorbed states of the $O_2$* and OOH* intermediates which would conclude in O-O cleavage and the formation of the $H_2O$ byproduct.[35]

In 2016, Wilson and Flaherty published a study in which they detailed the reaction mechanism as one in which the two electron oxygen reduction is coupled with the heterolytic oxidation of $H_2$ describing the pathways in terms of two half reactions, Figure 1.5.[36]

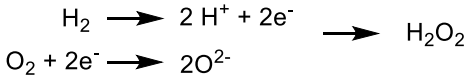


***Figure 1.5.*** *Two half equations present in the direct synthesis of $H_2O_2$ as proposed by Wilson and Flaherty.* [36]

They deduced this mechanism from the strong dependence of $H_2O_2$ and $H_2O$ formation on $H_2$ pressure while observing no change with $O_2$ pressure. These observations do not coincide with previously predicted Langmuir-Hinshelwood mechanisms which would involve the reduction of $O_2$* by sequential reaction with H* which would lead to $H_2O_2$ depending on $O_2$ and not $H_2$.[36]

This and other studies by Flaherty also show the important of $H^+$ concentration in the formation of $H_2O_2$. They observe an increase in the formation of $H_2O_2$ with an increase in $H^+$ concentration. This is then developed further to show that the formation is much greater in protic solvents, such as methanol and water, than in aprotic solvents, such as acetonitrile and dimethyl sulfoxide.[36,37]

When Pd is present it is debated whether metallic Pd or oxidised Pd, in the form of PdO, is the active centre for $H_2O_2$ production.

Wang *et al.* used density functional theory to look at the activation barriers for the different pathways on both PdO (101) and Pd (111) surface. They concluded that the activation barrier, for the production of $H_2O_2$, is lower (ca. 20 kJ $mol^{-1}$) on the PdO compared to the metallic surface and observed that the preferred product on PdO to be $H_2O_2$ and conversely $H_2O$ on the Pd surface. The higher activity and selectivity for $H_2O_2$ on the PdO surface was attributed to the weaker adsorption of $O_2$, $H_2$, $H_2O_2$ and the OOH intermediate which reduces their dissociation leading to $H_2O$.[38]

Burch *et al.* showed that for Pd catalysts supported on a variety of supports (C, $Al_2O_3$, $ZrO_2$, $TiO_2$ and $Fe_2O_3$ $Al_2O_3$ mixtures) a reductive heat treatment prior to use increased $H_2$ conversion and selectivity towards $H_2O_2$. Hence, they concluded that reduced $Pd^0$

species were more active and also more selective for $H_2O_2$ production.[39] However in a similar study Choudhary *et al.* looked at 2.5% Pd on a variety of oxide supports ($Al_2O_3$, $Ga_2O_3$, $ZrO_2$, $CeO_2$, $ThO_2$, $BPO_4$ and $SiO_2$) and compared the $H_2O_2$ activity of both the oxidised and reduced catalysts. They showed that although the $H_2$ conversion was greater over the reduced catalysts than oxidised the yield of $H_2O_2$ over the oxidised catalysts was greater. This was due to the much greater decomposition rates over the reduced catalysts leading to the oxidised catalysts showing a higher selectivity.[40]

Liu *et al.* produced and compared a fully reduced $Pd/SiO_2$, a fully oxidised $PdO/SiO_2$ and a $PdO/SiO_2$ catalyst which was reduced prior to use. The fully reduced samples provided the greatest activity for the production of $H_2O_2$ followed by the $PdO/SiO_2$ sample which was pre-reduced and the fully oxidised sample showed no activity. Hence from this study they concluded that metallic Pd is the active form for the production of $H_2O_2$.[41]

Flaherty has also contributed to the idea that metallic Pd is the active phase through observations that PdO based catalysts present induction times, ca. 30 minutes, for the formation of $H_2O_2$ which is in converse to Pd which produced $H_2O_2$ immediately.[35]

Ouyang *et al.* have investigated $Pd/TiO_2$ of vary concentrations of Pd and concluded that it is the interface between metallic Pd and PdO that produces the greatest activity and selectivity. They showed that at the interface of Pd particles and $TiO_2$ is a PdO layer which at the surface has more metallic Pd. In a sample with an increased ratio of $Pd^{2+}$:$Pd^0$ (65.7 %) they concluded that there were not enough $Pd^0$ centres which lead to a limit in the dissociative activation of $H_2$. Once the sample was reduced decreasing $Pd^{2+}$ (47.6%) to equal quantities of $Pd^0$ the activity and selectivity increased as the interfaces between $Pd^0$ and PdO were enhanced leading to both sites for $H_2$ activation and activation of $O_2$ being present.[42]

However, what can be agreed on amongst the community is that Pd active species under reaction conditions of both $H_2$ and $O_2$ can always change and extensive *in-situ* characterisation is required for full determination of the active species present.

#### 1.3.1.1.2 Synergistic effects.

Several Au catalysts have also been investigated but were found to be much less active than the equivalent Pd monometallic catalysts but have shown higher selectivity with decreased $H_2O_2$ degradation observed.[26,43,44]

Edwards *et al.* have observed that alloying the two metals, Au and Pd, to produce bimetallic supported catalysts induced a synergy between the metals, producing superior catalytic activity, Table 1.2.[45]

***Table 1.2.*** *Productivity of $H_2O_2$ for corresponding Au, Pd and AuPd supported on $TiO_2$ catalysts.*

| Catalyst | Productivity / $mol_{H_2O_2}\ kg_{cat}^{-1}\ hr^{-1}$ | $H_2$ selectivity / % | $H_2$ conversion / % |
|---|---|---|---|
| 5 % $Au/TiO_2$ | 7 | Too low to determine | Too low to determine |
| 5 % $Pd/TiO_2$ | 30 | 21 | 29 |
| 2.5 % Au 2.5% $Pd/TiO_2$ | 64 | 70 | 21 |

***Reaction conditions;*** *0.01 g catalyst, 2.9 g water, 5.6 g methanol, 420 psi 5 % $H_2$ in $CO_2$, 160 psi 25 % $O_2$ in $CO_2$, 2 °C, 30 minutes, 1200 RPM.*[45]

Ishihara and co-workers also showed that alloying Au and Pd increased $H_2O_2$ formation. With increasing concentrations of Au an increasing concentration of $H_2O_2$ was observed, this was attributed to decreasing the degradation rates of $H_2O_2$.[46] DFT studies then concluded that the decrease in $H_2O_2$ decomposition on the AuPd surface compared to the Pd surface was due to less active Au weakening the interaction between $H_2O_2$ and the AuPd surface. Hence the decreased adsorption of $H_2O_2$ on AuPd compared to Pd makes the release of $H_2O_2$ more favourable compared to O-O scission, increasing $H_2O_2$ selectivity.[47,48]

When alloying Au with Pd the disruption of Pd ensembles on the catalyst surface is observed.[49,50] Chen *et al.* concluded that promotional effects of Au were caused by the isolation of single Pd sites which decreases the adsorption of surface species.[49] Edwards *et al.* observed with increasing Au content an increase in Pd dispersion on the catalyst is observed which decreases the large Pd ensembles which have shown to have greater activity for $H_2O$ formation.[51] Hans and Mullins have noted that with increasing Pd content in bimetallic AuPd catalysts the dissociation energy of $O_2$ decreases.[52] The dissociation of $O_2$ leads to the formation of $H_2O$ rather than $H_2O_2$ as the O-O bond must be maintained for the formation of $H_2O_2$.[33] Hence with a decrease in $O_2$ dissociation energy an increase in $H_2O$ formation can be expected leading to a

decreased catalyst selectivity. These are morphology effects that are attributed to the synergistic effect of Au and Pd.

It has also been postulated that there is an electronic effect causing synergistic effects. The electronic structures of both Au and Pd are altered upon alloying. XPS analysis of AuPd catalysts have shown lower binding energies for both the Au $4f_{7/2}$ and Pd $3d_{3/2}$ peaks which indicates the movement of net charge into both Au and Pd.[53,54] Han *et al.* observed that there is a net charge from Pd into the s and p orbitals of Au which is coupled with a net charge from Au into Pd d orbitals.[54] This electronic modification can also increase selectivity by decreasing the $O_2$ dissociation on the catalyst surface.[54] It is also postulated that the addition of Au can stabilise the Pd on the catalyst surface by stabilising the oxidation state of Pd increasing re-usability of the catalyst also.[55]

#### 1.3.1.1.3 Particle morphology.

Edwards and Hutchings have shown by Transition Electron Microscopy (TEM) analysis the structural compositions of the bimetallic AuPd catalysts.[56] They observed that the composition of the nanoparticles was dependant on the nature of the support, Figure 1.6. With most common oxide supports, the composition of particles showed core-shell structures, with an Au-rich core and Pd-rich shell. It was suggested that this formation on oxide supports was attributed to the oxidation efficiency of the support. This enhances the formation of PdO which consequently leads to surface segregation. Conversely, with carbon which is a reducing support the formation of PdO species and segregation is unfavoured and hence a random alloy nature was observed.[45,56]

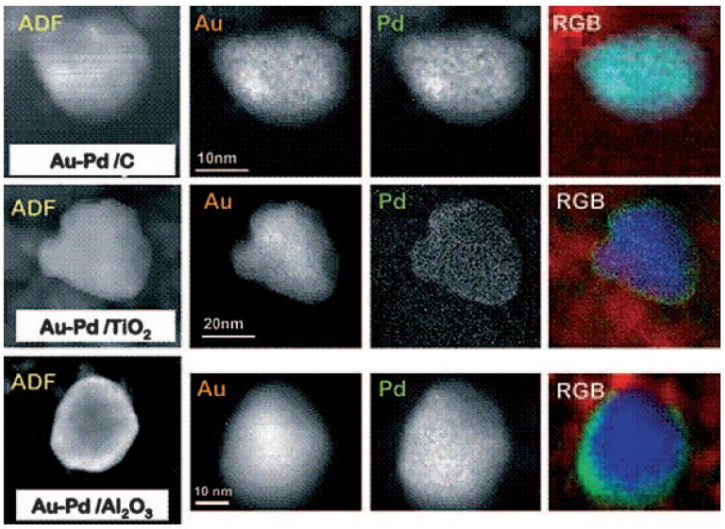


***Figure 1.6.*** *TEM images of AuPd nanoparticle catalysts supported on carbon, $TiO_2$ and $Al_2O_3$ after calcination. High-angle annular dark-field (HAADF) image is shown in first column, Au map in second, Pd map in third and the overlay of Au (blue) and Pd (green) RGB in fourth.[56] Copyright © 2008 WILEY-VCH Verlag GmbH & Co. KGaA, Weinheim*

It was shown that, for the carbon support, that a random alloy structure could be observed.[56,57] With the oxide supports with increasing calcination temperature composition switched from homogeneous alloys to core-shell at temperatures of 400 °C. The core-shell structures though were shown to be less active were more stable and had consistent activity with recycling tests. Here it was seen that catalysts that did not undergo high temperature heat treatments leached a considerable, over 80 %, of the metals from the catalyst and hence a decrease in productivity is seen for successive tests.[45]

#### 1.3.1.1.4 Support material.

The support is known to have a substantial effect on the selectivity and yield of $H_2O_2$ produced.[34,51,57–64] The extent of these enhancements has shown to be dependent on the support being investigated. The isoelectric point, IEP, of a support defines the pH at which the support molecules have no net charge. This has shown to have an effect on both the productivity of the catalyst as well as the enhancement seen with pre-treatments. The correlation between IEP and productivity has shown that supports with lower IEP show the highest productivity, Figure 1.7. This is coordinated with increasing IEP and decreasing acidity of the support increasing the degradation of $H_2O_2$, Figure 1.8, and hence leading to a decrease in yield and productivity.[58]

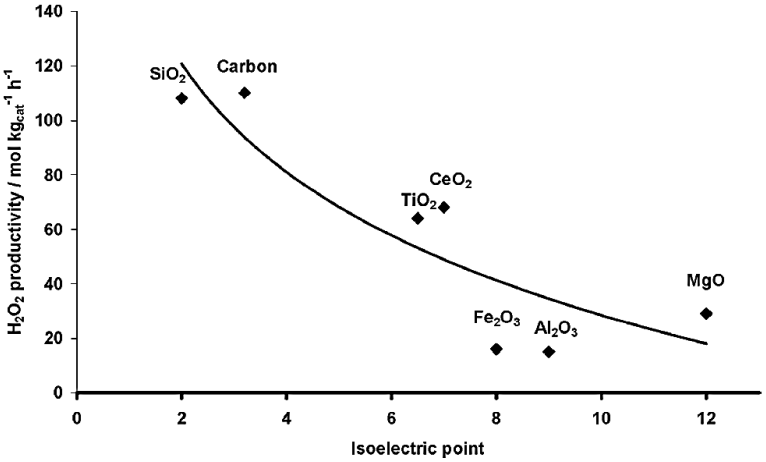


***Figure 1.7.*** *The correlation seen between the isoelectronic point of a support and the $H_2O_2$ productivity seen for bimetallic, AuPd, catalysts.[58]Reproduced from Ref. 58 with permission from The Royal Society of Chemistry.*

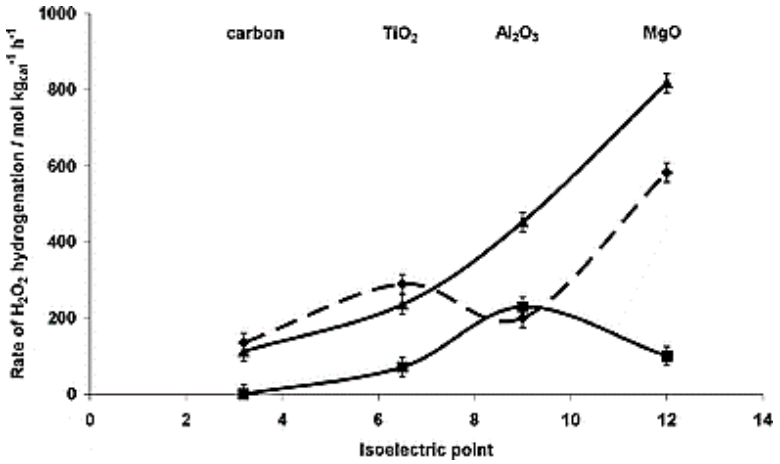


***Figure 1.8.*** *The correlation seen between the isoelectronic point of a support and the hydrogenation of $H_2O_2$ seen for; Pd ◆, Au ■, and AuPd ▲ catalysts.[58] Reproduced from Ref. 58 with permission from The Royal Society of Chemistry.*

Comparing carbon, with a low IEP, and MgO, with a high IEP, it was also shown that a lesser improvement of the productivity from acid pre-treatment was seen with higher IEPs.[65]

#### 1.3.1.1.5 Acid addition.

The decomposition of $H_2O_2$ is known to be catalysed, and enhanced, under basic conditions. Hence it has been found that the yield of $H_2O_2$ can be increased with the addition of acid additives or with the use of acidic supports.[51,58,65]

Pospelova first showed in 1961 that the addition of inorganic acids reduced the decomposition of $H_2O_2$ believed to be due the inhibition of deprotonation of $H_2O_2$ to form $^{\bullet}OOH$ which leads to $H_2O_2$ decomposition.[66]

Choudhary has shown for metallic Pd catalysts in aqueous mediums very limited $H_2O_2$ is produced due to the rapid decomposition of $H_2O_2$ over the metallic surface. With the addition of oxoacids ($H_3PO_4$, $H_2SO_4$ and $HNO_3$) this decomposition was dramatically reduced.[67]

Along with reducing the decomposition of $H_2O_2$ it is now postulated that $H^+$ ions can also be involved in the formation of $H_2O_2$.[36,37,68] Abate *et al.* proposed that $H^+$ could directly react with adsorbed $O_2$ forming OOH on the catalyst surface before further reaction with $H_2$ forming $H_2O_2$ with the release of $H^+$, Figure 1.9.[68]

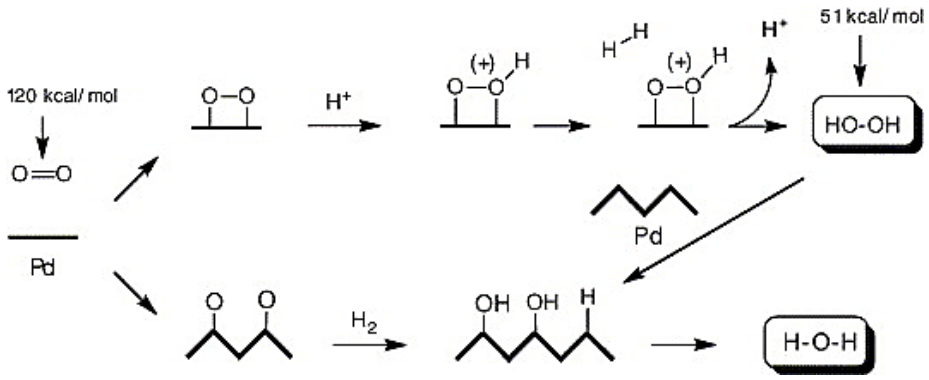


***Figure 1.9*** *Mechanism of $H_2O_2$ over Pd catalyst surface (illustrated in bold) proposed by Abate et al, including the bond dissociation energies of the O-O bond in $O_2$ and $H_2O_2$.[68]Copyright © 2005 Elsevier B.V. All rights reserved.*

Wilson and Flaherty have more recently investigated the mechanism of $H_2O_2$ formation on Pd clusters.[36] They also concluded that $H^+$ were imperative in the formation via the reduction of $O_2$ in the two electron oxygen reduction reaction. A correlation between the $H_2O_2$ turnover rates and the concentration of $H^+$ were observed with the highest $H_2O_2$ concentrations produced in protic solvents, showing the importance of $H^+$.[36] They followed this further by investigating AuPd clusters and discovered a similar dependence on $H^+$ ions.[37]

However, it should be noted that the concentration of acid in solution must be carefully controlled as at increased concentrations of acid metals can leach from the catalyst into the reaction solution.[31,69] This then introduces problems with catalyst stability and reusability as well as the need to remove the metal from the solution. Hence the use of acidic supports which avoids the direct addition of acid to a reactor could be favourable.

Edwards *et al.* have shown that the acid pre-treatment of $TiO_2$ and $SiO_2$ supports before impregnation of AuPd showed an increased productivity and selectivity.[51,61] By TEM, it was shown that the acid pre-treatment had the effect to re-disperse the gold within the particles, and to produce a tighter distribution of particle size.[51] The acid pre-treatment was also investigated with AuPd/C catalysts where the degradation of $H_2O_2$ could be eradicated, giving selectivities of greater than 98 %. Here it was shown that the best results were produced with acetic and nitric acid.[34]

#### 1.3.1.1.6 Halide addition.

It has been shown that the addition of halides, especially $Br^-$, acts to supress $H_2O_2$ decomposition believed to be due to changing the surface charge or by possible poisoning of catalyst sites responsible for hydrogenation of $H_2O_2$.[70] The promotional

addition of $Br^-$ has been reported both with solution species[71] and the incorporation of $Br^-$ into the catalyst support or with the Pd metal.[72,73]

Halides are often reported as catalyst poisons in heterogenous catalysis.[24] This is no exception in the case of $H_2O_2$ synthesis catalysts however here the increased selectivity to $H_2O_2$ is attributed to the selective poisoning of the catalyst sites responsible for the formation of $H_2O$.[74] Binding of halides onto these catalyst active sites onto which $O_2$ adsorbs and is subsequently cleaved can increase the selectivity towards $H_2O_2$ as the cleavage of $O_2$ leads to $H_2O$ formation.

Further studies into the promotional effects of halides have suggested that the halide prevents the back donation of electrons from the catalyst surface into the $O_2$ $2\pi^*$ orbital which maintains the O-O bond and again reduces formation of $H_2O$.[75]

Samanta and Choudhary observed that for halide promoted $Pd/Al_2O_3$ catalysts there was an optimum loading of $Br^-$ on the catalyst of 2% which provided the greatest activity and selectivity towards $H_2O_2$.[73] Above this optimum loading $Br^-$ ions would begin to non-selectively poison catalytic sites where a decrease in $H_2$ conversion indicated that the sites for $H_2O_2$ formation were now being blocked as well as those responsible for its degradation.[73]

Hans and Lunsford have also suggested that the addition of halides inhibits the formation of Pd ensembles and hence the promotional effect observed is similar to those observed from the alloying of Au and Pd.[32] The Pd ensembles have been attributed to O-O dissociation which leads to the degradation of $H_2O_2$ and an increase in $H_2O$ formation.[49,76] Hence the reduction in Pd ensembles can increase selectivity towards $H_2O_2$.

#### 1.3.1.1.7 Alternative metals to Au.

More recently, the potential of the addition or substitution of other metals into the catalyst has been explored.[77-89]

Xu *et al.* have shown that the addition of Pt to Pd can have promotional effects on the $H_2O_2$ synthesis.[77] As also observed for Au,[54] the addition of Pt is believed to lead to electron transfer from Pt to Pd which decreases the strength of the Pd-O bond which decreases the dissociation of $O_2$ and increases $H_2O_2$ selectivity.[77]

Further on from this Edwards *et al.* showed that very small amounts of metallic Pt, up to 0.20 wt. %, added to a $AuPd/TiO_2$ catalyst has a positive effect on productivity.[78] With very small additions, 0.05 wt. % Pt, the subsequent hydrogenation of $H_2O_2$ was decreased, compared to $AuPd/TiO_2$, and hence an increase in catalytic selectivity seen. However, with increased amounts of Pt, 0.10 and 0.20 wt. %, an increase in hydrogenation was observed, and a decrease in yield of $H_2O_2$ seen. From TEM, it was shown that the Pt promoted AuPd catalysts led to a narrower size distribution of the particles. It also showed a redistribution of the metals with much smaller Pd rich particles along with alloy particles which showed decreasing amounts of Pd with increasing particle size. This is a similar effect that is seen for $AuPd/TiO_2$ but to a greater extend with the addition of Pt.[78]

Samanta and Choudhary demonstrated that the addition of Rh or Ru to 2.5 % $Pd/ZrO_2$ was detrimental to $H_2O_2$ yield despite an increase in $H_2$ conversion compared to monometallic 2.5% $Pd/ZrO_2$. This was attributed to an increase in $H_2O_2$ decomposition over the RhPd and RuPd catalysts which was greater than the increase in $H_2O_2$ production.[40] On the contrary Ntainjua *et al.* observed a positive enhancement on $H_2O_2$ yield with alloying Ru and Pd.[79] However, they did note that the synergistic effects were loading dependant with Ru loading of 0.25 – 1% promoting the catalytic activity but above 2.5% Ru a detrimental effect was observed. The optimum ratio was observed at 0.5% Ru 4.5% $Pd/TiO_2$ which gave a productivity of 143 $mol_{H_2O_2}kg_{cat}^{-1}hr^{-1}$ which was a large enhancement on both monometallic catalysts, 5 % $Ru/TiO_2$ 14 $mol_{H_2O_2}kg_{cat}^{-1}hr^{-1}$ and 5% $Pd/TiO_2$ 30 $mol_{H_2O_2}$ $kg_{cat}^{-1}$ $hr^{-1}$.[79]

Freakley *et al.* discovered that Au could be replaced by the non-noble metal, Sn, in the $AuPd/TiO_2$ bimetallic catalyst while still maintaining similar productivities and enhancing catalytic selectivity.[76] With the appropriate oxidation reduction oxidation (ORO) heat treatment, the degradation of $H_2O_2$ could be eliminated completely, producing selectivities of 96 %. This showed that Sn was playing a beneficial role in inhibiting subsequent hydrogenation and decomposition of $H_2O_2$. The reduction in the degradation is believed to be due to Sn forming a $SnO_x$ layer which encapsulated small Pd rich particles, which are known to excel the hydrogenation of $H_2O_2$,[62,80–82] Figure 1.10 Insert C. The larger PdSn alloy particles were uncovered by this film and hence accessible for direct synthesis, Figure 1.10 Insert D.[76]

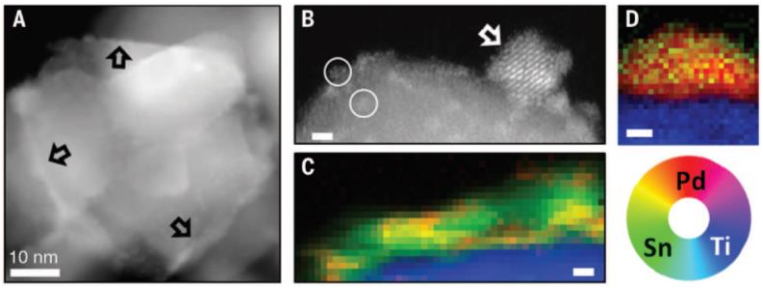


***Figure 1.10.*** *STEM-HAADF greyscale images (A and B) and RGB maps (C and D), showing particle composition, 3% Pd 2 % Sn/$TiO_2$. Scale bars represented are 1 nm.*[76]*Copyright © 2016, Copyright © 2016, American Association for the Advancement of Science*

Multiple heat treatments were implemented to produce the morphology of the SnPd/$TiO_2$ catalysts which provided the high catalytic selectivity. First the dried catalyst was calcined (500 °C, 3 hours, static air) which although showed appreciable $H_2O_2$ synthesis activity (68 $mol_{H_2O_2}$ $kg_{cat}^{-1}$ $hr^{-1}$) also showed significant $H_2O_2$ degradation activity (65 $mol_{H_2O_2}$ $kg_{cat}^{-1}$ $hr^{-1}$) and the catalyst was not stable to subsequent uses. An additional reduction heat treatment was then used (200 °C, 2 hours, 5% $H_2$/Ar) this still provided high $H_2O_2$ activity (60 $mol_{H_2O_2}$ $kg_{cat}^{-1}$ $hr^{-1}$) which was stable to multiple re-uses. However, this produced a large proportion of reduced Pd species which are known to be active for the $H_2O_2$ degradation and hence an increase in $H_2O_2$ degradation (300 $mol_{H_2O_2}$ $kg_{cat}^{-1}$ $hr^{-1}$) was observed. Finally, an additional calcination (400 °C, 4 hours, static air) was implemented to re-oxidise the exposed Pd surfaces. This combined ORO heat treatment produced an active catalyst (61 $mol_{H_2O_2}$ $kg_{cat}^{-1}$ $hr^{-1}$) which was stable over multiple runs and showed no degradation of $H_2O_2$ leading to $H_2O_2$ selectivity of 96%.[76]

This study began to investigate and show the possibility of replacing precious metals with more earth abundant metals without a compromise on the catalytic ability for direct synthesis of $H_2O_2$. Within this study 0.5% Pd 4.5% X/$TiO_2$ catalysts where X is Ni, Ga, Zn, Co and In were also studied where all catalyst showed no degradation of $H_2O_2$ and with Ni showing the highest productivity of 32 $mol_{H_2O_2}$ $kg_{cat}^{-1}$ $hr^{-1}$.[76]

Following on from this 0.5% Pd 4.5% Ni/$TiO_2$ catalysts were further investigated by Crole *et al.* in both batch and flow systems using water solvent at ambient temperatures.[83] This catalyst maintained high $H_2O_2$ selectivities 97 % and 85 % in batch and flow system respectively. In a flow system the concentration of $H_2O_2$ could be maintained with no loss of activity over a 10 hour time period.[83] This illustrated the

use of a stable catalyst, with a low precious metal content, utilised under benign, green conditions.

Many combinations of Pd with non-precious metals have now been observed in the literature including Ga and In,[84] Ag,[85] Sb,[86] Te,[87] Zn[88] and Na.[89] Showing the versatility of metals which can provide promotional effects on Pd for the direct synthesis of $H_2O_2$.

#### 1.3.1.1.8 Conclusions.

In conclusion, catalysts for $H_2O_2$ synthesis are varied in both their activity and selectivity with Pd at the foundation of the catalyst, Table 1.3. Many additives, such as acids and halides, can be added to increase $H_2O_2$ selectivity but the addition of these come with complications of separation and a potential contamination for further uses. The addition of secondary metals are a promising aspect of catalyst design especially with the use of non-precious metals. The incorporation of non-precious metals is an obvious economic benefit and if selectivity to $H_2O_2$ can still be maintained are an obvious future option for $H_2O_2$ synthesis.

***Table 1.3.*** *Notable $H_2O_2$ catalysts and their activity in the current literature.*

| Catalyst | Conditions | $H_2O_2$ productivity / $mol_{H_2O_2}\ kg_{cat}^{-1}\ hr^{-1}$ | $H_2O_2$ degradation / $mol_{H_2O_2}\ kg_{cat}^{-1}\ hr^{-1}$ |
|---|---|---|---|
| 2.5% Au 2.5% $Pd/TiO_2$[51] | 2 °C, $CO_2$ gas diluent, water/methanol | 64 | 200 |
| 3% Sn 2% $Pd/TiO_2$[76] | 2 °C, $CO_2$ gas diluent, water/methanol | 61 | 0 |
| 0.5% Au 0.5% $Pd/TiO_2$[90] | 25 °C, $CO_2$ gas diluent, water/methanol | 75 | 350 |
| 0.5% Au 0.5% $Pd/TiO_2$[90] | 25 °C, $N_2$ gas diluent, water | 13 | 1025 |

It has also been noted that $H_2O_2$ can be utilised as a non-toxic reagent in many applications. Most obviously it is an effective and benign oxidant and it is well noted in the literature that $H_2O_2$ can be utilised for both the oxidation of cyclohexane[91–96] and benzyl alcohol[97–99] which are both discussed in this thesis.

## 1.4 Oxidation of cyclohexane.

The oxidation of cyclohexane produces two primary oxidation products; the alcohol, cyclohexanol, and the ketone, cyclohexanone, which as a mixture is known as KA oil, Scheme 1.5.[100]

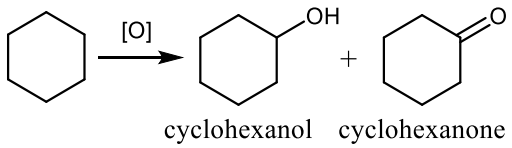


***Scheme 1.5.*** *A generic reaction scheme for the oxidation of cyclohexane, where [O] denotes a generic oxidant.*

### 1.4.1 Industrial production and importance.

Industrially the transformation is done, most commonly, in the presence of a cobalt naphthenate complex, Figure 1.11. This comes with the obvious drawbacks of a homogeneous catalyst as the recovery of the catalyst can be difficult and the stability of the catalyst at high temperature can also be an issue. The process is carried out at 150 to 180 °C under 10 to 12 bar $O_2$. The reaction has to be run at low conversions, of less than 10%, to reduce the over oxidation of the KA oil products and maintain selectivity to around 80%.[101]

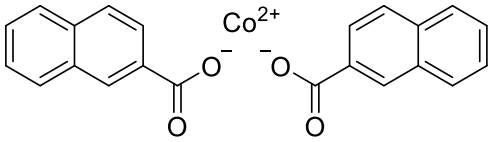


***Figure 1.11.*** *The industrially used Co naphthenate catalyst.*

The industrialisation of cyclohexane oxidation was introduced by DuPont in the 1940's with this Co naphthenate complex, $O_2$ as the oxidant and cyclohexanone initiator at 145 °C.[102] Although much research has been conducted into the advancement of both the catalyst and reaction system, it can be seen that the industrial process has scarcely change in the past 70 years.[103–109]

The industrial relevance of cyclohexane oxidation stems from the oxidation products, predominantly cyclohexanone, which are used for the production of nylon precursors.[110,111] Cyclohexanone can be further oxidised to the ring opened diacid, adipic acid.[101] Adipic acid reacts with the diamine, hexadiamine, via a condensation reaction to produce Nylon 6,6, Figure 1.12.

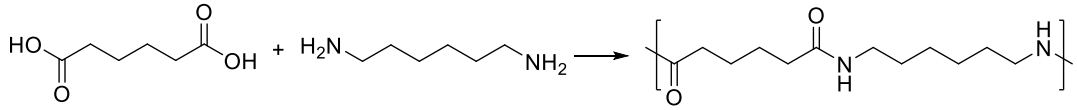


***Figure 1.12.*** *The production of Nylon 6,6 from adipic acid and hexadiamine.*

Nylon 6,6 has abundant uses in the polymer industry, such as fillers, fibres, internal lubricants, and impact modifiers.[101] It is estimated that the global market for Nylon 6,6 is to grow to $8830 million in 2024 up from $7630 million in 2019 showing a compound annual growth rate (CAGR) of 2.5%.[112]

### 1.4.2 Autoxidation process.

The aerobic oxidation of cyclohexane is known to proceed via a radical mechanism, named as an autoxidation process, via the activation of $O_2$, Scheme 1.6.[113]

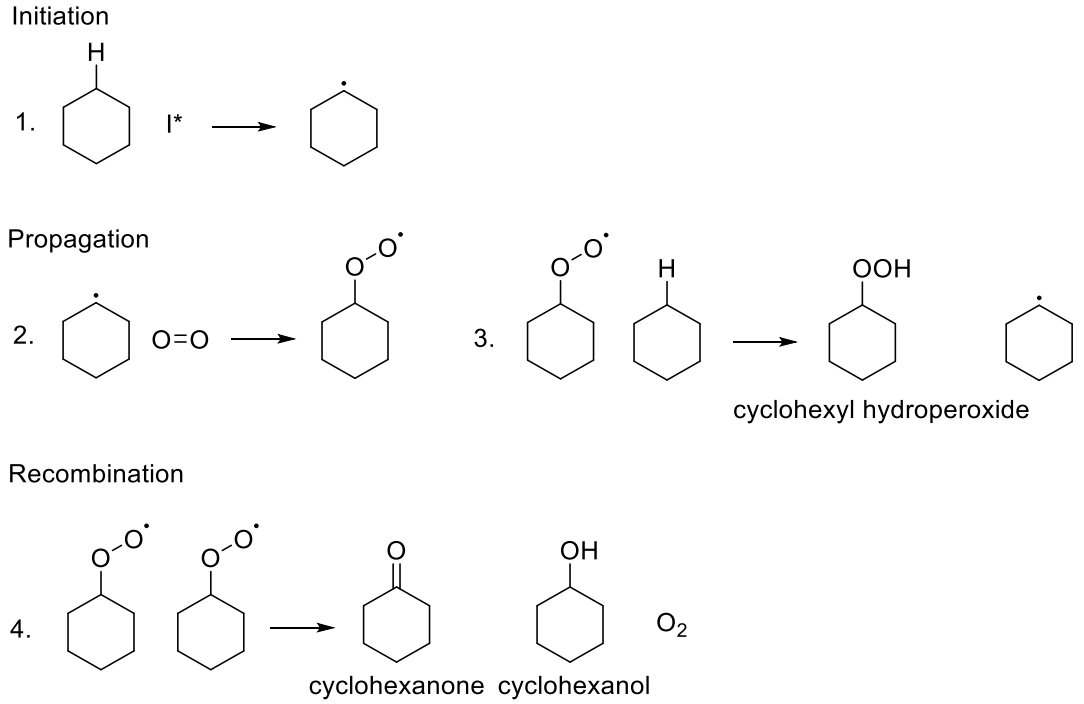


***Scheme 1.6.*** *The autoxidation of cyclohexane with molecular oxygen.*[113–116]

The initiating species, denoted as $I^*$ in Scheme 1.6, refers to anything in the reaction medium that can abstract a H from a cyclohexane molecule, such as *tert*-butyl hydroperoxide [117] or metal catalysts [118]. Steps 2 and 3 are propagating reactions and step 4 a termination reaction. This reaction pathway should produce a 1:1 ratio of cyclohexanol to cyclohexanone. However, the key intermediate, cyclohexyl hydroperoxide (CHHP), can break down via two additional pathways; H abstraction produces the peroxy radical which breaks down to produce cyclohexanone, and homolytic scission of the O-O which eventually produces additional alcohol, Scheme 1.7.[115]

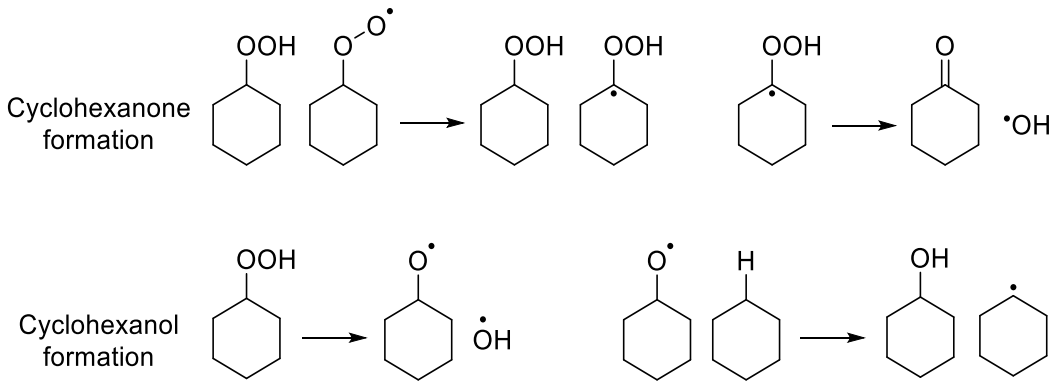


***Scheme 1.7.*** *Additional propagation reactions of the cyclohexyl hydroperoxide intermediate.*[115]

Within the literature, a variety of homogeneous [119–121] and heterogeneous catalysts[123-133] have been investigated to try and improve the yield, conversions and selectivity of the desired KA oil products. Again, here it is the heterogeneous studies that are explored for this literature review.

### 1.4.3 Heterogeneous catalysis.

The role of the metal within the catalytic oxidation of cyclohexane is still debated and seems to depend on the catalyst system used.[92,114–116,122–125] It is questioned whether the metal acts to just promote an autoxidation pathway or catalyses the reaction. For Au catalysts it has been argued that Au is acting to just initiate the autoxidation reaction,[122] but has also been indicated that Au acts to initiate and accelerate the reaction hence acting in a catalytic manner.[114]

Within the literature, different oxidising agents have been named most commonly; molecular $O_2$,[122] $H_2O_2$[126] and tert-butyl hydroperoxide (t-BHP)[127]. All have their advantages. $O_2$ is a well understood oxidant that is readily available and cheap to use. However, additional initiating species, such as peroxides, are often implemented to reduce lengthy induction periods.[122]

Throughout the literature a variety of different supported metals have been utilised providing a wide array of activity. To name a few; Cu[128], Mo and Co[129], Fe[125,130], V[94,131] and Ce[132] have all been investigated.

#### 1.4.3.1 Oxygen oxidant.

Electron paramagnetic resonance, EPR, spin trapping experiments can be used to see the radicals formed during the breakdown of the cyclohexyl hydroperoxide, CHHP, intermediate. From interpretation of the spin adducts formed during EPR insights into the mechanism can be realised. Liu *et al.* produced AuPd/MgO catalysts which

produced high conversions and selectivities, 11 and 95 % respectively, for the aerobic oxidation of cyclohexane.[133] This promising catalyst was investigated by EPR, and the difference between the distribution spin adducts formed by this catalyst were compared with those from the industrially used Co naphthenate catalyst. These studies were used to try to elucidate the mechanism by which the AuPd catalyst acts. The AuPd catalyst increased the amount of alkoxyl rather than peroxyl species compared to the Co catalyst which would follow a complete autoxidation pathway. This suggests that the AuPd catalyst has a stronger binding to the CHHP intermediate which results in the increased homolytic cleavage of the O-O bond, producing the alkoxyl species, Scheme 1.7, this leads to an increased selectivity towards cyclohexanol. However, the spin adducts seen were identical between the two catalysts and hence it was evident that the AuPd catalyst was still acting via the autoxidation mechanism. From this it was concluded that AuPd was acting both as an initiator and as a catalyst, by enhancing the rate yield of alkoxyl intermediates.[133]

Xu *et al.* produced an Au catalyst supported on graphite tested under mild conditions of 70 °C, with molecular oxygen used as the oxidant, which produced conversions around 5 % and selectivities of 20 % with no initiator, but upwards of 90 % with halide additives.[134] Increased reaction times of up to 40 hours were investigated and with increasing reaction time the conversion of cyclohexane increased, close to linearly. However, this was met with a decrease in selectivity to KA oil which dropped from 98 % at 10 hours to less than 20 % at 40 hours due to the accumulation of ring opened over oxidation products. From this it could be concluded that selectivity is a function of conversion which in turn was a function of reaction time.[134] This showed the importance of reaction time on product yield and how increased reaction times can decrease selectivity due to over oxidation of the primary products. This study then compared the corresponding Pt and Pd catalysts under the same conditions and saw no significant variations in the conversions or selectivities. Hence here it was concluded that the metal was not in fact of great importance and that reaction time played a much greater role in product distribution.[134] On the contrary, Mayani *et al.* studied Au, Pd and AuPd catalyst anchored onto carbon composites for cyclohexane oxidation with $H_2O_2$ and discovered that there was a considerable difference in the yields produced by the different metals. Here two carbon cages of differing sizes were

used and it was found that the larger the internal pores of the channels the greater the yield of the oxidation reaction.[126]

Sadiq *et al.* used bimetallic SnPt catalysts supported onto reduced graphene oxide under aerobic oxidation conditions in a solvent free system.[135] The selectivity towards cyclohexanol and cyclohexanone were observed over a period of 12 hours. A large increase of selectivity was seen up to 3 hours, where after it gradually decreases. This indicated the presence and prevalence of over oxidation products at reaction times greater than 3 hours.[135]

Liu *et al.* have shown that Ag nanoparticles, supported on MgO, can also be effective oxidation catalysts with selectivity to KA oil of 97 % and conversion of 4.6 %.[136] They were studied in solvent less conditions with oxygen at 140 °C for 17 hours. The corresponding bimetallic AgPd/MgO catalysts were also investigated and shown to have a synergistic effect towards oxidation of cyclohexane. The bimetallic catalysts showed higher conversions (9.5 %) while still maintaining high selectivity (89 %). Within this study the preparation method was investigated by comparing catalysts made by sol immobilisation and wet impregnation. It was found that the monometallic 1% Ag/MgO catalysts synthesised via sol immobilisation (4.6% conversion) were more active compared to wet impregnation (2.6% conversion) believed to be due to small metallic Ag particles whereas with impregnation methods $Ag_2O$ particles were seen which were not as active.[136]

Gui *et al.* has reported that that the addition of propylene carbonate (PC) as a solvent increased the yield of KA oil using a 1% $Au/SiO_2$ catalyst prepared by sol gel method.[137] At 140 °C under 15 bar $O_2$ with additional TBHP initator the addition of 5 ml of the PC solvent produced an increase of twelve times, from 1.8 % to 21.9 % mol conversion of cyclohexane, compared to the solventless system. Dimethyl carbonate, diethyl carbonate, dipropyl carbonate, ethylene carbonate, 1,2-butylene carbonate and acetone were also studied for comparison and propyelene carbonate was found to be best. This was assigned to the PC high polarity which ensued from it's high dipole moment. This high polarity can enhance the decomposition of the CHHP intermiediate and hence increase KA oil yield. [137]

### 1.4.3.2 $H_2O_2$ oxidant.

Cyclohexane oxidation with $H_2O_2$ as the main oxidant has been widely reported in the literature.[91–96] With $H_2O_2$ as an oxidant an excess of oxidant to substrate is usually used, due to the thermal decomposition of $H_2O_2$, but under milder conditions, compared to $O_2$ alone, such as 70 °C for 8 hours[126] and even as low as room temperature and ambient pressures.[138]

Throughout the literature, a diverse range of supports have been employed. Titanium silicate-1, TS-1, has been well researched for several oxidation reactions.[139] TS-1 is a zeolitic material where some Si atoms have been substituted for Ti atoms. It has been shown to catalyse an assortment of oxidation reactions, several with $H_2O_2$.[139] TS-1 is believed to activate $H_2O_2$ by the formation of a reactive five coordinate, Ti(IV), Ti-OOH species and hence via this intermediate can oxidise reactants.[140] It has also been shown to be an effective catalyst, with $H_2O_2$, for cyclohexane oxidation with high selectivity to cyclohexanone.[141] Within the internal pores of the structure, cyclohexanol is selectively oxidised to cyclohexanone. However, on the exterior of the structure small amounts of cyclohexanone is further oxidised to over-oxidation, ring opened products, which can reduce the overall selectivity of the reaction.[142] Recently, Dai *et al*. produced a TS-1 W coupled catalyst, $H_2WO_4$/TS-1, which via a bi-functionality catalysed cyclohexane oxidation all the way through to adipic acid with $H_2O_2$. Cyclohexane was oxidised to cyclohexanone, directly and from oxidation of cyclohexanol, via the Ti-OOH sites. Cyclohexanone was then further oxidised to adipic acid via the W-OOH sites.[123]

Solvents have shown to influence the conversion of the oxidation reaction with $H_2O_2$ as the oxidant. Acidic solvents, such as acetic acid, have shown to enhance conversion due to stabilising the $H_2O_2$ and reducing its decomposition to water,[143] as previously mentioned.[65] In addition, methanol and acetone have also been explored as solvents however, under the same reaction conditions have not produced as high conversions or selectivities.[143,144]

More recent research into cyclohexane oxidation has focussed on different, non-noble metals as the base of the catalyst.[95,115,118,124,128,144–150] Antony *et al*. used +2 complexes of the transition metals Cu, Co and Ni anchored onto an amine functionalised $SiO_2$ support as a heterogeneous catalyst with $H_2O_2$ as the oxidant.[138] Here the reaction

conditions were investigated finding the optimum temperature of 70 °C and 8 hours reaction time. It was seen that conversion increased with increasing reaction time up to 8 hours, and here after plateaued. With these increased reaction times an increase in cyclohexanone selectivity was also seen.[138]

Martins *et al.* have investigated first-row transition metal silica coated $Fe_3O_4$ particles for the oxidation of cyclohexane in the presence of $H_2O_2$, at 2:1 ratio $H_2O_2$:cyclohexane.[130] Here the magnetic $Fe_3O_4$ particles are utilized as a magnetic, easily recoverable catalyst with the silica coating implemented to avoid the accumulation of the magnetic particles. The silica coating has then been modified in different ways using a variety of different metals; $Mn^{2+}$, $Co^{2+}$, $Cu^{2+}$and $Zn^{2+}$. It was proposed that the transition metal sites form hydroxy and hydroperoxyl radicals from $H_2O_2$ which can then proceed to initiate the oxidation reaction mechanism. Here the $Mn^{2+}$ and $Cu^{2+}$ modified catalysts showed the greatest activity when utilized at 80 ºC under microwave assisted heating (10W) and showed sustained catalytic activity over 5 runs.[130]

However, the direct use of $H_2O_2$ for oxidation transformations requires a high molar excess and the production of $H_2O_2$ is a highly energy intensive process requiring the hydrogenation and oxidation of anthraquinone which then requires the transportation of highly concentrated solutions of $H_2O_2$.[20,23] Due to this the proposal of producing smaller, more selective, amounts of $H_2O_2$ *in-situ* in an oxidation reaction is an obvious advantage.

In 2014 Santonastaso *et al.* investigated the addition of $H_2$ to the aerobic oxidation of benzyl alcohol to produce $H_2O_2$ *in-situ*.[151] Condition screening was also conducted which investigated several intermediate points between the ideal conditions for the direct synthesis of $H_2O_2$ and the oxidation reaction.[151] Though the reaction being investigated here is not within this part of the project there is some important experimental investigations for the use of *in-situ* $H_2O_2$ from which this project can take inspiration from.

#### 1.4.3.3 tert-Butyl hydroperoxide (TBHP) oxidant.

*tert*-butyl hydroperoxide, TBHP, is a powerful oxidising agent and hence lesser amounts are needed for the same oxidising ability. Although the oxidation reaction

produces the by-product *tert*-butanol which is a flammable chemical that will need to be disposed of accordingly.[20]

Wang *et al.* used an ionic liquid medium and a TS-1 catalyst to oxidise cyclohexane with both $H_2O_2$ and TBHP.[152] They showed that at 90 °C for the equivalent reaction time, 24 hours, TBHP increased the conversion from 0.18% to 13.0% compared to $H_2O_2$. This shows the potency of TBHP in the oxidation reaction and also led to lower reaction times to be explored with 6 % conversion being observed at 6 hours.[152]

#### 1.4.3.4 Conclusions.

As has been discussed here a wide range of reaction conditions and catalysts have been explored for the oxidation of cyclohexane, Table 1.4. High temperature and radical initiators are often utilised to initiate the radical mechanism. It has also been presented that the use of $H_2O_2$ as an oxidant, compared to $O_2$ alone, can reduce the reaction temperature but the use of large excesses of concentrated $H_2O_2$ is required.

***Table 1.4.*** *Notable cyclohexane oxidation catalytic activity and the conditions under which they were tested in the literature.*

| Catalyst | Conditions | Cyclohexane conversion / % | Selectivity to KA oil / % |
|---|---|---|---|
| 1% Au/MgO[114] | 140 °C, 17 hours, 3 bar $O_2$ | 1.9 | 81 |
| 0.5% Au 0.5% Pd/MgO[133] | 140 °C, 17 hours, 3 bar $O_2$ | 11.0 | 94 |
| 10 % Au/C[126] | 25 °C, 4 hours, $H_2O_2$ | 7.7 | 100 |

It has also been presented that the conditions for optimal $H_2O_2$ production is often lower reaction temperatures and the addition of acid or halide promoters. Hence the coupling of these two reactions conditions for both $H_2O_2$ and cyclohexane oxidation will be the first thing to be explored and the bridging of this conditions gap will provide the greatest challenge.

It is hypothesised that the use of $H_2O_2$ produced *in-situ* will facilitate the use of lower reaction temperatures, where $H_2O_2$ can enable the initiation of the reaction mechanism and avoid the use of hazardous concentrated $H_2O_2$ solution.

## 1.5 Oxidation of benzyl alcohol.

The oxidation of benzyl alcohol to produce benzaldehyde is an important organic transformation in the pharmaceutical, fragrances and agricultural industries.[153] It has

been widely explored within the literature due to its well defined reaction scheme and is often used as a model reaction for catalyst investigation.

### 1.5.1 Industrial process and its uses.

The oxidation of benzyl alcohol can produce a total of 5 different oxidation products, Scheme 1.8, of which most have industrial relavence.[154] Benzaldehyde is a sweet smelling molecule and hence has found uses in the flavours and fragrances industries, as well as being a feedstock for the pharmaceutical and agricultural industry. Benzoic acid and benzyl benzoate are also important feedstocks for industrial pharmaceutical and chemical transformations, especially in the plastic industry.[155,156] Benzoic acid and it's benzoate salts can also be used as food additives to prolong product shelf life.[157]

Industrially the production of benzaldehyde, and benzyl alcohol, are yielded from the aerobic oxidation of toluene in a temperature range of 170 - 220 °C under limited conversion of less than 10 %.[158]

### 1.5.2 Reaction scheme and by-products.

The primary oxidation of benzyl alcohol is the oxidative dehydrogenation of the alcohol functionality to the aldehyde, benzaldehyde. Benzaldehyde can be further oxidised to benzoic acid which can react with an unreacted molecule of benzyl alcohol to form benzyl benzoate. Toluene can also be formed as a by-product via the disproportionation of benzyl alcohol, here two moles of benzyl alcohol react to form one mole toluene and one mole benzaldehyde.[159–161] Often the distinction between benzaldehyde formed from the oxidation reaction and that formed from direct oxidation of benzyl alcohol is made.[162]

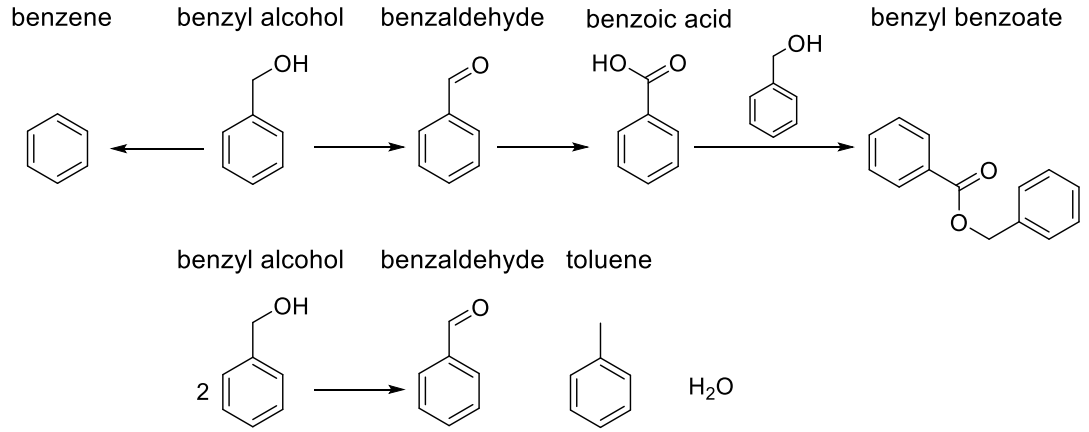


***Scheme 1.8.*** *A reaction scheme for the oxidation of benzyl alcohol.*

The further oxidation of benzaldehyde to benzoic acid is a facile oxidation which is known to occur spontaneously under ambient temperatures on exposure to air.[163] The oxidation of benzaldehyde has also been shown in the literature to oxidise under mild conditions using metal catalysts,[164–166] often the same as used in benzaldehyde oxidation, Au.[167–169] Despite the ease of over oxidation of benzaldehyde, to benzoic acid, the selectivity of benzyl alcohol oxidation is often high (>90 %)[55,153,169–172] indicating that the over oxidation of benzaldehyde is actually limited. Hence Sankar *et al.* investigated the addition of benzyl alcohol to benzaldehyde oxidation.[173] They observed that even at small amounts, 2%, benzyl alcohol could limit the oxidation of benzaldehyde with 10% of benzyl alcohol showing almost no benzoic acid formation. They attributed this inhibition due to benzyl alcohol interrupting the benzoylperoxy radical via H transfer[173], which is a key intermediate in benzaldehyde oxidation.[174]

### 1.5.3 Heterogeneous catalysis.

The production of benzaldehyde from the aerobic oxidation of benzyl alcohol has been extensively displayed in the literature. Typically conditions used consist of continuous pressure of $O_2$ of between 1 to 3 bar and temperatures up to 120 °C.[154,170]

#### 1.5.3.1 Pd catalysts

Monometallic catalysts of Pd have been extensively studied for the oxidation of benzyl alcohol with focus on the tuning of the selectivity of the catalyst.[175-187]

Previous investigations have studied the structure-activity relationship between the size of Pd nanoparticles.[175,176] Chen *et al.* investigated Pd/$SiO_2$-$Al_2O_3$ of varying particles sizes between 2.2 -10 nm for aerobic benzyl alcohol oxidation. From initial rates, particles in the range of 3.6 – 4.3 nm gave the greatest intrinsic TOF. With the most active catalysts showing a conversion of 97% with 98% selectivity towards benzaldehyde after a 10 hour reaction.[175] Li *et al.* investigated Pd supported on NaX zeolites with similar Pd nanoparticles sizes, 2 – 10.5 nm. Here particle sizes of 2.8 nm showed the greatest activity of 66 % conversion with still high selectivity of 97 % to benzaldehyde. This was closely followed by 2.9 nm sized particles at 63% conversion and 94% selectivity. These particles also showed the greatest initial rates with the highest intrinsic TOF.[176] Both these studies indicate that small Pd nanoparticles, below 5 nm, are optimum for the aerobic oxidation of benzyl alcohol.

Ferri *et al.* used a combination of site-selective blocking by CO and isotope labelling combined with *in-situ* attenuated total reflection infrared (ATR-IR) to investigate the active sites of Pd supported on $Al_2O_3$.[177] This showed that while the oxidative dehydrogenation of the benzyl alcohol took place on all facets the decarbonylation, to form benzene, occurred preferentially on the (111) facets. Building on this Pang *et al.*[178] and Campisi *et al.*[179] have shown that blocking the (111) facet by either CO adsorption[178] or by a PVA layer[179], formed in catalyst sol immobilisation, can increase the selectivity to benzaldehyde. Xiong and co-workers have investigated Pd facets and shown that $O_2$ activation is greater over (100) compared to (111). This greater activation of $O_2$ leads to a greater influx of reactive oxidation species and hence lead to greater oxidation ability.[180,181]

Investigations into the oxidation state of Pd in catalysts have recently indicated the importance of $Pd^0$-PdO interfaces as has been identified important for $H_2O_2$ synthesis as discussed earlier.[42] Meher and Rana produced stable $Pd^0$-PdO particles on a reduced graphene oxide surface to highlight that the interface of $Pd^0$-PdO particles was key to the aerobic catalytic oxidation.[182] Interfaces of $Pd^0$-PdO are believed to be stable and where the interfaces occur PdO can be reduced forming O vacancies on the catalyst which are more active for the adsorption and hence activation of $O_2$.[183,184] This could explain the increased activities of $Pd^0$-PdO interfaces that have been observed.

However it should be noted that several studies also report Pd catalysts with high metallic $Pd^0$ content.[179,185–187] Though some of these attribute the activity to reduced metallic Pd for all catalysts a small amount of $Pd^{2+}$ is still present and hence it cannot be attributed to one oxidation state alone. Shinde *et al.* noted although fresh catalysts contained predominately metallic Pd upon use in the aerobic oxidation of benzyl alcohol surface $Pd^0$ was oxidised to $Pd^{2+}$. This used catalyst showed similar catalytic activity compared to the fresh and hence it was concluded that the oxidation state alone does not determine activity.[186]

#### 1.5.3.2 AuPd catalysts.

The synergistic effect of Au and Pd has previously been discussed for the direct synthesis of $H_2O_2$[49,51,56,90] but similar catalytic enhancements have also been observed for the aerobic oxidation of benzyl alcohol.[55,188–193]

Enache *et al.* investigated the aerobic oxidation of several alcohols using Pd, Au and AuPd catalysts supported on several supports; $Al_2O_3$, $TiO_2$, $Fe_2O_3$, $SiO_2$ and C.[55] For benzyl alcohol oxidation, $TiO_2$ supported catalysts showed after 30 minutes of reaction that Pd catalysts displayed a greater conversion than the bimetallic AuPd, Table 1.5. However, the bimetallic catalyst showed close to double the selectivity towards benzaldehyde. After 8 hours of reaction the AuPd catalyst converted greater benzyl alcohol than Pd and still at greater than 90% selectivity to benzaldehyde. This showed that AuPd could maintain much higher selectivity than Pd and could show greater activity at extended reaction times possibly also showing the greater stability of the bimetallic catalyst. Monometallic Au catalyst showed a much lower activity at both reaction times.[55]

***Table 1.5.*** *Comparative data for benzyl alcohol oxidation 0.5 hour and 8 hours of reaction. Reaction conditions; 373 K, 0.2 MPa $O_2$, and 1500 RPM stirrer speed.*[55]

| **Catalyst** | **Benzyl alcohol Conversion / %** | | **Benzaldehyde Selectivity / %** | |
|---|---|---|---|---|
| | **0.5 hours** | **8 hours** | **0.5 hours** | **8 hours** |
| 2.5% $Au/TiO_2$ | 0.6 | 15.3 | 96.7 | 63.9 |
| 2.5% $Pd/TiO_2$ | 13.4 | 60.1 | 51.3 | 54.4 |
| 2.5% Au 2.5% $Pd/TiO_2$ | 3.7 | 74.5 | 95.2 | 91.6 |

Prati *et al.* have conducted several investigations into bimetallic AuPd catalysts for aerobic oxidation of benzyl alcohol.[188–192] They original investigated monometallic Au, Pd and Pt and bimetallic AuPd and AuPt supported on C.[190] Positive synergistic effects were observed for 0.73% Au 0.27% Pd/C (96 % conversion in $H_2O$) over the monometallic catalysts (0% for 1% Au/C and 18 % for 1% Pd/C) in both water and toluene solvent, with greater conversion observed in water (96 %) compared to toluene (32 %). The bimetallic catalyst consisted of real alloy particles with the alloying of Au increasing interatomic distances indicating an electronic enhancement of the catalyst. The addition of Au to Pd decreased the $O_2$ coverage of the catalyst which decreases the deactivation and hence has increased catalyst stability. On the contrary, alloying of Au and Pt showed a decrease in activity compared to the monometallic catalysts.[190]

Investigations have shown that high Au:Pd ratios which result in Au core Pd shell nanoparticles are highly active catalysts for the selective oxidation of benzyl alcohol.[55,168,189,195,196] Interestingly, changing Au:Pd has not had a substantial effect on the selectivity of the catalysts, but with increasing Au content an increase in

conversion is observed, with Wang *et al.* observing an optimum Au:Pd ratio of 9:1 and Silva *et al.* 10:1.[189,195] Using density functional theory Silva *et al.* concluded that with low Pd content the adsorption of benzyl alcohol was limited and at concentrations higher than 10% Pd although adsorption was favoured the desorption of benzaldehyde was then limited.[189]

#### 1.5.3.3 Oxidation via the *in-situ* utilisation of $H_2O_2$.

In 2014 Santonastaso *et al.* investigated the addition of $H_2$ to the aerobic oxidation of benzyl alcohol to produce $H_2O_2$ *in-situ*.[151] They investigated different reaction conditions to couple the production of $H_2O_2$ which is performed at sub-ambient temperatures, to limit the production of $H_2O$, and the high temperature oxidation of benzyl alcohol. The oxidation of benzyl alcohol is believed to proceed via a radical process involving a hydroperoxy intermediate where normally high temperatures are utilised to produce these intermediates and hence this work focussed on using mixtures of $H_2$ and $O_2$ to produce these radicals *in-situ*. It was believed that the 2.5% Au 2.5% Pd/$TiO_2$ catalyst used generated $H_2O_2$ and its hydroperoxy intermediate, which was believed to aid the oxidation of benzyl alcohol at lower temperatures and result in higher selectivity to benzaldehyde.[151]

Different reaction parameters were investigated for this study. The temperature was varied from 2 ºC, to 25 ºC to 50 ºC. With increasing temperature increasing activity was observed, with very limited activity of 0.4 % conversion at 2 ºC, however this was coupled with a decrease in benzaldehyde selectivity from 85 % to 70 %, Figure 1.13. This was attributed to both the increased stability of $H_2O_2$ at low temperatures as well as the repression of the oxidation reactions.[151] This provides a great example of the problems trying to bridge the conditions gap between $H_2O_2$ synthesis and oxidation reactions as discussed previously.

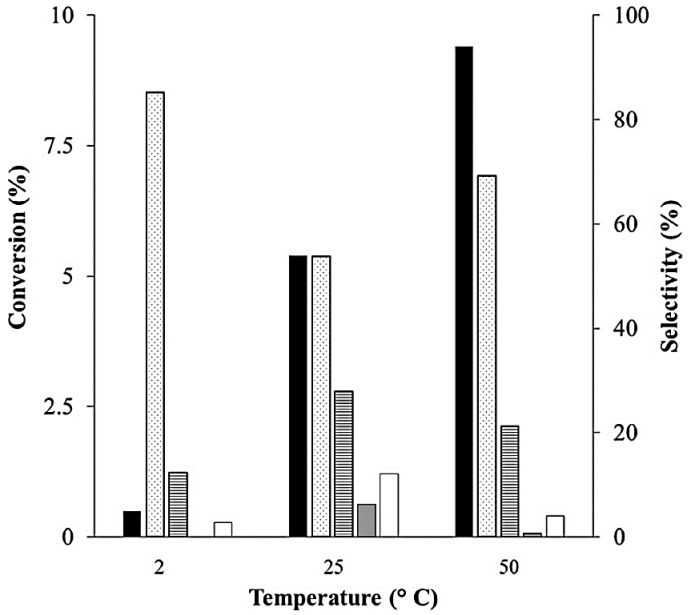


***Figure 1.13.*** *Conversion of benzyl alcohol and selectivity towards the major product during the oxidation of benzyl alcohol using in-situ generated $H_2O_2$ at different temperatures. Conversion: black bars. Selectivity: benzaldehyde, spotted bars; toluene, striped bars; benzyl benzoate, grey bars; and benzoic acid, white bars.*[151] *"Reprinted with permission from M. Santonastaso et al. Org. Process Res. Dev., 2014, 18, 1455–1460. Copyright 2014 American Chemical Society."*

Time-on-line studies were also conducted using 2.5% Au 2.5% Pd/$TiO_2$ with varying reaction times from 5 to 45 minutes, Figure 1.14. This showed a much greater initial reaction rate with the conversion of benzyl alcohol plateauing at 5.9 % after 30 minutes. Selectivity to benzaldehyde was maintained at 90 % at all reaction times. This indicated some deactivation of the catalyst throughout the reaction and re-use of the catalyst confirmed this with the re-use of the catalyst providing only half of the original activity. [151]

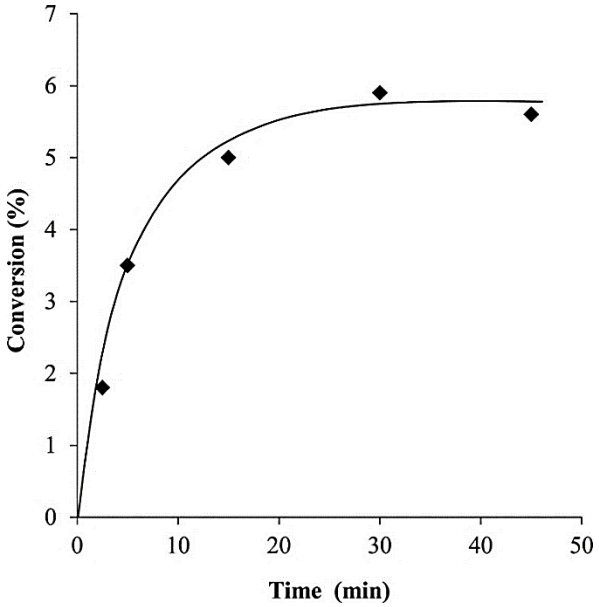


***Figure 1.14****. Oxidation of benzyl alcohol at varying reaction times. "Reprinted with permission from M. Santonastaso et al. Org. Process Res. Dev., 2014, 18, 1455–1460. Copyright 2014 American Chemical Society."*

A comparison of supports was also conducted looking at AuPd supported on MgO, $TiO_2$ and $CeO_2$. These catalysts supports are all known to provide high activity in aerobic oxidations, with the basic MgO leading to higher selectivity to benzaldehyde by reduction of toluene formation.[161] By changing the support from MgO to $TiO_2$ to $CeO_2$ an increase in benzyl alcohol conversion was observed from 1.8 % to 5.9 % to 8.6 % respectively.[151] This has shown that the support can have a significant effect on the oxidation activity and is in agreement with trends observed for $H_2O_2$, with more acidic supports providing greater activity due to the stabilisation of $H_2O_2$.[34,58] This indicated that under these conditions the selectivity of the catalyst towards $H_2O_2$ can affect the oxidation of benzyl alcohol.

Moreno *et al.* also investigated 2.5% Au 2.5% Pd catalyst this time supported on TS-1 for the oxidation of benzyl alcohol via the *in-situ* production of $H_2O_2$.[197] They prepared these catalyst both by wet impregnation and deposition precipitation methods and with varying amounts of silanization agent during the preparation of TS-1. All catalysts were tested for the *in-situ* oxidation at 2 °C and 30 °C with all catalysts showing very limited conversion, <1 %, at the lower temperature. The best catalyst showed a conversion of 7 % with selectivity to benzaldehyde of 92.6 % at 30 °C with both $H_2$ and $O_2$. This same catalyst showed 1.8 % conversion with only 69.1 % selectivity to benzaldehyde under the same conditions but with only $O_2$ present.[197] Again, this study has shown the importance of $H_2$ under mild conditions under which aerobic oxidation is limited.

#### 1.5.3.4 Conclusions.

In conclusion, high conversions of benzyl alcohol have been observed with AuPd catalysts using $O_2$ predominately as the oxidant, Table 1.6. Selectivity towards benzaldehyde are high and efforts have been made to reduce the disproportionation of benzyl alcohol to form an equimolar mixture of toluene and benzaldehyde. High selectivity to benzaldehyde have been observed with limited further oxidation to benzoic acid and Sankar *et al.* have demonstrated that this is due to benzyl alcohol inhibiting benzaldehyde oxidation.[173]

***Table 1.6.*** *Notable benzyl alcohol oxidation catalytic activity and the conditions under which they were tested in the literature.*

| Catalyst | Conditions | Benzyl alcohol conversion / % | Benzaldehyde selectivity / % |
|---|---|---|---|
| 2.5% Au 2.5% $Pd/TiO_2$[55] | 120 °C, 3 bar $O_2$, solvent free. | 74.5 | 91.6 |
| 2.5% Au 2.5% Pd $/TiO_2$[151] | 50 °C, $O_2$ and $H_2$, methanol | 5.9 | 90 |
| 2.5% Au 2.5% Pd /TS-1[197] | 30 °C, $O_2$ and $H_2$, water/methanol | 7.0 | 92.6 |

## 1.6 Fenton's Chemistry.

Fenton first discovered that tartaric acid could be oxidised by $H_2O_2$ in the presence of iron salts in 1894.[198] Since then iron systems have been used to produce $^{\bullet}OH$ radicals for a variety of advanced oxidation procedures mainly for the treatment of waste streams from paper bleaching, agriculture and industrial wastewater to name a few.[199,200]

Fenton's reagents consist of $Fe^{2+}$ which can react with $H_2O_2$ to form radicals in the sequences labelled equations 1.2 – 1.5. This also produces $Fe^{3+}$ which can also react to form radicals as shown in equations 1.6 – 1.7.[201,202]

$$Fe^{2+} + H_2O_2 \rightarrow Fe^{3+} + OH^{\bullet} + OH^{-} \quad \textit{Equation 1.2}$$

$$OH^{\bullet} + H_2O_2 \rightarrow H_2O + OOH^{\bullet} \quad \textit{Equation 1.3}$$

$$OOH^{\bullet} + H_2O_2 \rightarrow O_2 + H_2O + OH^{\bullet} \quad \textit{Equation 1.4}$$

$$Fe^{2+} + OH^{\bullet} \rightarrow Fe^{3+} + OH^{-} \quad \textit{Equation 1.5}$$

$$Fe^{3+} + H_2O_2 \rightarrow Fe^{2+} + OOH^{\bullet} + H^{+} \quad \textit{Equation 1.6}$$

$$Fe^{3+} + OOH^{\bullet} \rightarrow Fe^{2+} + H_2O^{+} \quad \textit{Equation 1.7}$$

Most Fenton's reagents are based on soluble ferrous salts which release $Fe^{2+}$ into the solutions for advanced oxidation processes.[199,200,203] However research has included immobilising $Fe^{2+}$ onto supports to limit the need to remove the metal from solution and for easy re-usability of the reagents.[199,200,204–209] Supports can be impregnated with $Fe^{2+}$ or zeolites have been exchanged with $Fe^{2+}$ and can act as efficient Fenton's catalysts, however these require the addition of large excesses of $H_2O_2$.[207,210–212] Hence investigations have also explored the use of bifunctional catalysts which can both produce $H_2O_2$ and form radicals via a Fenton's process.[204,205,208,209,213,214]

Underhill *et al.*[204] and Triki *et al.*[205] have both investigated PdFe catalysts supported on $TiO_2$ for the degradation of phenol via the *in-situ* production of $H_2O_2$. Underhill *et*

*al.* used diluted mixtures of $H_2$ and $O_2$ to produce $H_2O_2$ at 30 °C. This led to 78% conversion of phenol after 120 minutes, however it was discovered that substantial leaching of Fe from the catalyst was observed which had contributed to the catalytic degradation. They also observed that greater conversion of phenol was observed with *in-situ* $H_2O_2$ compared to *ex-situ* addition of $H_2O_2$.[204] Triki *et al.* used formic acid and $O_2$ to form $H_2O_2$ *in-situ* where the optimum catalyst provided 91% conversion over 6 hours at 25 °C. They investigated different loadings and ratios of Pd and Fe and found that 5% Pd 5% Fe/$TiO_2$ gave the greatest conversion. The lower loaded Pd catalysts produced greater amounts of $H_2O_2$ but did not show the greatest phenol degradation. This showed the importance of having a close interaction between the Pd and iron oxide species.[205]

In the literature Fe based heterogeneous Fenton's catalysts have been used to degrade and oxidise a variety of compounds such as antibiotics and drugs from waste pharmaceutical streams[215,216] as well as coloured pigments and dyes from textile waste water streams.[217,218] This shows the versatility of Fenton's reagents for chemical transformations.

## 1.7 Project aims and objectives.

This project planned to develop a novel catalyst which can produce, and use, *in-situ* $H_2O_2$ to oxidise cyclohexane and benzyl alcohol, working towards a catalyst which can produce high selectivities while working at higher conversions. Along with this, the project aimed for reactions to be carried out at lower temperatures than the currently used industrially and without the use of additional initiators.

An extensive screening of reaction conditions for the oxidation of cyclohexane will be carried out to provide a standard reaction protocol for which catalyst design will be tested against. The comparison between the autoxidation reaction, with no added catalyst, and the catalysed reaction will be looked at. It will be observed where the catalyst can enhance the oxidation reaction and how the selectivities and conversion can be changed at a variety of temperatures.

Catalyst design will include screening and development of different catalysts to see which can produce highest selectivities at high conversions. This will include exploring different metals including different combinations of bimetallic catalysts for

both the oxidation of cyclohexane and benzyl alcohol via the *in-situ* production of $H_2O_2$.

## 1.8 References.


1. M. Bowker, *The Basis and Applications of Heterogeneous Catalysis*, Oxford University Press, Incorporated, 1998.
2. K. Kakaei, M. D. Esrafili and A. Ehsani, *Interface Science and Technology*, Elsevier, 2019, pp. 1–21.
3. W. Ostwald, *Z Phys Chem*, 1894, **15**, 705–706.
4. The Nobel Prize in Chemistry 1909, https://www.nobelprize.org/prizes/chemistry/1909/ostwald/lecture/, (accessed February 6, 2020).
5. P. Serp and K. Philippot, *Nanomaterials in Catalysis*, John Wiley & Sons, 2012.
6. P. Anastas and N. Eghbali, *Chem. Soc. Rev.*, 2009, **39**, 301–312.
7. S. Bommarius and B. R. Riebel, *Biocatalysis*, Wiley-VCH Verlag GmbH & CoKGaA, Weinheim, FRG, 2005.
8. G. W. Parshall and S. D. Ittel, *Homogeneous catalysis*, Wiley, 1992.
9. P. W. N. M. van Leeuwen, *Homogeneous Catalysis: Understanding the Art*, Springer Science & Business Media, 2006.
10. G. C. Bond, *Heterogeneous Catalysis: Principles And Applications*, Oxford University Press, 2nd edn., 1987.
11. Chorkendorff and J. W. Niemantsverdriet, *Concepts of Modern Catalysis and Kinetics*, John Wiley & Sons, 2017.
12. R. J. Baxter and P. Hu, *J. Chem. Phys.*, 2002, **116**, 4379–4381.
13. W. H. Weinberg, *Acc. Chem. Res.*, 1996, **29**, 479–487.
14. C. Doornkamp and V. Ponec, *J. Mol. Catal. Chem.*, 2000, **162**, 19–32.
15. Z. Moshfegh, *J. Phys. Appl. Phys.*, 2009, **42**, 233001.
16. C.-J. Jia and F. Schüth, *Phys. Chem. Chem. Phys.*, 2011, **13**, 2457–2487.
17. L. J. Thenard, *Ann. Chim. Phys.*, 1818, **8**, 306–312.
18. C. W. Jones, *Applications of Hydrogen Peroxide and Derivatives*, Royal Society of Chemistry, 2007.
19. Y. Yi, L. Wang, G. Li and H. Guo, *Catal. Sci. Technol.*, 2016, **6**, 1593–1610.
20. C. Samanta, *Appl. Catal. Gen.*, 2008, **350**, 133–149.
21. H-J. Riedl and G. Pfieiderer, US2158525, 1939.
22. F. F. Desmedt, Y. Vlasselaer and P Miquel, US20150336796, 2013.
23. F. Moseley and P. N. Dyer, US4336240 A, 1982.
24. C. H. Bartholomew, *Appl. Catal. Gen.*, 2001, **212**, 17–60.
25. Otsuka and I. Yamanaka, *Electrochimica Acta*, 1990, **35**, 319–322.
26. P. Landon, P. J. Collier, A. J. Papworth, C. J. Kiely and G. J. Hutchings, *Chem. Commun.*, 2002, 2058–2059.
27. D. Hâncu and E. J. Beckman, *Green Chem.*, 2001, **003**, 80–86.
28. Z. Jianli, Z. Juncheng, S. Ji, G. Hongchen, W. Xiangsheng and G. Weimin, *Plasma Sci. Technol.*, 2009, **11**, 181.
29. R. J. Lewis and G. J. Hutchings, *ChemCatChem*, 2019, **11**, 298–308.
30. H. Henkel and W. Weber, US1108752A, 1914.
31. S. Chinta and J. H. Lunsford, *J. Catal.*, 2004, **225**, 249–255.
32. Y.-F. Han and J. H. Lunsford, *J. Catal.*, 2005, **230**, 313–316.

33. D. P. Dissanayake and J. H. Lunsford, *J. Catal.*, 2003, **214**, 113–120.
34. K. Edwards, B. Solsona, E. N. N, A. F. Carley, A. A. Herzing, C. J. Kiely and G. J. Hutchings, *Science*, 2009, **323**, 1037–1041.
35. D. W. Flaherty, *ACS Catal.*, 2018, **8**, 1520–1527.
36. N. M. Wilson and D. W. Flaherty, *J. Am. Chem. Soc.*, 2016, **138**, 574–586.
37. N. M. Wilson, P. Priyadarshini, S. Kunz and D. W. Flaherty, *J. Catal.*, 2018, **357**, 163–175.
38. F. Wang, C. Xia, S. P. de Visser and Y. Wang, *J. Am. Chem. Soc.*, 2019, **141**, 901–910.
39. R. Burch and P. R. Ellis, *Appl. Catal. B Environ.*, 2003, **42**, 203–211.
40. V. R. Choudhary, C. Samanta and T. V. Choudhary, *Appl. Catal. Gen.*, 2006, **308**, 128–133.
41. Q. Liu, K. K. Gath, J. C. Bauer, R. E. Schaak and J. H. Lunsford, *Catal. Lett.*, 2009, **132**, 342.
42. Ouyang, P. Tian, G. Da, X.-C. Xu, C. Ao, T. Chen, R. Si, J. Xu and Y.-F. Han, *J. Catal.*, 2015, **321**, 70–80.
43. D. H. Wells, W. N. Delgass and K. T. Thomson, *J. Catal.*, 2004, **225**, 69–77.
44. Okumura, Y. Kitagawa, K. Yamagcuhi, T. Akita, S. Tsubota and M. Haruta, *Chem. Lett.*, 2003, **32**, 822–823.
45. J. K. Edwards, A. F. Carley, A. A. Herzing, C. J. Kiely and G. J. Hutchings, *Faraday Discuss.*, 2008, **138**, 225–239.
46. Y. Nomura, T. Ishihara, Y. Hata, K. Kitawaki, K. Kaneko and H. Matsumoto, *ChemSusChem*, 2008, **1**, 619–621.
47. J. Li, A. Staykov, T. Ishihara and K. Yoshizawa, *J. Phys. Chem. C*, 2011, **115**, 7392–7398.
48. J. Li, T. Ishihara and K. Yoshizawa, *J. Phys. Chem. C*, 2011, **115**, 25359–25367.
49. Chen, D. Kumar, C.-W. Yi and D. W. Goodman, *Science*, 2005, **310**, 291–293.
50. D. Gudarzi, W. Ratchananusorn, I. Turunen, M. Heinonen and T. Salmi, *Catal. Today*, 2015, **248**, 58–68.
51. J. K. Edwards, E. Ntainjua N, A. F. Carley, A. A. Herzing, C. J. Kiely and G. J. Hutchings, *Angew. Chem. Int. Ed.*, 2009, **48**, 8512–8515.
52. S. Han and C. B. Mullins, *ACS Catal.*, 2018, **8**, 3641–3649.
53. P.A.P. Nascente, S. G. C. de Castro, R. Landers and G. G. Kleiman, *Phys. Rev. B*, 1991, **43**, 4659–4666.
54. Y.F. Han, Z. Zhong, K. Ramesh, F. Chen, L. Chen, T. White, Q. Tay, S. N. Yaakub and Z. Wang, *J. Phys. Chem. C*, 2007, **111**, 8410–8413.
55. D. I. Enache, J. K. Edwards, P. Landon, B. Solsona-Espriu, A. F. Carley, A. A. Herzing, M. Watanabe, C. J. Kiely, D. W. Knight and G. J. Hutchings, *Science*, 2006, **311**, 362–365.
56. J. K. Edwards and G. J. Hutchings, *Angew. Chem. Int. Ed.*, 2008, **47**, 9192–9198.
57. J. K. Edwards, A. Thomas, A. F. Carley, A. A. Herzing, C. J. Kiely and G. J. Hutchings, *Green Chem.*, 2008, **10**, 388–394.
58. E. Ntainjua, J. K. Edwards, A. F. Carley, J. A. Lopez-Sanchez, J. A. Moulijn, A. A. Herzing, C. J. Kiely and G. J. Hutchings, *Green Chem.*, 2008, **10**, 1162–1169.
59. G. Li, J. Edwards, A. F. Carley and G. J. Hutchings, *Catal. Today*, 2007, **122**, 361–364.

60. L. Torrente-Murciano, Q. He, G. J. Hutchings, C. J. Kiely and D. Chadwick, *ChemCatChem*, 2014, **6**, 2531–2534.
61. J. K. Edwards, S. F. Parker, J. Pritchard, M. Piccinini, S. J. Freakley, Q. He, A. F. Carley, C. J. Kiely and G. J. Hutchings, *Catal. Sci. Technol.*, 2013, **3**, 812–818.
62. J. K. Edwards, J. Pritchard, M. Piccinini, G. Shaw, Q. He, A. F. Carley, C. J. Kiely and G. J. Hutchings, *J. Catal.*, 2012, **292**, 227–238.
63. E. N. Ntainjua, M. Piccinini, S. J. Freakley, J. C. Pritchard, J. K. Edwards, A. F. Carley and G. J. Hutchings, *Green Chem.*, 2012, **14**, 170–181.
64. E. N. Ntainjua, M. Piccinini, J. C. Pritchard, J. K. Edwards, A. F. Carley, C. J. Kiely and G. J. Hutchings, *Catal. Today*, 2011, **178**, 47–50.
65. E. Ntainjua N., M. Piccinini, J. C. Pritchard, J. K. Edwards, A. F. Carley, J. A. Moulijn and G. J. Hutchings, *ChemSusChem*, 2009, **2**, 575–580.
66. T. A. Pospelova and N. I. Kobozev, *Russ. J. Phys. Chem.*, 1961, **35**, 584–587.
67. V. R. Choudhary, C. Samanta and P. Jana, *Appl. Catal. Gen.*, 2007, **317**, 234–243.
68. S. Abate, G. Centi, S. Melada, S. Perathoner, F. Pinna and G. Strukul, *Catal. Today*, 2005, **104**, 323–328.
69. V. R. Choudhary and C. Samanta, *J. Catal.*, 2006, **238**, 28–38.
70. V. R. Choudhary and P. Jana, *Catal. Commun.*, 2008, **9**, 2371–2375.
71. G . Blanco-Brieva, M. Montiel, F. Desmedt, P. Miquel, J. M. Campos-Martin and J. L. G. Fierro, *RSC Adv.*, 2016, **6**, 99291-99296.
72. E. Ntainjua N., M. Piccinini, J. C. Pritchard, Q. He, J. K. Edwards, A. F. Carley, J. A. Moulijn, C. J. Kiely and G. J. Hutchings, *ChemCatChem*, 2009, **1**, 479–484.
73. C. Samanta and V. R. Choudhary, *Appl. Catal. Gen.*, 2007, **330**, 23–32.
74. T. Deguchi and M. Iwamoto, *J. Phys. Chem. C*, 2013, **117**, 18540–18548.
75. S. T. Marshall and J. W. Medlin, *Surf. Sci. Rep.*, 2011, **66**, 173–184.
76. S. J. Freakley, Q. He, J. H. Harrhy, L. Lu, D. A. Crole, D. J. Morgan, E. N. Ntainjua, J. K. Edwards, A. F. Carley, A. Y. Borisevich, C. J. Kiely and G. J. Hutchings, *Science*, 2016, **351**, 965–968.
77. J. Xu, L. Ouyang, G.-J. Da, Q.-Q. Song, X.-J. Yang and Y.-F. Han, *J. Catal.*, 2012, **285**, 74–82.
78. J. K. Edwards, J. Pritchard, P. J. Miedziak, M. Piccinini, A. F. Carley, Q. He, C. J. Kiely and G. J. Hutchings, *Catal. Sci. Technol.*, 2014, **4**, 3244–3250.
79. E. N. Ntainjua, S. J. Freakley and G. J. Hutchings, *Top. Catal.*, 2012, **55**, 718–722.
80. Q. Liu, J. C. Bauer, R. E. Schaak and J. H. Lunsford, *Angew. Chem. Int. Ed Engl.*, 2008, **47**, 6221–6224.
81. Tian, L. Ouyang, X. Xu, C. Ao, X. Xu, R. Si, X. Shen, M. Lin, J. Xu and Y.-F. Han, *J. Catal.*, 2017, **349**, 30–40.
82. S. Kim, D.-W. Lee, K.-Y. Lee and E. A. Cho, *Catal. Lett.*, 2014, **144**, 905–911.
83. D. A. Crole, S. J. Freakley, J. K. Edwards and G. J. Hutchings, *Proc R Soc A*, 2016, **472**, 20160156.
84. S. Wang, R. J. Lewis, D. E. Doronkin, D. J. Morgan, J.-D. Grunwaldt, G. J. Hutchings and S. Behrens, *Catal. Sci. Technol.*, 2020, **10**, 1925 -1932.
85. J. Gu, S. Wang, Z. He, Y. Han and J. Zhang, *Catal. Sci. Technol.*, 2016, **6**, 809–817.

86. D. Ding, X. Xu, P. Tian, X. Liu, J. Xu and Y.-F. Han, *Chin. J. Catal.*, 2018, **39**, 673–681.
87. Tian, X. Xu, C. Ao, D. Ding, W. Li, R. Si, W. Tu, J. Xu and Y.-F. Han, *ChemSusChem*, 2017, **10**, 3342–3346.
88. S. Wang, K. Gao, W. Li and J. Zhang, *Appl. Catal. Gen.*, 2017, **531**, 89–95.
89. Y.-H. Cho, G.-H. Han, S. S. Han, M. Seo and K.-Y. Lee, *Mol. Catal.*, 2019, 110732.
90. Santos, R. J. Lewis, G. Malta, A. G. R. Howe, D. J. Morgan, E. Hampton, P. Gaskin and G. J. Hutchings, *Ind. Eng. Chem. Res.*, 2019, **58**, 12623–12631.
91. M. R. Toosi, M. H. Peyrovi, S. Hejazian, V. Abbaspour and V. Amani, *React. Kinet. Mech. Catal.*, 2013, **111**, 569–576.
92. M. M. Vinogradov, Y. N. Kozlov, A. N. Bilyachenko, D. S. Nesterov, L. S. Shul'pina, Y. V. Zubavichus, A. J. L. Pombeiro, M. M. Levitsky, A. I. Yalymov and G. B. Shul'pin, *New J Chem*, 2015, **39**, 187–199.
93. Raja and P. Ratnasamy, *Catal. Lett.*, 1997, **48**, 1–10.
94. M. Rezaei, A. Najafi Chermahini and H. A. Dabbagh, *Chem. Eng. J.*, 2017, **314**, 515–525.
95. T. F. S. Silva, A. J. Silvestre, B. G. M. Rocha, M. R. Nunes, O. C. Monteiro and L. M. D. R. S. Martins, *Catal. Commun.*, 2017, **96**, 19–22.
96. X. Lyu, H. Mao, K. Zhu, Y. Kong and M. Kobayashi, *Microporous Mesoporous Mater.*, 2017, **252**, 1–9.
97. M. P. Chaudhari and S. B. Sawant, *Chem. Eng. J.*, 2005, **106**, 111–118.
98. N. Jiang and A. J. Ragauskas, *Tetrahedron Lett.*, 2005, **46**, 3323–3326.
99. S. Tareq, M. I. Saiman, T.-Y. Y. Hin, A. H. Abdullah and U. Rashid, *Bull. Chem. React. Eng. Catal.*, 2018, **13**, 373–385.
100. V. Berezin, E. T. Denisov and N. M. Emanuel, *The Oxidation of Cyclohexane*, Pergamon Press, 1966.
101. F. Cavani and S. Alini, in *Sustainable Industrial Chemistry*, eds. F. Cavani, G. Centi, S. Perathoner and F. Trifiró, Wiley-VCH Verlag GmbH & Co. KGaA, 2009, pp. 367–425.
102. D. J. Loder, US2223494, 1940.
103. K. J. Balkus and A. G. Gabrielov, US005830429A, 1998.
104. P. Beatty, US8541057, 2013.
105. K. Qu, J. He, W. Jiang, M. Lin, Y. Yang, X. Shu and X. Wang, CN102757303 (A), 2012.
106. K. Whiston, L. Xi and G. Hutchings, WO2013114330 (A1), 2013.
107. Saleh, M. Adalla and K. Khairou, WO2016116776 (A1), 2016.
108. X. Liu, H. Wang, L. Song, K. Qiao and L. Wang, CN109248699 (A), 2019.
109. H. L. Cates, J. O. Punderson and R. W. Wheatcroft, US2851496, 1958.
110. C. E. Carraher, *J. Chem. Educ.*, 1978, **55**, 51.
111. H. Ichihashi and H. Sato, *Appl. Catal. Gen.*, 2001, **221**, 359–366.
112. R. and M. ltd, Polyamides (Nylon 6, Nylon 6.6) 2020 Global Market Review and Forecast to 2029, https://www.researchandmarkets.com/reports/4995073/polyamides-nylon-6-nylon-6-6-2020-global, (accessed April 21, 2020).
113. W. Partenheimer, *Catal. Today*, 1995, **23**, 69–158.
114. M. Conte, X. Liu, D. M. Murphy, K. Whiston and G. J. Hutchings, *Phys. Chem. Chem. Phys.*, 2012, **14**, 16279–16285.
115. M. Conte, X. Liu, D. M. Murphy, S. H. Taylor, K. Whiston and G. J. Hutchings, *Catal. Lett.*, 2015, **146**, 126–135.

116. Hermans, J. Peeters and P. A. Jacobs, *J. Phys. Chem. A*, 2008, **112**, 1747–1753.
117. G. J. Hutchings, S. Carrettin, P. Landon, J. K. Edwards, D. Enache, D. W. Knight, Y.-J. Xu and A. F. Carley, *Top. Catal.*, **38**, 223–230.
118. W. Yao, Y. Chen, L. Min, H. Fang, Z. Yan, H. Wang and J. Wang, *J. Mol. Catal. Chem.*, 2006, **246**, 162–166.
119. A. Alshaheri, M. I. M. Tahir, M. B. A. Rahman, T. B. S. A. Ravoof and T. A. Saleh, *Chem. Eng. J.*, 2017, **327**, 423–430.
120. G. S. Mishra, T. F. S. Silva, L. M. D. R. S. Martins and A. J. L. Pombeiro, *Pure Appl. Chem.*, 2009, **81**, 1217–1227.
121. F. Vailati, R. D. Huelsmann, E. Martendal, A. J. Bortoluzzi, F. R. Xavier and R. A. Peralta, *New J. Chem.*, 2020, **44**, 2514–2526.
122. P. C. Hereijgers and B. M. Weckhuysen, *J. Catal.*, 2010, **270**, 16–25.
123. J. Dai, W. Zhong, W. Yi, M. Liu, L. Mao, Q. Xu and D. Yin, *Appl. Catal. B Environ.*, 2016, **192**, 325–341.
124. Denicourt-Nowicki, A. Lebedeva, C. Bellini and A. Roucoux, *ChemCatChem*, 2016, **8**, 357–362.
125. Van-Dúnem, A. P. Carvalho, L. M. D. R. S. Martins and A. Martins, *ChemCatChem*, 2018, **10**, 4058–4066.
126. J. Mayani, S. V. Mayani and S. W. Kim, *Chem. Eng. Commun.*, 2016, **203**, 539–547.
127. S. Klein, S. Thorimbert and W. F. Maier, *J. Catal.*, 1996, **163**, 476–488.
128. B. Sarkar, P. Prajapati, R. Tiwari, R. Tiwari, S. Ghosh, S. S. Acharyya, C. Pendem, R. K. Singha, L. N. S. Konathala, J. Kumar, T. Sasaki and R. Bal, *Green Chem.*, 2012, **14**, 2600–2606.
129. P. Unnarkat, T. Sridhar, H. Wang, S. M. Mahajani and A. K. Suresh, *Catal. Today*, 2018, **310**, 116-129.
130. N. M. R. Martins, A. J. L. Pombeiro and L. M. D. R. S. Martins, *Catal. Commun.*, 2019, **125**, 15–20.
131. N. Pal, M. Pramanik, A. Bhaumik and M. Ali, *J. Mol. Catal. Chem.*, 2014, **392**, 299–307.
132. S. Yasyerli, G. Dogu and T. Dogu, *Catal. Today*, 2006, **117**, 271–278.
133. Liu, M. Conte, M. Sankar, Q. He, D. M. Murphy, D. Morgan, R. L. Jenkins, D. Knight, K. Whiston, C. J. Kiely and G. J. Hutchings, *Appl. Catal. Gen.*, 2015, **504**, 373–380.
134. Y.J. Xu, P. Landon, D. Enache, A. F. Carley, M. W. Roberts and G. J. Hutchings, *Catal. Lett.*, **101**, 175–179.
135. M. Sadiq, S. Sadiq, M. Abid Zia, M. Ali, K. Saeed, M. Sohail Ahmad and R. Ali, *C*, 2016, **2**, 8.
136. Liu, M. Conte, Q. He, D. Knight, D. Murphy, S. Taylor, K. Whiston, C. Kiely and G. J. Hutchings, *Chem. Eur. J.*, 2017, **23**,11834-11842.
137. Gui, W. Cao, L. Chen and Z. Qi, *Catal. Commun.*, 2015, **64**, 58–61.
138. R. Antony, S. T. D. Manickam and S. Balakumar, *J. Inorg. Organomet. Polym. Mater.*, 2016, **27**, 418–426.
139. C. Perego, A. Carati, P. Ingallina, M. A. Mantegazza and G. Bellussi, *Appl. Catal. Gen.*, 2001, **221**, 63–72.
140. F. Bonino, A. Damin, G. Ricchiardi, M. Ricci, G. Spanò, R. D'Aloisio, A. Zecchina, C. Lamberti, C. Prestipino and S. Bordiga, *J. Phys. Chem. B*, 2004, **108**, 3573–3583.

141. G. Li, J. Edwards, A. F. Carley and G. J. Hutchings, *Catal. Commun.*, 2007, **8**, 247–250.
142. E. V. Spinace, H. O. Pastore and U. Schuchardt, *J. Catal.*, 1995, **157**, 631–635.
143. S. E. Dapurkar, A. Sakthivel and P. Selvam, *J. Mol. Catal. Chem.*, 2004, **223**, 241–250.
144. Bellifa, D. Lahcene, Y. N. Tchenar, A. Choukchou-Braham, R. Bachir, S. Bedrane and C. Kappenstein, *Appl. Catal. Gen.*, 2006, **305**, 1–6.
145. Sakthivel and P. Selvam, *J. Catal.*, 2002, **211**, 134–143.
146. S. S. Acharyya, S. Ghosh, S. K. Sharma and R. Bal, *New J. Chem.*, 2016, **40**, 3812–3820.
147. Z.-Q. Zhang, J. Huang, L. Zhang, M. Sun, Y.-C. Wang, Y. Lin and J. Zeng, *Nanotechnology*, 2014, **25**, 435602.
148. R. Antony, S. T. D. Manickam, P. Kollu, P. V. Chandrasekar, K. Karuppasamy and S. Balakumar, *RSC Adv.*, 2014, **4**, 24820–24830.
149. S. Khare, P. Shrivastava, R. Chokhare, J. S. Kirar and S. Parashar, *J. Porous Mater.*, 2016, **24**, 855–866.
150. M. R. Sazegar, A. Dadvand and A. Mahmoudi, *RSC Adv.*, 2017, **7**, 27506–27514.
151. M. Santonastaso, S. J. Freakley, P. J. Miedziak, G. L. Brett, J. K. Edwards and G. J. Hutchings, *Org. Process Res. Dev.*, 2014, **18**, 1455–1460.
152. J. Wang, H. Zhao, X. Zhang, R. Liu and Y. Hu, *Chin. J. Chem. Eng.*, 2008, **16**, 373–375.
153. E. Chan-Thaw, A. Savara and A. Villa, *Catalysts*, 2018, **8**, 431.
154. E. Nowicka, S. Althahban, T. D. Leah, G. Shaw, D. Morgan, C. J. Kiely, A. Roldan and G. J. Hutchings, *Sci. Technol. Adv. Mater.*, 2019, **20**, 367–378.
155. T. Maki and K. Takeda, *Ullmann's Encyclopedia of Industrial Chemistry*, American Cancer Society, 2000.
156. F. Alberici, L. Pagani, G. Ratti and P. Viale, *Br. J. Dermatol.*, 2000, **142**, 969–972.
157. D. Warth, *Appl. Environ. Microbiol.*, 1991, **57**, 3410–3414.
158. J. Bonnart and G. Poilane, US3387036A, 1963.
159. F. Galvanin, M. Sankar, S. Cattaneo, D. Bethell, V. Dua, G. J. Hutchings and A. Gavriilidis, *Chem. Eng. J.*, 2018, **342**, 196–210.
160. E. Nowicka, J. P. Hofmann, S. F. Parker, M. Sankar, G. M. Lari, S. A. Kondrat, D. W. Knight, D. Bethell, B. M. Weckhuysen and G. J. Hutchings, *Phys. Chem. Chem. Phys.*, 2013, **15**, 12147–12155.
161. S. Meenakshisundaram, E. Nowicka, P. J. Miedziak, G. L. Brett, R. L. Jenkins, N. Dimitratos, S. H. Taylor, D. W. Knight, D. Bethell and G. J. Hutchings, *Faraday Discuss.*, 2010, **145**, 341–356.
162. M. Sankar, E. Nowicka, R. Tiruvalam, Q. He, S. H. Taylor, C. J. Kiely, D. Bethell, D. W. Knight and G. J. Hutchings, *Chem. Eur. J.*, 2011, **17**, 6524–6532.
163. R. Sheldon, *Metal-Catalyzed Oxidations of Organic Compounds: Mechanistic Principles and Synthetic Methodology Including Biochemical Processes*, Elsevier, 2012.
164. W. P. Jorissen and P. A. A. van der Beek, *Recl. Trav. Chim. Pays-Bas*, 1930, **49**, 138–141.
165. P. Fristrup, L. B. Johansen and C. H. Christensen, *Chem. Commun.*, 2008, 2750–2752.

166. M. Conte, H. Miyamura, S. Kobayashi and V. Chechik, *Chem. Commun.*, 2010, **46**, 145–147.
167. M. Alhumaimess, Z. Lin, W. Weng, N. Dimitratos, N. F. Dummer, S. H. Taylor, J. K. Bartley, C. J. Kiely and G. J. Hutchings, *ChemSusChem*, 2012, **5**, 125–131.
168. N. Dimitratos, J. A. Lopez-Sanchez, D. Morgan, A. Carley, L. Prati and G. J. Hutchings, *Catal. Today*, 2007, **122**, 317–324.
169. I. Enache, D. Barker, J. K. Edwards, S. H. Taylor, D. W. Knight, A. F. Carley and G. J. Hutchings, *Catal. Today*, 2007, **122**, 407–411.
170. Q. He, P. J. Miedziak, L. Kesavan, N. Dimitratos, M. Sankar, J. A. Lopez-Sanchez, M. M. Forde, J. K. Edwards, D. W. Knight, S. H. Taylor, C. J. Kiely and G. J. Hutchings, *Faraday Discuss.*, 2013, **162**, 365–378.
171. Cao, M. Sankar, E. Nowicka, Q. He, M. Morad, P. J. Miedziak, S. H. Taylor, D. W. Knight, D. Bethell, C. J. Kiely, A. Gavriilidis and G. J. Hutchings, *Catal. Today*, 2013, **203**, 146–152.
172. P. Miedziak, M. Sankar, N. Dimitratos, J. A. Lopez-Sanchez, A. F. Carley, D. W. Knight, S. H. Taylor, C. J. Kiely and G. J. Hutchings, *Catal. Today*, 2011, **164**, 315–319.
173. M. Sankar, E. Nowicka, E. Carter, D. M. Murphy, D. W. Knight, D. Bethell and G. J. Hutchings, *Nat. Commun.*, 2014, **5**, 3332.
174. M. F. R. Mulcahy and I. C. Watt, *Nature*, 1951, **168**, 123–124.
175. J. Chen, Q. Zhang, Y. Wang and H. Wan, *Adv. Synth. Catal.*, 2008, **350**, 453–464.
176. Li, Q. Zhang and Y. Wang, *Appl. Catal. Gen.*, 2008, **334**, 217–226.
177. D. Ferri, C. Mondelli, F. Krumeich and A. Baiker, *J. Phys. Chem. B*, 2006, **110**, 22982–22986.
178. S. H. Pang, A. M. Román and J. W. Medlin, *J. Phys. Chem. C*, 2012, **116**, 13654–13660.
179. S. Campisi, D. Ferri, A. Villa, W. Wang, D. Wang, O. Kröcher and L. Prati, *J. Phys. Chem. C*, 2016, **120**, 14027–14033.
180. R. Long, K. Mao, M. Gong, S. Zhou, J. Hu, M. Zhi, Y. You, S. Bai, J. Jiang, Q. Zhang, X. Wu and Y. Xiong, *Angew. Chem. Int. Ed Engl.*, 2014, **53**, 3205–3209.
181. R. Long, K. Mao, X. Ye, W. Yan, Y. Huang, J. Wang, Y. Fu, X. Wang, X. Wu, Y. Xie and Y. Xiong, *J. Am. Chem. Soc.*, 2013, **135**, 3200–3207.
182. S. Meher and R. K. Rana, *Green Chem.*, 2019, **21**, 2494–2503.
183. M. M. Wolf, H. Zhu, W. H. Green and G. S. Jackson, *Appl. Catal. Gen.*, 2003, **244**, 323–340.
184. C. T. Campbell, *Phys. Rev. Lett.*, 2006, **96**, 066106.
185. J.-D. Grunwaldt, M. Caravati, M. Ramin and A. Baiker, *Catal. Lett.*, 2003, **90**, 221–229.
186. V. M. Shinde, E. Skupien and M. Makkee, *Catal. Sci. Technol.*, 2015, **5**, 4144–4153.
187. Q. Wang, X. Cai, Y. Liu, J. Xie, Y. Zhou and J. Wang, *Appl. Catal. B Environ.*, 2016, **189**, 242–251.
188. Savara, C. E. Chan-Thaw, J. E. Sutton, D. Wang, L. Prati and A. Villa, *ChemCatChem*, 2017, **9**, 253–257.
189. T. A. G. Silva, E. Teixeira-Neto, N. López and L. M. Rossi, *Sci. Rep.*, 2014, **4**, 1–5.

190. N. Dimitratos, A. Villa, D. Wang, F. Porta, D. Su and L. Prati, *J. Catal.*, 2006, **244**, 113–121.
191. Savara, I. Rossetti, C. E. Chan-Thaw, L. Prati and A. Villa, *ChemCatChem*, 2016, **8**, 2482–2491.
192. M. Olmos, L. E. Chinchilla, A. Villa, J. J. Delgado, A. B. Hungría, G. Blanco, L. Prati, J. J. Calvino and X. Chen, *J. Catal.*, 2019, **375**, 44–55.
193. X. Yang, C. Huang, Z. Fu, H. Song, S. Liao, Y. Su, L. Du and X. Li, *Appl. Catal. B Environ.*, 2013, **140–141**, 419–425.
194. M. Morad, M. Sankar, E. Cao, E. Nowicka, T. E. Davies, P. J. Miedziak, D. J. Morgan, D. W. Knight, D. Bethell, A. Gavriilidis and G. J. Hutchings, *Catal. Sci. Technol.*, 2014, **4**, 3120–3128.
195. D. Wang, A. Villa, F. Porta, L. Prati and D. Su, *J. Phys. Chem. C*, 2008, **112**, 8617–8622.
196. R. C. Tiruvalam, J. C. Pritchard, N. Dimitratos, J. A. Lopez-Sanchez, J. K. Edwards, A. F. Carley, G. J. Hutchings and C. J. Kiely, *Faraday Discuss.*, 2011, **152**, 63–86.
197. Moreno, N. F. Dummer, J. K. Edwards, M. Alhumaimess, M. Sankar, R. Sanz, P. Pizarro, D. P. Serrano and G. J. Hutchings, *Catal. Sci. Technol.*, 2013, **3**, 2425–2434.
198. H. J. H. Fenton, *J. Chem. Soc. Trans.*, 1894, **65**, 899–910.
199. J. J. Pignatello, E. Oliveros and A. MacKay, *Crit. Rev. Environ. Sci. Technol.*, 2006, **36**, 1–84.
200. R. Andreozzi, *Catal. Today*, 1999, **53**, 51–59.
201. Haber, J. Weiss and W. J. Pope, *Proc. R. Soc. Lond. Ser. Math. Phys. Sci.*, 1934, **147**, 332–351.
202. W. G. Barb, J. H. Baxendale, P. George and K. R. Hargrave, *Nature*, 1949, **163**, 692–694.
203. M. S. Yalfani, A. Georgi, S. Contreras, F. Medina and F.-D. Kopinke, *Appl. Catal. B Environ.*, 2011, **104**, 161–168.
204. R. Underhill, R. J. Lewis, S. J. Freakley, M. Douthwaite, P. J. Miedziak, O. Akdim, J. K. Edwards and G. J. Hutchings, *Johns. Matthey Technol. Rev.*, 2018, **62**, 417–425.
205. M. Triki, S. Contreras and F. Medina, *J. Sol-Gel Sci. Technol.*, 2014, **71**, 96–101.
206. Liu, Q. Fan, Y. Liu and J. Wang, *J. Environ. Manage.*, 2018, **214**, 252–260.
207. S. Navalon, M. Alvaro and H. Garcia, *Appl. Catal. B Environ.*, 2010, **99**, 1–26.
208. Georgi, M. Velasco Polo, K. Crincoli, K. Mackenzie and F.-D. Kopinke, *Environ. Sci. Technol.*, 2016, **50**, 5882–5891.
209. S. Contreras, M. S. Yalfani, F. Medina and J. E. Sueiras, *Water Sci. Technol.*, 2011, **63**, 2017–2024.
210. M. Rios-Enriquez, N. Shahin, C. Durán-de-Bazúa, J. Lang, E. Oliveros, S. H. Bossmann and A. M. Braun, *Sol. Energy*, 2004, **77**, 491–501.
211. Y. Qin, M. Sun, H. Liu and J. Qu, *Electrochimica Acta*, 2015, **186**, 328–336.
212. M. Munoz, Z. M. de Pedro, J. A. Casas and J. J. Rodriguez, *Appl. Catal. B Environ.*, 2015, **176–177**, 249–265.
213. M. S. Yalfani, S. Contreras, F. Medina and J. Sueiras, *Appl. Catal. B Environ.*, 2009, **89**, 519–526.
214. M. S. Yalfani, S. Contreras, J. Llorca, M. Dominguez, J. E. Sueiras and F. Medina, *Phys. Chem. Chem. Phys.*, 2010, **12**, 14673–14676.

215. S. Zha, Y. Cheng, Y. Gao, Z. Chen, M. Megharaj and R. Naidu, *Chem. Eng. J.*, 2014, **255**, 141–148.
216. T. Van, L. H. Nguyen, T. K. Hoang, T. T. Nguyen, T. N. H. Tran, T. B. H. Nguyen, X. H. Vu, M. T. Pham, T. P. Tran, T. T. Pham, H. D. Nguyen, H.-P. Chao, C.-C. Lin and X. C. Nguyen, *Environ. Technol. Innov.*, 2020, **18**, 100670.
217. M. Atta, Y. M. Moustafa, H. A. Al-Lohedan, A. O. Ezzat and A. I. Hashem, *ACS Omega*, 2020, **5**, 2829–2842.
218. S. Karthikeyan, A. Titus, A. Gnanamani, A. B. Mandal and G. Sekaran, *Desalination*, 2011, **281**, 438–445.

# 2 Experimental.

## 2.1 Introduction.

A variety of monometallic and bimetallic supported metal catalysts have been synthesised. This chapter discussed the materials used to synthesise these catalysts along with their experimental testing and characterisation.

## 2.2 Materials Used.

### 2.2.1 Metal Precursors for catalyst synthesis.

- $PdCl_2$ (Sigma Aldrich, 99.999 % trace metal basis)
- $HAuCl_4.3H_2O$ (Sigma Aldrich, 99.99%)
- $FeCl_3.6H_2O$ (Sigma Aldrich, ≥ 99% trace metal basis)
- $CuCl_2$ (Sigma Aldrich, 99.999% trace metal basis)
- $MnCl_2.4H_2O$ (Fisher Chemicals, 99% trace metal basis)
- $CeCl_3.7H_2O$ (Sigma Aldrich, 99.9% trace metal basis)
- $CoCl_2.6H_2O$ (Alfa Aesar, 98% trace metal basis)
- $VCl_3$ (Sigma Aldrich, 97% trace metal basis)
- $NiCl_2.6H_2O$ (Sigma Aldrich, 99.999% trace metal basis)
- HCl (Fisher Chemicals, 37%)
- $NH_4VO_3$ (Sigma Aldrich, ≥ 99.0%)
- $C_2H_2O_4$ (Sigma Aldrich, 98%)
- $HNO_3$ (Fisher Chemicals, 67%)

### 2.2.2 Catalyst support materials.

- $TiO_2$ (P25, Degussa, 99.5% trace metal basis)
- $SiO_2$ (Sigma Aldrich)
- $CeO_2$ (Sigma Aldrich, powder, 99.995 % trace metal basis
- MgO (BDH)
- Carbon (CABOT Vulcan XC-72, Sigma Aldrich)
- $V_2O_5$ (Sigma Aldrich, ≥98%)
- $V_2O_4$ (Sigma Aldrich, >99%)

### 2.2.3 Reagents.

- Water (Fisher Scientific, HPLC gradient grade)
- Methanol (Fisher Scientific, ≥ 99.5 %)

- $H_2O_2$ (Fluka, 50wt. % in water)
- $NH_2Fe(SO_4).6H_2O$ (Alfa Aesar, 0.025 M aqueous solution)
- $Ce(SO_4)_2$ (Sigma Aldrich)
- $H_2SO_4$ (Fisher Scientific UK, >95 %)
- $FeSO_4.6H_2O$ (BDH)
- Cyclohexane (Honeywell, ≥ 99.9%)
- Tert-butanol (Acros organics, 99.5 %)
- Cyclohexanol (Sigma Aldrich, 99%)
- Cyclohexanone (Sigma Aldrich, ≥ 99.0%)
- Mesitylene (Sigma Aldrich, 98 %)
- Triphenyl phosphine (Sigma Aldrich, 99%)
- Benzyl alcohol (Alfa Aesar, 99%)
- Benzaldehyde (Sigma Aldrich, ≥99.5%)
- Benzoic acid (Sigma Aldrich, ≥99.5%)
- Toluene (Fisher Scientific, 99%)
- Benzyl Benzoate (Sigma Aldrich, ≥99.0%)
- 5,5-Dimethyl-1-pyrroline N-Oxide (Tokyo Chemical Industry, >97%)

### 2.2.4 Gases.

- 5% $H_2$ /$CO_2$ (BOC gases, 99.99%)
- 25% $O_2$ /$CO_2$ (BOC gases, 99.99%)
- 5% $H_2$ /$N_2$ (BOC gases, 99.99%)
- 25% $O_2$ /$N_2$(BOC gases, 99.99%)

## 2.3 Catalyst Preparation.

### 2.3.1 Wet impregnation.

Based on established methodology,[1] typically 2 g of 0.5 wt.% Au 0.5 wt.% Pd (1:1 Au:Pd weight ratio) supported catalyst were made as follows, Figure 2.1. Solid $PdCl_2$ (0.0166 g) was added to an aqueous solution of $HAuCl_4 \cdot 3H_2O$ (0.816 ml, 12.25 mg $ml^{-1}$) and stirred with heating (80 °C) until the palladium salt had completely dissolved. The support was then added (1.98 g) with continuous stirring. The solution was stirred at 85 °C until it formed a paste, this paste was then dried at 110 °C for 16 h. The dried catalyst was collected and ground before a portion (0.5 g) was calcined in static air (400 °C, 3 h, ramp rate 20 °C $min^{-1}$).

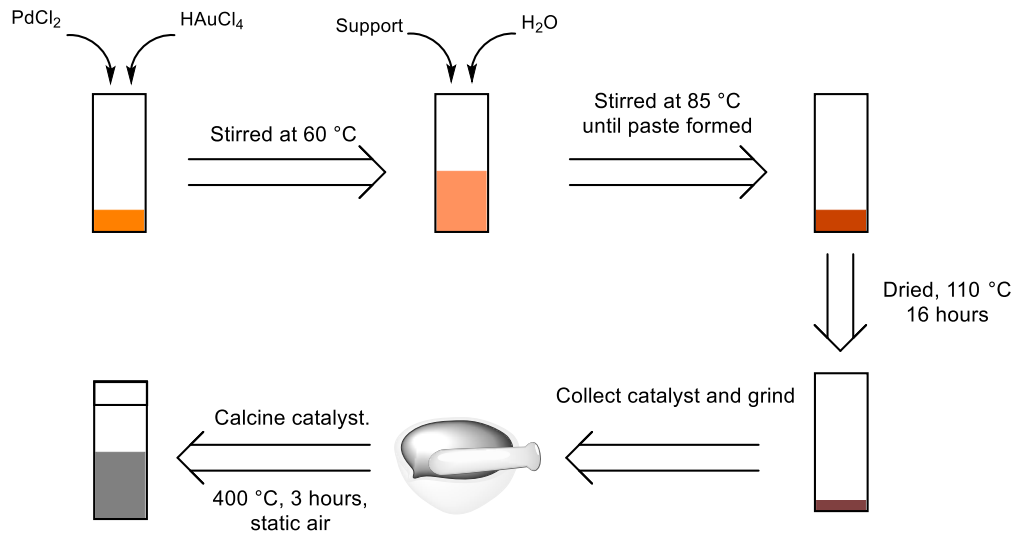


***Figure 2.1*** *A general schematic for the preparation of a bimetallic AuPd catalyst prepared by conventional wet impregnation.*

### 2.3.2 Modified impregnation.

Based on established methodology,[2] typically 2 g of 0.5 wt.% Au 0.5 wt.% Pd supported catalyst were made as follows (1:1 Au:Pd weight ratio), Figure 2.2. An acidified solution of $PdCl_2$ (1.667 ml, 6 mg $ml^{-1}$, 0.58 M HCl) was added to a predetermined volume of an aqueous solution of $HAuCl_4 \cdot 3H_2O$ (0.816 ml, 12.25 mg $ml^{-1}$) in a 50 ml round bottom flask. The volume of the solution was adjusted using deionized water to ensure a total volume of 16 ml before stirring and heating (60 °C). The support was then slowly added (1.98 g) with continuous stirring. The solution was stirred at 95 °C (16 h) to form a dry solid. The dried catalyst was collected and ground before a portion (0.5 g) of the dried catalyst was then heat treated under flowing 5 % $H_2$/Ar (500 °C, 4 h, ramp rate 10 °C $min^{-1}$).

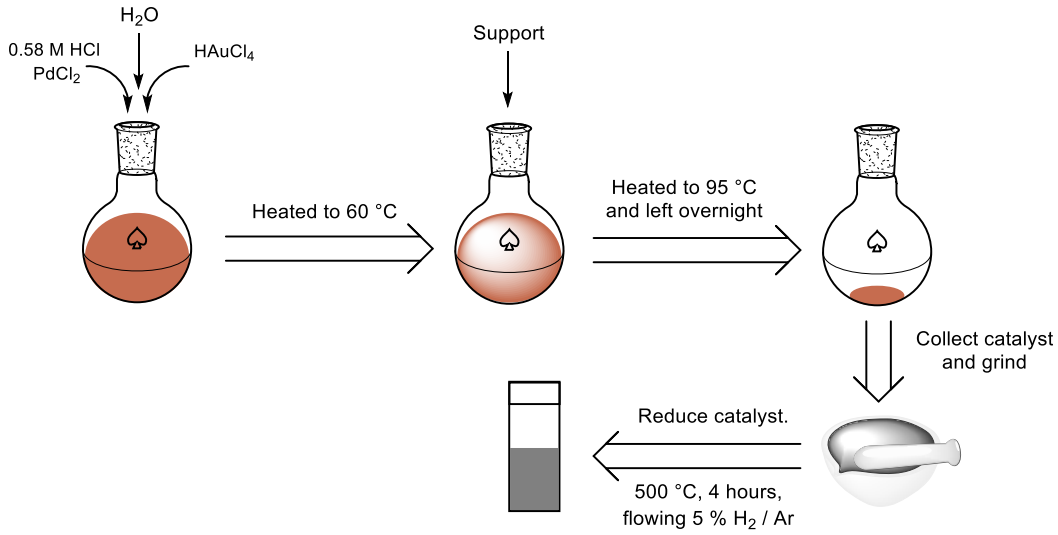


***Figure 2.2.*** *General schematic for the preparation of a bimetallic AuPd catalyst prepared by modified impregnation.*

### 2.3.3 Sol immobilisation.

Based on established methodology,[3] typically 1 g of 0.5 wt.% Au 0.5 wt.% Pd supported catalyst were made as follows (1:1 Au:Pd weight ratio), Figure 2.3. An aqueous solution of $PdCl_2$ (0.833 ml, 6 mg $ml^{-1}$) and an aqueous solution of $HAuCl_4 \cdot 3H_2O$ (0.408 ml, 12.25 mg $ml^{-1}$) were added to 400 ml deionised water and stirred. The required amount of a PVA solution (1.3 ml, 1 wt.% aqueous solution, Aldrich, MW=10 000, 80% hydrolysed) was added to achieve a ratio of PVA/(Au + Pd) (w/w) of 1.3. A freshly prepared solution of $NaBH_4$ (3.618 ml, 0.1 M) was added to give a ratio of $NaBH_4$/(Au + Pd) (mol/$mol^{-1}$ ) of 5. After 30 min of sol generation, the colloid was immobilised by adding the support material (0.99 g). The solution was acidified using $H_2SO_4$ (75 wt.%, Fisher Scientific) until a pH of 1 was reached. After 2 hours, the slurry was filtered, and the catalyst was washed thoroughly with 2 L of distilled water and then dried (110 °C, 16 h). The dried catalyst was collected and ground before a portion (0.5 g) of the dried catalyst was then calcined in static air (400 °C, 3 h, ramp rate 20 °C $min^{-1}$).

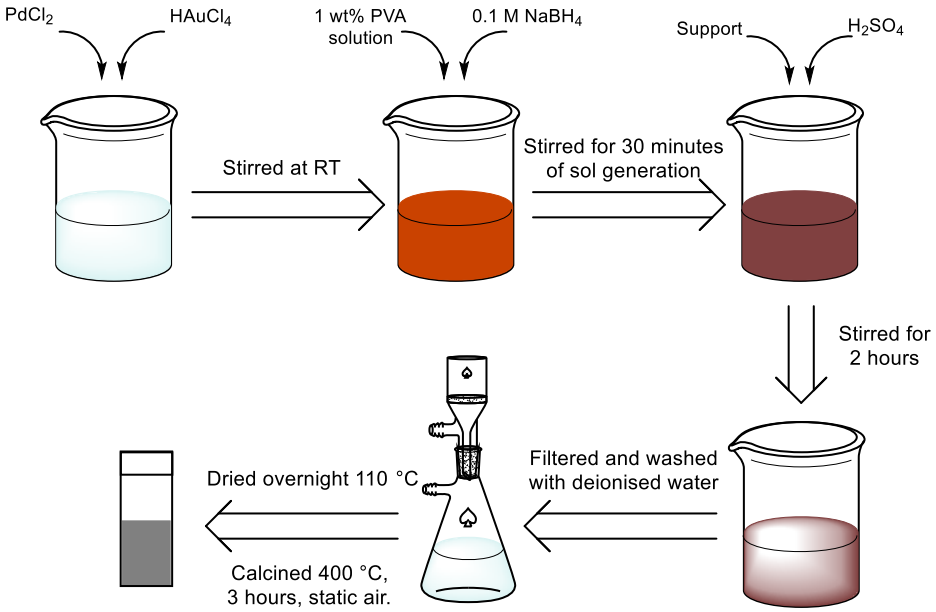


***Figure 2.3.*** *A general schematic for the preparation of a bimetallic AuPd catalyst prepared via sol immobilisation.*

### 2.3.4 Wet impregnation – Vanadia promoted catalysts.

Adapted from previous methodology[4] vanadia promoted $Pd/TiO_2$ catalysts were synthesised as follows. Typically, catalysts were synthesised in 2g batches with 0.5 wt.% Pd and varying V content from 0.5 wt.% to 3 wt.% on $TiO_2$. The requisite amount of solid $PdCl_2$ (0.0166 g) was added to 10 ml deionised water in a 50 ml round bottom flask. The solution was heated and stirred at 80 °C until full dissolution of the solid.

Ammonium metavanadate (0.0230 to 0.137 g) and oxalic acid (0.159 g) were added to the solution and left to stir until a paste had formed. This paste was dried (110 ºC, 16 hours). The catalyst was then recovered ground and a portion (0.5 g) was calcined in static air (550 ºC, 6 hours, ramp rate 20 °C $min^{-1}$). Some samples were also treated to further reductive heat treatments as detailed later.

### 2.3.5 $Pd/VO_x/TiO_2$ supported catalysts.

$Pd/VO_x/TiO_2$ catalysts were prepared by adaption from the methodology of Barthos *et al.*[5,6] Typically, catalysts were synthesised in 2g batches with 1 wt.% Pd with both 1 and 3 wt. % V on $TiO_2$. Firstly, the $TiO_2$ was impregnated with V. A decavanadate ($V_{10}O_{56}^{6-}$) solution was prepared from ammonium metavanadate (5 g) dissolved in deionised water (500 $cm^3$) and the stepwise addition of nitric acid (0.1 mol $dm^{-3}$) until a pH of 4 was reached. The $TiO_2$ (5 g) was then impregnated with the required decavanadate solution (11.48 $cm^3$ for 1% V, 33.45 $cm^3$ for 3% V) and dried (110 °C, 16 hours). The impregnated $TiO_2$ was then calcined in static air (400 °C, 4 hours, 10 °C $min^{-1}$). The impregnated supports were impregnated with $PdCl_2$ solution (6 mg $ml^{-1}$) via a wet impregnation procedure previously reported. A portion of the catalysts (0.5g) were then either calcined in static air or reduced under flowing 5% $H_2$/Ar (400 °C, 4 hours, ramp rate 10 °C $min^{-1}$).

## 2.4 Catalyst testing.

### 2.4.1 Direct synthesis of $H_2O_2$.

The direct synthesis of $H_2O_2$ has been investigated in 50 ml Parr Instruments stainless steel autoclave. Catalyst (0.01 g), water (2.9 g) and methanol (5.6 g) were added to the reactor. The reactor was purged with 10 bar 5% $H_2/CO_2$ three times and then filled with 5 % $H_2/CO_2$ (29 bar, 2.51 mmol $H_2$) and 25 % $O_2/CO_2$ (11 bar, 4.77 mmol $O_2$). The reactor was then stirred (1200 RPM) for 30 minutes at 25 °C. Once the reaction was complete the catalyst was separated by filtration. The $H_2O_2$ productivity was then determined by titration of aliquots of the post reaction solution with acidified $Ce(SO_4)_2$ ($8 \times 10^{-3}$ mol $dm^{-3}$) and using ferroin as an indicator.[7] Gas analysis was determined by gas chromatography using a Varian CP-3380 fitted with a Porapak Q column.

The catalytic activity towards the synthesis of $H_2O_2$ has been presented in terms of productivity. The concentration of $H_2O_2$ was determined and standardised by the mass of catalyst and time, as shown in Equation 2.1.

$$Productivity\left(mol_{H_2O_2}\ kg_{cat}^{-1}\ hr^{-1}\right) = \frac{moles\ H_2O_2\ produced}{mass\ of\ catalyst\ (kg) \times time\ (hr)} \qquad \textit{Equation 2.1}$$

For $H_2$ conversion blank reactions were run, where no catalyst was present but all conditions remained the same to as described above, after reaction a gas sample was taken and analysed by GC, this gave the $H_2$ area for 0% conversion. The area of $H_2$ was divided by $CO_2$ to give $H_2/CO_2$ as $CO_2$ was designated as the internal standard. Gas samples were then also taken post reaction and the ratio of the peak areas, $H_2/CO_2$, was compared to the blank to calculate $H_2$ conversion, Equation 2.2.

$$H_2\ Conversion = \frac{area\ H_2/area\ CO_{2_{blank}} - area\ H_2/area\ CO_{2_{reaction}}}{area\ H_2/area\ CO_{2_{blank}}} \times 100\ \% \qquad \textit{Equation 2.2}$$

Using the ideal gas equation the initial moles of $H_2$ in the reactor could be calculated, Equation 2.3, from this the moles of $H_2$ that had been converted during the reaction could be calculated. Using the moles of $H_2$ converted and the moles of $H_2O_2$ produced in the reaction the selectivity could also been determined, Equation 2.4.

$$n = \frac{pV}{RT} \qquad \textit{Equation 2.3}$$

*Where; n is the moles of gas, p is pressure of the gas, V is the volume, R is the universal gas constant and T is temperature.*

$$Selectivity = \frac{moles\ H_2O_2}{moles\ H_2 converted} \times 100\% \qquad \textit{Equation 2.4}$$

### 2.4.2 Degradation of $H_2O_2$.

The degradation of $H_2O_2$ was also investigated in 50 ml Parr Instruments stainless steel autoclave. Catalyst (0.01 g), $H_2O_2$ (0.68 g, 50 wt.% $H_2O_2$), water (2.22 g) and methanol (5.6 g) were added to the reactor producing an approximate 4 wt.% solution of $H_2O_2$. The reactor is purged with 10 bar 5 % $H_2/CO_2$ 3 times and then filled with 5 % $H_2/CO_2$ (29 bar, 2.51 mmol $H_2$). The reactor was stirred (1200 RPM) for 30 minutes at 25 °C. Once the reaction is complete the catalyst was separated by filtration. The $H_2O_2$ concentration was determined before and after reaction by titration of aliquots of the pre and post reaction solution with acidified $Ce(SO_4)_2$ ($8 \times 10^{-3}$ mol $dm^{-3}$) and using ferroin as an indicator. The comparison of pre and post reaction $H_2O_2$ concentration is used to calculate the degradation of $H_2O_2$.

The catalytic activity towards the degradation of hydrogen has also been presented in terms of productivity. The concentration of $H_2O_2$ that had been degraded was determined and standardised by the mass of catalyst and time. It has also been displayed as a percentage where the moles of $H_2O_2$ that has degraded is calculated as a percentage of the initial moles of $H_2O_2$.

### 2.4.3 Oxidation of cyclohexane via the *in-situ* production of $H_2O_2$.

The oxidation of cyclohexane has been investigated in 50 ml Parr Instruments stainless steel autoclave. Catalyst (0.05 g), tert-butanol (6.375 g) and cyclohexane (2.125 g, 25 mmol) are added to the reactor along with 0.5 ml of the internal standard mesitylene (0.43 g, 3.58 mmol). The reactor was purged with 10 bar 5 % $H_2/N_2$ and then filled with 5 % $H_2/N_2$ (29 bar, 2.51 mmol $H_2$) and 25 % $O_2/N_2$ (11 bar, 4.77 mmol $O_2$). The reactor was stirred (500 RPM) until the temperature (80 °C) was reached and then stirred (1200 RPM) for 17 hours. Once the reaction was complete the reactor was cooled in an ice bath to 15 °C and catalyst was separated by filtration. The yield of KA oil was determined by gas chromatography using a Varian 3200 GC equipped with a flame ionization detector. A CP Wax 42 column was used to separate products. Gas analysis was determined by gas chromatography using a Varian CP-3380 fitted with a Porapak Q column and $H_2$ conversion was calculated.

For product quantification mixtures of cyclohexane, cyclohexanol, cyclohexanone and the internal standard mesitylene were prepared at varying concentrations to calibrate the GC response. The area ratios of the compounds and the internal standard were plotted against the known moles of compounds in the calibration mixture to produce calibration curves, Figure 2.4 and 2.5. From these calibrations curves the response factors of each compound were calculated and used to quantitatively analyse the post reaction mixtures.

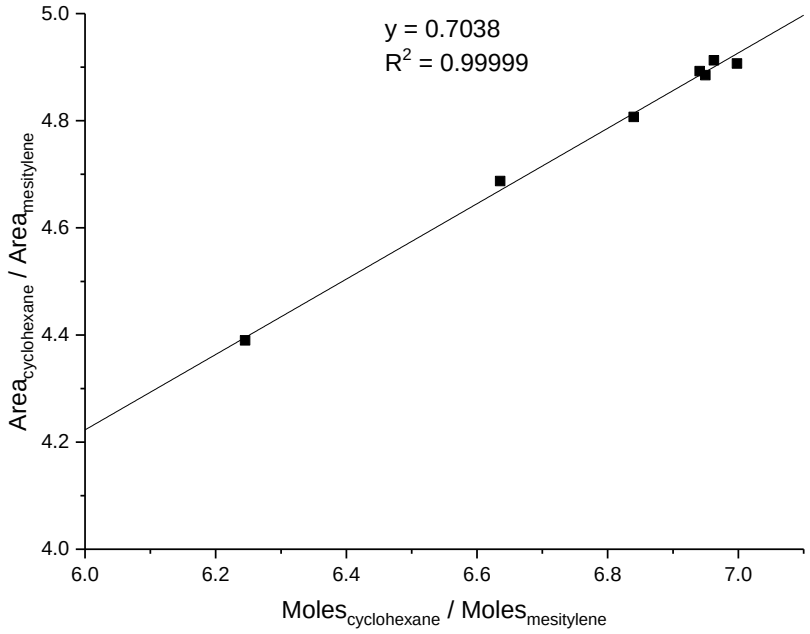


***Figure 2.4.*** *Calibration curve used to calculate the moles of cyclohexane present in post reaction mixtures for the oxidation of cyclohexane.*

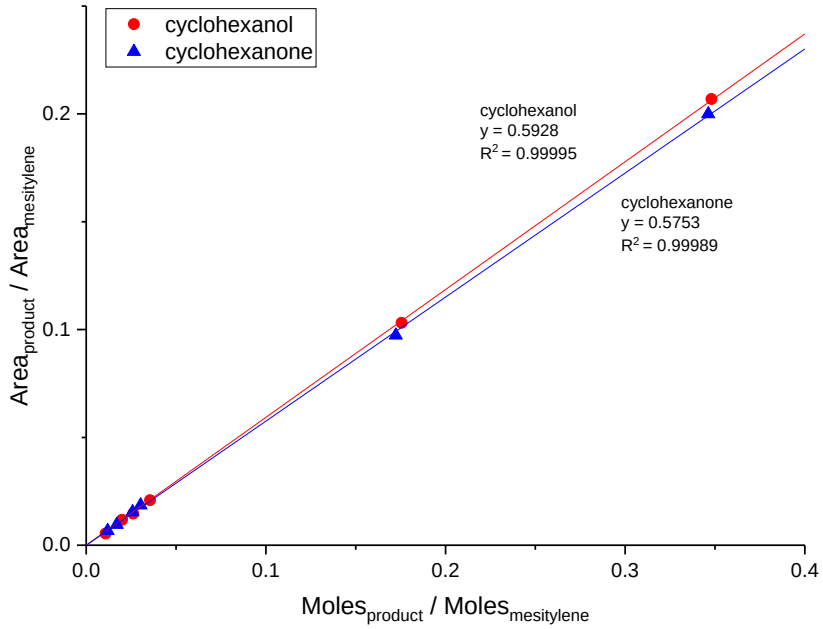


***Figure 2.5.*** *Calibration curve used to calculate the moles of cyclohexanol and cyclohexanone present in post reaction mixtures for the oxidation of cyclohexane.*

As $N_2$ was used as the diluent the conversion of $H_2$ was determined by the comparison of $H_2$ area post reaction and a blank reaction, Equation 2.5. $C_6$ product selectivity has been calculated based on $H_2$ conversion as defined in Equation 2.6.

$$H_2\ Conversion = \frac{area\ H_{2\,blank} - area\ H_{2\,reaction}}{area\ H_{2\,blank}} \times 100\ \% \qquad \textit{Equation 2.5}$$

$$C_6 Product\ Selectivity\ (\%) = \frac{Total\ product\ (mmol)}{H_2\ conversion\ (mmol)} \times\ 100\ \% \qquad \textit{Equation 2.6}$$

Quantification of the peroxide intermediate cyclohexyl hydroperoxide (CHHP) is determined by reacting a 2 ml aliquot of the post reaction mixture with an excess of triphenyl phosphine (0.13 g, 0.5 mmol). Reaction of triphenyl phosphine and CHHP produces cyclohexanol and hence comparison of GC analysis for cyclohexanol pre and post treatment with triphenyl phosphine can determine the yield of CHHP.

For catalyst re-use 0.15g of catalyst was utilised under the standard conditions described above. After reaction the catalyst and reaction solution were separated by filtration and the catalyst was washed with cyclohexane (5 times, 2 ml). The catalyst was then dried under vacuum at 30 °C, 16 hours.

### 2.4.4 Oxidation of benzyl alcohol via the *in-situ* production of $H_2O_2$.

The oxidation of benzyl alcohol has been investigated in 50 ml Parr Instruments stainless steel autoclave. Catalyst (0.01 g), methanol (7.13 g) and benzyl alcohol (1.04 g, 9.6 mmol) were added to the reactor along with 0.5 ml of the internal standard

mesitylene (0.43 g, 3.58 mmol). The reactor was purged with 5 % $H_2/CO_2$ three times and then filled with 5 % $H_2/CO_2$ (29 bar, 2.51 mmol $H_2$) and 25 % $O_2/CO_2$ (11 bar, 4.77 mmol $O_2$). The reactor was heated to 50 °C and once the temperature was reached it was then stirred (1200 RPM) for 30 minutes. Once the reaction was completed the reactor was cooled in an ice bath to 15 °C and the catalyst was separated by filtration. The yield of all products was determined by gas chromatography using a Varian 3200 GC equipped with a flame ionization detector. A CP Wax 42 column was used to separate products. Gas analysis was determined by gas chromatography using a Varian CP-3380 fitted with a Porapak Q column and $H_2$ conversion was calculated as detailed above in Section 2.4.1.

For product quantification mixtures of benzyl alcohol and all known products were prepared at varying concentrations to calibrate the GC response. The area ratios of the compounds and the internal standard, mesitylene, were plotted against the known moles of compounds in the calibration mixture to produce calibration curves, Figure 2.6 and 2.7. From these calibrations curves the response factors of each compound were calculated and used to quantitatively analyse the post reaction mixtures.

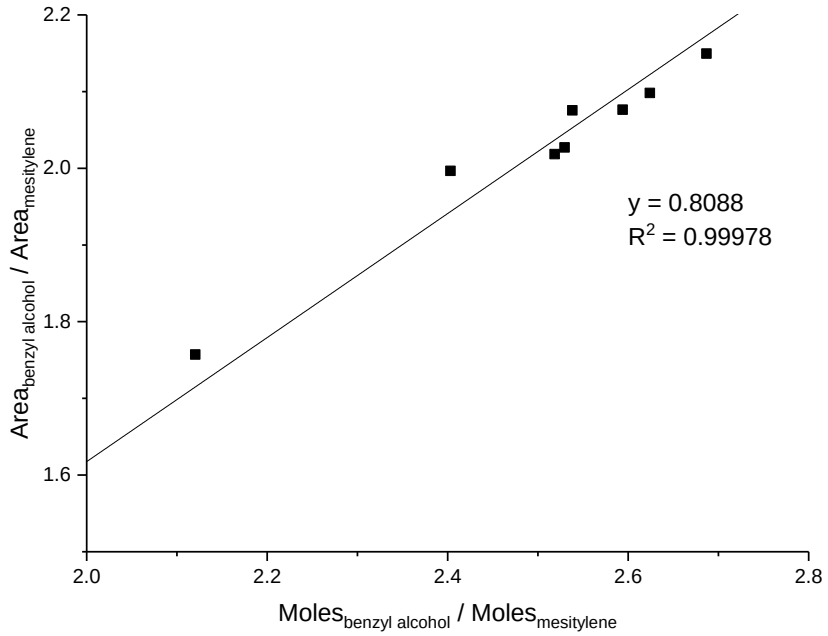


***Figure 2.6.*** *Calibration curve used to calculate the moles of benzyl alcohol present in post reaction mixtures for the oxidation of benzyl alcohol.*

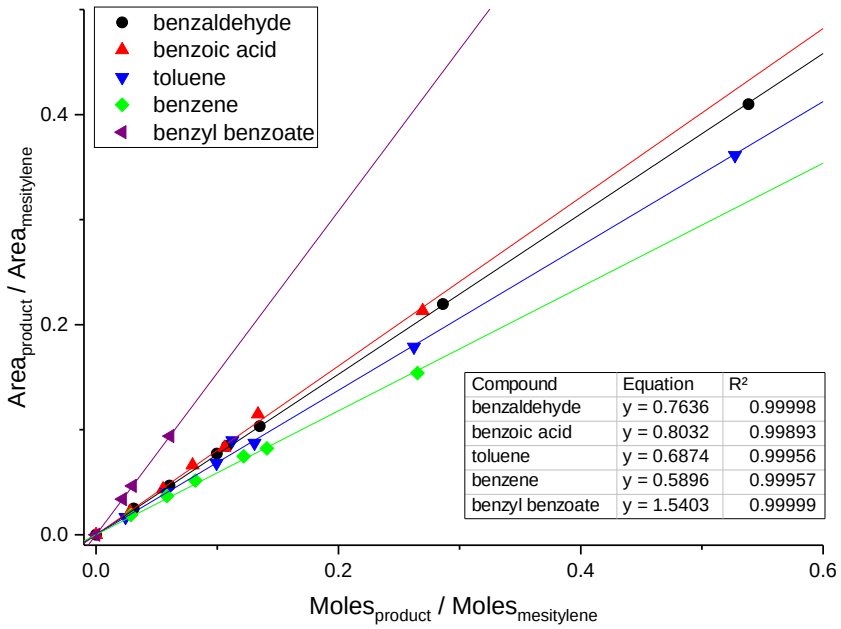


***Figure 2.7.*** *Calibration curve used to calculate the moles of products present in post reaction mixtures for the oxidation of benzyl alcohol.*

For catalyst re-use 0.5g of catalyst was utilised under the standard conditions described above. After reaction the catalyst and reaction solution were separated by filtration and the catalyst was washed with methanol (5 times, 2 ml). The catalyst was then dried under vacuum at 30 °C, 16 hours.

Sequential reactions were conducted under identical conditions to those outlined above for standard reactions, however after 30 minutes the reactor was cooled in an ice bath to 25 °C and gas sample was taken for analysis and the remaining gas removed from the reactor. The reactor was then purged again with 5% $H_2/CO_2$ and filled with 5 % $H_2/CO_2$ (29 bar, 2.51 mmol $H_2$) and 25 % $O_2/CO_2$ (11 bar, 4.77 mmol $O_2$). The reactor was then heated (50 °C) and the reaction commenced again for 30 minutes. After the required sequential reactions the catalysts and solution were separated and analysed as detailed above.

### 2.4.5 Radical trapping experiments with Electron Paramagnetic Resonance.

The oxidation of benzyl alcohol has been investigated in 50 ml Parr Instruments stainless steel autoclave. Catalyst (0.01 g), methanol (7.13 g) and benzyl alcohol (1.04 g, 9.6 mmol) were added to the reactor along with 5,5-dimethyl-1-pyrroline N-oxide (12 µL). The reactor was purged three times with 5 % $H_2/CO_2$ and then filled with 5 % $H_2/CO_2$ (29 bar, 2.51 mmol $H_2$) and 25 % $O_2/CO_2$ (11 bar, 4.77 mmol $O_2$). The reactor was then heated to 50 °C and once the temperature was reached stirring (1200

RPM) was commenced for 30 minutes. Once the reaction was complete the reactor was cooled in an ice bath to 15 °C and was purged with 20 bar $N_2$ for 20 minutes before the catalyst was separated by filtration and the filtered solution submitted for analysis by EPR spectroscopy. Reactions were also conducted in a water (9.0 g). Various blank reactions were also submitted for EPR spectroscopy to determine any background activity.

All EPR spectroscopy were ran and interpreted by Rebekah Taylor and Andrea Folli. Continuous wave X-band EPR spectra were recorded at 298K using a Bruker EMX MicroX spectrometer operating at 9.75 GHz, with 100 kHz field modulation, 1 G modulation amplitude, and 2 mW microwave power, equipped with a Bruker dielectric resonator (ER 4123d). EPR spectra were simulated using the EasySpin toolbox running on MathWorks Matlab program.

### 2.4.6 Gas Chromatography.

Gas Chromatography (GC) is imperative in Chemistry for analysing reaction mixtures. GC is an analytical technique used for separating compounds from a chemical mixture. It does this by exploiting the different affinities of the different compounds in a mixture for the static and mobile phases.[8]

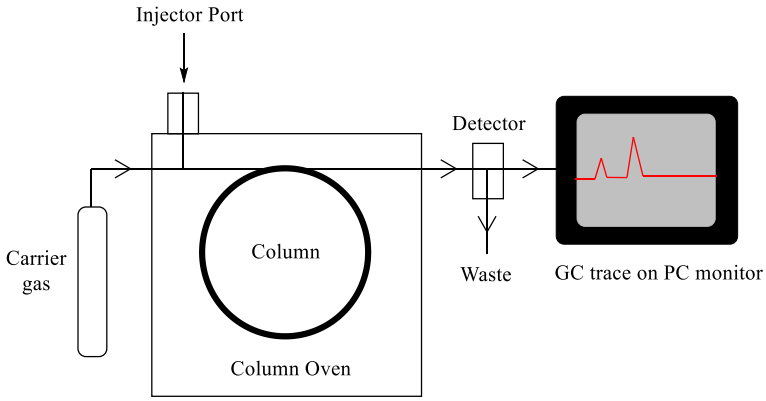


***Figure 2.8.*** *The general schematic diagram of a gas chromatography.*

The mixtures are injected and liquid samples are immediately vaporised and carried through the mobile phase by the carrier gas and delivered to the stationary phase, the column, which is heated by the column oven, Figure 2.8. The column is normally one of two forms; capillary or packed. Capillary columns, which are considered more efficient, are thin columns with diameters in the order of 0.1 mm. They can be subdivided again into wall-coated open tubular (WCOT), where the walls have been covered in a liquid stationary phase, or support-coated open tubular (SCOT) where a

support material is coated onto the walls onto which a stationary phase is then adsorbed. Packed columns are larger with internal diameters in the order of a few millimetres. These consist of a powdered support material, often silica based, which is coated in a stationary phase.[8]

The separation of the different constituents of the injected mixtures occur due to each constituent moving through the column at different velocities. These differences in velocities occur due to each component having different affinities for the stationary phase. Those compounds with stronger interactions with the stationary phase proceed through the column faster than those with weaker interactions. This leads to an increased time in which the compound is detected.

The carrier gas is used to move the gaseous analytes through the column. The carrier must not react with the analytes and hence must be chemically inert. The most commonly used gases are nitrogen, helium, argon and carbon dioxide and the selection of gas is normally governed by the type of detector in the GC. The carrier gas system often contains a molecular sieve to remove water and other impurities at the initial point of injection.

There are several detectors available for GC depending on the compounds being detected and the sensitivity required. Electron Capture Detectors (ECD) these use a beta emitter, often $^{63}Ni$ or $^{3}H$, to ionize the carrier gas. These beta particles collide with the carrier gas producing a plasma which contains free moving electrons and hence produces a current. When the GC effluent passes through any molecules which contain electronegative functional groups collide with these free electrons and hence the resulting current is reduced. The comparison between current produced from the carrier gas with and without sample gives quantifiable information on the sample components. These detectors work best with compounds with high electron affinities and hence are used most commonly for organohalide detection.

Flame Ionisation Detectors (FID) are best used for hydrocarbons and organic compounds but cannot detect small molecules such as nitrogen or carbon dioxide gases. These consist of a $H_2$ flame. As the compounds of the effluent pass through the flame they combust and produce ions and electrons which are attracted to a biased electrode. The charged particles produce a measurable current flow in the gap between two electrodes in the detector and can be measured. The current measured is

proportional to the concentration of the hydrocarbons. Though these detectors are very sensitive for organic molecules due to the sample being destroyed during detection the sample cannot be recovered.

Thermal Conductivity Detectors (TCD) are universal detectors and can measure both hydrocarbons and small molecules. These consist of two parallel tubes containing heating coils and carrier gas. As the GC effluent passes through one of the tubes the thermal conductivity is measured of both tubes and the comparison between reference carrier and the sample is made. Most compounds have lower thermal conductivities than that of the common carrier gas, helium, resulting in a decrease in thermal conductivity and a signal detection. Although a TCD can be less sensitive than a FID the sample is not destroyed and hence can be recovered post detection.

Mass Spectrometry (MS) can also be coupled with GC for qualitative and quantitative detections. The effluent is firstly ionised by an ionisation source and then pass into the mass spectrometer and are separated by their mass-to-charge ratios by the relative motion of the ions in an electromagnetic field.[8]

### 2.4.7 Electron Paramagnetic Resonance Spectroscopy.

Electron Paramagnetic Resonance (EPR) Spectroscopy is a technique that is used to investigate paramagnetic species, which by definition contains one or more unpaired electrons.[9] Unpaired electrons have electrons spins, $M_s$, and due to this spin the electron bears a magnetic moment, $\mu_s$. The spin has only two allowed orientations, +1/2 and -1/2. EPR uses a magnetic field to interact with the electrons magnetic moment and to move electrons between the two allowed states. The electrons can sit either parallel, when $M_s = 1/2$, or antiparallel, when $M_s = -1/2$ to the applied magnetic field, Figure 2.9.[10]

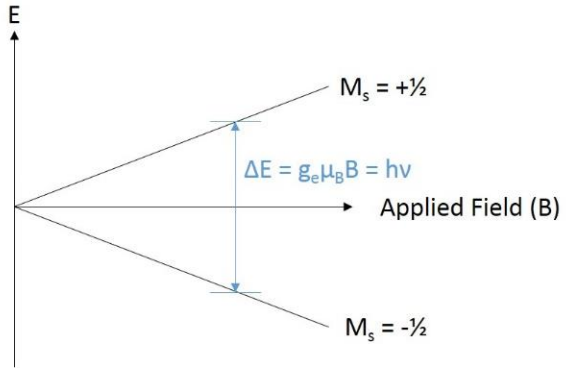


***Figure 2.9*** *A depiction of the energy levels of an unpaired electron in an external magnetic field. Where; $g_e$ is the free electron g value, $\mu_B$ is the Bohr magneton, B is the applied magnetic field flux density, h is Planks constant and v is the frequency of electromagnetic radiation.*

Movement of electrons between the two energy levels can occur when exposed to electromagnetic radiation which is equal to that of the energy difference between the two states. In most application the frequency of the radiation lies in the microwave region of the electromagnetic spectrum. The adsorption of this energy is what is measured by EPR spectroscopy with first derivative of this absorption which is presented in spectra. [10]

Radicals, including hydroxyl and hydroperoxyl, can be detected by EPR spectroscopy owing to their unpaired electrons. However, in the case of hydroxyl and hydroperoxyl radicals these radicals are very short lived and react quickly, hence to extend their lifetime enough to be detected by EPR a radical trap is used to form a radical adduct which is longer lived. For O based radicals 5,5-dimethyl-1-pyrroline N-oxide (DMPO) is often employed to form a DMPO adduct where the radical is located on the oxygen of the nitrous bond, as illustrated in Figure 2.10.[11]

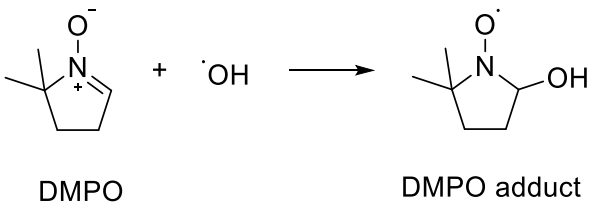


***Figure 2.10*** *The reaction between DMPO and hydroxyl radicals.*

## 2.5 Catalyst Characterisation.

### 2.5.1 X-Ray Diffraction.

Powder X-ray Diffraction (XRD) is a bulk characterisation technique which uses monochromatic X-ray radiation to determine the composition of compounds. It has the ability to provide information on the crystal structure, unit cell dimensions and atomic spacing of a sample.[12]

X-rays are produced by a cathode ray tube, and filtered to produce monochromatic radiation, which is directed towards the sample. These X-rays are then scattered by atoms that reside in an ordered lattice. X-rays can penetrate solids and hence the X-rays are diffracted by multiple crystal planes within the solid, the scattering of the X-rays from different crystal planes can interfere constructively. The X-rays constructively interfere when the distance travelled between the crystal planes is an integer number of wavelength of the incoming X-rays, according to the Bragg's relation, Equation 2.7.[12]

$$n\lambda = 2d\ sin\ \theta$$ *Equation 2.7*

*Where; n is an integer; the order of reflection, λ is the wavelength of incoming X-rays, d is the distance between lattice planes, θ is the angle between X-Rays and the crystal planes.*

The X-ray source is kept stationary and the detector moves throughout different angles to measure intensity as a function of angle.

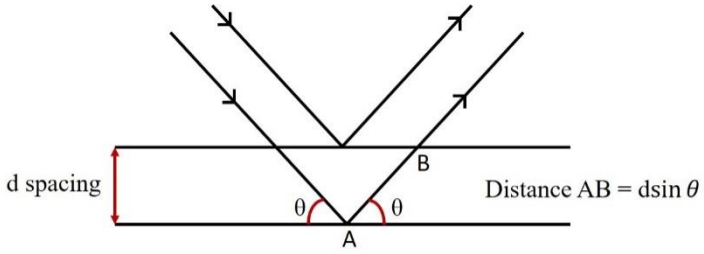


***Figure 2.11*** *A diagram to show the diffraction of incoming X-Rays on succeeding lattice planes.*

Diffractograms are measured and presented as a function of 2θ and from these angles the lattice spacings can be calculated according to Braggs relation, Figure 2.11. Each mineral has a set of unique d-spacings and hence from the comparison of d-spacings samples can be identified.[13]

X-Ray diffraction data was obtained using a (θ-θ) PANalytical X'pert Pro powder diffractometer using a Cu Kα radiation source operating at 40 KeV and 40 mA. Standard analysis was performed using a 40 minute scan between 2θ values of 10-80° with the samples supported on an amorphous silicon wafer. Diffraction patterns of phases were identified using the International Centre for Diffraction Data (ICDD) data base.

### 2.5.2 X-Ray Photoelectron Spectroscopy.

X-Ray Photoelectron Spectroscopy (XPS) is a surface sensitive analysis technique, only probing the first few atomic layers (< 10 nm) of a solid structure. It provides information predominately on the elemental composition and oxidation state of elements within a compound.[13]

XPS focusses a beam of photons from high energy X-rays onto the sample. These photons cause core electrons to be emitted from elements of the sample. Due to electrons being easily absorbed by any materials present measurements have to be undertaken in a vacuum to ensure all electrons reach the detector. According to the photoelectric effect, Equation 2.8, the kinetic energy at which electrons are emitted are related to the energy of the incident photons, the binding energy of the electrons emitted and the work function of the spectrometer, Figure 2.12.[14]

$$h\nu = E_K + E_B + \phi_{sp}$$ *Equation 2.8*

*Where; $h\nu$ is the photons incident energy, $E_K$ is the kinetic energy of the emitted electron, $E_B$ is the binding energy of the electron, $\phi_{sp}$ is the work function of the spectrometer.*

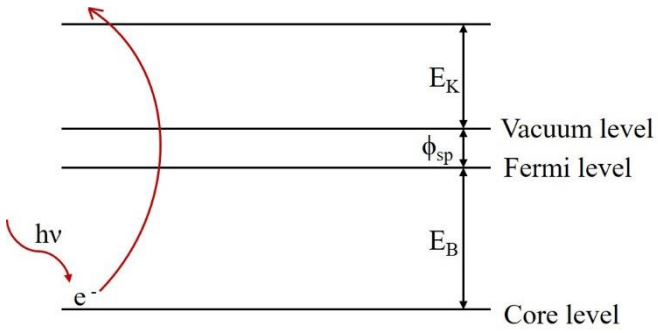


***Figure 2.12.*** *A diagram showing the theory of the electrons emission during XPS.*

By keeping the energy of the incident X-rays constant a XPS spectra may be given as the number of emitted electrons vs. their kinetic energy values or, as according to Equation 2.8, the number of electrons emitted at a certain kinetic energy vs. binding energy. From these binding energies the elemental identity, chemical state, and quantity of a detected element can be characterised.[10]

A Thermo Scientific K-Alpha+ photoelectron spectrometer was used to collect XP spectra utilising a micro-focused monochromatic Al Kα X-ray source operating at 72 W. Data was collected over an elliptical area of approximately 400 $\mu m^2$ at pass energies of 40 and 150 eV for high-resolution and survey spectra, respectively. Sample charging effects were minimised through a combination of low energy electrons and Ar+ ions, consequently this resulted in a C(1s) line at 284.8 eV for all samples. All data was processed using CasaXPS v2.3.20 rev 1.2H using a Shirley background, Scofield sensitivity factors and an energy dependence of −0.6. The intensities of the Pd(3d) and other metal (X) features were used to derive the X:Pd and $Pd^0$:$Pd^{2+}$ surface ratios.

### 2.5.3 Transmission Electron Microscopy.

Transmission Electron Microscopy (TEM) can be used to image objects on a nanoscale. It is hence a useful technique in catalysis to indicate nanoparticle size and when coupled with Energy-Dispersive X-Ray (EDX) spectroscopy can also identify the chemical composition.[15]

It uses a beam of electrons focusing on a small area of sample. When an electron beams hits a surface it can be reflected or penetrate through a sample leading to many possibly pathways of electrons which can be detected, Figure 2.13. In TEM analysis the

electrons that are transmitted through the sample are measured and hence the detectors are place below the sample.[10]

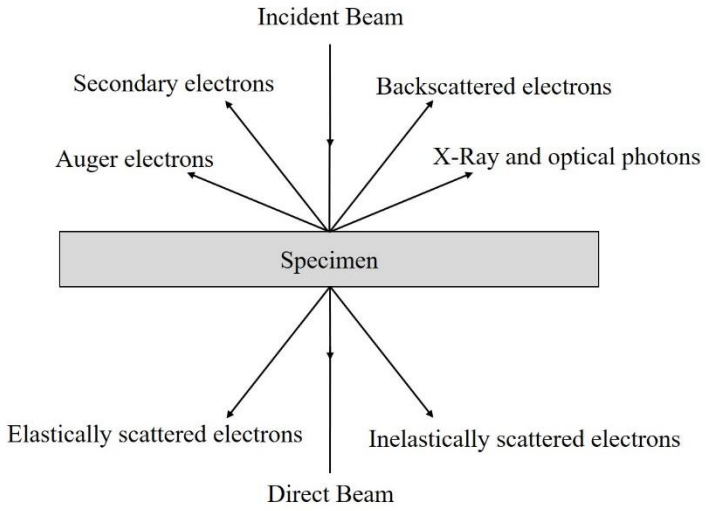


***Figure 2.13.*** *A diagram of all the potential way an electron can interact with a thin sample.*

TEM requires electrons to pass through a sample and hence requires thin samples for probing. Electron microscopes work on the concept that electrons have wavelengths on the order of magnitude of atoms, much shorter than visible light, and hence can interact with atoms present in a sample. Increasing the velocity at which electrons are directed at the sample, by increasing accelerating voltage, decreases their wavelength and hence increases the resolution of the electron microscope according to de Broglie's relationship, Equation 2.9.

$$\lambda = \frac{h}{mv}$$ *Equation 2.9*

*Where; $\lambda$ is the de Broglie wavelength, $h$ is Plank's constant, $m$ is mass, $v$ is velocity.*

When the electron beam is focussed onto the sample the electron that pass through the sample can either be reflected along the same path as the indecent beam or be deflected at varying angles, Figure 2.14. Dark field images can be produced when the electron beam is diffracted at a low angle. If the beam is diffracted at larger angles then high angle annular dark field (HAADF) images can be detected. As electrons are diffracted greatest by heavier elements a correlation between the contrast of the image and the atomic number can be made.[16]

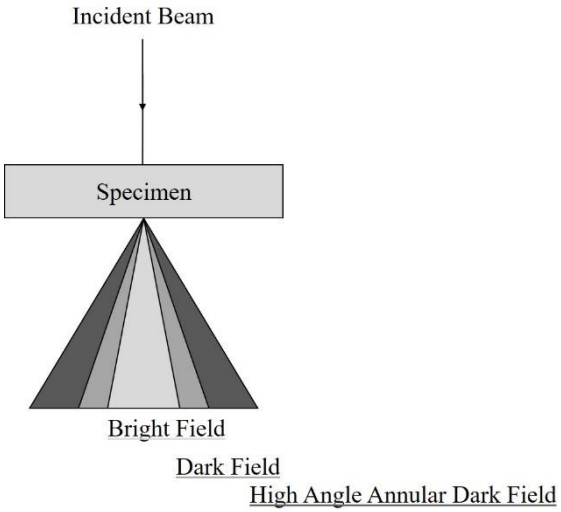


***Figure 2.14.*** *A diagram of the different detection regions in a TEM.*

As the electron beam hits the sample surface electrons within the elemental composition can be excited and emitted as X-rays which can be detected. TEM is often coupled with energy disperse X-ray (EDX) analysis. As the energy emitted is related to the specific energy levels present in an element EDX can be used for elemental analysis.[15]

Transmission electron microscopy (TEM) was performed in Cardiff University on a JEOL JEM-2100 operating at 200 kV. Samples were prepared by dispersion in ethanol by sonication and deposited on 300 mesh copper grids coated with holey carbon film. Energy dispersive X-ray (EDX) analysis was performed using an Oxford Instruments X–Max$^N$ 80 detector and the data analysed using the Aztec software.

Aberration corrected scanning transmission electron microscopy (AC-STEM) was conducted by Xi Lui in Shanghai Jiao Tong University and was performed using a probe-corrected Hitachi HF5000 S/TEM, operating at 200 kV. The instrument was equipped with bright field (BF) and high angle annular dark field (HAADF) detectors for high spatial resolution STEM imaging experiments. This microscope was also equipped with a secondary electron detector and dual Oxford Instruments XEDS detector (2 x 100 mm$^2$) having a total collection angle of 2.02 sr.

### 2.5.4 Thermogravimetric Analysis.

Thermogravimetric Analysis (TGA) is used to measure changes in weight as a function of temperature or time, and hence when a significant drop in weight coincides either with loss of solvent of decomposition of components. Analysis can be determined in an atmosphere of nitrogen, helium, air or under a vacuum. The

technique can be used quantify loss of weight from the catalyst surface. This loss in weight can be attributed to loss of solvent, amount of metallic catalytic residue remaining on support or after use can show the loss of products or coking from the catalyst.[10]

Thermogravimetric analysis was performed on Perkin Elmer Thermogravimetric analyser TGA 4000. The sample (approximately 50 mg) was placed in an aluminium crucible and heated to 800 °C at a ramp rate of 10 °C $min^{-1}$ under either air or nitrogen atmosphere to study the thermal stability of the samples.

### 2.5.5 Temperature Programmed Reduction.

Temperature Programmed Reduction (TPR) is used to probe the oxidation states of metals present on a catalyst. $H_2$ consumption is measured as a function of temperature. A flow of $H_2$ in an inert gas is passed over the sample and using a thermal conductivity detector (TCD) the consumption of gas is measured as the temperature of the sample is linearly increased. It can determine the number of reducible species present on the catalyst surface and reveals the temperature at which the reduction of each species occurs. It can also provide information on the temperature require to produce the desired reduced species on a catalyst, which can be useful for catalyst preparation.[17]

TPR were recorded using a Thermo 1100 series TPDRO. 0.05 g of sample was loaded into the sample tube between two pieces of quartz wool. Helium (15 ml $min^{-1}$) was then passed through the system while it was heated from room temperature to 110 °C at 5 °C $min^{-1}$, where it was held for 30 minutes. The sample was allowed to cool to room temperature and following this the gas was switched to 10% $H_2$ / Ar with a flow rate of 30 ml $min^{-1}$ and the sample was heated up to 800 °C with a 5 °C $min^{-1}$ ramp rate. The profile was recorded using a TCD with positive polarity.

### 2.5.6 Inductively Coupled Plasma Mass Spectroscopy.

Inductively Coupled Plasma Mass Spectroscopy (ICP-MS) is used to quantify trace elements in a mixture. It can detect metals in a solution down to ppb level and hence can be used to determine any metals present in a reaction solution as a result of leaching from the catalyst support.

ICP-MS works by ionising a liquid sample using an inductively coupled plasma. The inductively couple plasma is produced by inductively heating a gas, usually argon, using an electromagnetic coil. The sample then passes into the plasma which ionizes

the individual elements present. A mass spectrometer is then used to separate the ions by mass to charge ratio to identify the elements present. The intensity of the peaks present in the spectrum can then be calibrated with standard known solutions for quantification.[18]

Total metal leaching from the supported catalyst was quantified via ICP-MS of post-reaction solutions. All ICP-MS were run by Simon Waller in Cardiff University Analytical Services. Solutions were analysed using an Agilent 7900 ICP-MS equipped with I-AS auto-sampler. All samples were diluted by a factor of 10 using HPLC grade $H_2O$ (1% $HNO_3$ and 0.5% HCl matrix). All calibrants were matrix matched and measured against a five-point calibration using certified reference materials purchased from Perkin Elmer and certified internal standards acquired from Agilent.

### 2.5.7 Microwave Plasma Atomic Emission Spectroscopy.

Microwave Plasma Atomic Emission Spectroscopy (MP-AES) works in a very similar way to ICP-MS. Here microwaves are used to heat and ionize the nitrogen gas to produce the plasma in which the sample is passed through. Here atomic emission spectroscopy is used to determine the elements present, this works on the principle that when an atom is excited an electron can be promoted to a higher energy level. When this electron then relaxes back to ground state it emits a photon of a certain energy equivalent to the energy gap between the two energy levels, Figure 2.15. Due to all elements having unique electronic structures these characteristic atomic emissions can be used to determine the elements present in a sample and by again by the comparison of peak intensity to standard solutions can be used for quantification.[19]

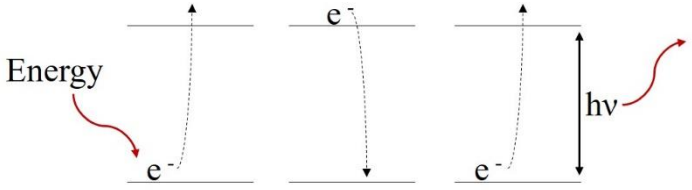


***Figure 2.15.*** *The concept of atomic emission, where a characteristic photon is released.*

For the quantification of metals in catalysts 50 mg of catalyst was dissolved in 10 ml aqua regia and left (16 hours) for the metals to dissolve into solution. The solutions were then diluted to 50 $cm^3$ using deionised water. The analysis was performed in an Agilent 4100 MP-AES. Metal concentrations were determined by response at two characteristic emission wavelengths for Au (242.8, 267.6 nm) and Pd (340.5, 363.5 nm). The concentration responses of Au and Pd were calibrated using commercial

reference standards (Agilent); using concentrations 5mg $ml^{-1}$, 10 mg $ml^{-1}$ and 15 mg $ml^{-1}$, in all cases $r^2 > 0.99$.

## 2.6 References.


1. J. C. Pritchard, Q. He, E. N. Ntainjua, M. Piccinini, J. K. Edwards, A. A. Herzing, A. F. Carley, J. A. Moulijn, C. J. Kiely and G. J. Hutchings, *Green Chem.*, 2010, **12**, 915–921.
2. M. Sankar, Q. He, M. Morad, J. Pritchard, S. J. Freakley, J. K. Edwards, S. H. Taylor, D. J. Morgan, A. F. Carley, D. W. Knight, C. J. Kiely and G. J. Hutchings, *ACS Nano*, 2012, **6**, 6600–6613.
3. J. Pritchard, L. Kesavan, M. Piccinini, Q. He, R. Tiruvalam, N. Dimitratos, J. A. Lopez-Sanchez, A. F. Carley, J. K. Edwards, C. J. Kiely and G. J. Hutchings, *Langmuir*, 2010, **26**, 16568–16577.
4. T. Garcia, W. Weng, B. Solsona, E. Carter, A. F. Carley, C. J. Kiely and S. H. Taylor, *Catal. Sci. Technol.*, 2011, **1**, 1367–1375.
5. R. Barthos, G. Novodárszki and J. Valyon, *Reac Kinet Mech Cat*, 2017, **121**, 17–29.
6. R. Barthos, A. Hegyessy, G. Novodárszki, Z. Pászti and J. Valyon, *Appl. Cat. A: Gen*, 2017, **531**, 96–105.
7. P. Landon, P. J. Collier, A. J. Papworth, C. J. Kiely and G. J. Hutchings, *Chem. Commun.*, 2002, 2058–2059.
8. R. L. Grob and E. F. Barry, *Modern Practice of Gas Chromatography*, John Wiley & Sons, 2004.
9. J. Daintith, *A Dictionary of Chemistry*, Oxford University Press, 2000.
10. B. Imelik and J. C. Vedrine, Eds., *Catalyst Characterization: Physical Techniques for Solid Materials*, Springer US, 1994.
11. G. R. Buettner and R. P. Mason, *Methods in Enzymology*, 1990, **186**, 127 - 133.
12. J. W. Niemantsverdriet, *Spectroscopy in Catalysis: An Introduction*, John Wiley & Sons, 2007.
13. G. Leofanti, G. Tozzola, M. Padovan, G. Petrini, S. Bordiga and A. Zecchina, *Catal. Today*, 1997, **34**, 307–327.
14. C. R. Brundle and A. D. Baker, *Electron Spectroscopy: Theory, Techniques and Applications*, Academic Press, London, 1978, vol. 2.
15. P. L. Gai, E. D. Boyes and E. D. Boyes, *Electron Microscopy in Heterogeneous Catalysis*, CRC Press, 2003.
16. S. J. Pennycook, A. R. Lupini, M. Varela, A. Borisevich, Y. Peng, M. P. Oxley, K. Van Benthem and M. F. Chisholm, in *Scanning Microscopy for Nanotechnology*, eds. W. Zhou and Z. L. Wang, Springer New York, New York, NY, 2006, pp. 152–191.
17. M. Fadoni and L. Lucarelli, *Studies in Surface Science and Catalysis*, 1999, **120**, 177–225.
18. W. Boorn and R. F. Browner, *Anal. Chem.*, 1982, **54**, 1402–1410.
19. L. Balcaen, E. Bolea-Fernandez, M. Resano and F. Vanhaecke, *Analytica Chimica Acta*, 2015, **894**, 7–19.

# 3 Investigations into standard reaction conditions for the selective oxidation of cyclohexane.

## 3.1 Introduction.

The primary focus of work in this project has been on the optimisation of reaction conditions for the oxidation of cyclohexane, Figure 3.1, via the *in-situ* production of hydrogen peroxide ($H_2O_2$). Preliminary testing concentrated on the purely aerobic oxidation using constant low pressure of $O_2$ (3 bar) in glass reactors, work then moved to aerobic conditions in a Parr Autoclave (12 bar 25%$O_2$/$N_2$) before ultimate investigations begun into introducing gas mixtures of both $H_2$ and $O_2$ to produce $H_2O_2$ *in-situ*.

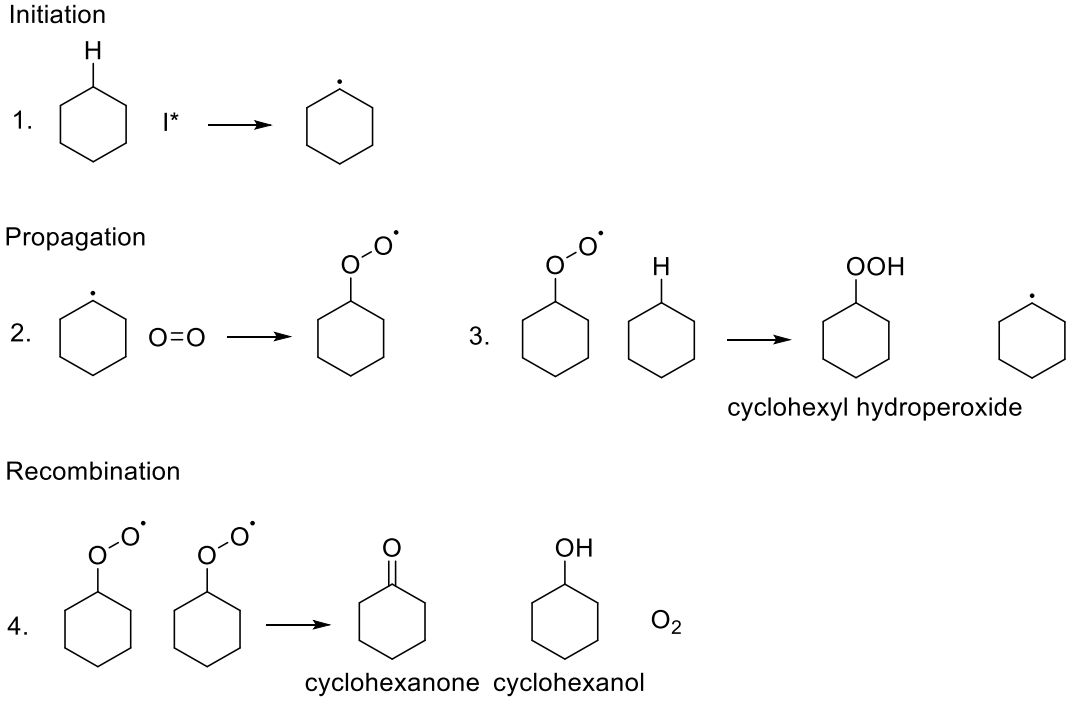


***Figure 3.1.*** *The autoxidation of cyclohexane with molecular oxygen.*[1–4]

## 3.2 Initial Aerobic Testing.

Initial catalytic testing focused on the aerobic oxidation of cyclohexane using glass Colaver reactors. The first positive results for the oxidation came from the repetition of conditions from a 2012 paper by Conte *et al*.[1] This piece of literature used aerobic conditions for the solvent free oxidation of cyclohexane at 140 °C for 17 hours under 3 bar $O_2$ and it is these conditions that have been replicated, Table 3.1.

***Table 3.1.*** *Comparison of previously reported MgO catalysts for the aerobic oxidation of cyclohexane.*

| | Catalyst | Conversion / % |
|---|---|---|
| Conte *et al.*[1] | 1% Au /MgO | 1.9 |
| Liu *et al.*[5] | 1% Pd/ MgO | 0.5 |
| Liu *et al.*[6] | 0.5% Au 0.5% Pd/MgO | 11.0 |
| This work | 5% Au/MgO | 0.16 |
| | 5% Pd/MgO | 0.91 |
| | 2.5% Au 2.5% Pd/MgO | 0.38 |

***Reaction conditions;*** *6 mg catalyst, 7.79 g cyclohexane, 3 bar $O_2$, 140 °C, 17 hours.*

Conte *et al.* investigated Au catalysts supported on MgO for comparison with autoxidation, where there is no additional catalyst. Conte *et al.* observed a slightly greater activity when the catalyst, 1% Au/MgO, was present compared to autoxidation at 1.9 and 1.1 % respectively. However, it should be noted that the autoxidation did show appreciable activity but at a lower selectivity to cyclohexanol and cyclohexanone and an increased selectivity to the CHHP intermediate. They also added radical initiators that increased the activity of the catalyst up to 5.0% but autoxidation activity was also increased to 6.7 % conversion, indicating both catalysed and uncatalyzed the reaction mechanism is radical based.[1]

### 3.2.1 Colaver glass reactors

#### 3.2.1.1 Effect of catalyst; different metals and support

Firstly, monometallic Au, Pd and bimetallic AuPd catalyst supported on both $TiO_2$ and MgO were investigated. Catalysts were prepared by wet impregnation with a total metal loading of 5 wt.% as discussed in Chapter 2, Section 2.3.1. Initially, the catalysts were tested for the synthesis and degradation of $H_2O_2$, Table 3.2. Experiments to determine the synthesis and degradation of $H_2O_2$ were carried out in two separate reactions as detailed in Chapter 2, Sections 2.4.1 and 2.4.2.

***Table 3.2.*** *$H_2O_2$ synthesis and degradation activity for Au, Pd and AuPd supported on $TiO_2$ and MgO.*[7]

| Catalyst | $H_2O_2$ synthesis / $mol_{H_2O_2}\ kg_{cat}^{-1}\ hr^{-1}$ | $H_2O_2$ degradation / $mol_{H_2O_2}\ kg_{cat}^{-1}\ hr^{-1}$ |
|---|---|---|
| 5% Au/$TiO_2$ | 7 | 24 |
| 5% Pd/$TiO_2$ | 30 | 247 |
| 5% AuPd/$TiO_2$ | 64 | 129 |
| 5% Au/MgO | 0 | 12 |
| 5% Pd/MgO | 29 | 405 |
| 5% AuPd/MgO | 29 | 535 |

***Reaction conditions;*** *Synthesis; 0.01 g catalyst, 2.9 g $H_2O$, 5.6 g MeOH, 2.9 MPa 5%$H_2$/$CO_2$, 1.1 MPa 25% $O_2$/$CO_2$, 2 °C, 1200 rpm. Degradation; 0.01 g catalyst, 0.68 g 50 wt.% $H_2O_2$, 2.22 g $H_2O$, 5.6 g MeOH, 2.9 MPa 5%$H_2$/$CO_2$, 2 °C, 1200 RPM.*

$TiO_2$ is a commonly used support for the direct synthesis of $H_2O_2$[7] and has also been investigated for the oxidation of cyclohexane.[8] MgO though not as efficient for $H_2O_2$ synthesis, due to its large degradation ability,[7] has been investigated for cyclohexane oxidation.[1,5,9]

These catalysts were then for tested cyclohexane oxidation under solvent free conditions in the Colaver glass reactors; 10 ml (93 mmol) cyclohexane, 6 mg catalyst, 3 bar constant pressure of $O_2$, 140 °C, 800 RPM, 17 hours, using 0.5 ml mesitylene external standard. For these tests, the CHHP intermediate has not been determined, however this is an important intermediate in KA oil production and it should be noted that this would be expected in addition to cyclohexanol and cyclohexanone. All catalysts tested, except 5% $Pd/TiO_2$, showed higher yields to KA oil than the autoxidation reaction without the additional catalyst, Figure 3.2.

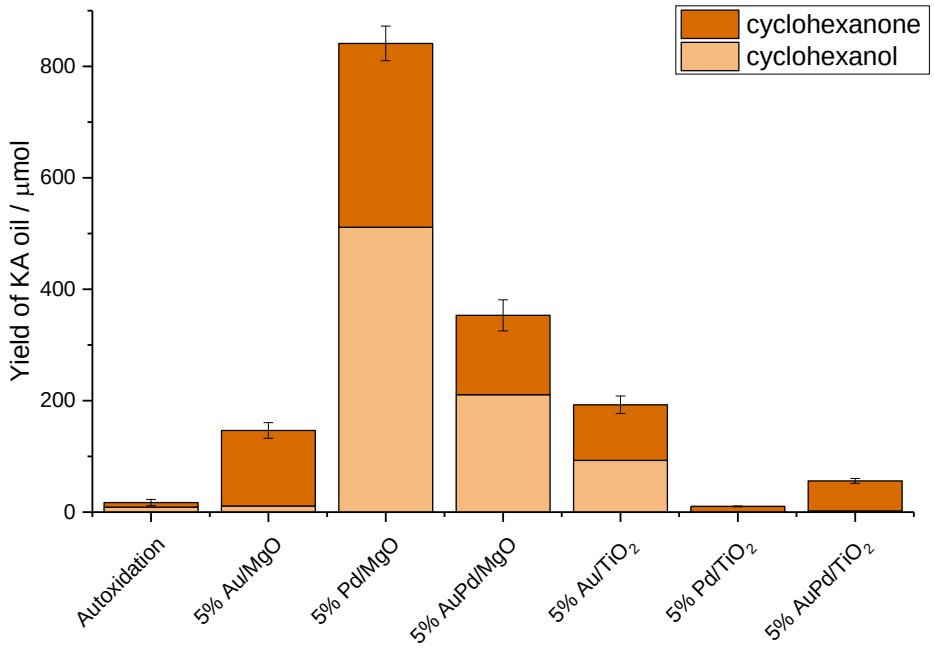


***Figure 3.2*** *The combined yield of cyclohexanol and cyclohexanone with Au, Pd and AuPd catalyst supported on MgO and $TiO_2$ and autoxidation.* ***Reaction conditions;*** *7.79 g (93 mmol) cyclohexane, 6 mg catalyst, 3 bar $O_2$, 140 °C, 17 hours, 800 RPM.*

For the $TiO_2$ supported catalysts the monometallic 5 % Au /$TiO_2$ gave the highest yield of KA oil (193 µmol). Contrast is seen in the activity of the monometallic 5 % Pd nanoparticles supported on $TiO_2$ and MgO. $TiO_2$ supported Pd showed very limited yield of both cyclohexanol and cyclohexanone (10 µmol) whereas when supported on MgO showed the highest yield (941 µmol), for the MgO catalysts. Comparison of the monometallic 5 % Au nanoparticles supported on both $TiO_2$ and MgO shows both producing similar yields of KA oil (193 and 147 µmol respectively). Overall, it could

be concluded that the MgO is the superior support under these experimental conditions. Although it has previously been shown that MgO alone can show some catalytic activity, with Conte *et al.* reporting 1.1 % conversion with MgO under identical conditions to those used here.[1] Hence some activity could be attributed to the support alone. In a patent released by Whiston *et al.* they have observed 1% AuPd/MgO to have greater activity than the corresponding $TiO_2$ supported catalyst at 11.0 and 4.5% conversions respectively. The MgO supported catalyst also showed a greater selectivity towards KA oil compared to $TiO_2$ at 95 and 63 % respectively.[10]

As reported in Table 3.1 Lui *et al.* have previously reported that the addition of Pd to Au/MgO catalyst increased the activity dramatically from 1.9% to 11% conversion, for 1% Au/MgO and 1% AuPd/MgO respectively.[6] Within the work reported here although the bimetallic catalyst has increased upon the activity of the 5% Au/MgO catalysts the 5% Pd/MgO gave the greatest activity. The catalysts reported here have 5 times greater active metal content compared to previously reported catalysts.[1,5,6] This increase in metal content has enhanced the activity of the monometallic Pd catalyst from 0.5%[5] to 0.9% conversion. However, the Au and AuPd catalysts have shown much lower activity, this could be attributed to increasing metal content decreasing the dispersion of the metals on the catalyst surface. With higher metal loadings and increased particle sizes the available surface area, and hence surface active sites, is decreased and this can decrease activity.[11] For Pd catalysts it has previously been observed that increasing metal loading does not have a significant effect on particle size and hence this could explain why no decrease in activity is observed for the higher metal loading.[12] To confirm whether the decrease in activity for these higher loaded catalysts were due to decreased metal dispersion and decreased available active sites chemisorption could be used to calculate the surface coverage to the catalyst. TEM imaging would be useful to determine if the particle sizes are increased with increased metal loading.

For this series of catalysts 5 % Pd/MgO has produced the highest yield of KA oil and hence it is this superior catalyst that was used for subsequent investigations.

### 3.2.1.2 Optimising reaction conditions for the aerobic oxidation of cyclohexane.

#### 3.2.1.2.1 Effect of temperature.

The current industrial oxidation conditions use high temperatures, in excess of 150 °C,[13,14] and hence there is an aim to reduce the temperature of the reaction while maintaining as high yield and selectivity as possible. This would begin to fulfil the aim to move to towards greener chemistry conditions within a catalytic system.[15] Hence the next parameter to be studied was temperature. The catalyst (5% Pd/MgO) was used in the temperature range of 80 to 140 °C and compared to the results produced under the uncatalysed, autoxidation, conditions, Figure 3.3.

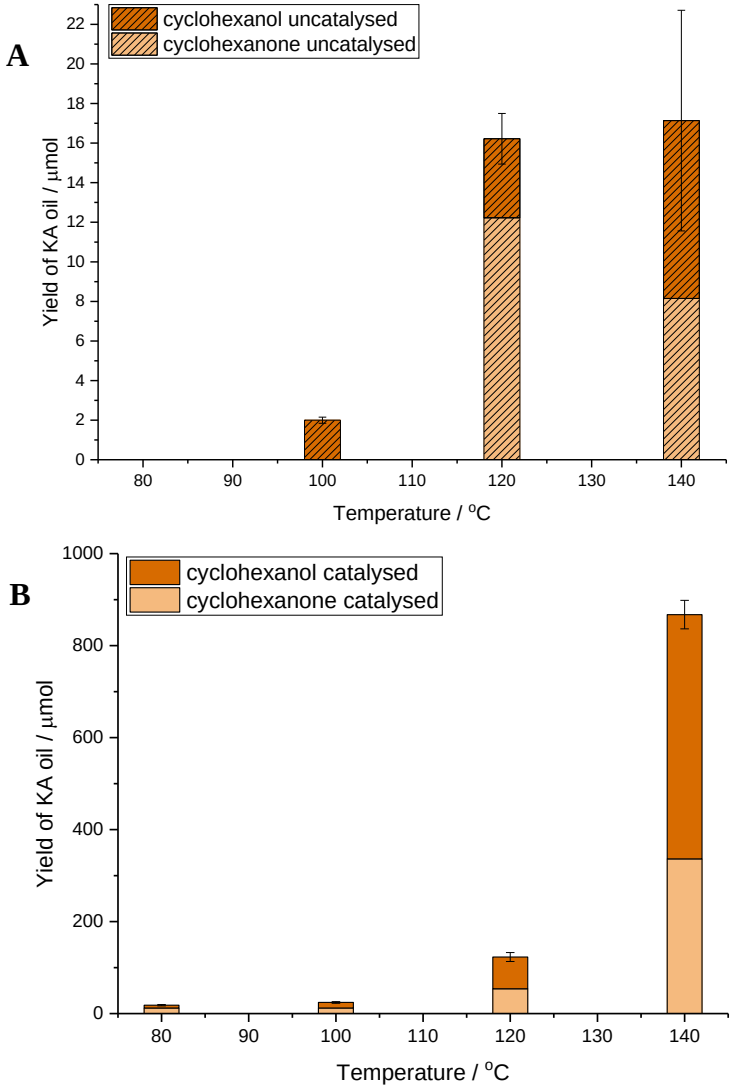


***Figure 3.3.*** *The yield of KA oil at varying temperatures for the un-catalysed autoxidation (A) and catalysed (B) with 5 % Pd/MgO.* ***Reaction conditions;*** *7.79 g (93 mmol) cyclohexane, 6 mg catalyst, 3 bar $O_2$, 17 hours, 800 RPM.*

With the added catalyst KA oil was yielded at all temperatures, whereas measurable yields were only seen above 120 °C when no catalyst is present. Both with and without

a catalyst it has been observed that an increase in temperature has led to an increase in the yield of KA oil. With the additional Pd catalyst, at lower temperatures up to 100 °C, a gradual increase in yield, from 18 µmol at 80 °C to 24 µmol at 100 °C is seen. Above 120 °C there is a more dramatic increase in the yield of products, from 123 mol at 120 °C to 867 µmol at 140 °C. It is promising that this catalyst has shown to produce higher yields, than without the catalyst, at lower temperatures.

#### 3.2.1.2.2 Effect of reaction time.

Current reaction times of 17 hours are utilised as standard[1], due to slow reactions and long induction times,[8] hence a screening of reaction times was conducted to see if this could be reduced through a catalysed pathway. Again 5 % Pd/MgO was employed in and compared to what is seen without a catalyst present, Figure 3.4. This product distribution as a function of reaction time was observed via a series of reactions, at different reaction times, under the same conditions of temperature and pressure.

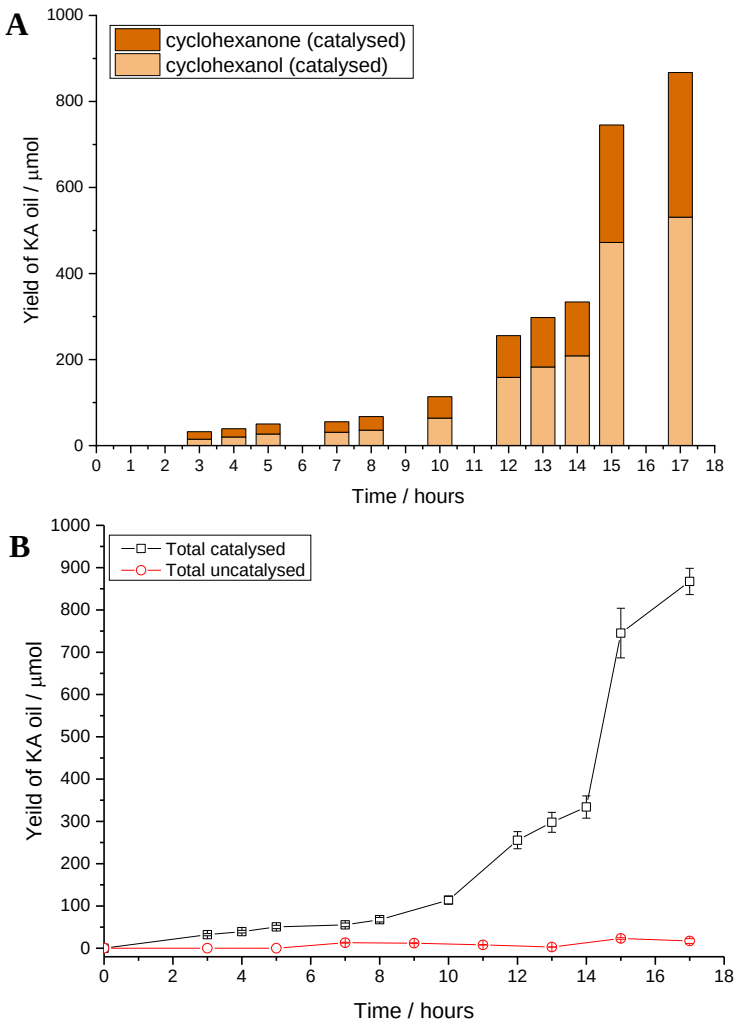


***Figure 3.4.*** *The combined yields of cyclohexanol and cyclohexanone produced with 5 % Pd / MgO catalyst (A) and the comparison between catalysed and uncatalyzed (B) at varying reaction times.* ***Reaction conditions;*** *7.79 g (93 mmol) cyclohexane, 6 mg catalyst, 3 bar $O_2$, 140 °C, 800 RPM.*

As expected, an increase in yield is seen with increasing reaction time. In the presence of the 5% Pd/MgO catalyst KA oil can be seen at all reaction times above 3 hours whereas without the catalyst yields are only seen after 7 hours. Initially, 3 to 10 hours, the catalyst shows a gradual increase in yield from 32 to 114 µmol where after this a more dramatic increase is seen up to 867 µmol at 17 hours. For autoxidation over the whole reaction time the increase in product yield is much less significant.

The less substantial increase in yield at lower reactions times for the 5 % Pd/MgO catalyst could indicate an induction period in the reaction. The initial stage of the reaction mechanism is initiation via H abstraction, Figure 3.1. The C-H bond dissociation energy is around 418 kJ $mol^{-1}$ and hence is a fairly strong bond which will require considerable energy to break.[16] Hence this induction period could be caused by the initiation step and increase in energy needed for this system to be able to cleave enough bonds for products to be observed. Another possibility is that within this time period the surface of the catalyst is altered to produce an active form, such as a change in particle size or metal oxidation state, increasing the product yield thereafter. Induction periods are well noted in hydrocarbon oxidation reaction and for cyclohexane.[8,17] In aerobic cyclohexane oxidation these induction periods have been attributed to the limit in the adsorption and activation of $O_2$ onto a catalyst surface. This induction period is the time for which it takes for free-radical concentration to increase to the point at which the propagation of the reaction can maintain the reaction.[17] The induction period is strongly affected by the initiation rate of the reaction.[17] It is believed that metal catalysts can increase the initiation rate of the aerobic oxidation and hence the observation of a shorter induction period when the catalyst is presence compared to absence could be attributed to this.[1,18] Conte *et al.* showed, via electron paramagnetic resonance (EPR), that the addition of 1% Au/MgO increases the concentration of oxygen based radicals from the cleavage of O-O bond in the CHHP intermediate. The 1% Au/MgO accelerated the radical chain reaction by the increase in these radical chain carriers.[1]

#### 3.2.1.2.3 Effect of stirring speed.

The chosen 5 % Pd/MgO catalyst has also been investigated to see the effect the stirring speed can have on the reaction products, Figure 3.5. With varying the stirring speed the contact between the catalyst and the reactants can be affected. Stirring of the reactants and catalyst can decrease diffusion limitations. Once more this has been

investigated in the Colaver reactors using a series of reactions under identical temperatures and pressures and varying each reaction with stirring speeds between 500 and 1300 RPM.

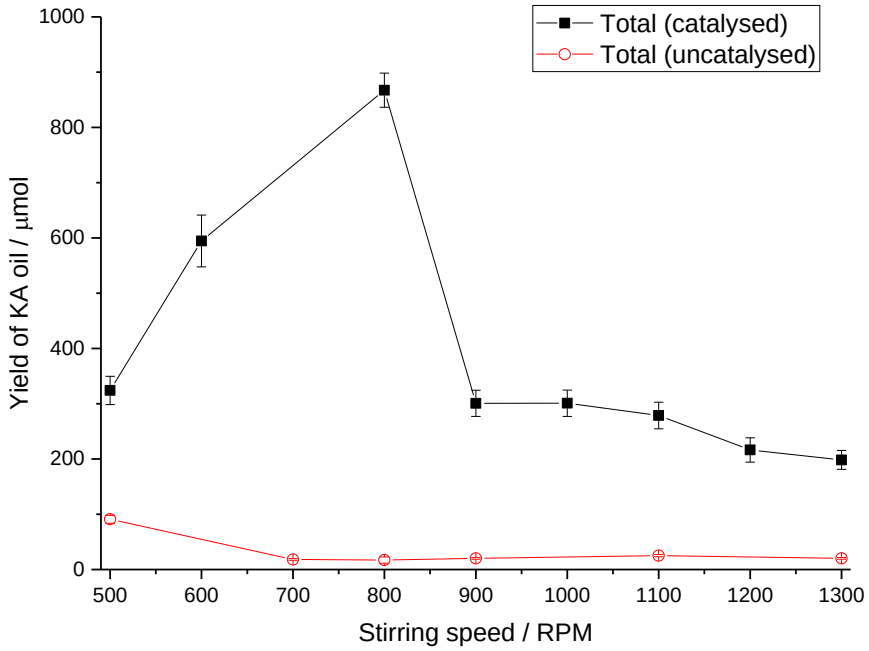


***Figure 3.5.*** *The combined yields of cyclohexanol and cyclohexanone produced with no additional catalyst, autoxidation, and with added 5 % Pd / MgO catalyst at different stirring speeds.* ***Reaction conditions;*** *7.79 g (93 mmol) cyclohexane, 6 mg catalyst, 3 bar $O_2$, 140 °C, 17 hours.*

In the presence of 5% Pd/MgO an increase in yield is observed with increasing stirring speed from 500 to 800 RPM due to better dispersion and improved diffusion of the reactants to the catalyst surface. However, a decrease and flatlining in yield is seen from 900 RPM and above, it is suggested that this occurs due to the catalyst accumulating on the sides of the reactor, limiting the availability of the catalyst surface to the reaction liquid. In the absence of the catalyst yields of KA oil are much lower at all stirring speeds. This indicates that at higher stirring speeds with the catalyst, there is still some contact with the catalyst but this has been dramatically reduced.

For autoxidation, there is a more gradual increase in yield with stirring speed but not as obvious trend or change as seen with the additional catalyst. This is to be expected as here it is only the diffusion of the gas into the liquid that could possibly be affected by stirring speed.

### 3.2.2 Parr Autoclave Reactor.

Some aerobic oxidation tests have also been performed in the high-pressure Parr autoclave. Again, solvent free conditions have been used with 6 mg catalyst. The

different metal and support combinations discussed in Section 3.2.1 have also been tested in the Parr autoclave. Here 12 bar 25% $O_2$ in $N_2$ is used which is equivalent to 3 bar pure $O_2$, which has been used in the Colaver reactors, Figure 3.6.

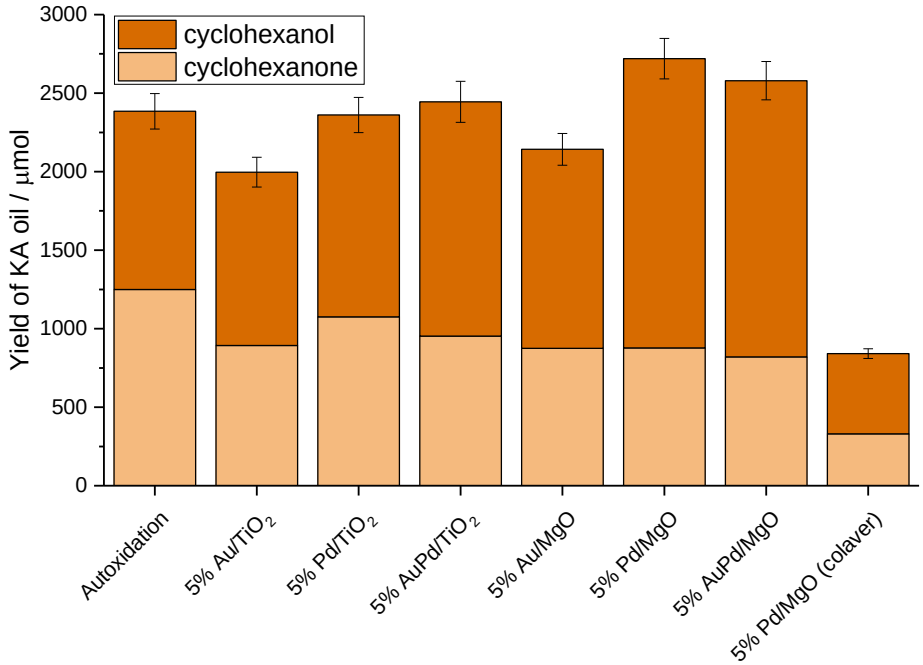


***Figure 3.6.*** *The combined yield of cyclohexanol and cyclohexanone with Au, Pd and AuPd catalyst supported on MgO and $TiO_2$.* ***Reaction conditions;*** *7.79 g (93 mmol) cyclohexane, 6 mg catalyst, 12 bar 25% $O_2$ in $N_2$, 140 °C, 17 hours, 800 RPM.*

The yield to KA oil in the autoclaves are on average a magnitude larger than those seen in the Colaver reactors. This is due to the increased gas pressure used in the autoclaves, despite the same molar quantity of $O_2$. Henry's law (Equation 3.1) states that, at a constant temperature, the solubility of a gas is directly dependent on the partial pressure of gas.[19]

$$C = kP_{gas} \qquad \textit{Equation 3.1}$$

*Where; C is solubility, k is Henry's constant and $P_{gas}$ is the partial pressure of the gas.*

Due to the dilution of the autoclave gas feed with nitrogen, four times the pressure is required for the same molar amount of $O_2$ and hence this increase in pressure increases solubility of the gas mixture. With an increase in solubility of the gas into the liquid reaction medium there is more $O_2$ gas available to react and hence increased yields have been observed for the autoclave reactor compared to the Colaver reactor. The increase in yield is also seen for autoxidation and the comparison between the catalyst and autoxidation is not as significant as is seen in the Colaver reactors.

## 3.3 Investigating standard reaction conditions using high pressure autoclaves for the oxidation of cyclohexane via the *in-situ* production of $H_2O_2$.

### 3.3.1 Introduction.

One of the main challenges facing *in-situ* oxidation is overcoming the conditions gap that exists between the direct synthesis of $H_2O_2$ and the aerobic oxidation of cyclohexane, as detailed in Table 3.3.

***Table 3.3.*** *Comparison of optimum conditions for $H_2O_2$ synthesis and cyclohexane oxidation.*

| Condition | $H_2O_2$ synthesis | Cyclohexane oxidation |
|---|---|---|
| Temperature | 2 ºC | 140 ºC |
| Time | 0.5 hours | 17 hours |
| Reactant gases | $H_2$ and $O_2$ diluted in $CO_2$ | $O_2$ |
| Solvent | Water/methanol | Solvent free |
| Acidic or basic | Acidic solution and acidic supports preferred | Basic catalyst supports (e.g. MgO[1]). |

One of the stark differences between optimum $H_2O_2$ synthesis and cyclohexane oxidation conditions is the operating temperatures. $H_2O_2$ is known to decompose at elevated temperatures and hence optimum reaction conditions have chosen sub ambient temperatures to reduce the formation of the by-product $H_2O$.[20] However for aerobic cyclohexane oxidation temperatures are often employed above the autoxidation temperature, 140 ºC, due to the high energy required to initiate the reaction.[18]

Direct synthesis of $H_2O_2$ is often carried out using mixtures of $H_2$ and $O_2$ diluted in $CO_2$ this is not only useful for safety reasons, to keep $H_2$ and $O_2$ out of the explosive region, 4 – 70% $H_2$ in $CO_2$,[21] but also $CO_2$ can act as an *in-situ* acid promoter to the reaction. In solution $CO_2$ can form carbonic acid which stabilises the production of $H_2O_2$.[22] Santos *et al.* observed when changing the diluting gas from $CO_2$ to $N_2$ a reduction in $H_2O_2$ productivity has been observed from 28 to 13 $mol_{H_2O_2}\ kg_{cat}^{-1}\ hr^{-1}$ at 25 ºC in water solvent using 1% AuPd/$TiO_2$.[23] For this reason $CO_2$ would be the preferred diluting gas for any oxidation via the *in-situ* production of $H_2O_2$. However when cyclohexane is mixed with $CO_2$ it becomes an expanding solvent [24] as such for safety reason $N_2$ must be used as the diluting gas for all *in-situ* experiments.

As discussed, acidic reaction solutions are preferred for $H_2O_2$ synthesis to reduce the formation of water and stabilise $H_2O_2$. Investigation into catalytic support materials also showed that acid supports can increased $H_2O_2$ productivity.[7,25] Both the acidic pre-treatment [25] of supports as well as increasing the isoelectric point of the support [7] have shown a positive effect on $H_2O_2$ production. Basic supports, such as MgO, have shown low selectivity towards to $H_2O_2$ due to increased degradation of $H_2O_2$.[7] However for aerobic oxidation MgO has been utilised as a support and shown increased activity upon more acidic supports.[5] This shows the difficulties that could arise not only in the condition requirements but also catalytic requirements for the *in-situ* oxidation of cyclohexane.

All these experiments in this section have been conducted with a 0.5% Au 0.5% $Pd/TiO_2$ catalyst prepared by the standard wet impregnation procedure as outlined in Chapter 2. This catalyst produced a $H_2O_2$ synthesis activity of 69 $mol_{H_2O_2}$ $kg_{cat}^{-1}$ $hr^{-1}$ and a degradation activity 239 $mol_{H_2O_2}$ $kg_{cat}^{-1}$ $hr^{-1}$ using ambient temperature in a water/methanol solvent. It has shown that this catalyst is effective in producing $H_2O_2$ however is non-selective as some degradation of $H_2O_2$ is also observed.

XPS analysis of the catalysis shows a Pd:Au surface ratio of 18.5 with a $Pd^0$:$Pd^{II}$ ratio of 1.3. With the 1:1 weight ratio used for the 1% $AuPd/TiO_2$ a Pd:Au molar ratio of 1.9 would be expected. This increased Pd:Au compared to experimentally calculated value indicated a core-shell structure with Pd predominately on the surface (shell) of the AuPd nanoparticles. The Pd present on the surface is a mixture of both metallic and $Pd^{2+}$.

TEM analysis has shown predominately sub-nanometer particles with an average particle size of 0.86 ± 0.2 nm, Figure 3.7. However, some larger particles, 20 – 40 nm, were also observed but not enough were seen for a particle count and hence have not been included in the average particle size.

In the literature AuPd catalysts prepared by conventional impregnation have been reported to show a Pd shell Au core structure with predominately PdO on the surface.[26] These observations support the previous literature.

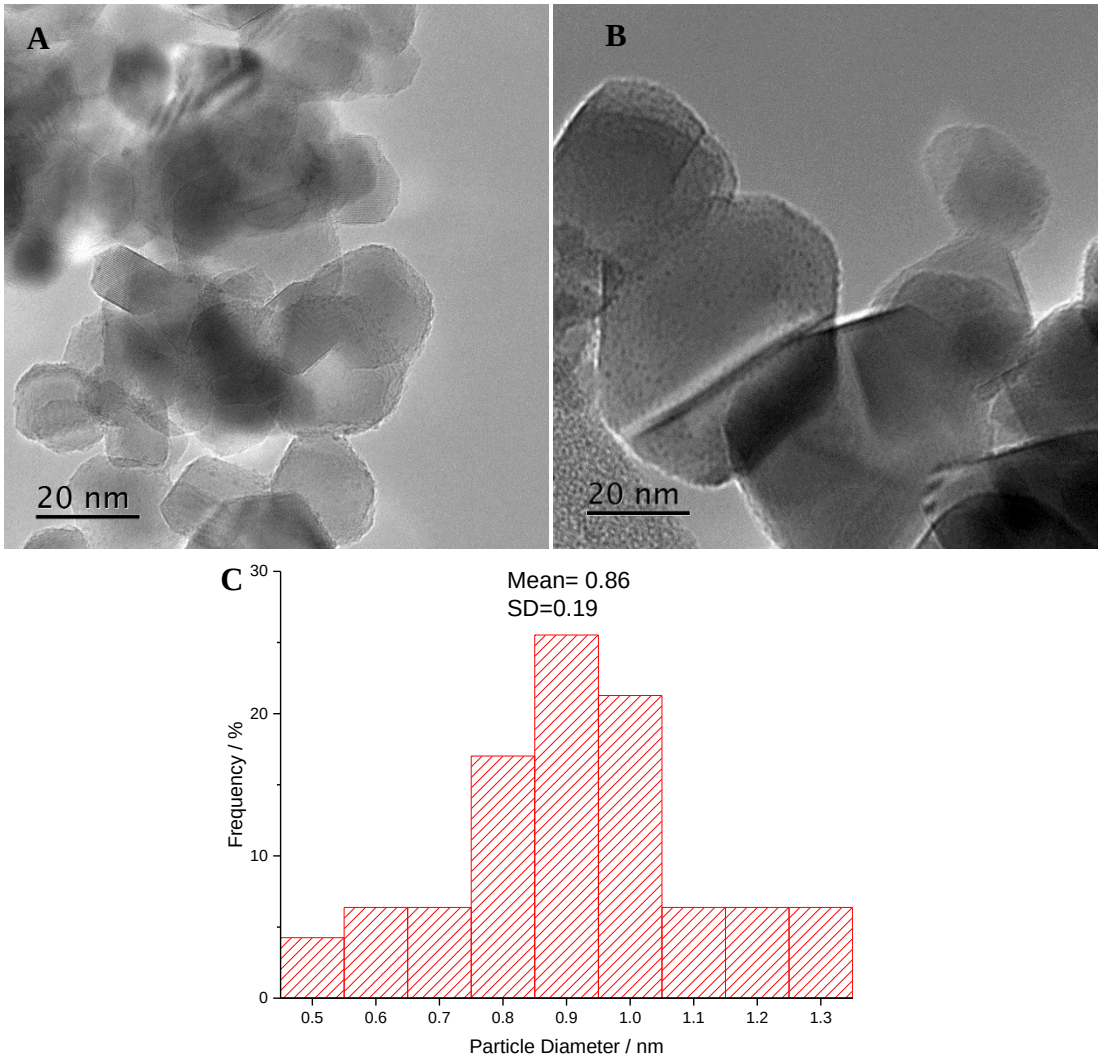


***Figure 3.7.*** *TEM images (A and B) and corresponding particle size distribution (C) for 1% AuPd/$TiO_2$.*

### 3.3.2 Choice of solvent.

Initial testing began with a methanol solvent in a 3:1 methanol:cyclohexane (vol/vol). Methanol was the first choice solvent as it is used in the standard $H_2O_2$ synthesis reaction and offers good solubility of both $H_2$ and $O_2$.[27,28] Firstly commercial $H_2O_2$ (4 wt.%) was added directly to the system prior to heating to determine if cyclohexane could be oxidised by $H_2O_2$ under these reaction conditions. Both products, cyclohexanol and cyclohexanone, were qualitatively identified by GC-MS. However, cyclohexane is immiscible in methanol and hence a biphasic reaction mixture was produced. This made for complications in the product analysis as the products could be seen in both phases. Hence work progressed onto looking at different solvents in which cyclohexane is miscible.

Cyclohexane was found to have better solubility in several solvents, including tert-butanol, iso-propanol and ethanol[29] and so these solvents were investigated. All solvents were first tested with $H_2O_2$ (4 wt. %) and 1% AuPd/$TiO_2$ and all showed presence of KA oil. All solvents were then tested using *in-situ* synthesised $H_2O_2$ and qualitatively analysed using GC-MS, Table 3.4.

***Table 3.4.*** *Qualitative results produced from GC-MS analysis from the use of different solvents in the in-situ oxidation of cyclohexane.*

| Solvent | Products | Other products | Hydrogen Conversion / % |
|---|---|---|---|
| Tert-butanol | Cyclohexanol and cyclohexanone | tert-butanol hydro peroxide | 95 |
| Ethanol | None | 1,1-diethoxyethane | 94 |
| Iso-propanol | Cyclohexanol | 2-isopropoxypropan-1-ol | 91 |

***Reaction conditions****; 80 °C, 17 hours, 0.050 g 1 % AuPd /$TiO_2$ catalyst, 6.37 g solvent, 2.13 g cyclohexane, 29 bar 5 % $H_2$ / $N_2$ and 11 bar 25 % $O_2$ / $N_2$, 1200 RPM.*

In tert-butanol both products were identified via GC-MS, whereas with iso-propanol only cyclohexanol can be seen and with ethanol no products were identified. Also, with iso-propanol and ethanol the solvents have reacted under the reaction conditions, Table 3.4, and hence here tert-butanol seems to be the preferred solvent system.

GC-MS has identified tert-butanol hydroperoxide (TBHP) peaks and hence this could be forming *in-situ* and could help oxidation as it is a stronger oxidant compared to $H_2O_2$. TBHP is known to be a strong oxidising agent, especially in cyclohexane oxidation [30] and hence could be a potentially powerful secondary oxidant.

### 3.3.3 *Ex-situ* vs. *in-situ* oxidation.

Under purely aerobic conditions (80 °C, 17 hours, 11 bar $O_2/N_2$) no yield of KA oil was seen. Hence it was investigated whether the *ex-situ* addition of $H_2O_2$ could also react under these conditions and whether *in-situ* production or directly adding the oxidant is optimal. The amount of $H_2O_2$ added was calculated as if all the $H_2$ present in the *in-situ* experiments (2.51 mmol) was converted to $H_2O_2$ (2.51 mmol, 0.085 g), this would be the highest concentration of $H_2O_2$ possible, Figure 3.8. The addition of *ex-situ* $H_2O_2$ was tested both under $O_2$ and $N_2$ to observe the differences between the direct oxidation by $H_2O_2$, under $N_2$, and the oxidation with $H_2O_2$ under aerobic coniditions. However, it should be noted that commercially sourced $H_2O_2$ has additional stabilisers present to increase shelf life by reducing thermal

decomposition.[31] These additional stabilisers could affect the reaction by stabilising the $H_2O_2$ or by changing the pH of the reaction medium or even interact with the catalyst surface.

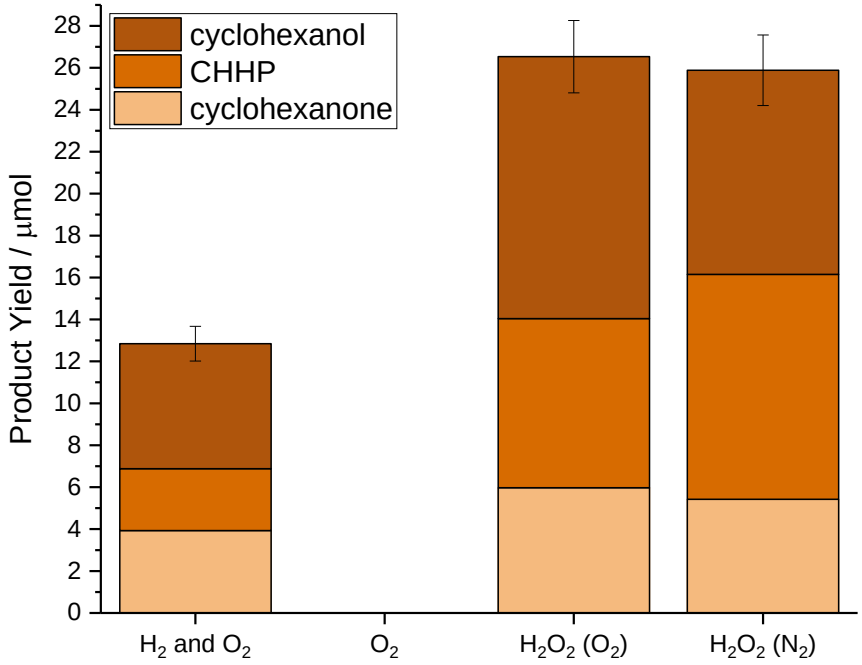


***Figure 3.8.*** *The comparison of KA oil yield with direct addition of $H_2O_2$ in a 1 wt. % concentration under both $O_2$ and $N_2$ and the in-situ production of $H_2O_2$.* ***Reaction conditions;*** *80 °C, 17 hours, 0.05g catalyst, 6.37 g tert-butanol, 2.13 g (25 mmol) cyclohexane, 0.17g 50 wt.% $H_2O_2$, 11 bar 25 % $O_2$ / $N_2$ and 29 bar $N_2$ or 40 bar $N_2$ or 29 bar 5 % $H_2$ / $N_2$ and 11 bar 25 % $O_2$ / $N_2$, 1200 RPM.*

It can be observed that *ex-situ* addition produced a greater yield than *in-situ* produced $H_2O_2$. However, it should be noted that the amount of $H_2O_2$ added was if all $H_2$ was converted directly to $H_2O_2$ under these reaction conditions not all the $H_2$ is converted and not all with 100% selectivity to $H_2O_2$. Some $H_2$ conversion could be attributed to the direction formation of $H_2O$ from $H_2$ and $O_2$. $H_2O_2$ is thermally unstable and hence some $H_2O_2$ will have decomposed during the heating up of the reactor. No $H_2O_2$ was measured, by titration, after the 17 hour oxidation reaction for both the *ex-situ* and *in-situ* $H_2O_2$. As discussed later in Section 3.3.9 the catalysts are reduced during the reaction and hence some $H_2$ conversion could be attributed to this also. Hence the concentration of $H_2O_2$ produced *in-situ* is likely to be much lower than added *ex-situ* and a full comparison cannot be made.

Very similar yields were obtained when $H_2O_2$ was used with $O_2$ and $N_2$ gases at 26.5 and 25.9 µmol respectively. This indicates that $H_2O_2$ is directly oxidising cyclohexane rather than acting as an initiator for the aerobic oxidation again indicating that under these mild reaction conditions that the aerobic autoxidation is very limited.

### 3.3.4 Effect of reaction time.

Different reaction times have been explored, keeping all other reaction conditions constant, Figure 3.9. With $O_2$ as an oxidant, harsh conditions such as 140 °C and 3 bar pure $O_2$ for long reaction times of 17 hours are usually used.[6] With $H_2O_2$ as an oxidant an excess of oxidant to substrate is usually used but under milder conditions and shorter reaction times. For example Mayani *et al.* used Au, Pd and AuPd supported on carbon with 2:1 $H_2O_2$:cyclohexane for only 8 hours.[32] Excesses of $H_2O_2$ are often utilised due to the increased decomposition of $H_2O_2$ at the elevated temperatures used for oxidation reactions. The aim with the use of $H_2O_2$ produced *in-situ* is that the excesses are not needed as the $H_2O_2$ can be produced and utilised in the oxidation reaction immediately.

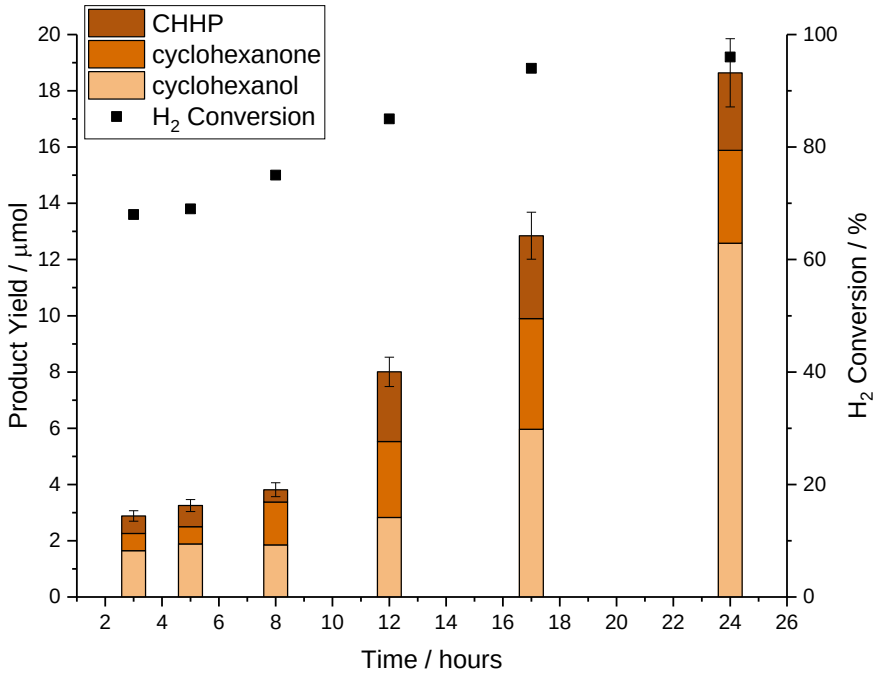


***Figure 3.9.*** *The yield of KA oil produced at varying reaction times.* ***Reaction conditions;*** *80 °C, 0.05 g 1 % AuPd/$TiO_2$ wet impregnation catalyst, 6.37 g tert-butanol, 2.13 g (25 mmol) cyclohexane, 29 bar 5 % $H_2$ / $N_2$ and 11 bar 25 % $O_2$ / $N_2$, 1200 RPM.*

As expected, a gradual increase in yield is seen as reaction time increases, although yields of KA oil have been observed at much shorter reaction times than normally employed in the aerobic oxidation.[1,5,6] High $H_2$ conversions can be seen for all reaction times. Starting from around 70 % $H_2$ conversion at 3 – 5 hours, increasing to 95% after 17 hours. This correlates with the increase in KA oil yield from 2.9 µmol at 3 hours up to 18.6 µmol at 24 hours, Figure 3.9. With this increasing $H_2$ conversion and increasing product yield the selectivity towards $C_6$ products based on $H_2$ increases as a function of reaction time, Table 3.5.

***Table 3.5.*** *$H_2$, cyclohexane conversion and selectivity as a function of reaction time.*

| Reaction time /h | $H_2$ Conversion / % | Total product yield / % | Selectivity to all $C_6^*$ products based on $H_2$ / % |
|---|---|---|---|
| 3 | 68 | 0.01 | 0.17 |
| 5 | 69 | 0.01 | 0.19 |
| 8 | 75 | 0.02 | 0.20 |
| 12 | 85 | 0.03 | 0.37 |
| 17 | 94 | 0.05 | 0.54 |
| 24 | 96 | 0.07 | 0.77 |

***Reaction conditions****; 80 °C, 17 hours, 0.050 g 1 % AuPd /$TiO_2$ catalyst, 6.37 g solvent, 2.13 g cyclohexane, 29 bar 5 % $H_2$ / $N_2$ and 11 bar 25 % $O_2$ / $N_2$, 1200 RPM. * $C_6$ products; cyclohexanol, cyclohexanone and CHHP.*

XPS analysis of the used catalyst at different reaction times has shown an increase in both the Pd:Au and $Pd^0$:$Pd^{2+}$ ratios with increasing reaction time, Table 3.6. This indicates either an enhancing of the particle Pd core Au shell morphology or an increase in particle size decreasing the dispersion of the Au and hence a signal is not detected due to the surface and depth limitation of XPS. An increase in $Pd^0$ content has previously been reported in the literature to increase the activity of $H_2O_2$ synthesis.[33–35] This increase in $Pd^0$ with increasing reaction time could increase the formation of $H_2O_2$ which could increase the cyclohexane oxidation activity.

***Table 3.6*** *XPS analysis of 1% AuPd/$TiO_2$ at varying reaction times.*

| Time / hours | Pd:Au | $Pd^0$:$Pd^{2+}$ |
|---|---|---|
| 0 | 18.5 | 1.3 |
| 3 | 34 | 1.6 |
| 8 | 28.8 | 4.9 |
| 12 | 29.9 | 2.7 |
| 17 | All Pd | 5.9 |
| 24 | All Pd | 9.8 |

These changes in the particle morphology and oxidation state of Pd are discussed further in Section 3.3.9 in regards to the activity of the catalyst.

### 3.3.5 Effect of temperature.

Initial investigations revealed that at 80 °C KA oil could only be observed when both $H_2$ and $O_2$ were in the gas mixtures (12.8 µmol) and not $O_2$ alone as the temperature used was far below autoxidation temperature.[18] Hence this showed that these conditions were not harsh enough for the solely aerobic reaction and that $H_2$ must be having an influence on the reaction. A range of temperatures were then investigated and compared to the aerobic reaction to determine the efficiency of reactive oxygen species generated *in-situ*. Temperatures in the range of 50 to 140 °C were tested; this

reflects the range of temperatures that have been used in the literature both when using $O_2$ and $H_2O_2$ as oxidants.[6,32,36–39] No significant change in $H_2$ conversion was seen throughout the temperature range with all $H_2$ conversions exceeding 70 %, Figure 3.10. Large conversion of $H_2$ under all reaction conditions have been partially attributed to the large solubility of the $H_2$ in the reaction solution and the long reaction times.

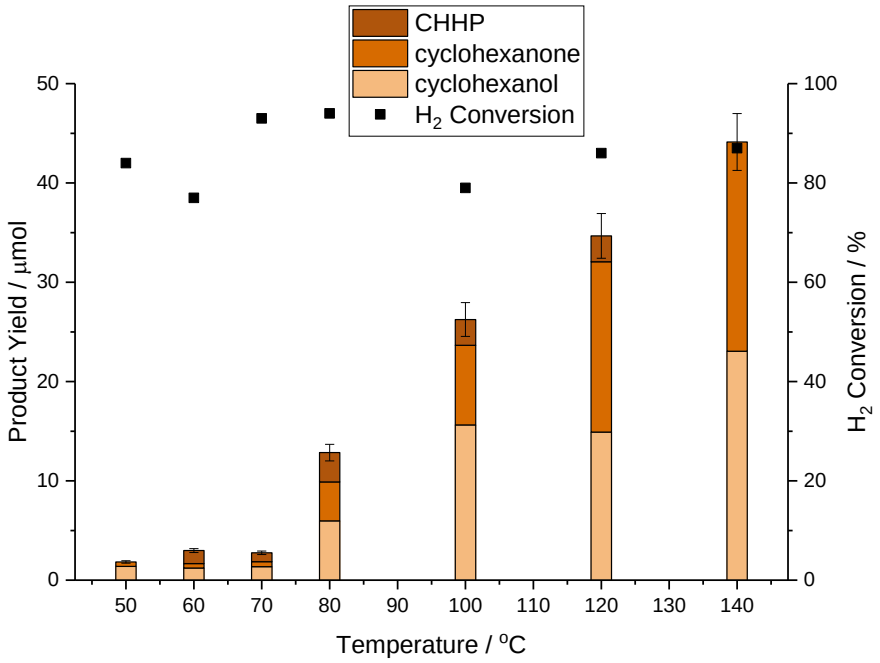


***Figure 3.10.*** *The effect of reaction temperature on the yield of KA oil.* ***Reaction conditions;*** *17 hours, 0.05 g 1 % AuPd/$TiO_2$ wet impregnation catalyst, 6.37 g tert-butanol, 2.13 g (25 mmol) cyclohexane, 29 bar 5 % $H_2$ / $N_2$ and 11 bar 25 % $O_2$ / $N_2$, 1200 RPM.*

As product yield has increased as a function of temperature in turn the selectivity to products based on $H_2$ has also increased, Table 3.7. However, as $H_2$ conversion is relatively consistent over all temperatures the contribution of aerobic oxidation increases as the temperature increases.

***Table 3.7.*** *$H_2$ conversion and selectivity as a function of reaction temperature.*

| Temperature / °C | $H_2$ Conversion / % | Total product yield / % | Selectivity to all $C_6$* products based on $H_2$ / % |
|---|---|---|---|
| 50 | 84 | 0.01 | 0.09 |
| 60 | 77 | 0.01 | 0.15 |
| 70 | 93 | 0.01 | 0.12 |
| 80 | 94 | 0.05 | 0.54 |
| 100 | 79 | 0.09 | 1.32 |
| 120 | 86 | 0.13 | 1.60 |
| 140 | 87 | 0.17 | 2.02 |

***Reaction conditions****; 80 °C, 17 hours, 0.050 g 1 % AuPd /$TiO_2$ catalyst, 6.37 g solvent, 2.13 g cyclohexane, 29 bar 5 % $H_2$ / $N_2$ and 11 bar 25 % $O_2$ / $N_2$, 1200 RPM. * $C_6$ products; cyclohexanol, cyclohexanone and CHHP.*

These temperatures have also been studied with only $O_2$ (11 bar 25% $O_2/N_2$, 4.77 mmol) to compare the effect of the addition of $H_2$ at all temperatures. The aerobic oxidation of cyclohexane is often reported at temperature approaching 140 °C [5] and it's important to see how these *in-situ* conditions compare to this, Figure 3.11.

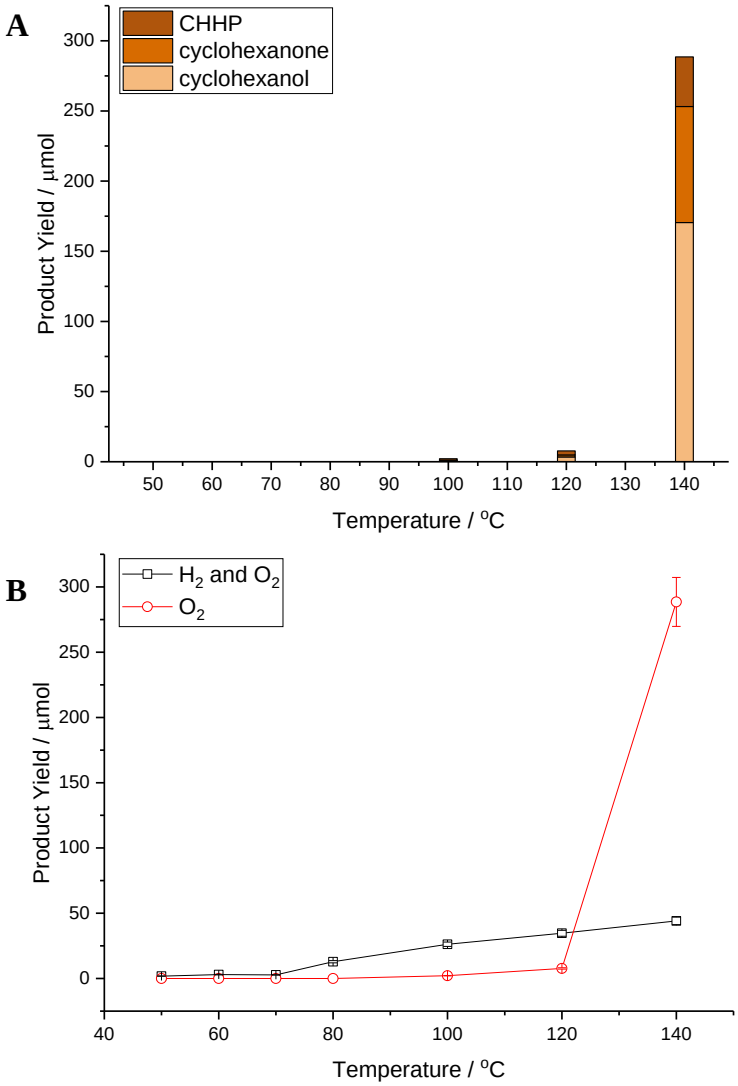


***Figure 3.11.*** *Aerobic oxidation (A) and the comparison between $O_2$ only and in-situ conditions (B) at all temperatures.* ***Reaction conditions;*** *17 hours, 0.05 g 1 % AuPd/$TiO_2$ wet impregnation catalyst, 6.37 g tert-butanol, 2.13 g (25 mmol) cyclohexane, 29 bar 5 % $H_2$ / $N_2$ and 11 bar 25 % $O_2$ / $N_2$, for in-situ results, 11 bar 25 % $O_2$ / $N_2$ for aerobic, 1200 RPM.*

At lower temperatures, ≤ 80 °C, KA oil was only measured when both $H_2$ and $O_2$ were present. At higher temperatures, ≥ 100 °C, KA oil was measured both under $H_2$ and $O_2$, and $O_2$ only conditions. However, KA oil yield under aerobic conditions exceeds that of *in-situ* at 140 °C. This is most likely due to under *in-situ* conditions $O_2$ is consumed to produce oxygen-based active species which may decompose, compared to the aerobic conditions where all the $O_2$ is available for oxidation.

### 3.3.6 Effect of catalyst mass.

The effect of catalyst mass on the oxidation conditions has also been investigated. It has previously been observed that for the synthesis of $H_2O_2$ productivity increases with increasing catalyst mass.[22,40,41] Edwards *et al.* observed with a 5% AuPd/$TiO_2$ that increasing the catalyst mass from 0.01 to 0.05 g increased the concentration of $H_2O_2$ from 0.07 to 0.23 wt.% at 2 °C.[40]

As it is postulated that cyclohexane oxidation proceeds via the *in-situ* production of $H_2O_2$ it is important to test the effect of catalyst mass on cyclohexane oxidation, Figure 3.12. The mass of catalyst used can also indicate whether the reaction is under mass transfer limited conditions or not. [42]

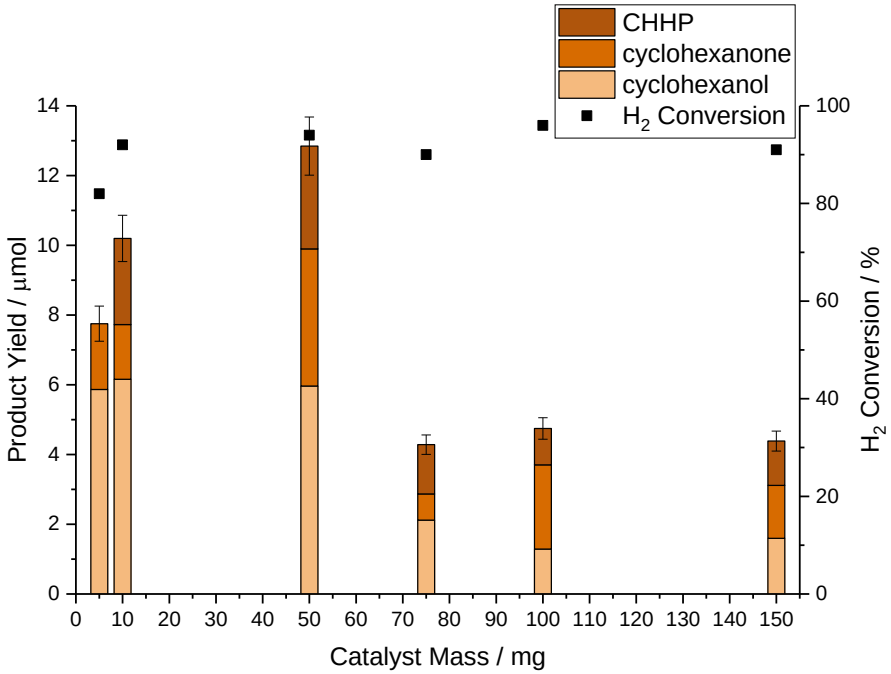


***Figure 3.12.*** *Effect of catalyst mass on the overall yield of KA oil.* ***Reaction conditions;*** *17 hours, 80 °C, 1 % AuPd/$TiO_2$ wet impregnation catalyst, 6.37 g tert-butanol, 2.13 g (25 mmol) cyclohexane, 29 bar 5 % $H_2$ / $N_2$ and 11 bar 25 % $O_2$ / $N_2$, 1200 RPM.*

An increase in KA oil yield can be observed from 7.8 µmol to 12.8 µmol when increasing catalyst mass from 5 mg to 50 mg after which increasing the catalyst mass further results in a decrease in product yield, 5 µmol, along with a decrease in $C_6$ selectivity, Table 3.8. This suggests that with increasing catalyst mass up to 50 mg the increase in metal and hence active surface increases, increasing yield. However, as the increase in activity is not linear it could indicate that some diffusion limitations are occurring with the catalyst and reactants. This could also indicate that with increasing catalyst mass an increase in degradation of $H_2O_2$ which could limit the oxidation. At

greater than 75 mg catalyst a decrease in catalytic activity is observed despite high $H_2O_2$ concentration expected.[22,40,41] At greater catalyst masses $H_2O_2$ concentrations should be greater, however reaction times under cyclohexane oxidation conditions are much greater than those normally utilised for $H_2O_2$ synthesis and hence it is difficult to make a direct comparison.[22,40,41] For effective cyclohexane oxidation $H_2O_2$ concentrations must be maintained and utilised effectively over the long reaction times. In the literature for large catalyst masses high $H_2$ conversion and $H_2O_2$ concentrations are observed at short reaction times, 30 minutes, it could be postulated that at extended reaction times the $H_2O_2$ synthesis activity cannot be maintained and the oxidation activity is reduced.

***Table 3.8.*** *$H_2$ conversion and selectivity as a function of catalyst mass.*

| Catalyst mass / mg | $H_2$ Conversion / % | Total product yield / % | Selectivity to all $C_6$ products based on $H_2$ / % |
|---|---|---|---|
| 5 | 82 | 0.03 | 0.38 |
| 10 | 92 | 0.04 | 0.44 |
| 50 | 94 | 0.05 | 0.54 |
| 75 | 92 | 0.02 | 0.18 |
| 100 | 96 | 0.02 | 0.20 |
| 150 | 91 | 0.02 | 0.19 |

***Reaction conditions****; 80 °C, 17 hours, 0.050 g 1 % AuPd /$TiO_2$ catalyst, 6.37 g solvent, 2.13 g cyclohexane, 29 bar 5 % $H_2$ / $N_2$ and 11 bar 25 % $O_2$ / $N_2$, 1200 RPM. * $C_6$ products; cyclohexanol, cyclohexanone and CHHP.*

Gemo *et al*. have previously showed that increasing the mass of Pd catalysts decreased the $H_2O_2$ productivity along with a decrease in $H_2O_2$ selectivity. With increasing catalyst mass an increase in $H_2O$ was observed indicating that with increasing catalyst mass an increase in $H_2O_2$ degradation occurs.[43] With an increase in $H_2O_2$ an increase in $H_2$ conversion resulting in a decrease in selectivity to $C_6$ products based on $H_2$ as has been observed, Table 3.8.

### 3.3.7 Effect of stirring speed.

Another potentially limiting factor to the reaction is the stirring speed. With increasing stirring speed the diffusion of the reactants to the catalyst can increase. If the stirring is not sufficient then diffusion limitation can occur. Hence the effect of stirring speed has been investigated to see under what conditions we are mass transfer limited by inefficient stirring, Figure 3.13.

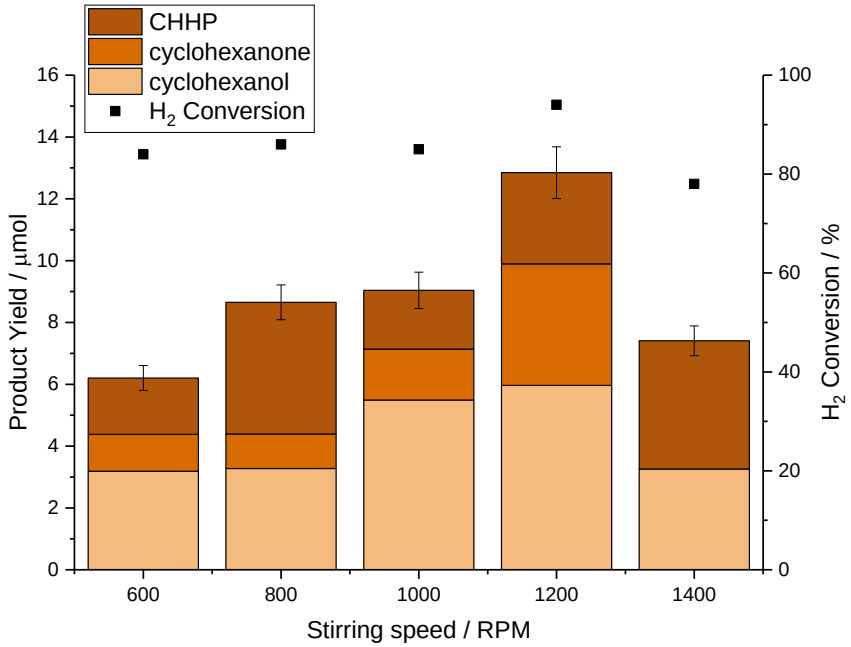


***Figure 3.13.*** *Effect of stirring speed on the yield of KA oil.* ***Reaction conditions;*** *17 hours, 80 °C, 0.05 g 1 % AuPd/$TiO_2$ wet impregnation catalyst, 6.37 g tert-butanol, 2.13 g (25 mmol) cyclohexane, 29 bar 5 % $H_2/N_2$ and 11 bar 25 % $O_2/N_2$.*

An increase in yield and $C_6$ selectivity is seen with increasing stirring speed up to 1200 RPM, Table 3.9, showing improved diffusion of reactants to the catalyst active site. However above 1200 RPM a decrease in yield and selectivity is seen indicating a limiting factor. Landon *et al.* have previously investigated the effect of stirring speed on $H_2O_2$ synthesis using 0.6% Pd/sulfonated carbon at 1 °C.[22] They observed an increase in $H_2$ conversion with increasing stirring speed up to 800 RPM after which the conversion plateaus. They concluded above 800 RPM gas-liquid mass transfer has been limited meaning the contact between the catalyst surface and the reactant gases was reduced.[22] Hence with increasing stirring speed an increase in $H_2O_2$ could be expected and hence lead to the increase observed in cyclohexane oxidation, up to 1200 RPM.

***Table 3.9.*** *$H_2$ conversion and selectivity as a function of stirring speed.*

| **Stirring speed / RPM** | **$H_2$ Conversion / %** | **Total product yield / %** | **Selectivity to all $C_6$ products based on $H_2$ / %** |
|---|---|---|---|
| 600 | 84 | 0.02 | 0.29 |
| 800 | 86 | 0.03 | 0.40 |
| 1000 | 85 | 0.04 | 0.42 |
| 1200 | 94 | 0.05 | 0.54 |
| 1400 | 78 | 0.03 | 0.38 |

***Reaction conditions****; 80 °C, 17 hours, 0.050 g 1 % AuPd /$TiO_2$ catalyst, 6.37 g solvent, 2.13 g cyclohexane, 29 bar 5 % $H_2$ / $N_2$ and 11 bar 25 % $O_2$ / $N_2$, 1200 RPM. * $C_6$ products; cyclohexanol, cyclohexanone and CHHP.*

The $H_2$ conversion also drops at 1400 RPM, Table 3.9, potentially indicating that we are now limited by the diffusion of the gas to the catalyst surface. It is postulated that with increasing stirring speed above 1200 RPM a vortex is produced in the reaction mixture which results in the catalyst depositing on the reactor wall decreasing the contact between the catalyst and reactants, as illustrated in Figure 3.14, this can explain the decreases in yield upon increase in stirring speed above 1200 RPM.

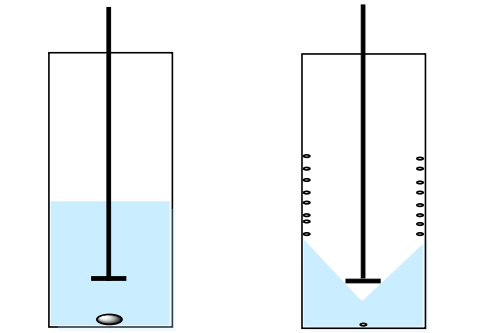


***Figure 3.14.*** *A depiction of catalyst deposition on the reactor at low and high stirring speeds.*

Although this vortex cannot be observed during the reaction post reaction the accumulation of catalyst on the reactor wall post has indicated that this is occurring.

### 3.3.8 Effect of gas ratio $H_2$:$O_2$.

The ratio of $H_2$:$O_2$ has shown to influence $H_2O_2$ synthesis rates. An optimum ratio of 1:1 has been observed to give the highest concentrations of $H_2O_2$, despite also giving the highest $H_2O_2$ degradation rates.[20,41] It is postulated that small amounts of $H_2O_2$ produced *in-situ* could be utilised to initiate the reaction and then maintain the oxidation with $O_2$. If this was possible small amounts of $H_2$ could be utilised.

For standard reaction conditions used in this work 29 bar 5% $H_2/N_2$ and 11 bar 25% $O_2/N_2$ are utilised, giving a $H_2$:$O_2$ ratio of 0.53, where $O_2$ is in excess of $H_2$. For these experiments the total pressure of gas, including $N_2$ has been kept constant and the ratio of $H_2$ and $O_2$ within this total changed, Appendix Table S.1.1. The effect of varying the $H_2$:$O_2$ ratio while maintaining constant pressure has been determined, Figure 3.15.

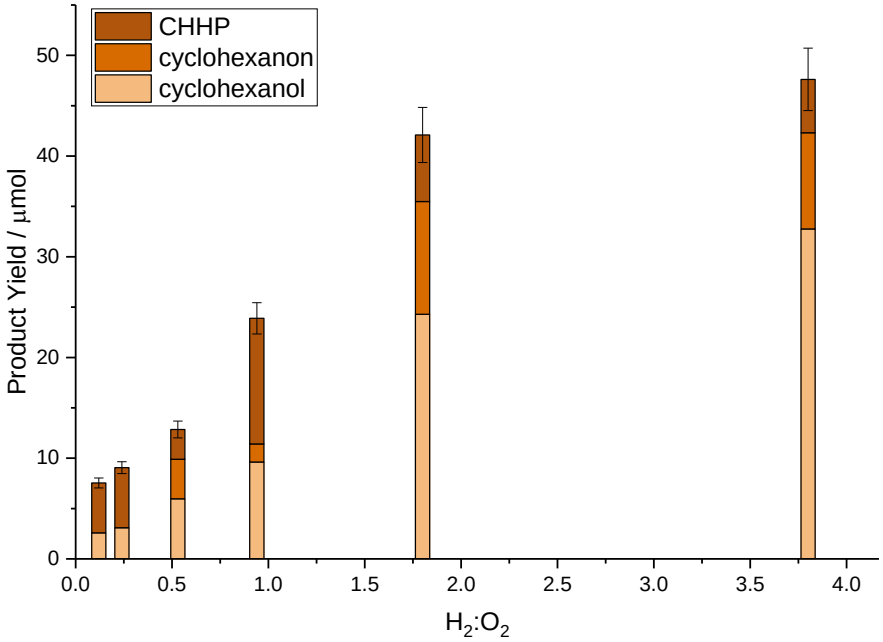


***Figure 3.15.*** *The effect of $H_2$:$O_2$ ratio on the yield of KA oil.* ***Reaction conditions;*** *17 hours, 80 °C, 0.05 g 1 % AuPd/$TiO_2$ wet impregnation catalyst, 6.37 g tert-butanol, 2.13 g (25 mmol) cyclohexane, 1200 RPM.*

It can be observed that with an increase in $H_2$:$O_2$ there is an increase in the yield of KA oil. This has shown once again the importance of the presence of $H_2$ in the reaction and it is this that is the limiting reagent. This could be due to the $H_2$ being used in reducing the catalyst surface and hence activating the catalyst surface. Additionally, this could be due to $H_2$ being wasted in side reactions such as the hydrogenation of $H_2O_2$ or possible direct combustion of $H_2$ and $O_2$ both producing $H_2O$ which reduces the amount of available $H_2$.

### 3.3.9 Re-use of catalyst.

The re-usability of a catalyst is an important characteristic as it shows its industrial viability and its stability under reaction conditions. For these reusability tests, 0.15 g of the catalyst were used and then recovered and dried under vacuum (30 °C, 16 h) prior to investigation under standard reaction conditions, as outlined in Chapter 2, Section 2.4.3.

Continual re-uses have shown that catalyst activity improves with additional use from 9.0 to 12.7 to 19.1 µmol, Figure 3.16. This could indicate that under these reaction conditions the catalyst is altered, resulting in an activation of the catalyst and thus an improvement in catalytic ability. It is proposed that this is due to a reduction of PdO to metallic Pd under the reaction conditions, Table 3.10.

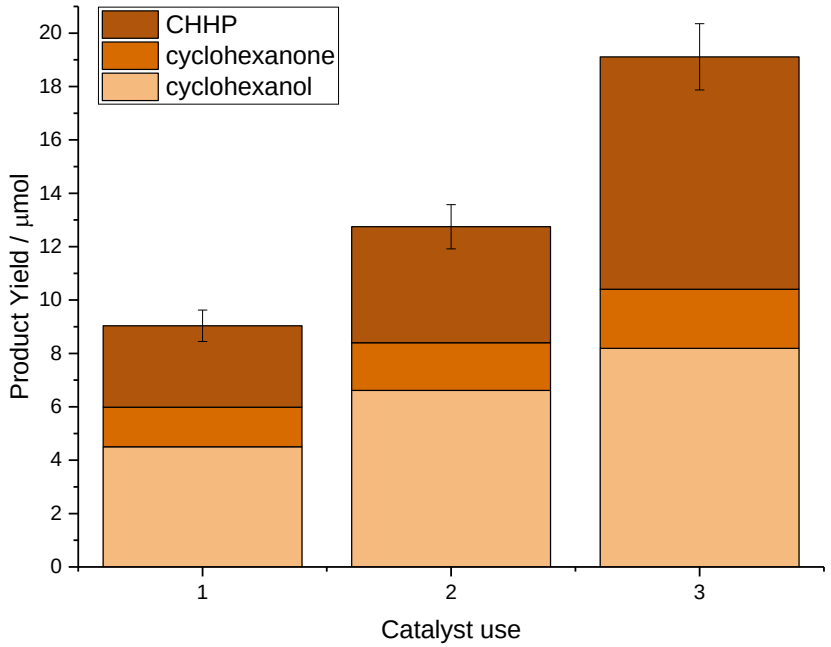


***Figure 3.16.*** *The yield of KA oil produced upon multiple re-uses of the catalyst.* ***Reaction conditions;*** *17 hours, 80 °C, 1 % AuPd/$TiO_2$ wet impregnation catalyst, 6.37 g tert-butanol, 2.13 g (25 mmol) cyclohexane, 29 bar 5 % $H_2$ / $N_2$ and 11 bar 25 % $O_2$ / $N_2$, 1200 RPM.*

XPS analysis has been performed on both fresh and used catalyst to see the changes in the surface species of the catalysts, Table 3.10. These results show that the standard wet impregnation 1% AuPd/$TiO_2$ catalyst has both $Pd^{2+}$ and $Pd^0$ species present after calcination. However, for almost all re-uses there is no Au signal present upon re-use of the catalyst. This could suggest either a change in the structure of the bimetallic nanoparticles to enhance the core-shell structures or could indicate leaching of Au species into solution or an increase in particle size decreasing the dispersion of Au.

***Table 3.10.*** *Surface composition of Pd and Au determined by XPS of 1 % AuPd/$TiO_2$ both fresh and used in the oxidation of cyclohexane.*

| **Description** | **Pd:Au** | **$Pd^0$:$Pd^{2+}$** | **Cl atomic concentration / %** |
|---|---|---|---|
| Fresh | 18.5 | 1.3 | 0.45 |
| 1st use | All Pd | 6.67 | 0.3 |
| 2nd use | All Pd | All $Pd^0$ | 0 |
| 3rd use | All Pd | All $Pd^0$ | 0 |

A decrease in Cl can also be seen with subsequent uses. Cl ions may have leached from the catalyst surface into solution during the oxidation reaction which can stabilise and aid $H_2O_2$ production.[44]

The fresh and used catalysts have both been digested in aqua regia and analysed by microwave plasma atomic emission spectra (MP-AES) Table 3.11, as described in Chapter 2, Section 2.5.7. These showed that in both the fresh and used samples Au was still present and no significant amount of either metal had been leached from the catalyst during reaction.

***Table 3.11.*** *Concentration of metal detected by MP-AES post digestion in aqua-regia for 1 % AuPd/$TiO_2$.*

| Catalyst | Au Loading / wt.% | Pd Loading / wt.% |
|---|---|---|
| Fresh | 0.63 | 0.46 |
| 1st use | 0.66 | 0.54 |
| 2nd use | 0.60 | 0.45 |
| 3rd use | 0.55 | 0.41 |

Hence MP-AES along with the XPS data suggests that the metal nanoparticles on the surface of the catalyst undergo a compositional rearrangement during the reaction conditions, Figure 3.17. This indicates an enhancement of the core-shell structure, however further high resolution microscopy would be needed to confirm this. It can then be inferred that both $Pd^0$ and core-shell morphology could be important features of the catalyst to improve activity.

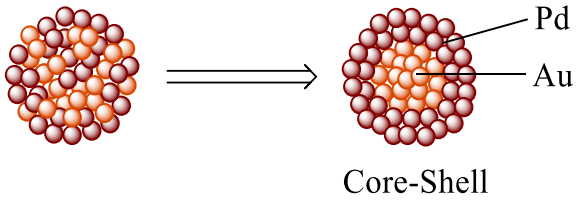


***Figure 3.17.*** *A visualisation of the re-structuring of the 1 % AuPd/$TiO_2$ upon use.*

It has been discussed within the literature the importance of $Pd^0$ on the synthesis of $H_2O_2$.[33,34,45,46] Reduced Pd species are postulated to be more active for the synthesis of $H_2O_2$ but also its degradation compared to PdO.[45] For the direct synthesis of $H_2O_2$ the selectivity is important to produce the greatest final concentration of $H_2O_2$. For cyclohexane oxidation reaction where it is postulated that the $H_2O_2$ is synthesized and utilised immediately the selectivity is less important. If $Pd^0$ can increase the $H_2$ conversion and hence the amount of $H_2O_2$ produced this can increase the oxidation activity. Metallic Pd surfaces have been suggested to be responsible for the activation and splitting of the O-O bond which leads to the degradation of $H_2O_2$.[47] However this could be beneficial for the oxidation reaction as the splitting of the O-O in $H_2O_2$ can lead to radical species which can aid in the radical oxidation mechanism.

Core-shell morphologies of AuPd particles for $H_2O_2$ synthesis have previously been reported, they have shown lower initial activities than random alloy morphologies however they were more stable and showed continual activity upon re-use.[48] This sustained production of $H_2O_2$ is important for the continual formation and utilisation of $H_2O_2$ for cyclohexane oxidation.

As mentioned in Section 3.3.1 TEM analysis analysis showed that fresh 1% AuPd/$TiO_2$ consisted predominately small sub 1 nm particles, Figure 3.18 A, with some larger particles. Upon the use of the catalyst further TEM analysis has shown the growth of the nanoparticles with no sub-nanomter particles being observed, Figure 3.18 . Large particles, >20 nm, have been observed in all the first, second and third use. It is postualted that these small particles were Pd rich and upon use these Pd-rich particles have been replaced with large agglomerated AuPd particles which could explain the loss of Au in the XPS spectra.

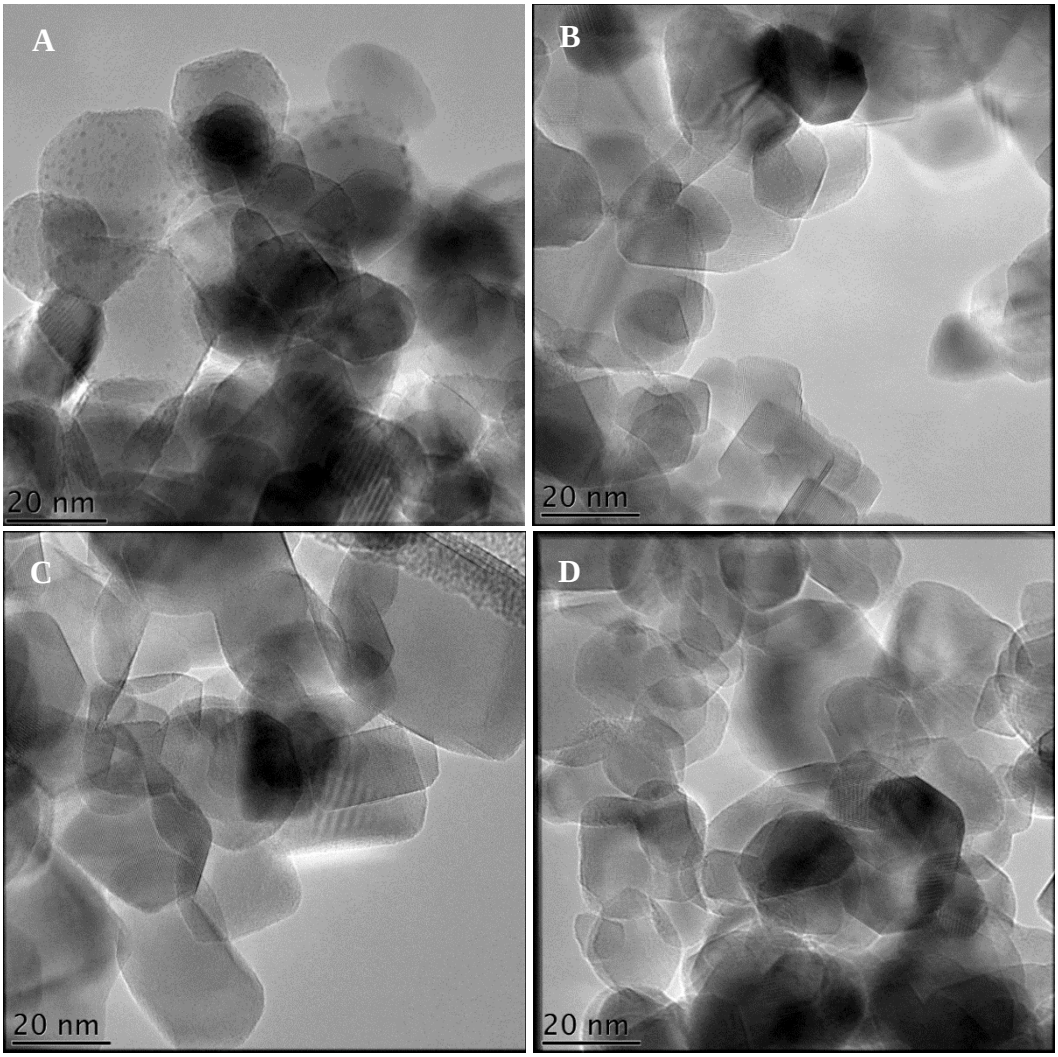


***Figure 3.18*** *TEM images of fresh and used 1% AuPd/$TiO_2$, (A) fresh catalyst, (B) first use, (C) second use and (D) third use.*

As TEM has shown an increase in the particle size the decrease in metal atomic concentrations observed by XPS can be partially be attributed to a decrease in dispersion on the catalysts. These large particles could still contain core-shell morphology as previously mentioned and as XPS is only a surface technique the whole particle will not be analysed.

It could be seen from the XPS data, Table 3.6, that no Au and only Pd was present on the surface of the catalyst after use. This could indicate that it is Pd that is playing the most important role in the catalytic activity and an increase in activity upon re-use could be due to more available Pd active species on the surface. To test this monometallic 1% $Pd/TiO_2$ and 1% $Au/TiO_2$ catalysts have been investigated, Figure 3.19. Both the monometallic catalysts show a reduced activity compared to the bimetallic catalyst.

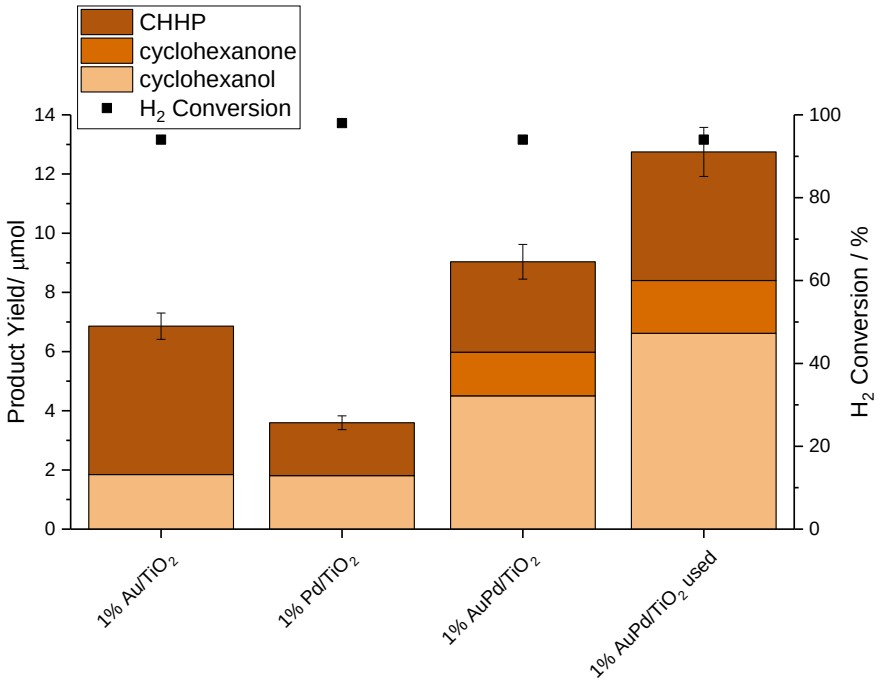


***Figure 3.19.*** *The yield of KA oil upon re-use of 1% $AuPd/TiO_2$ catalyst compared to monometallic 1% $Au/TiO_2$ and 1% $Pd/TiO_2$.* ***Reaction conditions;*** *17 hours, 80 °C, 0.05 g catalyst, 6.37 g tert-butanol, 2.13 g (25 mmol) cyclohexane, 29 bar 5 % $H_2$ / $N_2$ and 11 bar 25 % $O_2$ / $N_2$, 1200 RPM.*

The reduced activity of 1% $Pd/TiO_2$ could be partially due to Pd predominately in the $Pd^{2+}$ state compared to all $Pd^0$ in the used catalysts and hence could show that the oxidation state of Pd is important. The addition of Au into Pd catalysts is proposed to increase activity by electronic stabilisation of Pd.[49,50] Hence the synergy observed for the bimetallic catalyst could be partially attributed the influence of Au on the Pd oxidation state and stabilising the reduced Pd species upon catalyst re-use.

Hence to test the effect of varying amounts of reduced Pd species present in the catalyst a 1% AuPd/$TiO_2$ catalyst prepared by wet impregnation has been synthesised of which portions have been heat treated under a flow of 5% $H_2$/Ar, Figure 3.20. A variety of catalysts have been made with varying heat treatments;

- Calcined, static air, 400 °C, 3 hours (standard heat treatment)
- Reduced, 5% $H_2$/Ar, 400 °C, 3 hours.
- Calcined, static air, 400 °C, 3 hours. Then reduced, 5% $H_2$/Ar, 200 °C, 2 hours.

These gave varying $Pd^{II}$:$Pd^0$ depending on heat treatment as observed via XPS, Table 3.12. It was also believed that calcination followed by reduction will ensure the close to core-shell morphology normally seen for the only calcined conventional wet impregnation catalyst while providing a reduced Pd species. Hence these calcined then reduced catalyst should mimic the re-used the catalysts the most.

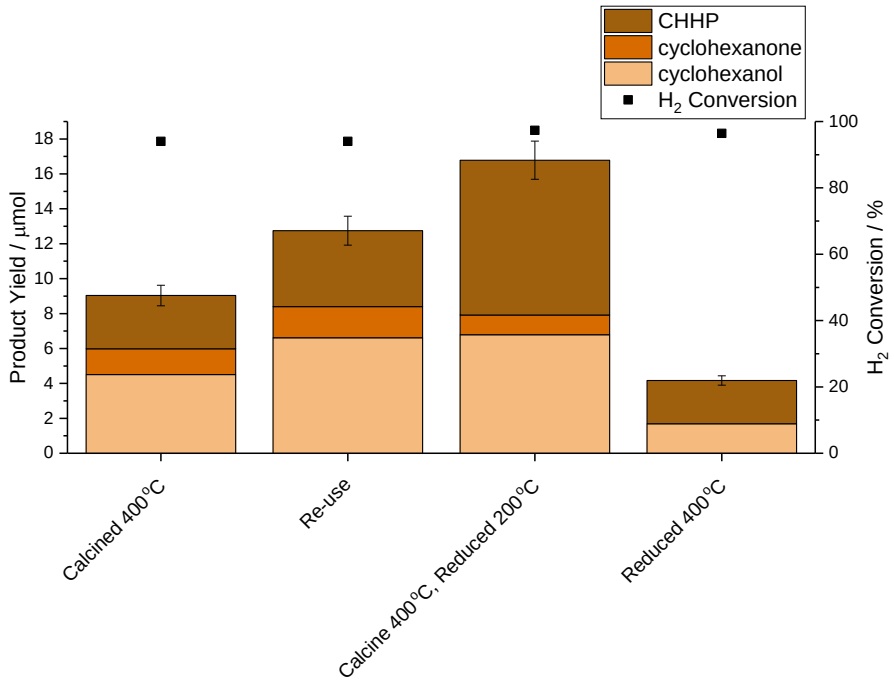


***Figure 3.20.*** *The yield of KA oil produced by a 1% AuPd/$TiO_2$ conventional wet impregnation, comparing the effect of different heat treatments during catalyst synthesis.* ***Reaction conditions;*** *17 hours, 80 °C, 0.05 g catalyst, 6.37 g tert-butanol, 2.13 g (25 mmol) cyclohexane, 29 bar 5 % $H_2$ / $N_2$ and 11 bar 25 % $O_2$ / $N_2$, 1200 RPM.*

From this it can be observed that the catalysts which has been calcined followed by a low temperature (200 °C) reduction has produced the highest yield of KA oil, 16.8 µmol. The catalyst which had not been calcined but only reduced (400 °C) produced the lowest yield. Sankar *et al.* have previously shown that reductive heat treatments for AuPd/$TiO_2$ catalysts produce random alloy structures.[51] This could show that not only the $Pd^0$:$Pd^{2+}$ ratio is important but also the morphology, which can be directed by

heat treatment, is important for catalytic activity. Although it should also be noted that with increasing the number of heat treatments an increase in particle size could be expected which can also have an effect on activity.[52] This effect could be even more prominent with increasing temperature of the second heat treatment by increasing the mobility of the Pd on the surface increasing agglomeration during the heat treatment. However as there has not been a detrimental effect on catalytic activity for the additional 200 °C heat treatment it could indicate that particle sizes have not been affected or that the size of the particles is not as prominent in controlling activity compared to oxidation state, as was observed for the re-use of the catalyst.

XPS data, Table 3.12, has shown that introducing a reductive heat treatment, even at low temperature (200 °C) the surface Pd can be fully reduced to $Pd^0$.

***Table 3.12.*** *Surface composition of Pd and Au determined by XPS of 1 % AuPd/$TiO_2$ which has undergone different heat treatments.*

| Catalyst heat treatment | Pd:Au | $Pd^0$:$Pd^{2+}$ |
|---|---|---|
| Calcined (400 C, 3 hrs) | 18.5 | 1.3 |
| Calcined then reduced (200 °C, 2hrs) | 22.5 | All $Pd^0$ |
| Reduced (400 °C, 3 hrs) | 16 | All $Pd^0$ |
| Calcined used | All Pd | All $Pd^0$ |
| Calcined then reduced (200 °C) used | * | * |
| Reduced used | 11.5 | All $Pd^0$ |

* No XPS data could be obtained due to weak signals.

A catalyst that has been used in the cyclohexane oxidation has also been tested for $H_2O_2$ synthesis to see if the changes in catalyst which increases yield of KA oil is due to an increase in $H_2O_2$ production, Table 3.13.

***Table 3.13.*** *Productivity and degradation of $H_2O_2$ for a fresh and used for cyclohexane oxidation 1% AuPd/$TiO_2$ catalyst.*

| Catalyst | Productivity / $mol_{H_2O_2}$ $kg_{cat}^{-1}$ $hr^{-1}$ | Degradation / $mol_{H_2O_2}$ $kg_{cat}^{-1}$ $hr^{-1}$ |
|---|---|---|
| 1% AuPd/$TiO_2$ fresh | 69 | 240 (14 %) |
| 1% AuPd/$TiO_2$ used (oxidation) | 22 | 71 (7 %) |

***Reaction conditions;*** *0.01 g catalyst, 2.9 g water, 5.6 g methanol, 30 minutes, 25 °C, 1200 RPM, 29 bar 5 % $H_2$ / $CO_2$ and 11 bar 25 % $O_2$ / $CO_2$, for synthesis, only 29 bar 5 % $H_2$ / $CO_2$ for degradation.*

It can be observed that the re-use of the catalyst does not have a positive effect on $H_2O_2$ production as it does with the oxidation of the cyclohexane. This indicates that the used catalyst increased oxidation activity is not attributed to an increase in $H_2O_2$ production. A decrease in the degradation of $H_2O_2$ has been observed for the used

catalyst and hence although the catalyst may not be producing more $H_2O_2$ it is doing so more selectively which could have influenced the activity of the oxidation reaction.

## 3.4 Conclusions.

These investigations have shown that cyclohexane could be oxidised with gas mixtures containing both $H_2$ and $O_2$ at temperatures where no reaction is observed under $O_2$ alone when a catalyst is present.

A variety of reaction parameters have been investigated to produce the optimum reaction conditions (reaction time, reaction temperature, catalyst mass, stirring speed) for the oxidation of cyclohexane. From these experiments standard reaction conditions for the oxidation of cyclohexane via the *in-situ* production of $H_2O_2$ have now been defined as; 0.05g catalyst, 80°C, 17 hours, 29 bar 5% $H_2/N_2$, 11 bar 25% $O_2/N_2$, 1200RPM, and it is these conditions which have been used for further studies (Chapter 4 and 5).

Using 1% $AuPd/TiO_2$ catalyst re-use studies were conducted to discover the stability of the catalyst in the system. These showed that the catalyst improved on successive re-use due to an increase in the $Pd^0$ species present on the surface of the catalysts after use coupled with a re-structuring of both Au and Pd on the surface.

## 3.5 References.

1. M. Conte, X. Liu, D. M. Murphy, K. Whiston and G. J. Hutchings, *Phys. Chem. Chem. Phys.*, 2012, **14**, 16279–16285.
2. W. Partenheimer, *Catal. Today*, 1995, **23**, 69–158.
3. M. Conte, X. Liu, D. M. Murphy, S. H. Taylor, K. Whiston and G. J. Hutchings, *Catal. Lett.*, 2015, **146**, 126–135.
4. Hermans, J. Peeters and P. A. Jacobs, *J. Phys. Chem. A*, 2008, **112**, 1747–1753.
5. X. Liu, M. Conte, Q. He, D. Knight, D. Murphy, S. Taylor, K. Whiston, C. Kiely and G. J. Hutchings, *Chem. Eur. J.*, 2017, **23**, 11834–11842.
6. X. Liu, M. Conte, M. Sankar, Q. He, D. M. Murphy, D. Morgan, R. L. Jenkins, D. Knight, K. Whiston, C. J. Kiely and G. J. Hutchings, *Appl. Catal. Gen.*, 2015, **504**, 373–380.
7. E. Ntainjua, J. K. Edwards, A. F. Carley, J. A. Lopez-Sanchez, J. A. Moulijn, A. A. Herzing, C. J. Kiely and G. J. Hutchings, *Green Chem.*, 2008, **10**, 1162–1169.
8. B. P. C. Hereijgers and B. M. Weckhuysen, *J. Catal.*, 2010, **270**, 16–25.
9. E. F. Aboelfetoh, M. Fechtelkord and R. Pietschnig, *J. Mol. Catal. Chem.*, 2010, **318**, 51–59.

10. K. Whiston, X. Liu and G. Hutchings, WO2013114330 (A1), 2013.
11. N. Dimitratos, J. A. Lopez-Sanchez, D. Lennon, F. Porta, L. Prati and A. Villa, *Catal. Lett.*, 2006, **108**, 147–153.
12. P. Tian, L. Ouyang, X. Xu, C. Ao, X. Xu, R. Si, X. Shen, M. Lin, J. Xu and Y.-F. Han, *J. Catal.*, 2017, **349**, 30–40.
13. H. L. Cates, J. O. Punderson and R. W. Wheatcroft, 2851496, 1958.
14. D. J. Loder, 2223494, 1940.
15. P. T. Anastas and J. C. Warner, *Green chemistry theory and practice*, Oxford University Press, 2000.
16. Z. Tian, A. Fattahi, L. Lis and S. R. Kass, *J. Am. Chem. Soc.*, 2006, **128**, 17087–17092.
17. V. Govindan and A. K. Suresh, *Ind. Eng. Chem. Res.*, 2007, **46**, 6891–6898.
18. Hermans, P. A. Jacobs and J. Peeters, *Chem. Eur. J.*, 2006, **12**, 4229–4240.
19. W. Henry, *Philos. Trans. R. Soc. Lond.*, 1803, **93**, 29–274.
20. M. Piccinini, E. N. N, J. K. Edwards, A. F. Carley, J. A. Moulijn and G. J. Hutchings, *Phys. Chem. Chem. Phys.*, 2010, **12**, 2488–2492.
21. N. Cohen, Flammability and explosion limits of $H_2$ and $H_2$/CO: a literature review, Aerospace Report TR-92(2534)-1, 1992.
22. P. Landon, P. J. Collier, A. F. Carley, D. Chadwick, A. J. Papworth, A. Burrows, C. J. Kiely and G. J. Hutchings, *Phys. Chem. Chem. Phys.*, 2003, **5**, 1917–1923.
23. Santos, R. J. Lewis, G. Malta, A. G. R. Howe, D. J. Morgan, E. Hampton, P. Gaskin and G. J. Hutchings, *Ind. Eng. Chem. Res.*, 2019, **58**, 12623–12631.
24. P. G. Jessop and B. Subramaniam, *Chem. Rev.*, 2007, **107**, 2666–2694.
25. J. K. Edwards, B. Solsona, E. N. N, A. F. Carley, A. A. Herzing, C. J. Kiely and G. J. Hutchings, *Science*, 2009, **323**, 1037–1041.
26. J. K. Edwards, A. F. Carley, A. A. Herzing, C. J. Kiely and G. J. Hutchings, *Faraday Discuss.*, 2008, **138**, 225–239.
27. L. Young, Ed., *Hydrogen and deuterium*, Pergamon Press, Oxford ; New York, 1st ed., 1981.
28. R. Battino and International Union of Pure and Applied Chemistry, Eds., *Oxygen and ozone*, Pergamon, Oxford ; New York, 1st ed., 1981.
29. Solvent Miscibility Table, https://www.sigmaaldrich.com/chemistry/solvents/solvent-miscibility-table.html, (accessed 1 May 2020).
30. J. Wang, H. Zhao, X. Zhang, R. Liu and Y. Hu, *Chin. J. Chem. Eng.*, 2008, **16**, 373–375.
31. Hydrogen peroxide solution 516813, https://www.sigmaaldrich.com/catalog/product/sigald/516813, (accessed 17 April 2020).
32. V. J. Mayani, S. V. Mayani and S. W. Kim, *Chem. Eng. Commun.*, 2016, **203**, 539–547.
33. R. Burch and P. R. Ellis, *Appl. Catal. B Environ.*, 2003, **42**, 203–211.
34. Q. Liu, K. K. Gath, J. C. Bauer, R. E. Schaak and J. H. Lunsford, *Catal. Lett.*, 2009, **132**, 342.
35. P. Priyadarshini and D. W. Flaherty, *AIChE J.*, 2019, **65**, e16829.
36. Sakthivel and P. Selvam, *J. Catal.*, 2002, **211**, 134–143.
37. Shi, B. Zhu, M. Lin, J. Long and R. Wang, *Catal. Today*, 2011, **175**, 398–403.

38. Y.-J. Xu, P. Landon, D. Enache, A. F. Carley, M. W. Roberts and G. J. Hutchings, *Catal. Lett.*, **101**, 175–179.
39. M. Rezaei, A. Najafi Chermahini and H. A. Dabbagh, *Chem. Eng. J.*, 2017, **314**, 515–525.
40. J. K. Edwards, A. Thomas, B. E. Solsona, P. Landon, A. F. Carley and G. J. Hutchings, *Catal. Today*, 2007, **122**, 397–402.
41. S. J. Freakley, M. Piccinini, J. K. Edwards, E. N. Ntainjua, J. A. Moulijn and G. J. Hutchings, *ACS Catal.*, 2013, **3**, 487–501.
42. Zamaniyan, Y. Mortazavi, A. A. Khodadadi and A. N. Pour, *J. Energy Chem.*, 2013, **22**, 795–803.
43. N. Gemo, S. Sterchele, P. Biasi, P. Centomo, P. Canu, M. Zecca, A. Shchukarev, K. Kordás, T. O. Salmi and J.-P. Mikkola, *Catal. Sci. Technol.*, 2015, **5**, 3545–3555.
44. V. R. Choudhary and C. Samanta, *J. Catal.*, 2006, **238**, 28–38.
45. V. R. Choudhary, C. Samanta and T. V. Choudhary, *Appl. Catal. Gen.*, 2006, **308**, 128–133.
46. N. M. Wilson and D. W. Flaherty, *J. Am. Chem. Soc.*, 2016, **138**, 574–586.
47. F. Wang, C. Xia, S. P. de Visser and Y. Wang, *J. Am. Chem. Soc.*, 2019, **141**, 901–910.
48. J. K. Edwards and G. J. Hutchings, *Angew. Chem. Int. Ed.*, 2008, **47**, 9192–9198.
49. M. Chen, D. Kumar, C.-W. Yi and D. W. Goodman, *Science*, 2005, **310**, 291–293.
50. Y.-F. Han, Z. Zhong, K. Ramesh, F. Chen, L. Chen, T. White, Q. Tay, S. N. Yaakub and Z. Wang, *J. Phys. Chem. C*, 2007, **111**, 8410–8413.
51. M. Sankar, E. Nowicka, R. Tiruvalam, Q. He, S. H. Taylor, C. J. Kiely, D. Bethell, D. W. Knight and G. J. Hutchings, *Chem. Eur. J.*, 2011, **17**, 6524–6532.
52. S. J. Freakley, Q. He, J. H. Harrhy, L. Lu, D. A. Crole, D. J. Morgan, E. N. Ntainjua, J. K. Edwards, A. F. Carley, A. Y. Borisevich, C. J. Kiely and G. J. Hutchings, *Science*, 2016, **351**, 965–968.

# Appendix.

***Table S3.1.*** *Pressures of 5% $H_2/N_2$ and 25% $O_2/N_2$ utilised for varying $H_2$:$O_2$ for cyclohexane oxidation via the in-situ production of $H_2O_2$.*

| $H_2$ pressure / bar | $O_2$ pressure / bar | $H_2$ moles / mmol | $O_2$ moles / mmol | $H_2$:$O_2$ ratio |
|---|---|---|---|---|
| 12 | 25 | 1.3 | 10.8 | 0.12 |
| 22 | 18 | 1.9 | 7.8 | 0.24 |
| 29 | 11 | 2.5 | 4.8 | 0.53 |
| 33 | 7 | 2.9 | 3.0 | 0.93 |
| 36 | 4 | 3.1 | 1.7 | 1.8 |
| 38 | 2 | 3.3 | 0.87 | 3.8 |

***Table S3.2*** *Surface composition of Pd and Au determined by XPS of 1 % $AuPd/TiO_2$ after varying reaction times for cyclohexane oxidation via the in-situ production of $H_2O_2$.*

| Time / hours | Atomic concentration / % | | |
|---|---|---|---|
| | Au | $Pd^0$ | $Pd^{2+}$ |
| 0 | 0.06 | 0.63 | 0.48 |
| 3 | 0.1 | 2.11 | 1.29 |
| 8 | 0.1 | 2.39 | 0.49 |
| 12 | 0.09 | 1.97 | 0.72 |
| 17 | 0 | 1.65 | 0.28 |
| 24 | 0 | 1.87 | 0.19 |

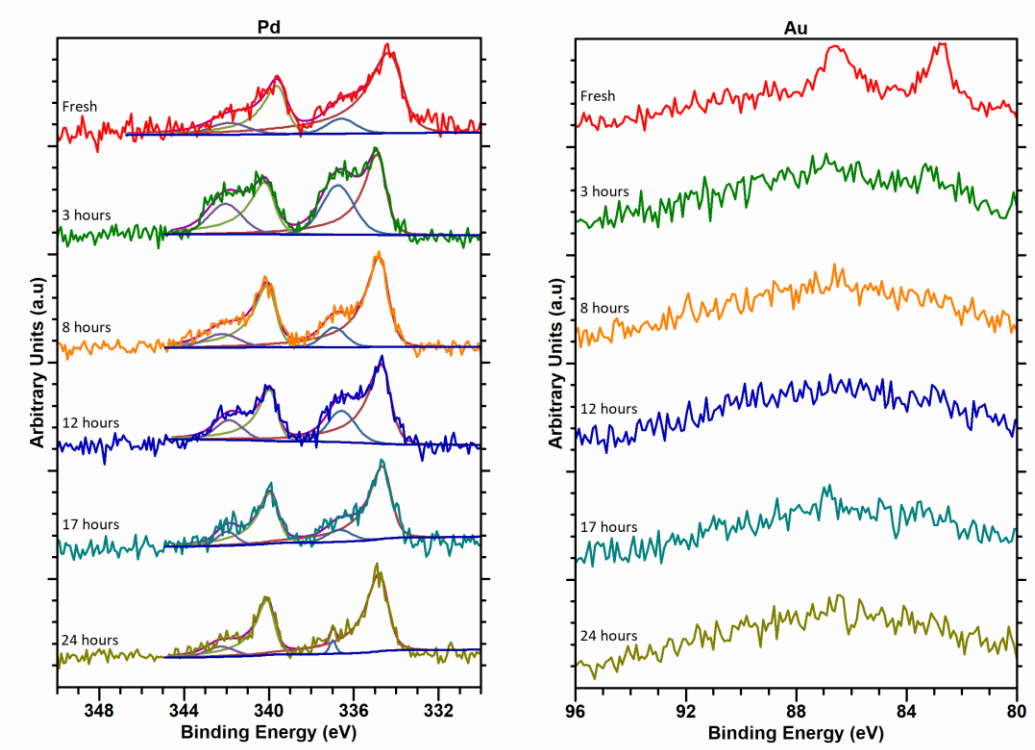


***Figure S3.1.*** *XPS spectra and fitting of Pd 3d and Au 4f regions for 1% $AuPd/TiO_2$ catalyst used at varying reaction times for cyclohexane oxidation via the in-situ production of $H_2O_2$.*

***Table S3.3.*** *Surface composition of Pd and Au determined by XPS of 1 % AuPd/$TiO_2$ both fresh and used for cyclohexane oxidation via the in-situ production of $H_2O_2$.*

| Description | Atomic concentration / % | | |
|---|---|---|---|
| | **Au** | **$Pd^0$** | **$Pd^{2+}$** |
| Dried catalyst | 0.44 | 0 | 0.7 |
| Calcined catalyst | 0.06 | 0.63 | 0.48 |
| Used (1st use) | 0 | 0.20 | 0.035 |
| Re-use (2nd use) | 0 | 0.1 | 0 |
| Re-use (3rd use) | 0 | 0.13 | 0 |

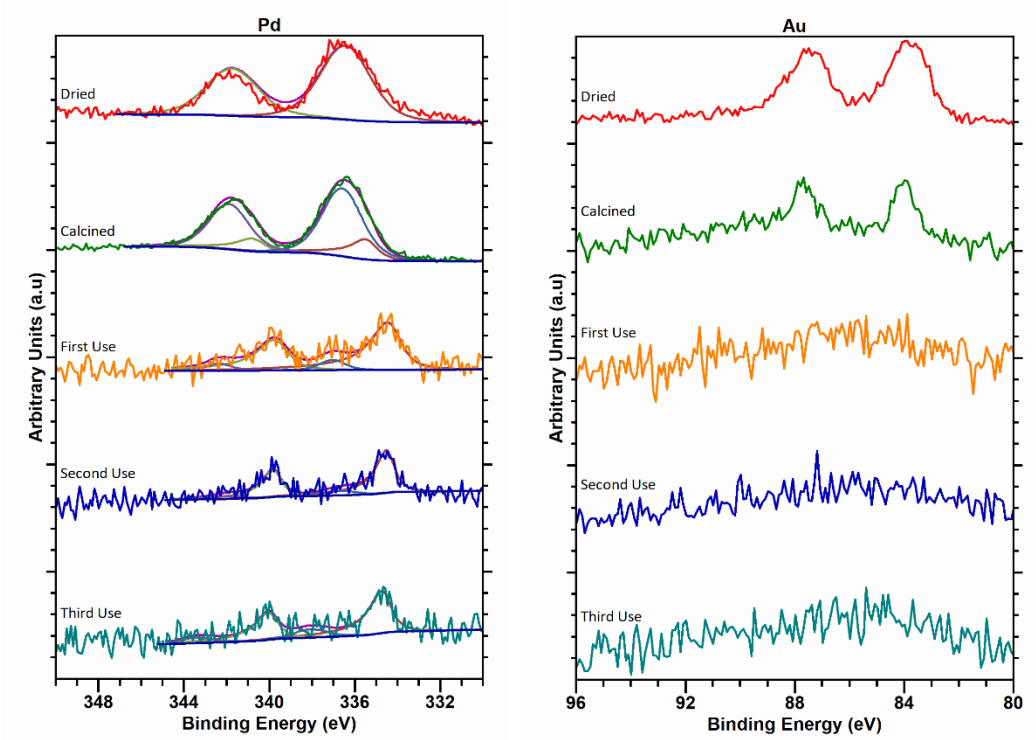


***Figure S3.2.*** *XPS spectra and fitting of Pd 3d and Au 4f regions for both fresh and used 1% AuPd/$TiO_2$ catalyst.*

***Table S3.4.*** *Surface composition of Pd and Au determined by XPS of 1% AuPd/$TiO_2$ which has undergone different heat treatments.*

| Catalyst | Atomic concentration / % | | |
|---|---|---|---|
| | **Au** | **$Pd^0$** | **$Pd^{2+}$** |
| Calcined (400 °C, 3 hrs) | 0.06 | 0.63 | 0.48 |
| Calcined then reduced (200 °C, 2hrs) | 0.02 | 0.45 | 0 |
| Reduced (400 °C, 3 hrs) | 0.03 | 0.48 | 0 |
| Calcined used | 0 | 0.20 | 0.035 |
| Calcined then reduced (200 °C) used | * | * | * |
| Reduced used | 0.02 | 0.23 | 0 |

* No XPS data could be obtained due to weak signals.

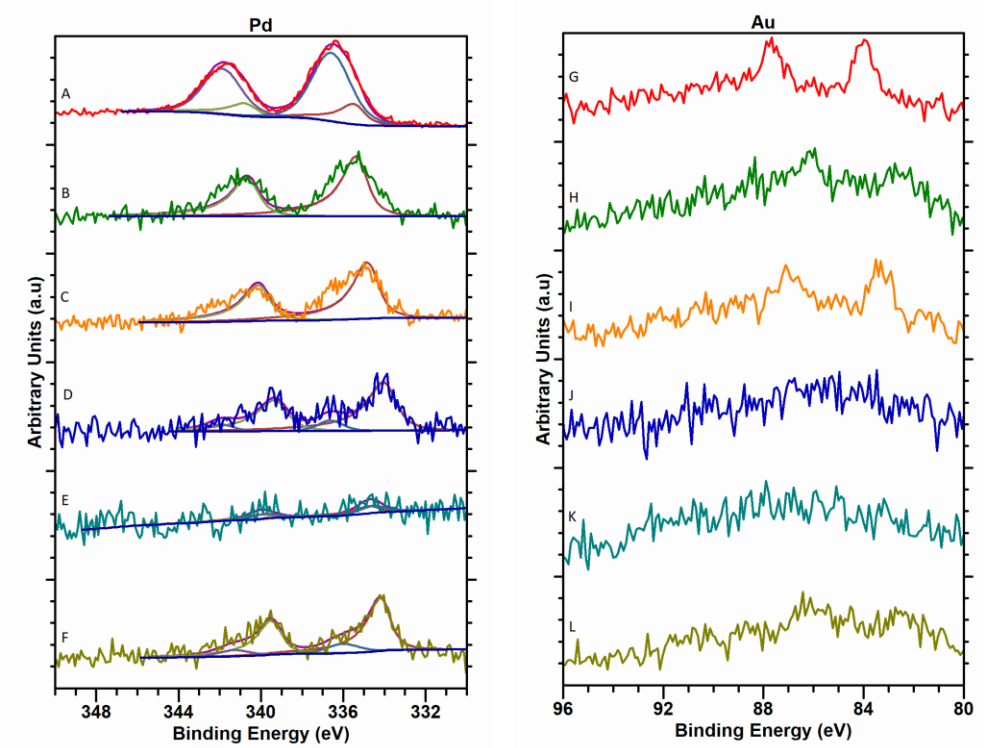


***Figure S3.3.*** *XPS spectra and fitting of Pd 3d and Au 4f regions for 1% AuPd/$TiO_2$ catalyst whicb has undergone different heat treatments in preparation.* ***A*** *and* ***G*** *calcined (400 °C),* ***B*** *and* ***H*** *calcined (400 °C) then reduced (200 °C),* ***C*** *and* ***I*** *reduced (400 °C),* ***D*** *and* ***J*** *calcined (400 °C) used,* ***E*** *and* ***K*** *calcined (400 °C) then reduced (200 °C) used, F and L reduced (400 °C) used.*

# 4. The effect of support on AuPd catalysts for the selective oxidation of cyclohexane via the *in-situ* production of $H_2O_2$.

## 4.1 Introduction.

Once initial studies on establishing reaction conditions had been completed, work focussed on catalyst design to further increase the observed yields of KA oil. In Chapter 3 a 1% AuPd/$TiO_2$ prepared by wet impregnation produced a total product yield of 12.8 µmol after 17-hour reaction.

Bimetallic, AuPd, catalysts with nominal metal loadings of 1 wt.% (Au:Pd, 1:1 wt/wt) were prepared on a variety of supports; $TiO_2$, $SiO_2$, $CeO_2$, MgO and carbon (XC-72R) via a variety of methods; wet impregnation, modified impregnation and sol immobilisation, as discussed in detail in Chapter 2. These catalysts were produced to compare not only the effect of different supports but also the method of catalyst preparation on the catalytic ability towards the direct synthesis of $H_2O_2$ and its subsequent degradation and the *in-situ* oxidation of cyclohexane.

***Table 4.1.*** *Comparison between the wet impregnation, modified impregnation and sol immobilisation catalyst preparation methods.*

| **Wet impregnation** [1–3] | **Modified impregnation** [4,5] | **Sol immobilisation** [6–8] |
|---|---|---|
| Simple preparation. | Simple preparation | More complex preparation, additional polymer stabilizers required |
| Calcined 400 ºC, 3 hours | Reduced 400 ºC, 4 hours | Calcined 400 ºC, 3 hours |
| Particle size 1-10 nm with some much larger particles >>10nm. | Small particle size 1-5 nm with tight size distribution | Small particle size (2-6 nm) with tight size distribution |
| Core-shell or random alloy particle morphology depending on support. | Random alloy particle morphology | Random alloy particle morphology, but can be changed depending on order of metal addition |
| High $Pd^{2+}$ content | High $Pd^0$ content | High $Pd^0$ content |

## 4.2 $H_2O_2$ synthesis and degradation.

### 4.2.1 Introduction.

As detailed in Chapter 3 the addition of $H_2$ has shown a dramatic increase on the aerobic oxidation of cyclohexane under mild temperatures, 80 °C. Hence it was postulated that $H_2O_2$, or it's intermediates, were important in the oxidation reaction. Therefore, initial design of a catalyst concentrated on the direct synthesis of $H_2O_2$.

### 4.2.2 Direct synthesis of $H_2O_2$.

Hutchings and co-workers have previously studied the effect of catalyst support for Au, Pd and AuPd catalysts for the synthesis and degradation of $H_2O_2$.[9–13] These have focussed on 5 wt.% catalysts tested in water/methanol solvents at 2 °C.[9–13] These studies showed for that for catalysts prepared by wet impregnation that supports with low isoelectric points (IEP) showed greater activity for the synthesis of $H_2O_2$ than higher IEP supports, Figure 4.1.[11–13] This is due to low IEP supports having greater acidity, contributing to the stabilisation of $H_2O_2$. They also observed the support influenced the particle morphology for bimetallic AuPd catalysts. For AuPd supported on carbon a random-alloy structure was observed but for oxide supports ($SiO_2$, $TiO_2$, MgO, $CeO_2$) a Pd-shell Au-core structure was observed. However, they did conclude that the morphology of the particles was not the leading factor in activity as both carbon and $SiO_2$ showed high activity despite showing different particle morphologies.[11–13]

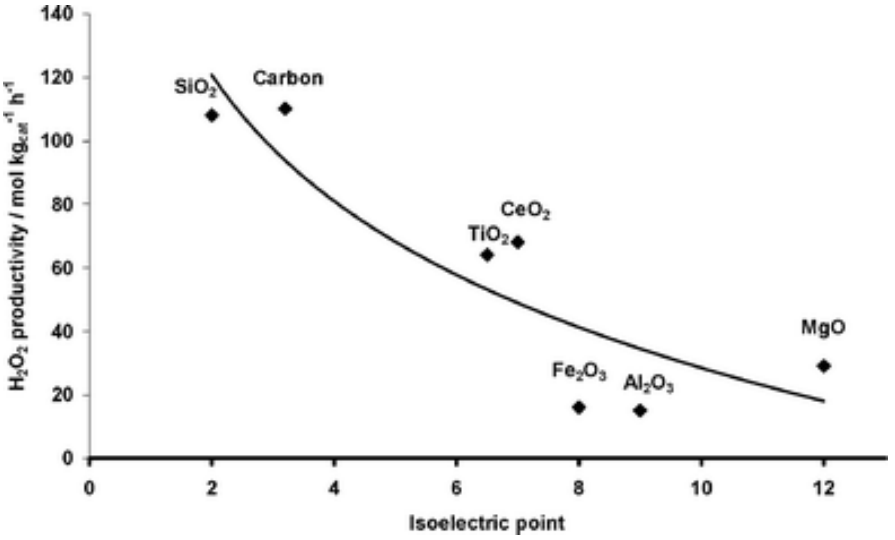


***Figure 4.1.*** *$H_2O_2$ productivity for bimetallic AuPd catalysts as a function of isoelectric point.[11]* ***Reaction conditions;*** *0.01 g catalyst, 2.9 g $H_2O$, 5.6 g methanol, 420 psi 5%$H_2$/$CO_2$, 160 psi 25%$O_2$/$CO_2$, 1200 rpm, 30 minutes. Reproduced from Ref. 11 with permission from The Royal Society of Chemistry.*

A series of bimetallic 0.5% Au 0.5% Pd catalysts have been prepared by different preparation methods (wet impregnation, modified impregnation and sol immobilisation) and produced on a variety of supports ($SiO_2$, $TiO_2$, $CeO_2$, MgO and C). Initially these catalysts were tested for the direct synthesis of $H_2O_2$ at ambient temperature. Figure 4.2 indicates that for the direct synthesis of $H_2O_2$ that catalysts prepared by wet impregnation produce the highest yield of $H_2O_2$ for all supports except $TiO_2$. In terms of supports $TiO_2$ is observed to offer the greatest productivity overall from all preparation methods.

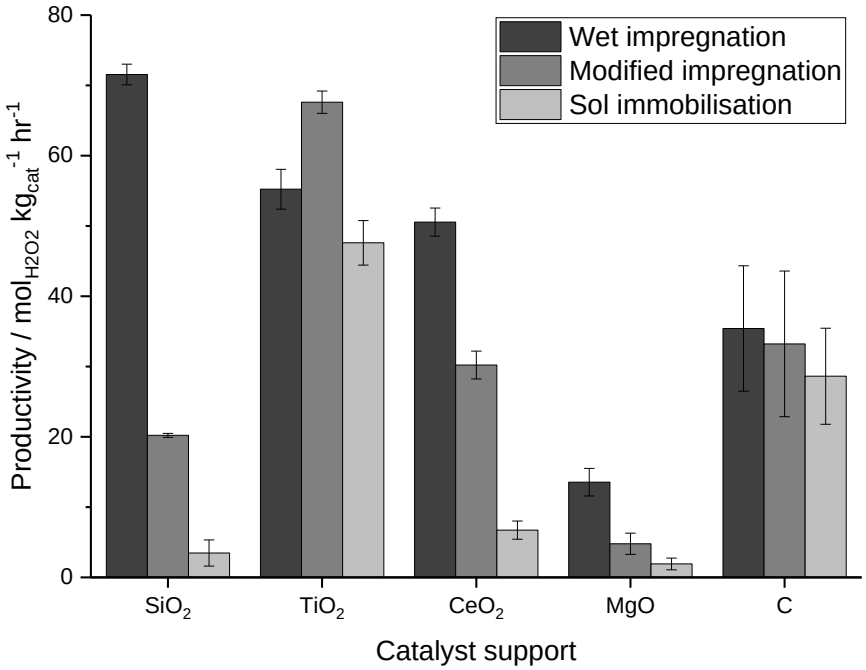


***Figure 4.2.*** *Catalytic activity of 1 % AuPd catalysts towards the synthesis of $H_2O_2$, comparison between catalyst preparation and support.* ***Reaction conditions;*** *0.01 g catalyst, 2.9 g water, 5.6 g methanol, 29 bar 5 % $H_2$ / $CO_2$, 11 bar 25 % $O_2$ / $CO_2$, 1200 RPM, 30 minutes, 25 °C.*

1% AuPd/$TiO_2$ synthesised by wet impregnation has shown a synthesis activity of 55 $mol_{H_2O_2}$ $kg_{cat}^{-1}$ $hr^{-1}$ under ambient temperatures. This is compared to previously reported 64 $mol_{H_2O_2}$ $kg_{cat}^{-1}$ $hr^{-1}$ for a 5 % AuPd/$TiO_2$ also prepared by wet impregnation and tested at 2 °C by Edwards *et al*.[3] It has been observed here that decreasing the metal loading by 5 times can still produce a similar amount $H_2O_2$ even under conditions which are less favourable for $H_2O_2$ synthesis.[14] This sustained activity despite a 5 times lower precious metal content can be attributed to the decrease in the undesired formation of $H_2O$ over the lower weight loaded catalyst. At 25 °C 1% AuPd/$TiO_2$ has shown a degradation activity of 212 $mol_{H_2O_2}$ $kg_{cat}^{-1}$ $hr^{-1}$, this is compared to 188 $mol_{H_2O_2}$ $kg_{cat}^{-1}$ $hr^{-1}$ for 5% AuPd/$TiO_2$ under conditions at which $H_2O_2$ is more stable, 2 °C.[15]

Santos *et al.* have previously investigated 0.5% Au 0.5% Pd/$TiO_2$ catalysts prepared by modified impregnation for the direct synthesis of $H_2O_2$ and tested under identical conditions to explored here. They observed a drop in productivity from 93 to 75 $mol_{H_2O_2}$ $kg_{cat}^{-1}$ $hr^{-1}$ when the reaction temperature is increased from 2 to 25 °C.[16] This decrease in productivity was coupled with a decrease in $H_2O_2$ selectivity from 44 to 14 % and was attributed to an increase in the degradation of $H_2O_2$ at 25 °C compared to 2 °C (350 and 255 $mol_{H_2O_2}$ $kg_{cat}^{-1}$ $hr^{-1}$ respectively).[16] This investigation illustrated the importance of AuPd catalysts for $H_2O_2$ synthesis under more industrially favourable reactions conditions. Although selectivity was decreased it showed that AuPd catalysts could still be stable under industrially favoured conditions and is the guide for future catalyst design.

Here 1% AuPd/$SiO_2$ when prepared via wet impregnation has given the highest activity at 72 $mol_{H_2O_2}$ $kg_{cat}^{-1}$ $hr^{-1}$ and the highest selectivity based on $H_2$, 66%, Table 4.2. Ntainjua *et al*. have previously reported a correlation between the isoelectric point of the support and the catalytic activity towards $H_2O_2$ synthesis for wet impregnation catalysts.[11] Within the catalyst prepared in this series $SiO_2$ has the highest isoelectric point and hence this could explain its superior activity and selectivity.

***Table 4.2.*** *$H_2$ conversion and selectivity based on $H_2$ for 1 % AuPd catalysts towards the synthesis of $H_2O_2$, comparison between catalyst preparation and support.*

| **Preparation method** | **Support** | **Productivity / $mol_{H_2O_2}kg_{cat}^{-1}hr^{-1}$** | **$H_2$ Conversion / %** | **$H_2$ Selectivity / %** |
|---|---|---|---|---|
| Wet impregnation | $SiO_2$ | 72 | 44 | 66 |
| | $TiO_2$ | 55 | 64 | 30 |
| | $CeO_2$ | 51 | 53 | 38 |
| | MgO | 14 | 43 | 11 |
| | C | 35 | 60 | 24 |
| Modified impregnation | $SiO_2$ | 20 | 67 | 17 |
| | $TiO_2$ | 68 | 55 | 38 |
| | $CeO_2$ | 30 | 36 | 29 |
| | MgO | 5 | 66 | 3 |
| | C | 33 | 43 | 34 |
| Sol immobilisation | $SiO_2$ | 3 | 65 | 2 |
| | $TiO_2$ | 48 | 46 | 40 |
| | $CeO_2$ | 7 | 4 | 65 |
| | MgO | 2 | 68 | 1 |
| | C | 29 | 60 | 21 |

***Reaction conditions;*** *0.01 g catalyst, 2.9 g water, 5.6 g methanol, 29 bar 5 % $H_2/CO_2$ and 11 bar 25 % $O_2/CO_2$, 1200 RPM, 30 minutes, 25 °C.*

By all preparation methods MgO has shown limited activity towards the synthesis of $H_2O_2$ despite similar $H_2$ conversion to other supports, Table 4.2. This is coupled with a low selectivity based on $H_2$ and indicates a lower selectivity towards $H_2O_2$ and an increased degradation of $H_2O_2$ and formation of $H_2O$. MgO is a basic support with a high isoelectric point and hence this would lead to the low selectivity of these catalysts.[11,17] Ntainjua *et al.* have previously reported that bare MgO support degrades a large amount of $H_2O_2$ (206 $mol_{H_2O_2}$ $kg_{cat}^{-1}$ $hr^{-1}$) at 2 °C and by comparison $TiO_2$ has shown no degradation using water/methanol solvent.[17] Hence the low selectivity of MgO catalyst is predominately due to the degradation of $H_2O_2$ due to the basic support.

Sankar *et al.* have previously compared a 1% AuPd/$TiO_2$ prepared by wet impregnation, modified impregnation and sol immobilisation for the synthesis of $H_2O_2$ at 2 ºC with all other conditions the same as investigated here. This showed an activity trend of modified impregnation > sol immobilisation > wet impregnation with productivity of 99, 32 and 23 $mol_{H_2O_2}kg_{cat}^{-1}hr^{-1}$ respectively.[4] They attributed the enhanced activity of modified impregnation procedure due to a small particle size with a random alloy composition with this composition being maintained throughout the sample.[4] This is compared to the Pd core Au shell morphology achieved via the calcination of wet impregnation prepared catalysts, with elemental content varying with particle size where small particles (< 5 nm) have been found to be Pd rich and large particles (>10 nm) Au rich.[3] However it should be noted that AuPd catalysts prepared by sol immobilisation have also shown random alloy compositions but have not shown the same enhanced activity. It could then be concluded the particle morphology may not be the only factor contributing to the catalytic activity.[4,6] A combination of this composition and electronic enhancement, from reductive heat treatments, have shown modified impregnation to improve catalyst activity and stability.[4]

### 4.2.3 The degradation of $H_2O_2$.

The degradation of $H_2O_2$ has also been investigated for the series of catalyst described above prepared by different methods and different supports, Figure 4.3. These degradation experiments were conducting independently of the synthesis reactions with a starting solution of approximately 4 wt.% $H_2O_2$ in water and methanol.

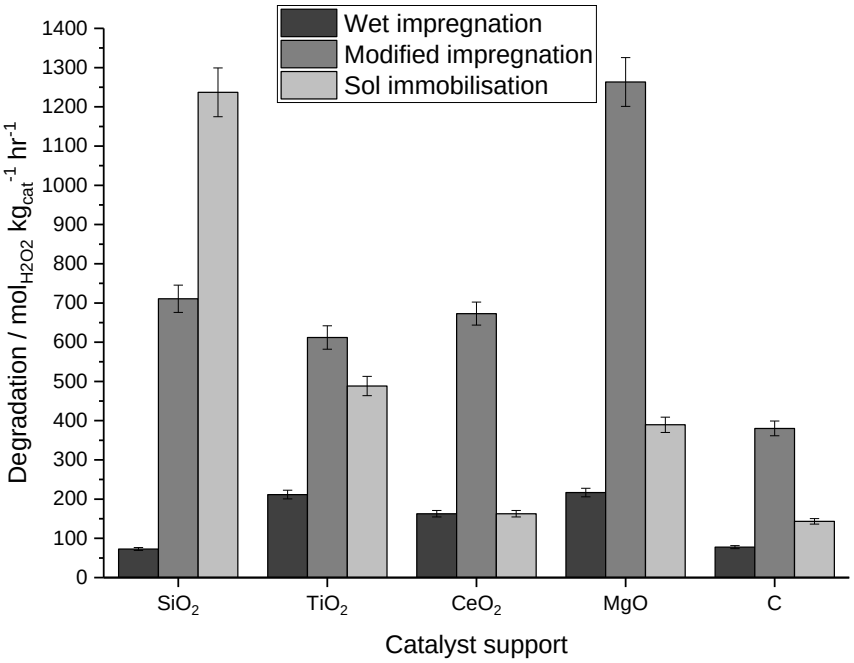


***Figure 4.3.*** *Catalytic activity of 1 % AuPd catalysts towards the degradation of $H_2O_2$, comparison between catalyst preparation and support.* ***Reaction conditions;*** *0.01g catalyst, 0.68 g $H_2O_2$, 2.22 g water, 5.6 g methanol, 29 bar 5 % $H_2/CO_2$, 1200 RPM, 30 minutes, 25 °C.*

Similar to productivity results (Figure 4.2), catalysts prepared by the wet impregnation method have shown the best activity with the lower degradation of $H_2O_2$ observed which results in the increased selectivity towards $H_2O_2$. Wet impregnation uses a calcination heat treatment and no reducing agents during catalyst preparation and hence it would be expected to give catalysts with high $Pd^{2+}$ content,[1,4,6] as reported for 1% AuPd/$TiO_2$ in Chapter 3. In the literature it has been suggested that PdO is more selective towards $H_2O_2$ formation with the degradation of $H_2O_2$ lower on PdO surfaces compared to metallic Pd.[18,19] Activation of O-O bond which results in the breaking of the bond and the formation of $H_2O$ [20] is greater over reduced Pd surfaces.[18,19] Therefore, it could be suggested that the decrease in $H_2O_2$ degradation over catalysts prepared by wet impregnation is in part due to the greater PdO content compared to modified impregnation or sol immobilisation catalysts. In the literature it has been reported that catalysts prepared by wet impregnation have a larger average particle size compared to those produced by modified impregnation and sol immobilisation.[1,4,6] However as noted in Chapter 3, Section 3.3, from TEM analysis showed that the average particle size of the 1% AuPd/$TiO_2$ was measured at 0.86 nm. Tian *et al.* have previously investigated the relationship between Pd particle size and $H_2O_2$ selectivity.[21] They observed that sub-nanometer particles, between 0.5 – 2.5 nm, showed the highest selectivity, 94 %, with nano particles, >2.5 nm, showing a drop in

selectivity, 40%. They also concluded that single site catalysts were not active due to the lack of interfaces of $PdO_x$/Pd where $Pd^{\delta+}$ led to the decrease in O-O cleavage increasing $H_2O_2$ selectivity.[21] Hence the low degradation, Table 4.3, and high selectivity observed in this work for the wet impregnation catalysts could be attributed to the optimum sub-nanometer particle sizes observed on this catalysts.

***Table 4.3.*** *Degradation activity of 1 % AuPd catalysts towards the synthesis of $H_2O_2$, comparison between catalyst preparation and support.*

| Preparation method | Support | $H_2O_2$ Degradation / % |
|---|---|---|
| Wet impregnation | $SiO_2$ | 4 |
| | $TiO_2$ | 11 |
| | $CeO_2$ | 8 |
| | MgO | 11 |
| | C | 4 |
| Modified impregnation | $SiO_2$ | 35 |
| | $TiO_2$ | 30 |
| | $CeO_2$ | 29 |
| | MgO | 62 |
| | C | 19 |
| Sol immobilisation | $SiO_2$ | 62 |
| | $TiO_2$ | 25 |
| | $CeO_2$ | 8 |
| | MgO | 20 |
| | C | 7 |

***Reaction conditions:*** *0.01g catalyst, 0.68 g $H_2O_2$, 2.22 g water, 5.6 g methanol, 29 bar 5 % $H_2$ / $CO_2$, 1200 RPM, 30 minutes, 25 °C.*

The effect of temperature on $H_2O_2$ degradation activity is well known with the 5% AuPd/$TiO_2$ catalyst prepared by wet impregnation, previously shown by Crole *et al.* to degrade 26% of 4wt.% $H_2O_2$ at 25 °C[22] compared to 9% at 2 °C.[15] Under identical reaction conditions the 1% AuPd/$TiO_2$ catalyst has degraded a much reduced 11% of the original $H_2O_2$ in solution (Table 4.3). By reducing the metal content of the catalyst, the unwanted degradation of $H_2O_2$ has been supressed, showing again the increased selectivity of these catalysts under ambient temperatures.

## 4.3 The oxidation of cyclohexane via the *in-situ* production of $H_2O_2$.

All the catalysts that have been investigated for their activity towards $H_2O_2$ synthesis and degradation have been tested for the *in-situ* oxidation of cyclohexane, Figure 4.4, at 80 °C for 17 hours, with these conditions optimised in Chapter 3. No clear correlations between the catalytic activity towards $H_2O_2$ productivity or degradation and oxidation yield have been observed.

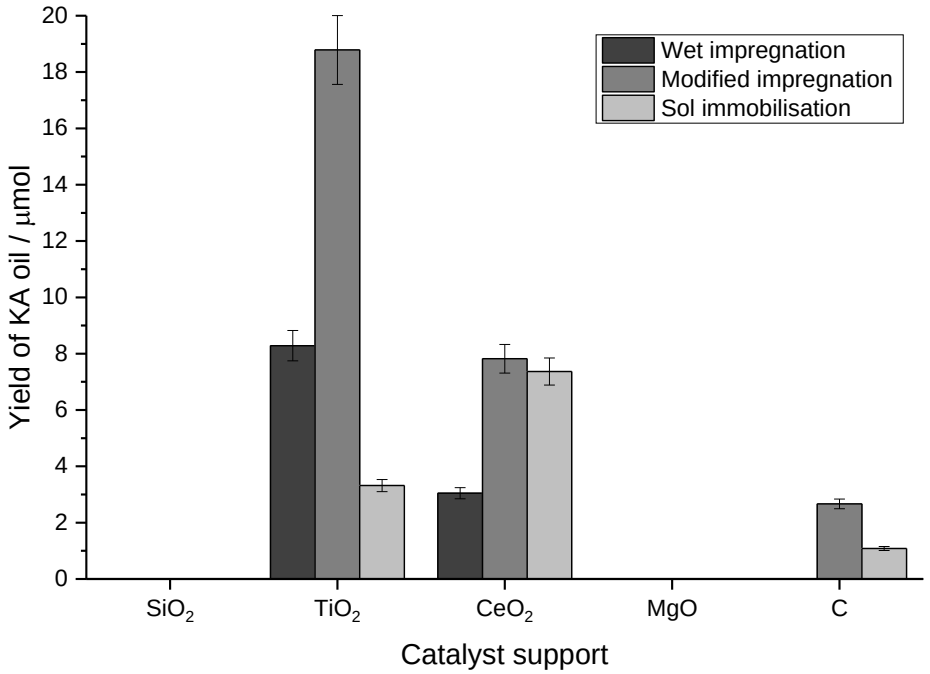


***Figure 4.4.*** *The yield of KA oil produced from 1 % AuPd catalyst immobilised on various supports and prepared via different preparation methods.* ***Reaction conditions;*** *17 hours, 80 °C, 0.05 g catalyst, 6.37 g tert-butanol, 2.13 g cyclohexane, 29 bar 5 % $H_2$ / $N_2$ and 11 bar 25 % $O_2$ / $N_2$ ,1200 RPM.*

MgO supported catalysts, which have been identified to offer low activity towards $H_2O_2$ synthesis as well as high $H_2O_2$ degradation rates, showed no yield of KA oil. This is despite MgO having been shown previously to be an ideal catalyst support for the aerobic oxidation of cyclohexane.[23–25] This illustrates again that under the *in-situ* conditions used within this work the contribution from aerobic oxidation is limited.

By comparison, $SiO_2$ supported catalysts which was reported to show high $H_2O_2$ synthesis activity and offer low degradation towards $H_2O_2$, when prepared by wet impregnation, also showed no yields of KA oil which was unexpected. This could be due to the $SiO_2$ catalyst having a high initial activity towards $H_2O_2$ which has not be sustained in the long reaction times of the oxidation reaction. It could also indicate that $H_2O_2$ may not be the reactive intermediate but is reactive oxygen species, such as ·OH and ·OOH, which may be responsible for the oxidation. It has previously been shown that •OH radicals can play a part in the radical mechanism for the oxidation of cyclohexane via the photoirradiation[26] or electrochemical[27] production of •OH. Tomat and Rigo also postulated that •OH radicals formed from $H_2O_2$ using TS-1 catalysts play a role in the oxidation of cyclohexane.[28]

$TiO_2$, $CeO_2$, and C did produce KA oil and in all cases the catalysts produced by modified impregnation gave the highest yield. This could indicate that the reaction favours neutral conditions as these catalysts all have moderate isoelectric points.

From X-ray photoelectron spectroscopy (XPS) analysis (Section 4.4.2, Table 4.4) it could be seen that the modified impregnation catalysts had greater proportion of metallic Pd species present on the surface compared to the wet impregnation. These results suggest that the nature of Pd is key in dictating catalytic activity for the oxidation of cyclohexane. It has previously been demonstrated by Sankar *et al.* that a greater $H_2O_2$ synthesis activity is observed for metallic Pd rather than PdO.[4] They also demonstrated that exposing the 1% AuPd/$TiO_2$ catalyst to a reductive heat treatment (400 °C, 4 hrs, 5% $H_2$/Ar) increased the productivity to 99 from 37 $mol_{H_2O_2}$ $kg_{cat}^{-1}$ compared to a calcination under the same conditions, 400 ºC for 4 hours, which they attributed to the greater $Pd^0$ content for the modified impregnation catalyst.[4] Reduced Pd species have been reported to less selective for $H_2O_2$ production than PdO.[18,19,29,30] However this reduced selectivity is coupled with increased $H_2$ conversion as the production of $H_2O_2$ is greater but it is also coupled with an increase in $H_2O_2$ hydrogenation.[19] During the oxidation reaction where it is hoped that $H_2O_2$ is utilised efficiently and quickly the selectivity towards $H_2O_2$ and its degradation may be less important. If the reduced Pd can produce greater amount of $H_2O_2$ this can be beneficial for the *in-situ* oxidation of cyclohexane. Han and Mullins have shown that reduced Pd islands, in bimetallic AuPd catalysts, show a greater dissociation of $O_2$ compared to Pd poor regions.[31] Dissanayake and Lunsford demonstrated that the cleavage of O-O bond leads to $H_2O$ in the synthesis of $H_2O_2$.[20] However if the O-O bond cleavage is greater in the $Pd^0$ rich modified impregnation catalysts this could lead to $^{\bullet}OH$ radicals formed on the catalyst surface which can be potent for the oxidation of cyclohexane as previously discussed.[26–28]

## 4.4 Catalyst characterisation.

### 4.4.1 XRD.

X-ray diffraction data has been collected for all heat-treated catalysts and compared to the untreated support materials, Figure 4.5 – 4.8. Due to the low metal loadings of the catalysts and the intense reflections of the supports it is hard to identify the metallic peaks. The characteristic peaks of Au would be expected at 2θ values of; 38, 44, 65,

78, 82, 98, 111, 115 and 135°.[32] For Pd peaks would be expected at; 40, 47, 68, 82, 87, 105, 119 and 125° (Reference code; 00-046-1043).[32]

The XRD pattern of pure $TiO_2$ (P25) shows both reflections for the rutile and anatase phases as expected for P25, Figure 4.5. Potential peaks for Au can be seen at 38 ° and 44 ° for all preparation methods, Figure 4.5, however this cannot be said for sure due to overlap with support peaks. Reflections for metallic Pd should be seen at 40, 47 and 68° however no peaks are observed at 40 and 47° if present at 68° are obstructed by the main reflections of the support.

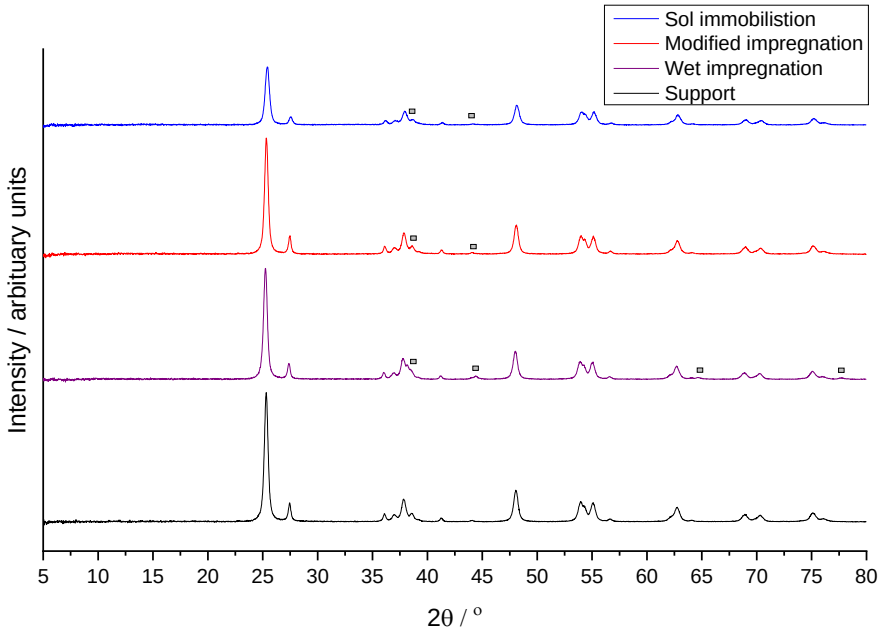


***Figure 4.5.*** *X-ray diffractogram of 1 % AuPd/$TiO_2$ catalysts produced via different preparation methods. Au reflections (■)*

For wet impregnation prepared catalysts, a reflection can be seen at 2θ value of 65° which indicates metallic Au. As this peak is only observed for the wet impregnation catalyst it could indicate that this sample has much larger Au particle size than the other samples. The larger mean particle size of wet impregnation catalyst prepared on $TiO_2$ compared to modified impregnation and sol immobilisation have previously been reported.[1,4,6] It is believed that these larger particle sizes can decrease the degradation of $H_2O_2$[29,30] and hence this observation by XRD of larger particles in the wet impregnation catalyst could explain the decreased $H_2O_2$ degradation observed for this catalyst, Table 4.3.

Silica shows only one broad peak between 15 and 30°, Figure 4.6, and hence it is easier to define the reflections associated with Pd and Au. These broad peaks occur due to

the amorphous nature of $SiO_2$ in comparison to the crystalline structures of the other supports.[33] Au reflections can be seen at 38, 44, 65 and 78° for both conventional and modified impregnation catalysts and weaker peaks are present in the sol immobilised sample. In the wet impregnation sample a reflection can be observed for PdO at 34°.[34]

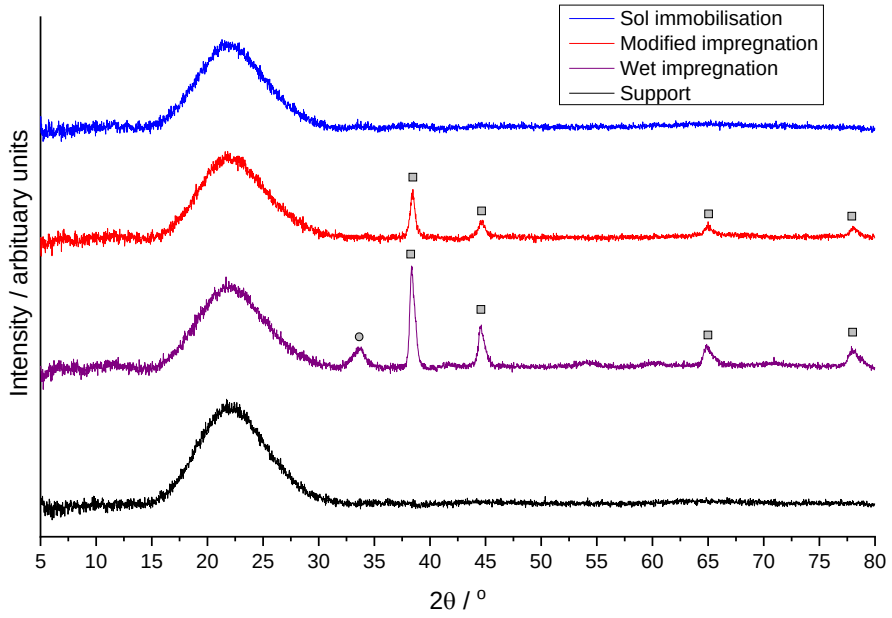


***Figure 4.6.*** *X-ray diffractogram data of 1 % AuPd/$SiO_2$ catalysts produced via different preparation methods. Au reflections (■), PdO reflections (●).*

The larger reflections observed for wet impregnation again indicates larger particle sizes on the catalyst along with PdO reflections indicating larger PdO compositions in these particles. The absence of either Au or Pd reflections in the sol immobilisation sample could indicate small particle sizes, confirming sol immobilisation form small nanoparticles.[30] These small particles could be the source of the high degradation observed for the sol catalyst, Figure 4.3.

Due to high crystallinity rising to strong reflections of the ceria support, Figure 4.7, it is hard to see the reflections of the metals however in the wet impregnation catalysts small reflections can be seen at 38 and 65 ° for Au, again indicating larger particles present in this preparation method. These large particles could contribute to the higher activity observed for the wet impregnation catalyst and its decreased $H_2O_2$ degradation. However, it should be noted that the $CeO_2$ catalyst prepared by sol immobilisation showed low degradation and synthesis activity despite suggesting small nanoparticles indicating that the particle size is not the only influencing factor.

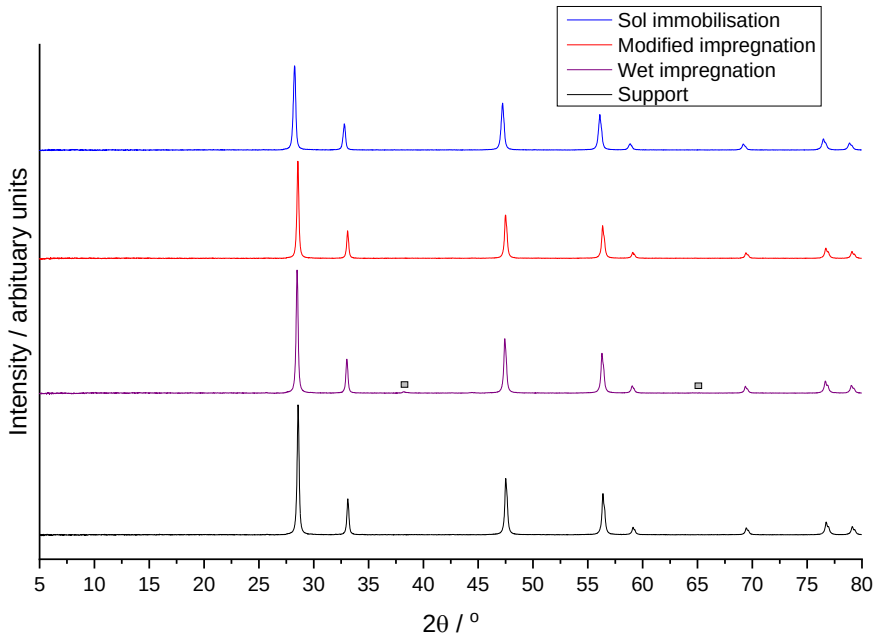


***Figure 4.7.*** *X-ray diffractogram data of 1 % AuPd/$CeO_2$ catalysts produced via different preparation methods. Au reflections (■).*

Again, the Au reflections expected between 30 to 40 ° cannot be determined due to overlap with the reflections associated with MgO, Figure 4.8. For wet impregnation, small shoulder reflections can be observed at 44 and 65° which could be attributed to Au.

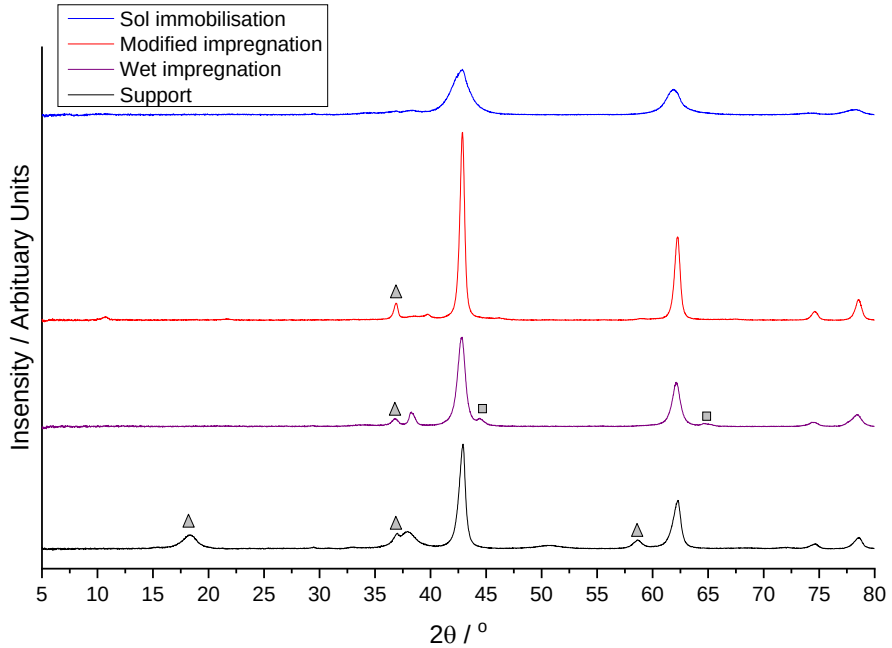


***Figure 4.8.*** *X-ray diffractogram data of 1 % AuPd/MgO catalysts produced via different preparation methods. Au reflections (■), MgOH reflections (▲)*

It can be observed that the reflections of the MgO support cannot be seen in the catalysts which could indicate a disruption to the crystalline structure via preparation or heat treatment of the catalysts. The reflections that are missing from catalysts that

are present in the support are attributed to MgOH.[35] Some reflections for MgOH are still present in the wet impregnation and modified impregnation catalyst at 37°. It has been widely reported that the thermal decomposition of MgOH can form MgO, at as low as 300 °C,[36] and hence the disappearance of some MgOH reflections could have occurred during the catalyst heat treatments. For sol immobilisation all MgOH reflections have gone and the MgO reflections widen indicating a loss in crystallinity during catalyst preparation. Sol immobilisation preparation involves acidification of the sol with $H_2SO_4$ as reported in detail in Chapter 2. This addition of acid can hydrolyse MgOH to MgO reducing the basicity of the support. Hence this decrease in basicity could explain the reduced degradation of $H_2O_2$ observed for the MgO sol immobilisation catalyst, compared to modified and wet impregnation, which has maintained the least MgO reflections.

### 4.4.2 XPS.

XPS analysis of the AuPd catalysts has been conducted with the results shown in Table 4.4. From these the ratio of Pd:Au can be calculated as well as $Pd^0$:$Pd^{2+}$.

***Table 4.4.*** *XPS analysis of Pd and Au determined by XPS of 1 % AuPd supported catalysts.*

| Support | Preparation Method | Pd:Au | $Pd^0$:$Pd^{2+}$ |
|---|---|---|---|
| $CeO_2$ | wet impregnation | 55.9 | 0.54 |
| | modified impregnation | 3.1 | 0.95 |
| | sol immobilised | 4.6 | 0.30 |
| $SiO_2$ | wet impregnation | 10 | All $Pd^{2+}$ |
| | modified impregnation | 2.5 | 0.67 |
| | sol immobilised | 1.7 | 1.8 |
| $TiO_2$ | wet impregnation | 18.5 | 1.3 |
| | modified impregnation | 3.9 | 4.4 |
| | sol immobilised | 3.9 | 1.6 |
| MgO | wet impregnation | 36.5 | 0.70 |
| | modified impregnation | 11.3 | 0.98 |
| | sol immobilised | 13.4 | 0.23 |

It has been observed, for all supports, that catalysts produced via wet impregnation have a higher ratio of Pd:Au than the other preparation methods. This indicates a larger concentration of surface Pd in comparison to Au suggesting that the nanoparticles immobilised upon the support are of a Pd-shell Au-core morphology or that the Pd present is better dispersed on the support. These core shell morphologies have previously been reported for 5% AuPd/$TiO_2$ and other oxide supports prepared by wet impregnation.[3] This core-shell morphology although was observed to be less active

than the corresponding random alloy morphology it did maintain it's structure and activity upon re-use. The core shell particle morphology was shown to stable up to 4 uses for the direct synthesis of $H_2O_2$.[3]

XPS also showed that the modified impregnation catalysts had the higher metallic Pd content compared to the wet impregnation and sol immobilised equivalents. These catalysts are exposed to a reductive heat treatment rather than calcined, as in the case of wet impregnation and sol immobilisation. Metallic Pd has previously been observed in the literature to provide higher activity for $H_2O_2$ synthesis.[4,18,19,37] Sankar *et al.* have previously reported that bimetallic catalysts prepared by modified impregnation show high activity for $H_2O_2$ synthesis which has been partially attributed to the large $Pd^0$ content.[4] This data could be used to explain reactivity trends seen in the oxidation of cyclohexane via the production of *in-situ* $H_2O_2$ where it is postulated that a larger proportion of reduced Pd leads to a higher catalytic activity due to an increase in $H_2O_2$ activity, as discussed in Chapter 3.

### 4.4.3 TGA.

Sol immobilisation catalysts employ stabilising agents to avoid the coalescent of nanoparticles during synthesis and result in small particle size with a tight size distribution.[6–8,30] However, after preparation of the catalyst the polymer stabilising agent are still bound to the nanoparticles, this can block the catalyst actives sites and be detrimental to catalytic activity.[38] Hence heat treatments can be employed to remove the stabiliser and to stabilise catalyst activity. However, it should be noted that heat treatments have shown to increase particle size and relative amounts of PdO on the particle surface.[6,38] Lopez-Sanchez *et al.* have previously shown that AuPd catalysts prepared by sol immobilisation offered high initial activities for $H_2O_2$ synthesis however the degradation of $H_2O_2$ was also high (up to 27% $H_2O_2$ degraded for 1% AuPd/$TiO_2$ at 2 °C).[7] Hence the addition of a calcination heat treatment have been introduced for these catalysts to increase PdO content to increase $H_2O_2$ selectivity.[19] It was also hoped that a calcination could increase the stability of the catalysts at the elevated temperatures used for the oxidation of cyclohexane. TGA analysis has been implemented to show the stability of the catalysts and to inform on calcination temperatures for the sol immobilisation catalysts, Figure 4.9.

During the preparation of sol immobilisation catalysts the required amount of a PVA solution (1 wt%) was added to give a PVA/(Au + Pd) (wt/wt) ratio of 1.3, as previously reported to be optimum by Pitchard *et al.*,[30] and hence on these catalyst a weight change of around 1.3 % would be expected if all the PVA was present on the catalyst and removed upon heating. According to the literature the decomposition of PVA ligand would be expected above 250 °C.[6]

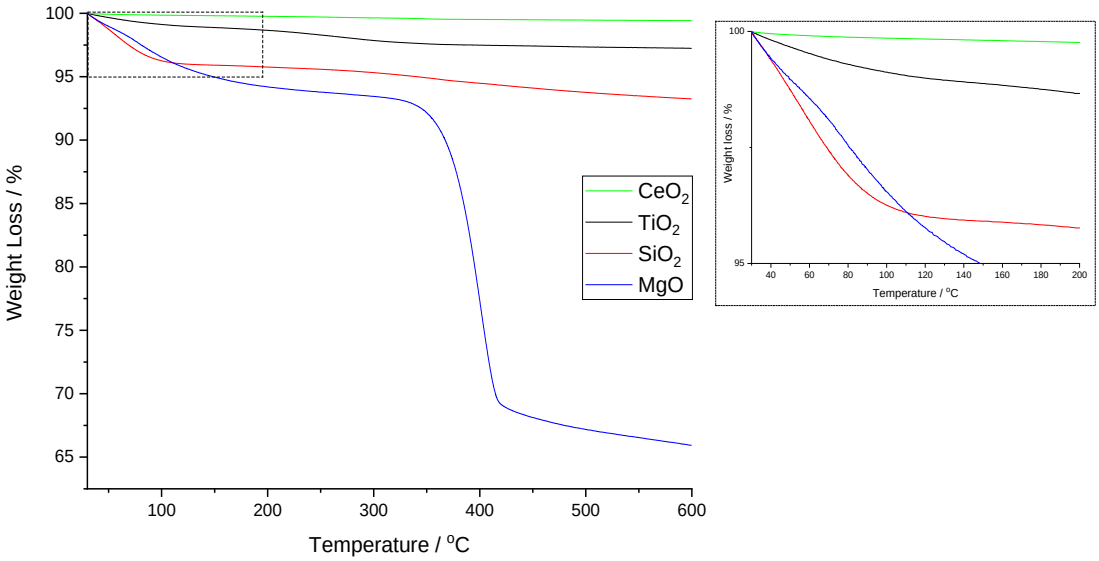


***Figure 4.9.*** *TGA analysis of 1 % AuPd different supports produced via sol immobilisation using PVA as the stabiliser. TGA conditions; 30 to 600 °C with a ramp rate of 10 °C min$^{-1}$ in air.*

Both $TiO_2$ and $CeO_2$ have shown no overall large decrease in mass. The small decreases in mass over the temperature region can be attributed to PVA decomposition or the loss of water from the catalyst surface and no overall decomposition of the catalyst.

For $SiO_2$ sample a larger mass loss can be seen in the initial heating to 100 °C after this no substantial mass loss can be seen. This could indicate that the catalyst and support is slightly unstable, and some decomposition occur below 100 °C, or could be attributed to a larger loss of $H_2O$ from the sample, compared to $TiO_2$ and $CeO_2$.

For MgO a dramatic loss in weight can be seen at 400 °C. This would indicate some decomposition of the catalyst and support and hence suggest some thermal instability of the catalyst around 400 °C. A change in the MgO support was observed by XRD during catalyst preparation with the loss of reflections corresponding to MgOH and a broadening of peaks indicating a loss of crystallinity for the sol immobilisation catalyst. Hence some of the instability observed by TGA for the MgO catalyst could

be attributed to this loss in crystallinity and led to the very limited catalytic activity observed for $H_2O_2$ synthesis (2 $mol_{H_2O_2}$ $kg_{cat}^{-1}$ $hr^{-1}$) and the subsequent oxidation of cyclohexane.

## 4.5 Conclusions and future work.

This chapter has focussed on a range of methodologies to enhance catalytic performance for the selective oxidation of cyclohexane via *in-situ* production of $H_2O_2$. Comparing preparation methods, catalysts prepared by modified impregnation have shown the highest activity for the oxidation of cyclohexane via the *in-situ* production of $H_2O_2$. The addition of acid and a reductive heat treatment could explain the superiority of this preparation method. The reductive heat treatment has introduced a greater amount of $Pd^0$ while maintaining PdO-Pd interfaces. Overall $TiO_2$ was shown to be the best support for the oxidation of cyclohexane via the *in-situ* production of $H_2O_2$. This is despite $SiO_2$ showing greater $H_2O_2$ synthesis activity illustrating that the direct correlation between $H_2O_2$ synthesis activity and *in-situ* oxidation cannot be made.

Following on from this future work will focus on catalysts supported onto $TiO_2$ and following the modified impregnation procedure to increase the catalytic performance for the *in-situ* oxidation of cyclohexane further.

## 4.6 References.

1. J. K. Edwards and G. J. Hutchings, *Angew. Chem. Int. Ed.*, 2008, **47**, 9192–9198.
2. J. K. Edwards, B. E. Solsona, P. Landon, A. F. Carley, A. Herzing, C. J. Kiely and G. J. Hutchings, *J. Catal.*, 2005, **236**, 69–79.
3. J. K. Edwards, A. F. Carley, A. A. Herzing, C. J. Kiely and G. J. Hutchings, *Faraday Discuss.*, 2008, **138**, 225–239.
4. M. Sankar, Q. He, M. Morad, J. Pritchard, S. J. Freakley, J. K. Edwards, S. H. Taylor, D. J. Morgan, A. F. Carley, D. W. Knight, C. J. Kiely and G. J. Hutchings, *ACS Nano*, 2012, **6**, 6600–6613.
5. M. Morad, M. Sankar, E. Cao, E. Nowicka, T. E. Davies, P. J. Miedziak, D. J. Morgan, D. W. Knight, D. Bethell, A. Gavriilidis and G. J. Hutchings, *Catal. Sci. Technol.*, 2014, **4**, 3120–3128.
6. J. Pritchard, M. Piccinini, R. Tiruvalam, Q. He, N. Dimitratos, J. A. Lopez-Sanchez, D. J. Morgan, A. F. Carley, J. K. Edwards, C. J. Kiely and G. J. Hutchings, *Catal. Sci. Technol.*, 2013, **3**, 308–317.
7. J. A. Lopez-Sanchez, N. Dimitratos, P. Miedziak, E. Ntainjua, J. K. Edwards, D. Morgan, A. F. Carley, R. Tiruvalam, C. J. Kiely and G. J. Hutchings, *Phys. Chem. Chem. Phys.*, 2008, **10**, 1921–1930.

8. N. Dimitratos, J. A. Lopez-Sanchez, D. Morgan, A. Carley, L. Prati and G. J. Hutchings, *Catal. Today*, 2007, **122**, 317–324.
9. S. J. Freakley, R. J. Lewis, D. J. Morgan, J. K. Edwards and G. J. Hutchings, *Catal. Today*, 2015, **248**, 10–17.
10. E. N. Ntainjua, M. Piccinini, J. C. Pritchard, J. K. Edwards, A. F. Carley, C. J. Kiely and G. J. Hutchings, *Catal. Today*, 2011, **178**, 47–50.
11. E. Ntainjua, J. K. Edwards, A. F. Carley, J. A. Lopez-Sanchez, J. A. Moulijn, A. A. Herzing, C. J. Kiely and G. J. Hutchings, *Green Chem.*, 2008, **10**, 1162–1169.
12. J. K. Edwards, A. Thomas, B. E. Solsona, P. Landon, A. F. Carley and G. J. Hutchings, *Catal. Today*, 2007, **122**, 397–402.
13. J. K. Edwards, A. Thomas, A. F. Carley, A. A. Herzing, C. J. Kiely and G. J. Hutchings, *Green Chem.*, 2008, **10**, 388–394.
14. M. Piccinini, E. N. N, J. K. Edwards, A. F. Carley, J. A. Moulijn and G. J. Hutchings, *Phys. Chem. Chem. Phys.*, 2010, **12**, 2488–2492.
15. J. C. Pritchard, Q. He, E. N. Ntainjua, M. Piccinini, J. K. Edwards, A. A. Herzing, A. F. Carley, J. A. Moulijn, C. J. Kiely and G. J. Hutchings, *Green Chem.*, 2010, **12**, 915–921.
16. Santos, R. J. Lewis, G. Malta, A. G. R. Howe, D. J. Morgan, E. Hampton, P. Gaskin and G. J. Hutchings, *Ind. Eng. Chem. Res.*, 2019, **58**, 12623–12631.
17. E. Ntainjua N., M. Piccinini, J. C. Pritchard, J. K. Edwards, A. F. Carley, J. A. Moulijn and G. J. Hutchings, *ChemSusChem*, 2009, **2**, 575–580.
18. F. Wang, C. Xia, S. P. de Visser and Y. Wang, *J. Am. Chem. Soc.*, 2019, **141**, 901–910.
19. V. R. Choudhary, C. Samanta and T. V. Choudhary, *Appl. Catal. Gen.*, 2006, **308**, 128–133.
20. D. P. Dissanayake and J. H. Lunsford, *J. Catal.*, 2003, **214**, 113–120.
21. P. Tian, L. Ouyang, X. Xu, C. Ao, X. Xu, R. Si, X. Shen, M. Lin, J. Xu and Y.-F. Han, *J. Catal.*, 2017, **349**, 30–40.
22. D. A. Crole, S. J. Freakley, J. K. Edwards and G. J. Hutchings, *Proc R Soc A*, 2016, **378**: 20160156.
23. M. Conte, X. Liu, D. M. Murphy, K. Whiston and G. J. Hutchings, *Phys. Chem. Chem. Phys.*, 2012, **14**, 16279–16285.
24. X. Liu, M. Conte, M. Sankar, Q. He, D. M. Murphy, D. Morgan, R. L. Jenkins, D. Knight, K. Whiston, C. J. Kiely and G. J. Hutchings, *Appl. Catal. Gen.*, 2015, **504**, 373–380.
25. X. Liu, M. Conte, Q. He, D. Knight, D. Murphy, S. Taylor, K. Whiston, C. Kiely and G. J. Hutchings, *Chem. Eur. J.*, 2017, **23**, 11834-11842.
26. H. Einaga, S. Futamura and T. Ibusuki, *Appl. Catal. B Environ.*, 2002, **38**, 215–225.
27. R. Tomat and A. Rigo, *J. Appl. Electrochem.*, 1980, **10**, 549–552.
28. E. V. Spinace, H. O. Pastore and U. Schuchardt, *J. Catal.*, 1995, **157**, 631–635.
29. S. J. Freakley, Q. He, J. H. Harrhy, L. Lu, D. A. Crole, D. J. Morgan, E. N. Ntainjua, J. K. Edwards, A. F. Carley, A. Y. Borisevich, C. J. Kiely and G. J. Hutchings, *Science*, 2016, **351**, 965–968.
30. J. Pritchard, L. Kesavan, M. Piccinini, Q. He, R. Tiruvalam, N. Dimitratos, J. A. Lopez-Sanchez, A. F. Carley, J. K. Edwards, C. J. Kiely and G. J. Hutchings, *Langmuir*, 2010, **26**, 16568–16577.
31. S. Han and C. B. Mullins, *ACS Catal.*, 2018, **8**, 3641–3649.

32. H. E. Swanson, United States and National Bureau of Standards, *Standard x-ray diffraction powder patterns*, U.S. Dept. of Commerce, National Bureau of Standards : For sale by the Supt. of Docs., U.S. G.P.O., Washington, DC, 1953.
33. C. Graf, *Kirk-Othmer Encyclopedia of Chemical Technology*, American Cancer Society, 2018, pp. 1–43.
34. G. K. Reddy, C. Ling, T. C. Peck and H. Jia, *RSC Adv.*, 2017, **7**, 19645–19655.
35. W. Sutapa, A. W. Wahab, P. Taba and N. L. Nafie, *Orient. J. Chem.*, 2018, **34**, 1016–1025.
36. F. Moodie and C. E. Warble, *J. Cryst. Growth*, 1986, **74**, 89–100.
37. N. M. Wilson, P. Priyadarshini, S. Kunz and D. W. Flaherty, *J. Catal.*, 2018, **357**, 163–175.
38. A. Lopez-Sanchez, N. Dimitratos, C. Hammond, G. L. Brett, L. Kesavan, S. White, P. Miedziak, R. Tiruvalam, R. L. Jenkins, A. F. Carley, D. Knight, C. J. Kiely and G. J. Hutchings, *Nat. Chem.*, 2011, **3**, 551–556.

# Appendix.

***Table S4.1*** *Atomic concentrations of Pd and Au determined from XPS analysis of 1 % AuPd supported catalysts.*

| Support | Preparation Method | Atomic concentration / % | | |
|---|---|---|---|---|
| | | Au | $Pd^0$ | $Pd^{2+}$ |
| $CeO_2$ | wet impregnation | 0.14 | 2.76 | 5.06 |
| | modified impregnation | 0.23 | 0.35 | 0.37 |
| | sol immobilised | 0.33 | 0.35 | 1.18 |
| $SiO_2$ | wet impregnation | 0.01 | 0 | 0.1 |
| | modified impregnation | 0.02 | 0.02 | 0.03 |
| | sol immobilised | 0.18 | 0.2 | 0.11 |
| $TiO_2$ | wet impregnation | 0.06 | 0.63 | 0.48 |
| | modified impregnation | 0.07 | 0.22 | 0.05 |
| | sol immobilised | 0.1 | 0.24 | 0.15 |
| MgO | wet impregnation | 0.02 | 0.3 | 0.43 |
| | modified impregnation | 0.07 | 0.39 | 0.4 |
| | sol immobilised | 0.09 | 0.23 | 0.98 |

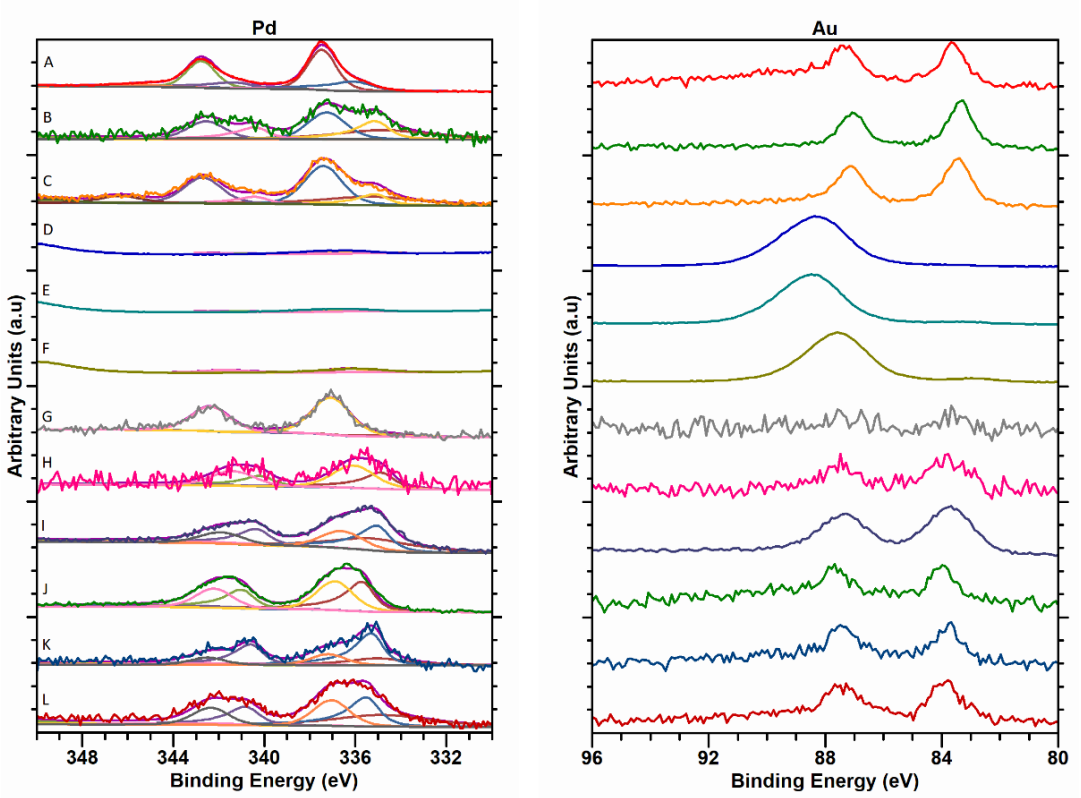


***Figure S4.10.*** *XPS spectra and fitting of Pd 3d and Au 4f regions for 1% AuPd/$TiO_2$ catalysts prepared by different preparation methods and on different supports. Supported on $CeO_2$ prepared by wet impregnation (**A**), modified impregnation (**B**) and sol immobilisation (**C**). Supported on MgO prepared by wet impregnation (**D**), modified impregnation (**E**) and sol immobilisation (**F**). Supported on $SiO_2$ prepared by wet impregnation (**G**), modified impregnation (**H**) and sol immobilisation (**I**). Supported on $TiO_2$ prepared by wet impregnation (**J**), modified impregnation (**K**) and sol immobilisation (**L**).*

# 5. Replacing Au for the selective oxidation of cyclohexane via the *in-situ* production of $H_2O_2$.

## 5.1 Introduction.

From initial studies in Chapter 3 it was observed for a 1% $AuPd/TiO_2$ that catalytic activity towards the oxidation of cyclohexane via the *in-situ* production of $H_2O_2$ improved upon re-use of the catalyst. It was determined that the increase in activity was due to an increase in $Pd^0$ centres and a re-structuring of the Au-Pd bimetallic nanoparticles to enhance the Au core-Pd shell morphology as suggested by XPS analysis. Reduced Pd species have previously been shown to offer increased activity in the direct synthesis of $H_2O_2$.[1] As a reduced Pd oxidation state was observed to enhance cyclohexane oxidation activity in Chapter 3 subsequent catalysts have been prepared via a modified impregnation procedure,[2] where a reductive heat treatment (500 °C, 4 hours) is used, have now been explored for the oxidation of cyclohexane.

As outlined in Chapter 1 the oxidation of cyclohexane is known to proceed via a radical mechanism,[3–8] as such the production of radicals *in-situ* is essential; and hence another important class of catalysts to explore are those in which Fenton's Chemistry, Figure 5.1, is apparent.[9–11] Fenton's Chemistry is the utilisation of Fe to convert $H_2O_2$ into hydroxyl and hydroperoxyl radicals. As such a series of Pd based catalysts incorporating Fentons or Fentons-like metals,[12,13] prepared via a modified impregnation methodology, have been studied for the direct synthesis of $H_2O_2$ and *in-situ* oxidation of cyclohexane.

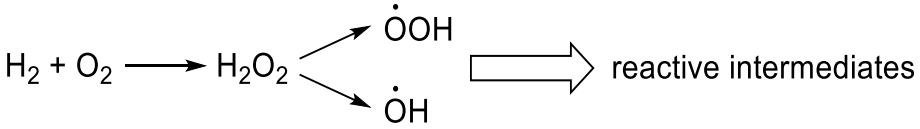


***Figure 5.1**. The reactive oxygen species that are produced from $H_2O_2$.*

## 5.2 Bimetallic Pd based catalysts for the direct synthesis of $H_2O_2$.

All catalysts produced were first tested for the direct synthesis of $H_2O_2$ to assess their performance for $H_2O_2$ formation, Figure 5.2. 1% $VPd/TiO_2$, 1% $MnPd/TiO_2$, $FePd/TiO_2$, 1% $CoPd/TiO_2$ and 1 % $AuPd/TiO_2$ have all shown an enhanced activity compared to monometallic 1% $Pd/TiO_2$ indicating a synergistic enhancement in these bimetallic catalysts.

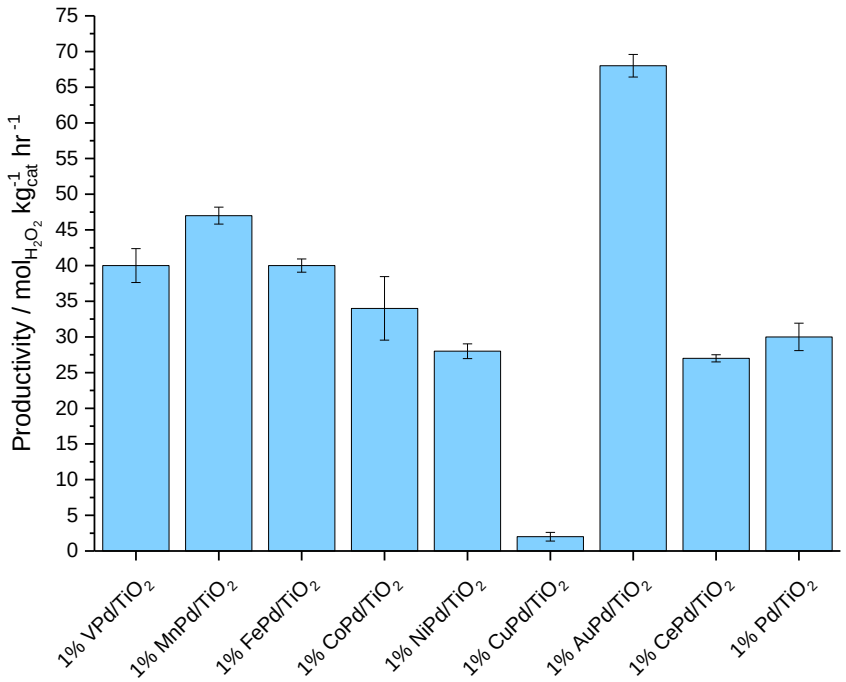


***Figure 5.2*** *The activity of bimetallic 1 % XPd/TiO$_2$ catalysts towards the synthesis of H$_2$O$_2$.* ***Reaction conditions;*** *0.01 g catalyst, 2.9 g water, 5.6 g methanol, 29 bar 5 % H$_2$/CO$_2$ and 11 bar 25 % O$_2$/CO$_2$, 1200 RPM, 30 minutes, 25 °C.*

1 % VPd/TiO$_2$, 1 % MnPd/TiO$_2$ and 1 % FePd/ TiO$_2$ catalysts are observed to have similar H$_2$O$_2$ activity and offer greater activity compared to X= Ce, Cu, Ni and Co. However, these catalysts are still much less active than the previously reported 1 % AuPd/TiO$_2$ (68 mol$_{H_2O_2}$ kg$_{cat}^{-1}$ hr$^{-1}$). This 1% AuPd/TiO$_2$ catalyst has previously been reported to offer a productivity of 75 mol$_{H_2O_2}$ kg$_{cat}^{-1}$ hr$^{-1}$ tested at 20 °C.[14] Very limited activity has been seen with 1 wt.% CuPd/TiO$_2$, showing that the addition of Cu has had a detrimental effect on catalytic activity. This is in keeping with previous investigations into AuPdCu supported on TiO$_2$, where the addition of 0.1 wt.% Cu reduced the activity of a 5% AuPd/TiO$_2$ from 83 to 10 mol$_{H_2O_2}$ kg$_{cat}^{-1}$ hr$^{-1}$.[15] In this study it was postulated that the addition of small amounts of Cu could increase the selectivity towards methanol in the oxidation of methane when H$_2$O$_2$ is both added and generated *in-situ*.[15] Joshi *et al.* demonstrated, by DFT calculations, that the addition of H$_2$ to form OOH was thermodynamically unfavourable on CuPd catalysts. The second H addition to form H$_2$O$_2$ is also unfavourable resulting in limited H$_2$O$_2$ yields from CuPd clusters.[16]

1% AuPd/TiO$_2$ has shown to be the most active catalyst towards the synthesis as well as the most selective based on H$_2$ conversion (38 %), Table 5.1. The lower selectivity for the other catalysts could be attributed to the Fenton's and Fenton's-like metals

which, by definition, break $H_2O_2$ into radicals ($^{\bullet}OH$) which could lead to the greater degradation of $H_2O_2$.

***Table 5.1.*** *The $H_2$ conversion and $H_2O_2$ selectivity of bimetallic 1 % XPd/$TiO_2$ catalysts towards the synthesis of $H_2O_2$.*

| Catalyst | Productivity / $mol_{H_2O_2}$ $kg^{-1}$ $hr^{-1}$ | $H_2$ Conversion / % | $H_2O_2$ Selectivity / % [a] |
|---|---|---|---|
| 1% Pd/$TiO_2$ | 30 | 29 | 21 |
| 1 % AuPd/$TiO_2$ | 68 | 57 | 38 |
| 1 % VPd/$TiO_2$ | 40 | 39 | 21 |
| 1 % MnPd/$TiO_2$ | 47 | 56 | 18 |
| 1 % FePd/$TiO_2$ | 40 | 58 | 14 |
| 1 % CoPd/$TiO_2$ | 34 | 48 | 16 |
| 1 % NiPd/$TiO_2$ | 28 | 30 | 19 |
| 1 % CuPd/$TiO_2$ | 2 | 18 | 2 |
| 1 % CePd/$TiO_2$ | 27 | 15 | 39 |

***Reaction conditions;*** *0.01 g catalyst, 2.9 g water, 5.6 g methanol, 29 bar 5 % $H_2/CO_2$ and 11 bar 25 % $O_2/CO_2$, 1200 RPM, 30 minutes, 25 °C. [a] Selectivity based on $H_2$ consumption.*

It can be observed that there is a correlation between $H_2$ conversion and productivity for the first row transition metals and Pd catalysts (Appendix, Figure S5.1) leading to all catalysts having similar selectivity, based on $H_2$, of 15 – 20 %.

Degradation data, Figure 5.3, have shown that all catalysts degrade $H_2O_2$ to a much lesser extent than the bimetallic 1 % AuPd/$TiO_2$ and monometallic 1% Pd/$TiO_2$.

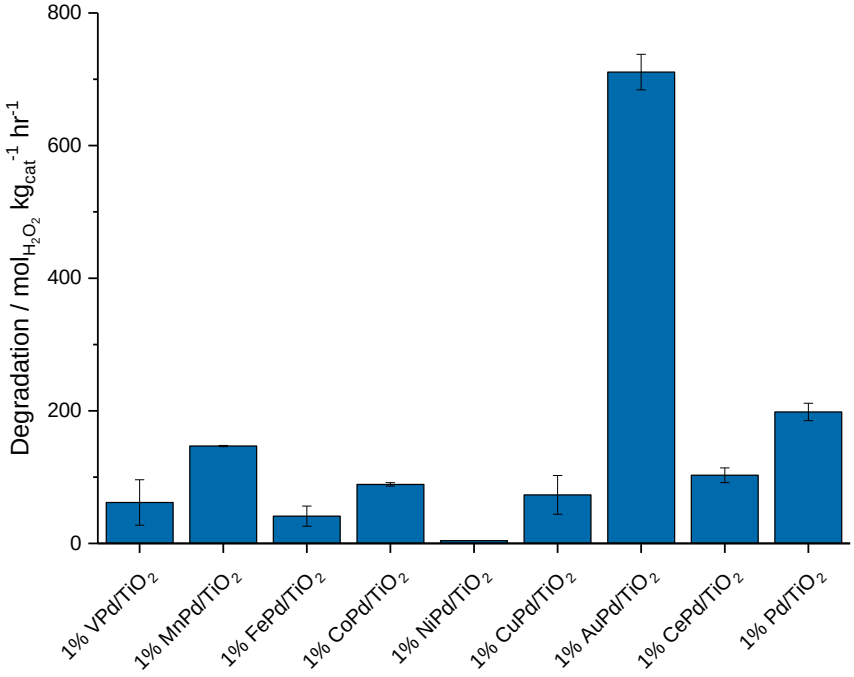


***Figure 5.3*** *The activity of bimetallic 1 % XPd/$TiO_2$ catalysts towards the degradation of $H_2O_2$.* ***Reaction conditions****; 0.01 g catalyst, 0.68 g 50 wt% $H_2O_2$, 2.22 g water, 5.6 g methanol, 29 bar 5 % $H_2/CO_2$, 1200 RPM, 30 minutes, 25 °C.*

All new catalysts are seen to offer similar rates of $H_2O_2$ degradation, with the exception of 1% NiPd/$TiO_2$ which shows negligible $H_2O_2$ degradation (10 $mol_{H_2O_2}$ $kg_{cat}^{-1}$ $hr^{-1}$). However, this is not surprising as both Crole and Freakley have previously reported that the addition of Ni to Pd catalysts can dramatically increase selectivity towards $H_2O_2$.[17,18]

The corresponding monometallic catalysts, 1% X/$TiO_2$, have also been synthesised and tested for the formation and degradation of $H_2O_2$, Table 5.2. However, all catalysts except 1% Pd/$TiO_2$ (30 $mol_{H_2O_2}$ $kg_{cat}^{-1}$) have shown very limited activity towards the direct synthesis of $H_2O_2$.

***Table 5.2.*** *The productivity, degradation, $H_2$ conversion and $H_2O_2$ selectivity of monometallic 1 % X/$TiO_2$ catalysts towards the synthesis of $H_2O_2$.*

| Catalyst | Productivity / $mol_{H_2O_2}$ $kg^{-1}$ $hr^{-1}$ | Degradation / $mol_{H_2O_2}$ $kg^{-1}$ $hr^{-1}$ | $H_2$ Conversion / % | $H_2O_2$ Selectivity* / % [a] |
|---|---|---|---|---|
| 1 % V/$TiO_2$ | 2 | 20 | 6 | 17 |
| 1 % Mn/$TiO_2$ | 2 | 0 | 3 | 13 |
| 1 % Fe/$TiO_2$ | 2 | 0 | 0 | N/D |
| 1 % Co/$TiO_2$ | 1 | 0 | 8 | 5 |
| 1 % Ni/$TiO_2$ | 0 | 0 | 0 | N/D |
| 1 % Cu/$TiO_2$ | 1 | 0 | 0 | N/D |
| 1 % Au/$TiO_2$ | 4 | 0 | 13 | 3 |
| 1 % Ce/$TiO_2$ | 2 | 0 | 0 | N/D |
| 1% Pd/$TiO_2$ | 30 | 198 | 29 | 21 |

***Reaction conditions;*** *0.01 g catalyst, 2.9 g water, 5.6 g methanol, 29 bar 5 % $H_2/CO_2$ and 11 bar 25 % $O_2/CO_2$, 1200 RPM, 30 minutes, 25 °C. * Selectivity based on $H_2$ consumption. Note N/D means not determined as $H_2$ conversion is 0%.*

Due to the low $H_2O_2$ synthesis activity of these monometallic catalysts they have not been explored further for the oxidation reaction via the *in-situ* production of $H_2O_2$.

## 5.3 Bimetallic Pd based catalysts for the oxidation of cyclohexane via the *in-situ* production of $H_2O_2$.

A series of bimetallic 1% XPd/$TiO_2$ catalysts have been tested for the oxidation of cyclohexane via the *in-situ* production of $H_2O_2$, with the data seen in Figure 5.4.

Introducing a secondary metal into Pd supported catalysts has dramatically increased the catalytic activity and selectivity for the *in-situ* oxidation of cyclohexane, Table 5.3. All catalysts are seen to offer a limited yield of KA oil in the presence of $O_2$ only compared to $H_2$ and $O_2$ despite the same quantities of $O_2$ present under both conditions. The introduction of $H_2$ leads to a significant increase in KA oil yield clearly

demonstrating the importance of $H_2$ in the reaction and indicating that peroxide based species are imperative in the oxidation reaction under these conditions.

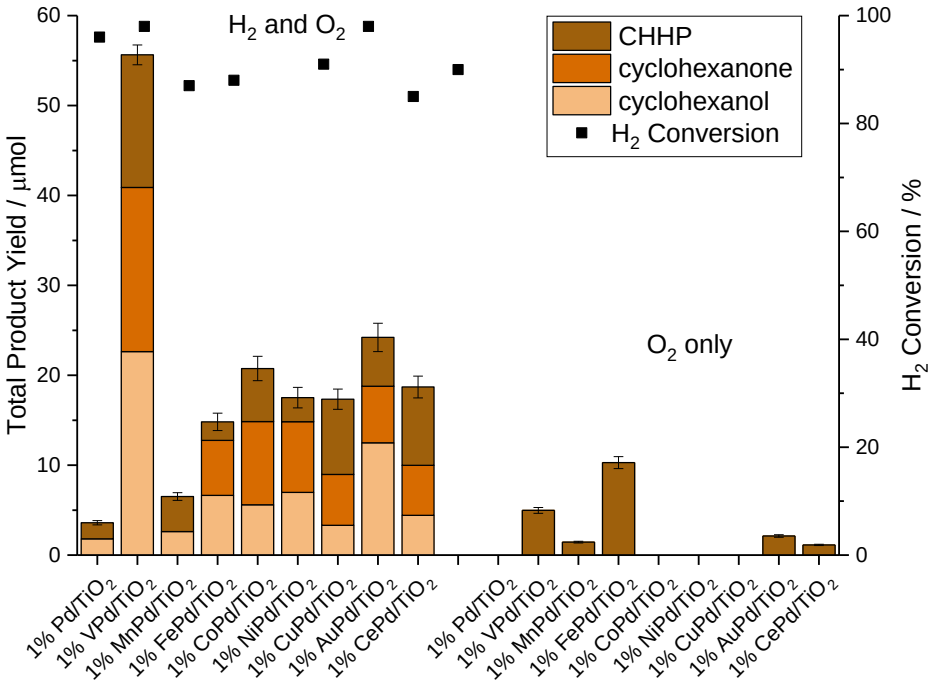


***Figure 5.4.*** *The activity of bimetallic 1 % XPd/$TiO_2$ catalysts towards the oxidation of cyclohexane. A comparison between in-situ and aerobic conditions.* ***Reaction conditions:*** *80 °C, 17 hours, 0.05 g catalyst, 6.37 g t-BuOH, 2.13 g (25 mmol) cyclohexane, 29 bar 5 % $H_2$ / $N_2$ and 11 bar 25 % $O_2$ / $N_2$ (only 29 bar $O_2$/$N_2$ present in $O_2$ only conditions), 1200 RPM.*

The alloying of Pd with secondary non-noble metals is generally reported to lead to yields of KA oil lower than the previously studied 1 % AuPd/$TiO_2$ catalyst, 18.8 µmol. This could be attributed to the decreased $H_2O_2$ activity observed for these catalysts compared to 1% AuPd/$TiO_2$. Perhaps more interestingly the 1 % VPd/$TiO_2$ catalyst is seen to outperform all catalysts, including 1 % AuPd/$TiO_2$, with a KA oil yield of 40.9 µmol observed, with this corresponding to a conversion of 0.27 %, compared to 0.10 % for 1% AuPd/$TiO_2$, Table 5.3. This is a doubling in the catalytic activity for 1% VPd/$TiO_2$ compared to 1% AuPd/$TiO_2$ despite a decrease in $H_2O_2$ productivity from 68 to 18 $mol_{H_2O_2}$ $kg_{cat}^{-1}$ $hr^{-1}$ for 1 % AuPd/$TiO_2$ and 1% VPd/$TiO_2$ respectively. This could indicate that $H_2O_2$ synthesis activity, measured at room temperature, is not necessarily a good metric for the oxidation. It should be noted that no correlation has been seen between either the synthesis or degradation of $H_2O_2$ and the oxidation of cyclohexane via the *in-situ* production of $H_2O_2$ (Appendix Figure S5.2).

Vanadium based catalysts have been explored in the literature for aerobic oxidations of various molecules, including cyclohexane.[19–24] A more detailed discussion of V catalysts is given in Section 5.4.

***Table 5.3.*** *$H_2$ conversion and selectivity to $C_6$ products during oxidation of cyclohexane.*

| Catalyst | $H_2$ Conversion / % | Total Product Yield / % | Selectivity to all $C_6^*$ products based on $H_2$ / % |
|---|---|---|---|
| 1% $Pd/TiO_2$ | 96 | 0.01 | 0.2 |
| 1% $VPd/TiO_2$ | 98 | 0.27 | 2.8 |
| 1% $MnPd/TiO_2$ | 87 | 0.03 | 0.3 |
| 1% $FePd/TiO_2$ | 88 | 0.06 | 0.7 |
| 1% $CoPd/TiO_2$ | 95 | 0.08 | 0.9 |
| 1% $NiPd/TiO_2$ | 91 | 0.07 | 0.8 |
| 1% $CuPd/TiO_2$ | 98 | 0.07 | 0.7 |
| 1% $AuPd/TiO_2$ | 95 | 0.10 | 1.0 |
| 1% $CePd/TiO_2$ | 90 | 0.07 | 0.8 |

***Reaction conditions;*** *80 °C, 17 hours, 0.05 g catalyst, 6.37 g t-BuOH, 2.13 g cyclohexane, 29 bar 5 % $H_2$ / $N_2$ and 11 bar 25 % $O_2$ / $N_2$, 1200 RPM. *$C_6$ products; cyclohexanol, cyclohexanone and CHHP.*

### 5.3.1 Catalyst characterisation.

Characterisation of the catalysts has focused on determining the oxidation states present on the surface using X-ray photoelectron spectroscopy (XPS). The catalysts have been analysed both as fresh samples and after use in cyclohexane oxidation to determine if any change in metal oxidation state occurs during the reaction, Table 5.4.

***Table 5.4.*** *XPS analysis of 1 % $XPd/TiO_2$ catalysts fresh and after use in the cyclohexane oxidation via in-situ $H_2O_2$ synthesis.*

| Catalyst | $Pd^0$:$Pd^{2+}$ | Pd:X | Expected Pd:X |
|---|---|---|---|
| 1 % $VPd/TiO_2$ | 3.3 | 0.19 | 0.48 |
| 1 % $VPd/TiO_2$ used | 3.8 | 0.18 | |
| 1 % MnPd/ $TiO_2$ | 2 | 0.34 | 0.52 |
| 1 % MnPd/ $TiO_2$ used | 2.83 | 0.34 | |
| 1 % FePd/ $TiO_2$ | 3.2 | 0.27 | 0.52 |
| 1 % FePd/ $TiO_2$ used | 13.5 | 0.41 | |
| 1 % CoPd/ $TiO_2$ | 17 | 0.21 | 0.55 |
| 1 % CoPd/ $TiO_2$ used | 3.2 | 0.25 | |
| 1 % $NiPd/TiO_2$ | 4 | 0.83 | 0.55 |
| 1 % $NiPd/TiO_2$ used | 2 | 0.81 | |
| 1 % CuPd/ $TiO_2$ | 16 | 0.28 | 0.60 |
| 1 % CuPd/ $TiO_2$ used | 4.86 | 0.38 | |
| 1 % AuPd/ $TiO_2$ | All $Pd^0$ | 2.27 | 1.85 |
| 1 % AuPd/ $TiO_2$ used | 10 | 11 | |
| 1 % CePd/ $TiO_2$ | All $Pd^0$ | 0.11 | 1.32 |
| 1 % CePd/ $TiO_2$ used | All $Pd^0$ | 0.08 | |

From the data shown in Table 5.4 it can be observed that in the fresh samples Pd is predominately present on the catalyst surface in the metallic form, as expected from the reductive heat treatment (500 °C, 4 hours) used in the preparation of the catalysts. Furthermore, the measured Pd:X ratio is generally lower than the expected ratio

calculated from the catalyst metal weight loadings, this is indicative of an increase in concentration of the secondary metal present on the surface in comparison to Pd. This could indicate larger particles sizes of the second metal which would lead to a decrease in dispersion of the metal.

No obvious changes can be seen in Pd:X ratio upon catalyst use, with the exception of 1 % AuPd/$TiO_2$ catalyst. This is in keeping with previous studies for an analogous catalyst, prepared via a wet impregnation, and is attributed to a restructuring of particle morphology resulting in the formation of Pd-shell Au-core particles, detailed in Chapter 3. Both the 1 % FePd/$TiO_2$ and 1 % MnPd/$TiO_2$ catalysts show an increase in $Pd^0$:$Pd^{II}$ after use in the oxidation of cyclohexane via *in-situ* $H_2O_2$ synthesis. Both 1 % CoPd/$TiO_2$ and 1 % CuPd have a higher $Pd^0$:$Pd^{II}$ as fresh catalysts compared to used and show a decrease in $Pd^0$:$Pd^{II}$ after use. These catalysts with an initial higher $Pd^0$:$Pd^{II}$, compared to used, have shown higher catalytic activity in the oxidation of cyclohexane. This can be attributed to previous investigations that showed that increase in reduced Pd species on the catalyst surface leads to increase in $H_2O_2$ synthesis activity.[25] The most active 1% VPd/$TiO_2$ has shown similar $Pd^0$:$Pd^{2+}$ and Pd:X both in the fresh and used catalyst potentially showing a stability of the electronic structure of Pd during use. The alloying of V and Pd could results in electronic enhancement of Pd as has previously been noted in the literature for Au and Pd.[26–28]

All post reaction solutions have been analysed by inductively coupled plasma mass spectrometry (ICP-MS) to detect if any leaching of active metal species occurs during the cyclohexane oxidation reaction, with the data seen in Table 5.5. Dissanayake and Lunsford have previously shown that colloidal Pd, in the form $PdCl_4^{2-}$, is an effective catalyst for the synthesis of $H_2O_2$ with low rates of $H_2O_2$ decomposition.[29] Homogeneous catalysts have been described in the literature for cyclohexane oxidation.[30–39] Most commonly Co based homogeneous catalysts have been used industrially for the oxidation of cyclohexane.[36,38–40] Alshaheri *et al.* have shown the use of highly selective (98%) divalent Ni, Co, Fe, Mn and Zn ions in Schiff bases as homogenous catalysts with $H_2O_2$ for cyclohexane oxidation at 70 °C, showing the versatility of non-noble metals for the homogeneous catalysis.[32] Mishra *et al.* have shown the efficiency of vanadium scorpionate complex for the aerobic oxidation of cyclohexane with high KA oil selectivity at 140 °C.[33] As it has been shown that

cyclohexane can be oxidised by homogeneous catalysts any leaching of the metals from the catalyst into solution must be considered as could add to the catalytic activity.

***Table 5.5.*** *ICP-MS analysis of post reaction solutions of 1 % XPd/$TiO_2$ used in the oxidation of cyclohexane, indicating the percentage of the metal leached.*

| Catalyst | % Pd leached (ppb) | % X leached (ppb) |
|---|---|---|
| 1 % VPd/$TiO_2$ | 0.29 (63) | 21 (4533) |
| 1 % MnPd/ $TiO_2$ | 0.58 (124) | 0.53 (116) |
| 1 % FePd/ $TiO_2$ | 2.7 (592) | 8.5 (1853) |
| 1 % CoPd/ $TiO_2$ | 0.75 (164) | 0.03 (6) |
| 1 % NiPd/$TiO_2$ | 0 (0) | 0 (0) |
| 1 % CuPd/ $TiO_2$ | 0.8 (178) | 58 (12641) |
| 1 % AuPd/ $TiO_2$ | 1.6 (353) | 0.46 (101) |
| 1 % CePd/ $TiO_2$ | 0.44 (96) | 0 (0) |

Through ICP-MS analysis of post reaction solutions, Table 5.5, it is possible to report only small amounts of Pd leaching for all catalysts tested. However, the extent of secondary metal leaching varies significantly, with Cu, V and to a lesser extent Fe, showing appreciable levels of leaching. It is likely that the extent of secondary metal leaching, in particular that of V, can be related to an improved catalytic activity for the oxidation of cyclohexane. Further studies have subsequently been conducted to determine if this is the case, with the findings discussed below in Section 5.4.4.

Garcia-Bosch and Siegler have utilised Cu complexes for the oxidation cyclohexane using $H_2O_2$ in a Fenton's-like regime with high yields, up to 50%, with cyclohexanol as the major product.[35] Large leaching has also be observed for Cu in the 1% CuPd/$TiO_2$ catalyst and hence some activity could be attributed to Fenton's activity of homogeneous Cu, however it should be noted that this catalyst showed limited $H_2O_2$ synthesis activity at room temperature. There has also been leaching of Fe from 1% FePd/$TiO_2$ and as solution Fe is well known to act as a Fenton's reagent in a variety of oxidation reactions[41–46], including cyclohexane,[47,48] this could also be contributing to the activity observed here.

## 5.4 Further investigation into 1 % VPd/$TiO_2$.

### 5.4.1 1% VPd/$TiO_2$ characterisation.

The 1% VPd/$TiO_2$ prepared by modified impregnation has shown an enhanced activity for the oxidation of cyclohexane compared to 1% AuPd/$TiO_2$, Figure 5.4. Extensive catalyst characterisation has been performed to determine any structure activity relationships.

Transmission electron microscopy (TEM) analysis of the 1 % VPd/$TiO_2$ conducted in Cardiff University has shown no clear nanoparticles on the catalysts surface, Figure 5.5 A and B. Around the edge of the $TiO_2$ particles it is clear there is some roughening, this could indicate very small, sub-nanometre, particles present on the support surface. Hence higher resolution high-angle annular dark-field scanning transmission electron microscopy (HAADF-STEM) imaging conducted at Diamond Light Source, Hartwell, Figure 5.5 C and D. This imaging has shown small sub-nanometre particles, Figure 5.5 C, along with some larger particle around 5 nm, Figure 5.5 D, however as these particles are sparce on the support a reliable mean particle size could not be conducted.

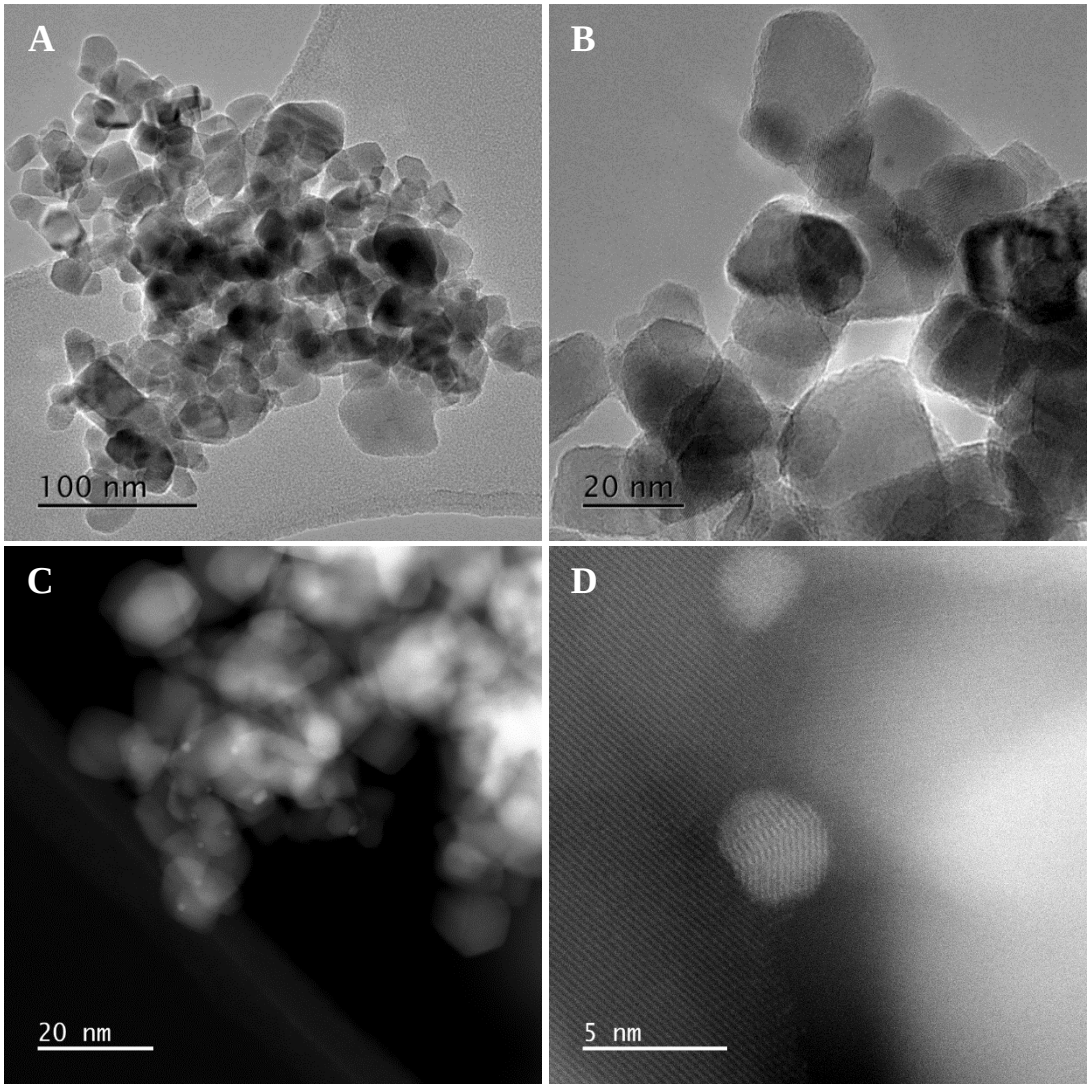


***Figure 5.5.*** *TEM (A and B) and HAADF-STEM (C and D) imaging of fresh 1 % VPd/$TiO_2$ catalyst.*

The distribution of metal nanoparticles over the $TiO_2$ surface, determined by Energy Dispersive X-Ray (EDX) mapping, shows a wide distribution, in particular V, over the support surface, Figure 5.6. This also suggests that there is no or limited alloying between V and Pd and that V is associated with the support with discrete Pd particles.

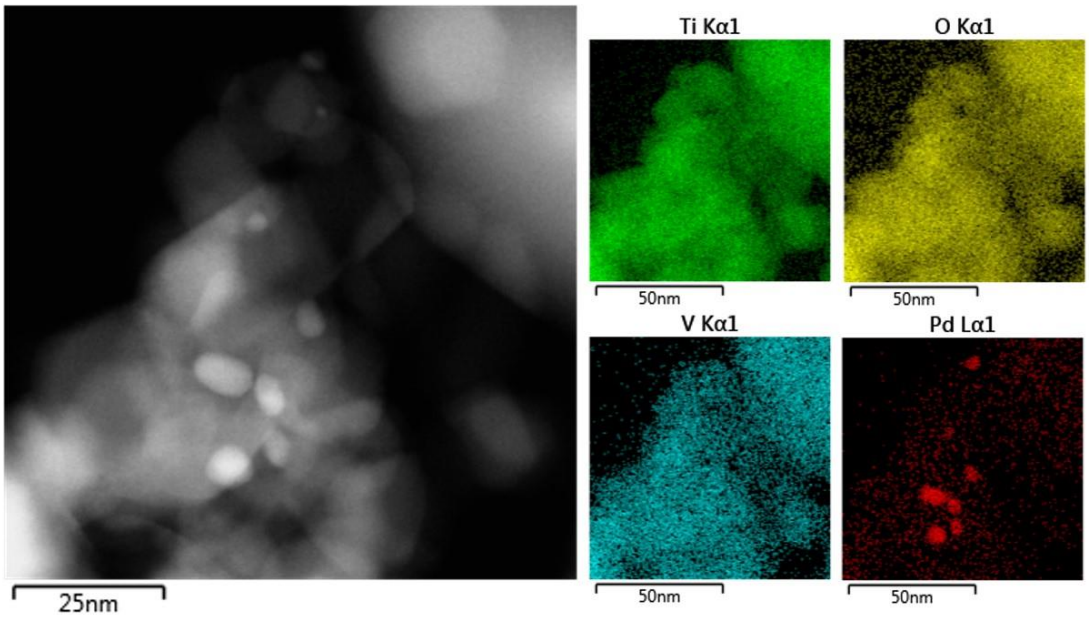


***Figure 5.6.*** *HAADF-STEM imaging and the corresponding EDX Mapping of Ti, O, V and Pd for fresh 1 % VPd/$TiO_2$.*

Wachs *et al.* have previously observed that the structure of $VO_x/TiO_2$ catalysts were strongly dependant on calcination temperature.[49] At low calcination temperatures, 110 – 200 °C, V is shown to exist as the precursor V salt – vanadium oxylate. Under optimum conditions, 350 – 575 °C, vanadia is present as a dispersed monolayer on $TiO_2$ and $V_2O_5$ crystallites. These complete monolayers of vanadia have been shown to be the most active for the oxidation of o-xylene. At elevated calcination temperatures, greater than 575 °C, a mixed V-Ti-O phase is produced which was shown to be detrimental to catalytic activity.[49,50] This illustrated the enhanced catalytic performance of vanadia monolayers and hence if this 1% $VPd/TiO_2$ does contain monolayer coverage of vanadia it could rationalise its improved catalytic activity. In the modified impregnation 1% $VPd/TiO_2$ $VCl_3$ was used as a precursor with a reductive heat treatment but further studies, detailed in Sections 5.4, have implemented ammonium metavanadate as the precursor and varying calcinations to encourage $VO_x$ formation.

TPR analysis of 1% $Pd/TiO_2$ have shown negative peak at 75 °C, Figure 5.7, which is attributed to the release of $H_2$ from Pd-H species that are formed at 25 °C when $H_2$ is initially flowed over the catalyst during sample pre-treatment.[51] In 1% $VPd/TiO_2$ it is unclear whether this peak has disappeared completely or shifted to a higher temperature, 123 °C, as highlighted in Figure 5.7. Both these indicate a stabilisation of Pd by V. The disappearance of the Pd-H peak could indicate an enhanced dispersion

of Pd on the catalyst and a stabilisation of the electronic structure of Pd. This electronic stabilisation of Pd has been reported previously for Au [52] and hence similar effects could have occurred through the alloying of Pd and V. Above 200 °C multiple reduction peaks can be observed for V species, indicating a high oxidation state of V.

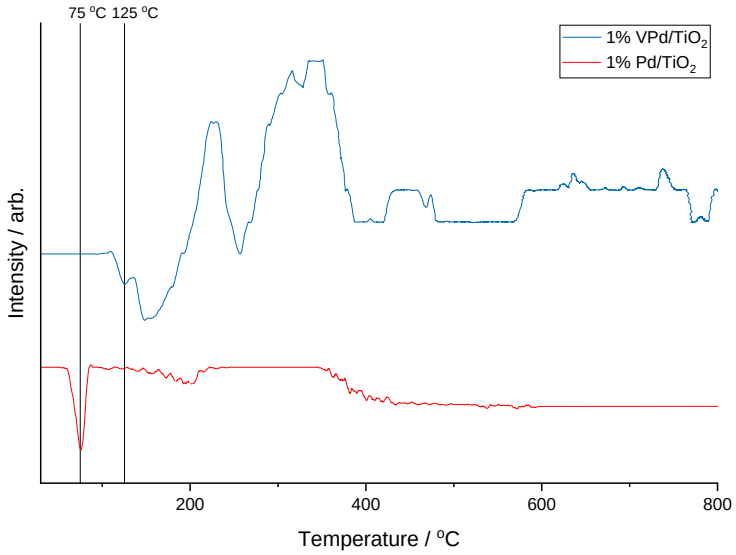


***Figure 5.7.*** *TPR profiles for 1% VPd/$TiO_2$ (blue) and 1% Pd/$TiO_2$ (red).*

It has been reported that the alloying of V and Pd increases the reducibility of V in the catalysts,[24,53–55] indicating a larger range of available oxidation states of V. Garcia *et al.* have also noted that the addition of Pd to V/$TiO_2$ catalysts increases the amount of polyvanadate species present on the surface of the catalyst. They have also noted that upon alloying there's an increase in the +4 oxidation state of V, compared to +5, and an increase in $Pd^{2+}$.[24] With V loading less than monolayer coverage (<1% V) on 0.5% Pd/$TiO_2$ Pd was present in only $Pd^{2+}$ but with increasing V small amounts of $Pd^0$ were also detected. Hence they concluded electronic influences of V on Pd, and Pd on V.[24]

### 5.4.2 Different ratios of V:Pd in 1% VPd/$TiO_2$.

A series of catalysts with nominal weight loading of 1 wt.% were synthesised in which the ratio of V:Pd has been modified, Figure 5.8. In total, 5 catalysts were produced with varying ratio of V:Pd. The aim of this study was to discover if varying the V:Pd could enhance catalytic activity. It was also postulated that with decreasing V loading the catalyst stability could be increased, by increasing the alloying between V and Pd, which could also sustain catalytic activity.

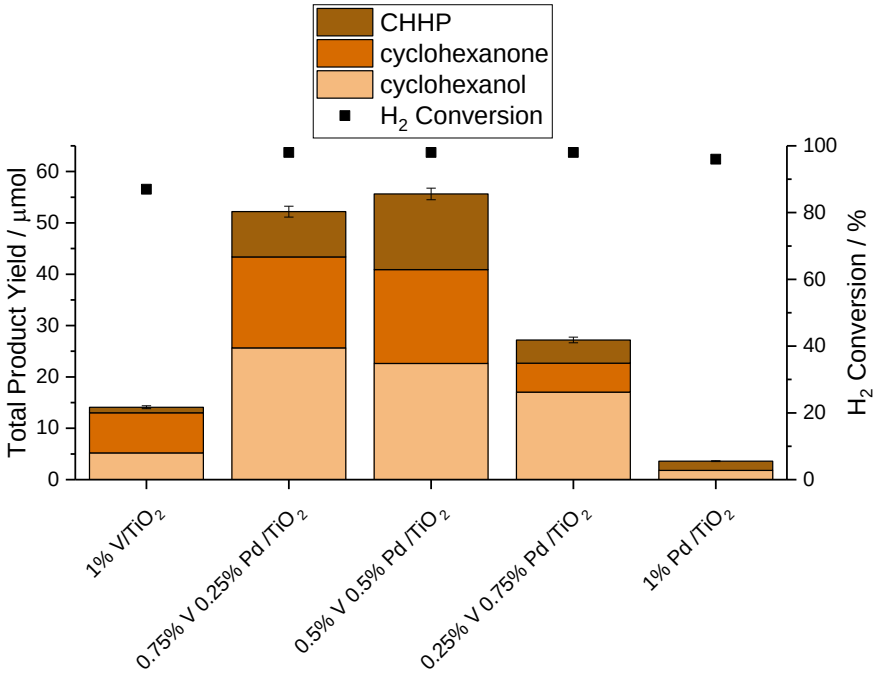


***Figure 5.8.*** *The activity of bimetallic 1 % VPd/$TiO_2$ with varying Pd content towards the oxidation of cyclohexane. A comparison between in-situ and aerobic conditions.* ***Reaction conditions;*** *80 °C, 17 hours, 0.05 g catalyst, 6.37 g t-BuOH, 2.13 g (25 mmol) cyclohexane, 29 bar 5 % $H_2$ / $N_2$ and 11 bar 25 % $O_2$ / $N_2$, 1200 RPM.*

It has been observed that catalysts with lower Pd content have shown greater activity than those with higher Pd content, along with a higher selectivity towards $C_6$ products, Table 5.6. This has shown that the precious metal content of the catalyst can be dramatically reduced to only 0.25% Pd and still maintain enhanced catalytic activity, 53 µmol, compared to the monometallic analogues. This suggests that the catalysis is not limited by the production of $H_2O_2$ as $H_2$ conversion is consistent, Table 5.6, however this is over extended reaction times of 17 hours. To better differentiate the activity of the catalysts shorter reaction times, where $H_2$ is not limited, could be conducted to determine initial rates and a comparison made.

***Table 5.6.*** *$H_2$ conversion and selectivity towards $C_6$ products for VPd catalysts with varying Pd content with a total metal loading of 1 wt.%.*

| Pd content / % | $H_2$ Conversion / % | Total Product Yield / % | Selectivity to all $C_6^*$ products based on $H_2$ / % |
|---|---|---|---|
| 0 | 87 | 0.06 | 0.6 |
| 25 | 98 | 0.21 | 2.1 |
| 50 | 98 | 0.22 | 2.3 |
| 75 | 98 | 0.11 | 1.1 |
| 100 | 96 | 0.01 | 0.2 |

***Reaction conditions;*** *80 °C, 17 hours, 0.05 g catalyst, 6.37 g t-BuOH, 2.13 g cyclohexane, 29 bar 5 % $H_2$ / $N_2$ and 11 bar 25 % $O_2$ / $N_2$, 1200 RPM. *$C_6$ products; cyclohexanol, cyclohexanone and CHHP.*

ICP-MS analysis of post reaction solutions clearly highlights that with increasing V content there is an increase in leaching of V species, Table 5.7. It was predicted that by decreasing total V content a decrease in V leaching and an increase in catalyst stability could be obtained, however similar percentage of V leaching (20 %) was still observed for 0.25% V 0.75 % $Pd/TiO_2$.

***Table 5.7.*** *ICP-MS analysis of post reaction solutions of the oxidation of cyclohexane using 1 % $VPd/TiO_2$ with varying V:Pd.*

| Catalyst | Pd leaching / % (ppb) | V leaching / % (ppb) |
|---|---|---|
| 1% $V/TiO_2$ | - | 71 (31351) |
| 0.75% V 0.25% $Pd/TiO_2$ | 0.11 (12) | 22 (7150) |
| 0.5% V 0.5% $Pd/TiO_2$ | 0.29 (63) | 21 (4533) |
| 0.25% V 0.75% $Pd/TiO_2$ | 0.02 (5) | 18 (1925) |
| 1% $Pd/TiO_2$ | 0.01 (4) | - |

XPS analysis, Table 5.8, showed for the fresh catalyst that with increasing V content a decrease in $Pd^0$:$Pd^{2+}$ ratio is observed, indicating an increase in $Pd^{2+}$ content. This increased $Pd^{2+}$ content could be responsible for the increased catalyst activity of these higher V loaded catalysts as higher $Pd^{2+}$ content has previously been reported to increase $H_2O_2$ production and decrease $H_2O_2$ degradation and hence could explain the increased $H_2$ selectivity of the bimetallic VPd catalysts compared to the monometallic analogues.[25] However it should be noted that the oxidation states measured for the fresh catalysts are unlikely to be the same under reaction conditions. This could indicate that the addition of V to Pd has had an electronic effect on Pd by stabilising the oxidation state of Pd. A decrease in Pd:V is also observed with increasing V content as expected.

***Table 5.8.*** *XPS analysis of 1 % $VPd/TiO_2$ catalysts, with varying V:Pd, fresh and after use in the cyclohexane oxidation via in-situ $H_2O_2$ synthesis.*

| Catalyst | $Pd^0$: $Pd^{2+}$ | Pd:V | $V^{5+}$:$V^{4+}$ |
|---|---|---|---|
| 1% $V/TiO_2$ | - | - | 2.00 |
| 0.75% V 0.25% $Pd/TiO_2$ | 0.83 | 0.06 | 1.19 |
| 0.5% V 0.5% $Pd/TiO_2$ | 3.3 | 0.20 | 1.00 |
| 0.25% V 0.75% $Pd/TiO_2$ | 0.83 | 0.06 | 0.78 |
| 1% $Pd/TiO_2$ | All $Pd^0$ | - | - |

V is present on the surface in both +4 and +5 oxidation state, which could indicate $V_2O_4$ or $V_2O_5$ species. With increasing V content a decrease in $V^{5+}$:$V^{4+}$ is observed with equal amount of both oxidation states present in the 0.5% V 0.5% $Pd/TiO_2$ catalyst. This exact balance of the V redox pair could explain the superior activity of

the 0.5% V 0.5% Pd/$TiO_2$ catalyst, with the $V^{5+}/V^{4+}$ redox pair well reported in the literature to be important for alkane oxidation, and in particular cyclohexane oxidation.[55–59] Abon *et al.* have previously observed the importance of $V^{5+}/V^{4+}$ in vanadium phosphorus oxides (VPO) for light alkane oxidations.[58] They observed that an excess of $V^{4+}$ content, in comparison to $V^{5+}$ sites, and the isolation of $V^{5+}$ sites caused an increase in butane oxidation activity.[58] Jian *et al*. have observed using VPO catalysts for cyclohexane oxidation a similar dependence on $V^{5+}/V^{4+}$ with a synergistic effect occurring between the two oxidation states leading to enhanced cyclohexane conversion during aerobic oxidation.[59] Kozlov *et al.* have demonstrated the combination of $V^{4+}$ and $V^{5+}$ with $H_2O_2$ for alkane oxidation using vanadium based complexes.[60] They observed $V^{4+}$ promotes the formation of $^{\bullet}OH$ radicals from $H_2O_2$ resulting in the formation of a $V^{5+}$ complex. These $^{\bullet}OH$ radicals then aid in the aerobic oxidation of alkanes by form alkyl radicals initiating the oxidation reaction mechanism. $V^{4+}$ complex is then reformed from the $V^{5+}$ form reacting with $^{\bullet}OOH$ radicals formed in the reaction.[60]

Hence a reaction mechanism is proposed, Figure 5.9, in which the Pd site directly synthesise $H_2O_2$ from $H_2$ and $O_2$ and the redox couple $V^{5+}/V^{4+}$ utilises the $H_2O_2$ to oxidise cyclohexane.

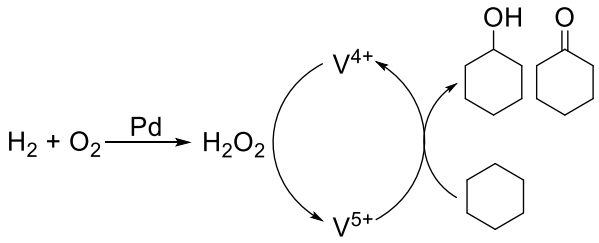


***Figure 5.9.*** *Proposed mechanism for the oxidation of cyclohexane using VPd catalysts.*

The direct synthesis of $H_2O_2$ activity of these 1% VPd/$TiO_2$ at varying V:Pd has also been evaluated, Figure 5.10, to determine whether with high V content if $H_2O_2$ is still synthesised. A volcano plot centring on 0.25% V 0.75% Pd/$TiO_2$ has been observed for the VPd catalyst. All catalysts with greater than 0.5% Pd have shown an enhancement of the both the monometallic V and Pd catalysts. This has shown that a small addition of V has had a promotional effect on the $H_2O_2$ synthesis activity. This promotional effect could be due to electronic enhancement of Pd and the stabilisation of Pd oxidation states. With increasing V content above 0.5% the lack of active Pd metal decreases the $H_2O_2$ formation. Nonetheless, a direct correlation between $H_2O_2$ synthesis activity and cyclohexane oxidation is not present.

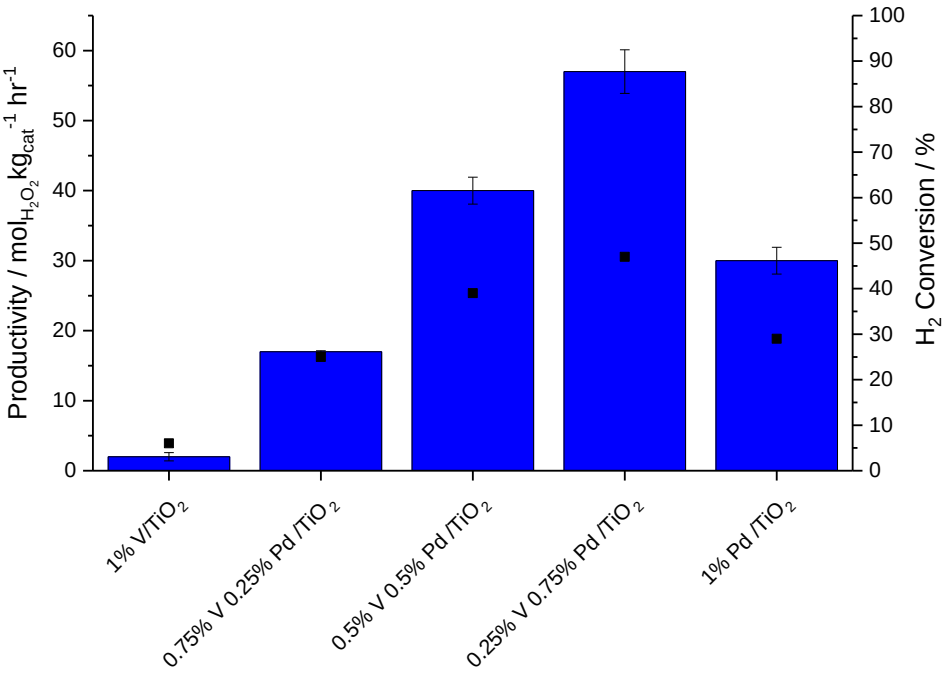


***Figure 5.10.*** *Catalytic activity of 1 % VPd catalysts, with varying V:Pd ratios, towards the synthesis of $H_2O_2$.* ***Reaction conditions;*** *0.01 g catalyst, 2.9 g water, 5.6 g methanol, 29 bar 5 % $H_2$ / $CO_2$ and 11 bar 25 % $O_2$ / $CO_2$, 1200 RPM, 30 minutes, 25 °C.*

This has indicated that a 1:1 weight ratio of 1% VPd/$TiO_2$ is the optimum catalyst for the oxidation of cyclohexane via the *in-situ* production of $H_2O_2$ and hence it is this ratio that has been investigated further.

### 5.4.3 Catalyst re-use.

ICP-MS analysis of post reaction solution indicated 21% of the initial V present on the catalyst had leached into solution, leading to 4.5 ppm of V in solution. Hence, it was postulated that the superior activity of 1 % VPd/$TiO_2$ catalyst could be due to the leaching of the V and that these homogeneous V species could be catalysing the reaction. V has often been implemented as a catalyst for the oxidation of cyclohexane, with vanadium oxide supported upon metal oxides widely studied.[61,62] Homogeneous V species have also been explored in the literature with some success reported for non-zero valent V complexes. Mishra *et al.* have observed 13 % conversion of cyclohexane after 18 hours at 140 °C under 15 atm of $O_2$ using V-scorpionate complexes under solvent free conditions.[33] Homogeneous catalysts that employ V with oxo and peroxo complexes have also been reported in which these radicals species can abstract the initial hydrogen leading to KA oil formation.[63,64] Hence it is plausible that V species present in the reaction solution or on the catalyst surface could be providing catalytic activity.

To try to determine if the loss of V from the catalyst support had a detrimental effect on catalytic activity a used 1 % VPd/$TiO_2$ catalyst was studied for the oxidation of cyclohexane, Figure 5.11.

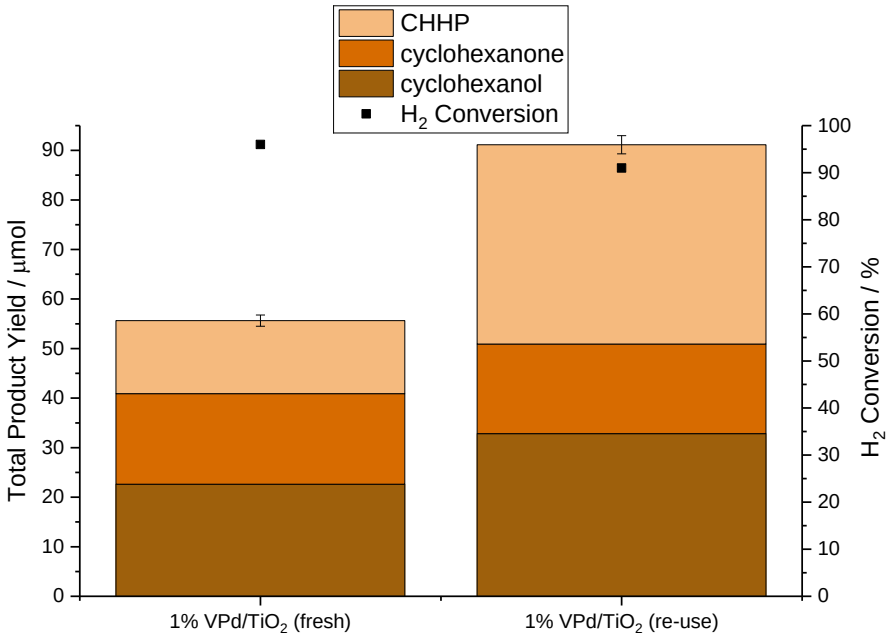


***Figure 5.11.*** *The effect on the yield of KA oil upon re-use of 1 % VPd/$TiO_2$.* ***Reaction conditions;*** *80 °C, 17 hours, 0.05 g catalyst, 6.37 g t-BuOH, 2.13 g (25 mmol) cyclohexane, 29 bar 5 % $H_2/N_2$ and 11 bar 25 % $O_2$ / $N_2$, 1200 RPM.*

An increase in catalytic activity upon re-use of the 1 % VPd/$TiO_2$ has been observed from a yield of KA oil of 43 to 51 µmol with an increase in the intermediate CHHP also observed, from 17 to 40 µmol. This indicated that despite the loss of V from the catalyst surface the catalyst has still maintained catalytic activity. This can be attributed to the Pd still present on the surface, the active metal, for $H_2O_2$ formation. An enhancement of Pd by V is still present nonetheless as a much greater activity has been observed compared to the monometallic Pd catalyst. Similar increases in activity upon use were reported in Chapter 3 for 1% AuPd/$TiO_2$ prepared by wet impregnation. The increase in activity here was attributed to the increase in $Pd^0$ with successive uses. With the 1% VPd/$TiO_2$ the $Pd^0$:$Pd^{2+}$ is maintained post reaction (Table 5.4) but due to the reductive heat treatment used in catalyst preparation the $Pd^0$ was already the most prominent oxidation state. A change is V oxidation state is also observed after use with both $V^{4+}$ and $V^{5+}$ being present on the fresh catalyst and only $V^{4+}$ observed on the used catalyst.

ICP-MS results show that on the first use 21 % of the original V had leached from the catalyst during testing. Upon second use leaching had reduced but was still significant

(14 %), Table 5.9. This suggests that there is continual leaching of V metal from the catalyst rather than an initial loss of weakly bound surface species. This could still indicate that homogeneous V species are contributing to the catalytic activity. However, on re-use of the catalyst there is a reduction in the concentration of V species in solution but a greater product yield was observed. This could indicate that if V species have contributed to activity their contribution is minimal.

***Table 5.9.*** *ICP-MS analysis of post reaction solutions of the oxidation of cyclohexane using 1 % VPd/$TiO_2$.*

| Catalyst use | % Pd leached (ppb) | % V leached (ppb) |
|---|---|---|
| 1st use | 0.29 (63) | 21 (4533) |
| 2nd use | 0.33 (73) | 14 (3090) |

XPS analysis of the fresh and used catalysts has shown no changes in the catalyst surface, Table 5.10. The $Pd^0$:$Pd^{2+}$ is unchanged after use and this could rationalise the maintained activity of the catalyst upon re-use. The maintaining of the $Pd^0$:$Pd^{2+}$ at 3.8 means that both $Pd^{2+}$ and $Pd^0$ are both still present on the surface. This also means that interfaces of Pd-PdO could still be present and these interfaces have been postulated to be the most active for $H_2O_2$ synthesis.[65]

***Table 5.10.*** *XPS analysis of fresh and used (1st and 2nd use) for 1 % VPd/$TiO_2$ used for the oxidation of cyclohexane via the in-situ production of $H_2O_2$.*

| Catalyst use | $Pd^0$:$Pd^{2+}$ | Pd:X |
|---|---|---|
| Fresh | 3.3 | 0.19 |
| 1st use | 3.8 | 0.18 |
| 2nd use | 3.8 | 0.23 |

Upon use in the cyclohexane oxidation reaction a similar structure of the catalyst is observed by TEM with rough edges on the $TiO_2$ particles, Figure 5.12 A. However, on closer inspection some areas of the sample show sintering of Pd into larger, around 10 nm, particles, Figure 5.12 B.

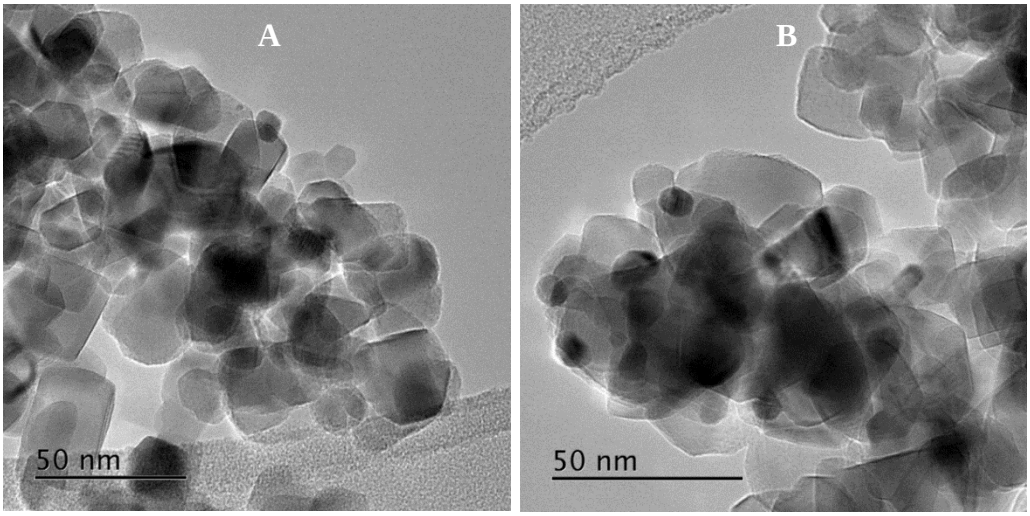


***Figure 5.12.*** *TEM images of 1 % VPd/$TiO_2$ after use in the oxidation of cyclohexane.*

HAADF-STEM with EDX mapping, Figure 5.13, has shown these larger particles, up to 20 nm, which are still Pd in nature with V still dispersed over the support material. Despite sintering of Pd on the sample catalytic activity has still been maintained this could indicate that the dispersion of Pd was not imperative for the enhanced catalytic activity of 1% VPd/$TiO_2$.

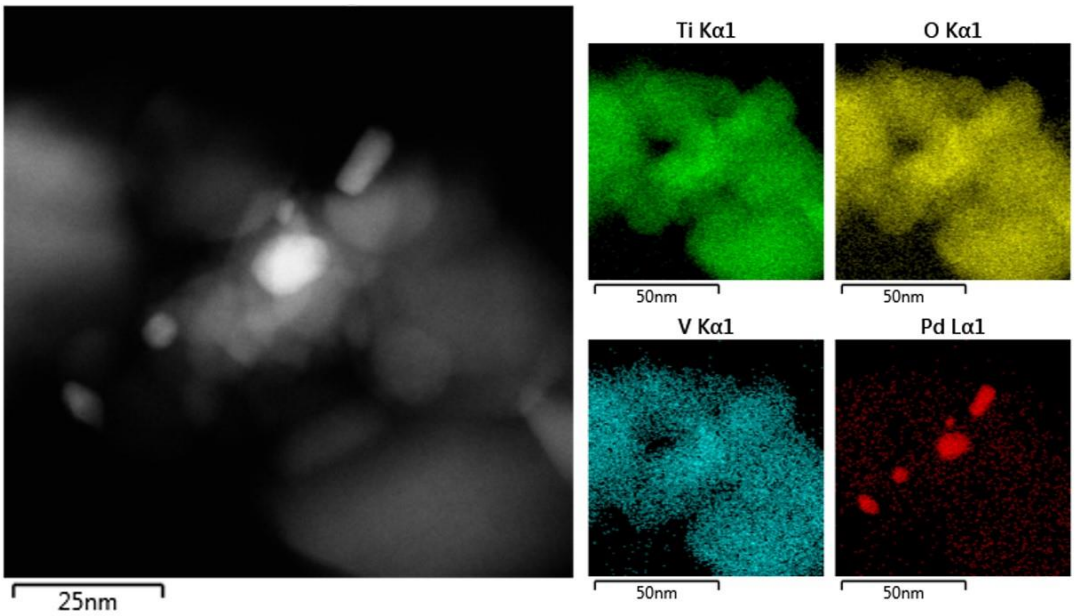


***Figure 5.13.*** *HAADF-STEM and the corresponding EDX mapping of 1% VPd/$TiO_2$ after use in the oxidation of cyclohexane.*

### 5.4.4 Efficacy of homogenous V species.

#### 5.4.4.1 Hot filtration.

In order to determine if the leached V species were active for the oxidation of cyclohexane alone hot filtration experiments have also been conducted, where the 1% VPd/$TiO_2$ heterogeneous catalyst is removed via filtration and the post reaction

solution is re-used under standard *in-situ* oxidation conditions. These results are shown in Figure 5.14.

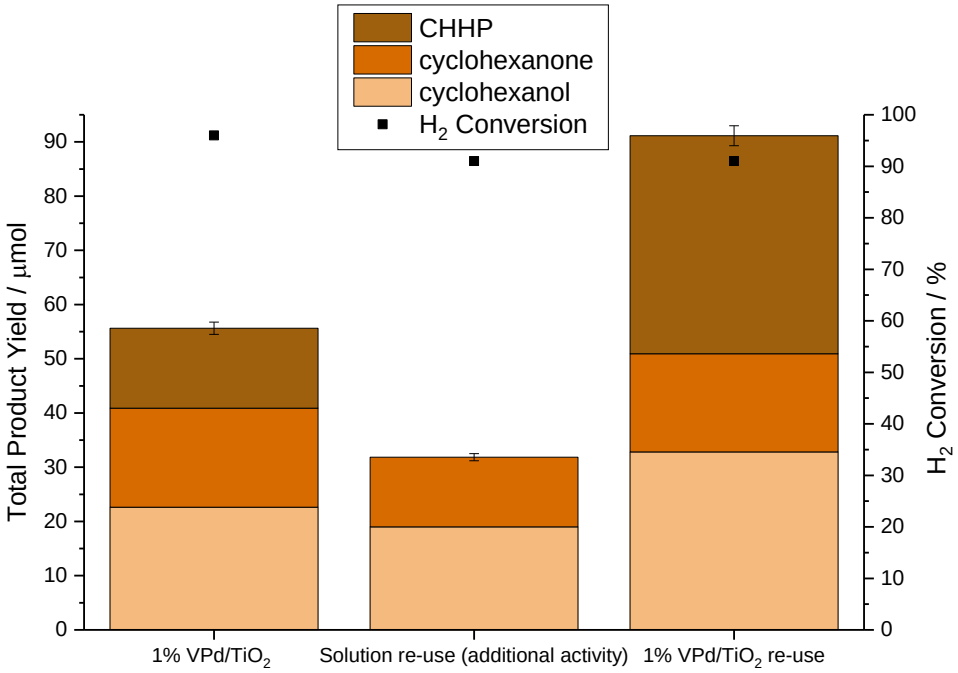


***Figure 5.14.*** *The re-use of the reaction solution from 1 % VPd/$TiO_2$ and comparison to catalyst reuse.* ***Reaction conditions;*** *80 °C, 17 hours, 0.05g catalyst, 6.37 g t-BuOH, 2.13 g (25 mmol) cyclohexane, 29 bar 5 % $H_2$ / $N_2$ and 11 bar 25 % $O_2$ / $N_2$, 1200 RPM.*

Overall an increase in yield of KA oil has been observed upon re-use of the reaction solution, an additional 32 µmol of product has been observed. No CHHP has been observed upon solution reuse and hence it can be deduced that some activity has come from the conversion of CHHP to KA oil. This additional activity of the solution could indicate that V species in the reaction solution have been active for the oxidation of cyclohexane. There were also small amounts (63 ppb) of Pd leached from the catalyst into solution and it should be noted that colloidal Pd has been noted in the literature to catalyse the direct synthesis of $H_2O_2$.[29] Thus some activity could have arisen from colloidal Pd present. The increased activity upon solution re-use (32 µmol of product) is not as great as the increase upon catalyst re-use (91 µmol of product). This indicates that the heterogenous catalysis is still important for the oxidation and both homogenous and heterogeneous catalytic routes have a role to play in the reaction.

However, a similar additional activity upon solution re-use has been also observed for 1% AuPd/$TiO_2$, Figure 5.15, which showed minimal metal leaching (353 ppb Pd, 101 ppb Au). This could show that some additional activity has occurred from the extended reaction time and once the reaction has commenced further activity could be initiated by temperature alone.

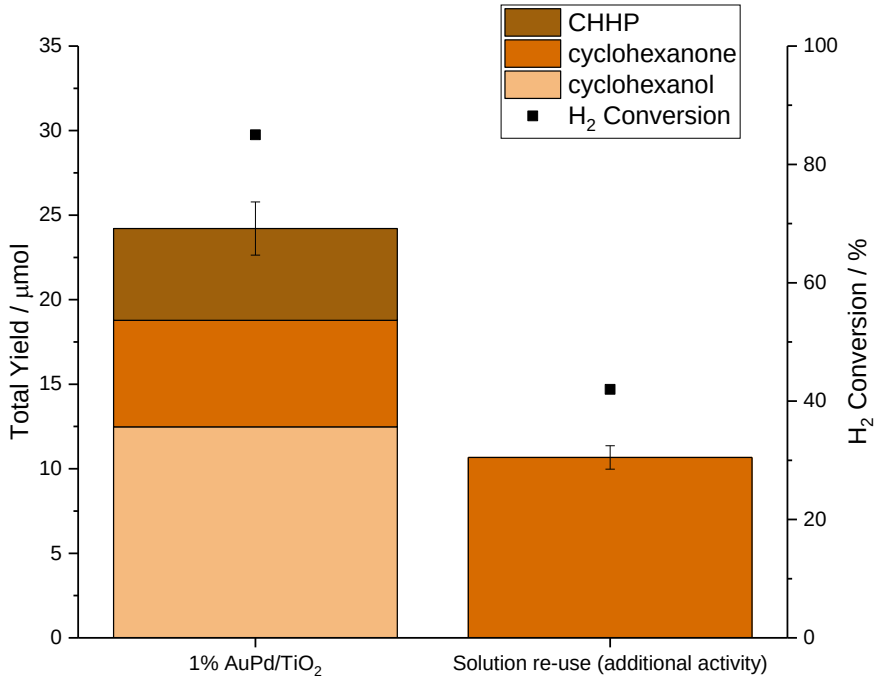


***Figure 5.15*** *The re-use of the reaction solution from 1 % AuPd/$TiO_2$.* ***Reaction conditions;*** *80 °C, 17 hours, 0.05 g catalyst, 6.37 g t-BuOH, 2.13 g (25 mmol) cyclohexane, 29 bar 5 % $H_2$ / $N_2$ and 11 bar 25 % $O_2$ / $N_2$, 1200 RPM.*

### 5.4.4.2 Addition of carbon sequester.

Activated carbon has also be added to the reaction in the presence of 1 % VPd/$TiO_2$ catalyst to sequester any leached V species and to reduce any contribution from homogeneous species, with the results shown in Figure 5.16. It has previously been reported that the addition of Vulcan XC72R and carbon extrudates in the oxidation of glucose can sequester Pt leached from a 5 % Pt/$TiO_2$ catalysts.[66] Hence the same methodology has been implemented here. Firstly, the carbon materials were tested alone to indicate if any background oxidation could occur, with a limited activity observed.

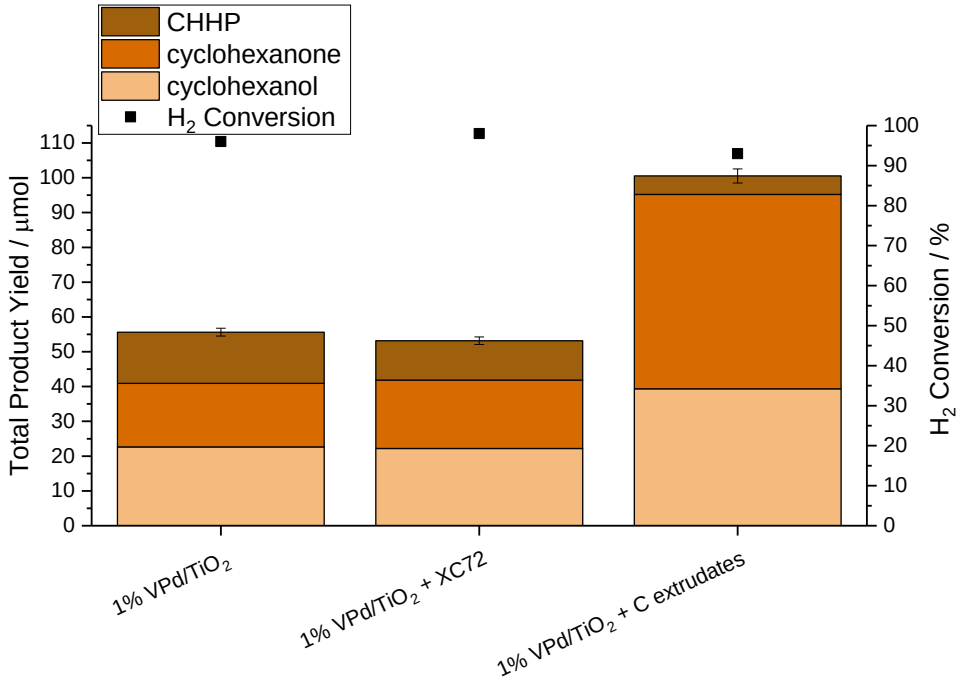


***Figure 5.16.*** *The effect of activated carbon on addition to 1 % VPd/$TiO_2$.* ***Reaction conditions;*** *80 °C, 17 hours, 0.05 g catalyst, 0.05 g carbon, 6.37 g t-BuOH, 2.13 g (25 mmol) cyclohexane, 29 bar 5 % $H_2$ / $N_2$ and 11 bar 25 % $O_2$ / $N_2$, 1200 RPM.*

The addition of XC72 carbon to the cyclohexane oxidation reaction is seen to have no substantial effect on the product yield compared to 1 % VPd/$TiO_2$ catalyst alone. However, further investigation via ICP-MS have demonstrated that the addition of carbon was unsuccessful in reducing the concentration of V in solution, Table 5.11.

***Table 5.11.*** *ICP-MS analysis of post reaction solutions from the oxidation of cyclohexane using 1% VPd/$TiO_2$ in the presence of carbon.*

| Catalyst | % Pd leached (ppb) | % V leached (ppb) |
|---|---|---|
| 1% VPd/$TiO_2$ | 0.29 (63) | 21 (4533) |
| 1% VPd/$TiO_2$ + XC72 | 0.11 (24) | 23 (5137) |
| 1% VPd/$TiO_2$ + C extrudates | 0.02 (4) | 17 (3810) |

Further studies investigating the addition of carbon extrudates is seen to dramatically increase the yield of oxidation products despite having limited catalytic activity by itself. XPS analysis of the carbon extrudates reveal the presence of Na (1071 eV), O (533 eV); this could indicate $SiO_2$ or C-O or C=O functionalisation, S (164 eV); this could show R-SH thiol functionalisation and Si (103 eV); present as $SiO_2$. These possible C, O, Si and S functional groups could interact with cyclohexane and could begin to explain its enhanced activity. Gurdazi *et al.* have previously reported that oxygen containing functional groups on activated carbon have shown control over activity and selectivity for $H_2O_2$ synthesis, by reducing $H_2O$ formation.[26] Edwards *et al.* have previously reported carbon as an efficient support for AuPd catalysts for the

direct synthesis of $H_2O_2$.[67] This could indicate that the addition of carbon could increase $H_2O_2$ production. Edwards *et al.* also noted that the carbon used contained many metallic impurities, including Fe.[67] Again these impurities could've contributed to the additional activity observed when the carbon was present. In the literature a variety of carbons have been described as good oxidation catalysts for various oxidation reactions such as sulfuric acid, methanol and oxalic acid oxidation.[68] These catalytic properties have been widely reported to be enhanced by the chemical functionalisation of the carbon.[69]

For completeness $H_2O_2$ synthesis testing has also be conducted in the presence of the carbon extrudates to see if the increase in oxidation activity could be due to an increase in $H_2O_2$ activity. As shown in Table 5.12 the addition of carbon has increased $H_2O_2$ productivity slightly along with increasing $H_2$ conversion but with no overall change in selectivity based on $H_2$.

***Table 5.12.*** *The activity of bimetallic 1 % VPd/$TiO_2$ catalysts towards the synthesis and degradation of $H_2O_2$ with and without the addition of carbon extrudates.*

| Catalyst | Productivity/ $mol_{H_2O_2}$ $kg_{cat}^{-1}$ $hr^{-1}$ | $H_2$ Conversion / % | $H_2O_2$ Selectivity / % | Degradation / $mol_{H_2O_2}$ $kg_{cat}^{-1}$ $hr^{-1}$ (%) |
|---|---|---|---|---|
| 1 % VPd/$TiO_2$ | 37 | 39 | 18 | 96 (5) |
| 1 % VPd/$TiO_2$ and C extrudates | 49 | 57 | 17 | 129 (7) |

***Synthesis:*** *0.01 g catalyst, 2.9 g water, 5.6 g methanol, 29 bar 5 % $H_2/CO_2$ and 11 bar 25 % $O_2/CO_2$, 1200 RPM, 30 minutes, 25 °C.* ***Degradation:*** *0.01 g catalyst, 0.68 g 50 wt% $H_2O_2$, 2.22 g water, 5.6 g methanol, 29 bar 5 % $H_2/CO_2$, 1200 RPM, 30 minutes, 25 °C.*

It has previously reported that the addition of Cs-exchanged phosphotungstic acids as recoverable solid acid additives using AuPd/$TiO_2$ catalysts can dramatically increase the synthesis of $H_2O_2$.[70] These solid acid additives were compared to the promotional effect of common oxides and non-halo acids and it was shown that a decrease in pH had a beneficial effect on $H_2O_2$ synthesis. [70] The addition of carbon in these investigations could have decreased the pH of the $H_2O_2$ synthesis solution and hence resulted in the increase in $H_2O_2$.

Although a small increase in activity for both the synthesis and degradation of $H_2O_2$ has been observed these are still not as high as with 1% AuPd/$TiO_2$ alone and hence the increase in activity for the oxidation of cyclohexane cannot be attributed to this

alone. This has indicated that C extrudates could be used as effective catalyst additive in future investigations.

### 5.4.4.3 $VCl_3$ solution.

To determine the efficacy of the homogenous catalyst precursor material 77.2 µL of $VCl_3$ solution (3.239 mg $ml^{-1}$) was added to the reactor as a homogenous catalyst. The amount added was equal to the total weight of metal that is added with heterogeneous 1 % $VPd/TiO_2$. It was anticipated that this $VCl_3$ could emulate any V species that have leached from the catalyst and indicate how effective homogeneous V species are in the oxidation of cyclohexane. The comparison between 1 % $VPd/TiO_2$, $VCl_3$ and 1 % $Pd/TiO_2$ have been made in Figure 5.17.

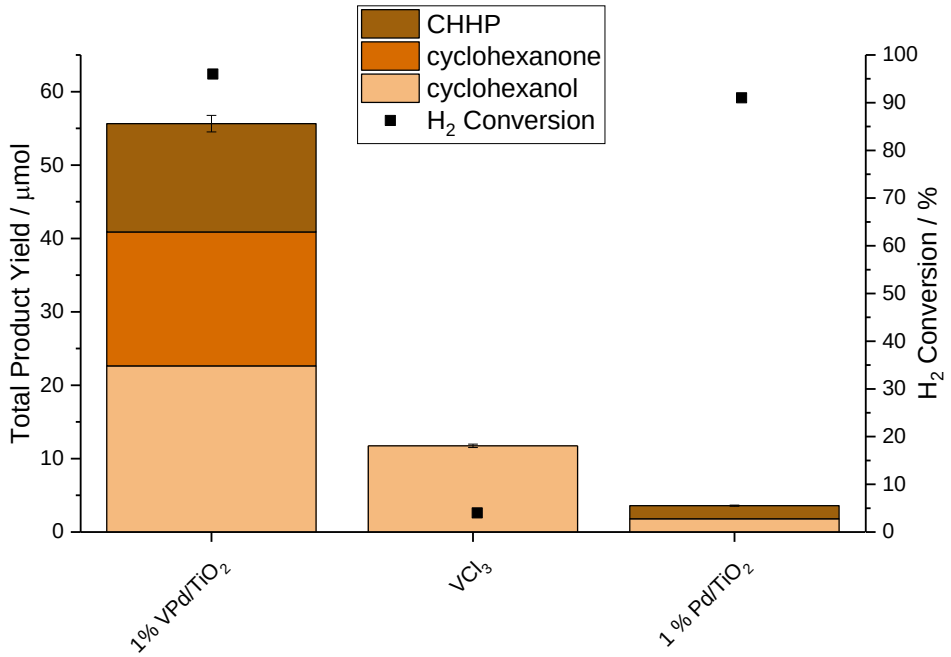


***Figure 5.17.*** *The effect of 1 % $VPd/TiO_2$ and $VCl_3$ on the oxidation of cyclohexane.* ***Reaction conditions;*** *80 °C, 17 hours, 0.05 g heterogeneous catalysts, 77 µL $VCl_3$, 6.37 g t-BuOH, 2.13 g (25 mmol) cyclohexane, 29 bar 5 % $H_2$ / $N_2$ and 11 bar 25 % $O_2$ / $N_2$, 1200 RPM.*

Limited activity has been observed for $VCl_3$ showing that at least these homogeneous species are not active in the oxidation of cyclohexane and could indicate leaching of other V species. A low $H_2$ conversion was also observed for $VCl_3$ showing its inability to produce $H_2O_2$/reactive oxygen species which could explain its lack of catalytic activity. A dark green solution was added to the reactor and after reaction a yellow-brown solid was recovered, so this could indicate not a true homogeneous alternative or comparison to the 1 % $VPd/TiO_2$. XPS analysis has identified peaks at 517.2 eV indicating V still in a +3 oxidation state but in the form of $V_2O_3$. Peaks have also highlighted Cr and Fe species, these are possibly $FeCl_2$ or $Fe_2O_3$ (710 eV) and Cr in

oxide form, most likely $Cr_2O_3$ and $CrO_3$ (577 and 586 eV respectively). It is believed these Fe and Cr species have occurred from corroding of the reactor parts into the reaction solution, further highlighting the need to completely immobilise V.

### 5.4.5 Extended studies on V based catalysts.

#### 5.4.5.1 Vanadium oxide based catalysts.

XPS analysis of all $VPd/TiO_2$ catalyst showed V is present on the surface predominately in +4 and +5 oxidation state which could indicate $V_2O_4$ or $V_2O_5$ species present on the surface. Hence $V_2O_4$ and $V_2O_5$, which are well known oxidation catalysts,[23,24,54,71–75] have been tested as well as a physical mixtures with 1 % $Pd/TiO_2$, Figure 5.18.

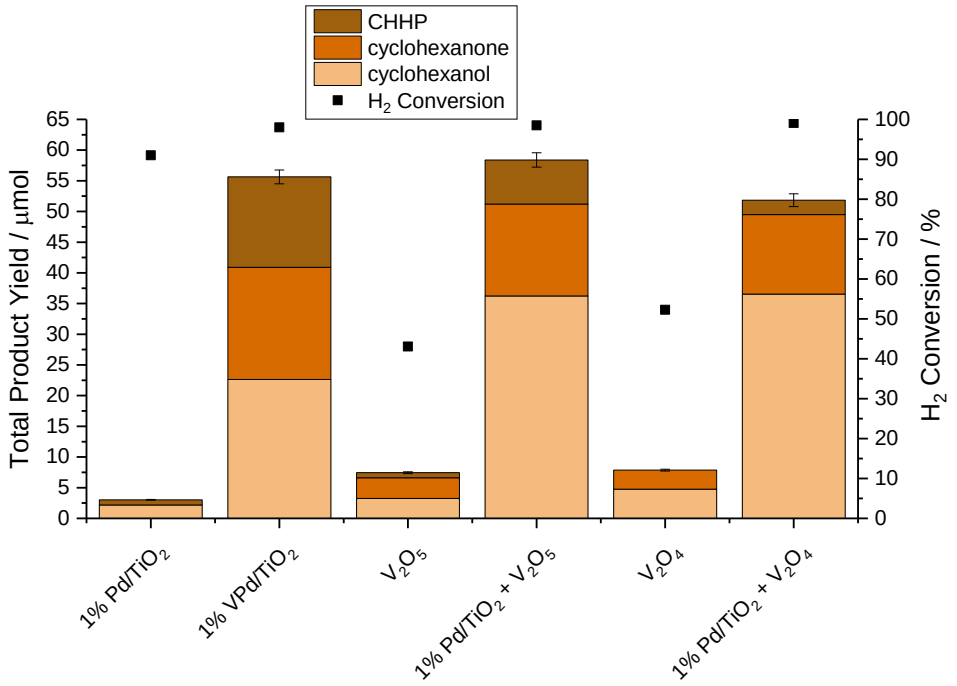


***Figure 5.18.*** *The activity of 1% $Pd/TiO_2$, 1 % $VPd/TiO_2$, $V_2O_5$, $V_2O_4$, and physical mixtures of 1 % $Pd/TiO_2$ and vanadium oxides towards the oxidation of cyclohexane.* ***Reaction conditions;*** *80 °C, 17 hours, 0.05 g catalyst, 6.37 g t-BuOH, 2.13 g (25 mmol) cyclohexane, 29 bar 5 % $H_2$ / $N_2$ and 11 bar 25 % $O_2$ / $N_2$, 1200 RPM.*

It can be observed that some limited catalytic activity has been observed for both oxides alone at a much reduced $H_2$ conversion, Table 5.13. This indicates that predominately aerobic oxidation is occurring over these oxide catalysts.

***Table 5.13.*** *$H_2$ conversion and selectivity to $C_6$ products during oxidation of cyclohexane using 1% $VPd/TiO_2$ and vanadium oxides.*

| Catalyst | $H_2$ Conversion / % | Total Product Yield / % | Selectivity to all $C_6^*$ products based on $H_2$ / % |
|---|---|---|---|
| 1% $Pd/TiO_2$ | 96 | 0.01 | 0.2 |
| 1% $VPd/TiO_2$ | 98 | 0.22 | 2.3 |
| $V_2O_5$ | 43 | 0.02 | 0.7 |
| 1% $Pd/TiO_2$ + $V_2O_5$ | 99 | 0.23 | 2.4 |
| $V_2O_4$ | 52 | 0.03 | 0.6 |
| 1% $Pd/TiO_2$ + $V_2O_4$ | 99 | 0.20 | 2.1 |

***Reaction conditions;*** *80 °C, 17 hours, 0.05 g catalyst, 6.37 g t-BuOH, 2.13 g cyclohexane, 29 bar 5 % $H_2$ / $N_2$ and 11 bar 25 % $O_2$ / $N_2$, 1200 RPM. *$C_6$ products; cyclohexanol, cyclohexanone and CHHP.*

Here the physical mixtures of 1% $Pd/TiO_2$ and vanadium oxides have shown a greater activity and selectivity than both vanadium oxides and 1% $Pd/TiO_2$ catalyst alone. This activity shown for the physical mixtures is comparable to that observed for the bimetallic 1% $VPd/TiO_2$ catalyst. It can be observed that both $V^{4+}$ and $V^{5+}$ oxides have been active as physical mixtures showing the diversity and activity of V multiple oxidation states. Garcia *et al.* have previously reported that mixed oxidation states of both $V^{4+}$ and $V^{5+}$ present on vanadia promoted $Pd/TiO_2$ catalysts, indicating both oxidation states can be active for oxidation. They also noted that the alloy of Pd and V led to the increased reducibility of V allowing varying oxidation states which enhances the V redox properties which important in catalytic oxidations.[55]

From the activity of these physical mixtures it can be noted that the mixture of both the 1% $Pd/TiO_2$, which has been shown to be a good $H_2O_2$ synthesis catalyst,[76] and vanadium oxides which are well known oxidation catalysts[77] has given the greater activity. As previously discussed in Section 5.4.2, V present on the surface of supported VPd catalysts is in a mixture of +4 and +5 oxidation states. Within the literature the redox coupling between $V^{+4}$ and $V^{+5}$ is important in selective alkane, in particular cyclohexane, oxidation.[55–57] Hence this could indicate that the enhanced activity of 1% $VPd/TiO_2$ could be attributed to this combination of sites for $H_2O_2$ synthesis and disperse redox active vanadia sites for the oxidation and not necessarily to alloying of the two metals.

When $V_2O_4$ and $V_2O_5$ have been utilised here complete solubility of the oxides into solution has resulted in large concentrations of V in solution and the difficult recovery of the vanadium oxide component of the catalyst mixture and hence do not show an enhancement on the 1% $VPd/TiO_2$ catalysts.

Unsupported vanadium oxide catalysts have been shown to be good oxidation catalyst as soluble metal catalysts.[74,77] Nonetheless as these are soluble catalysts the associated problems with catalyst separation occur.[78] Within the literature investigations hence then moved to more stable and reusable catalysts where vanadia is supported upon other oxide materials which disperses the vanadia over the support maintaining isolated active sites.[77] Purely vanadia supported catalysts, without Pd, will be explored later in Section 5.4.5.3.

### 5.4.5.2 Vanadia promoted palladium-titania catalysts.

Garcia *et al.* have previously detailed the synthesis of vanadia promoted Pd supported on $TiO_2$ for the oxidation of volatile organic compounds.[24] They described the synthesis of 1 % VPd/$TiO_2$ catalysts via a wet impregnation method using ammonium metavanadate as the V precursor. These catalysts contained high $V^{4+}$ and $V^{5+}$ content with $VO_x$ present as a monolayer dispersion on the surface. The addition of Pd to V/$TiO_2$ although decreased the Pd dispersion and alloying was not observed, it increased the reducibility of the V species. It was suggested that the observed increased catalyst activity was connected to these enhanced redox properties of the catalysts.[23,55] The same procedure for alumina supported catalysts showed that the co-impregnation of both V and Pd precursors provided the highest oxidation activity and it is this preparation method that has been utilised in this work.[79] The incorporation of vanadia species on to the catalyst is aimed to reduce the solubility issues that occurred when pure vanadium oxides were used while still maintaining isolated vanadia sites as a monolayer.

Different heat treatments have been investigated for these vanadia promoted catalysts. Calcinations were previously investigated for 6 hours at 550 C° [55] and these conditions have been replicated (donated as wi in Figure 5.19). Catalysts have also been calcined and then undergone a low temperature reduction, 200 °C for 2 hours 5% $H_2$/Ar, to reduce the Pd species on the surface as reduced Pd has previously shown to be active for the *in-situ* oxidation of cyclohexane. For $H_2O_2$ synthesis a reductive heat treatment post calcination of a PdSn/$TiO_2$ catalyst removes small Pd nanoparticles which are active for $H_2O_2$ degradation[17] which could decrease the $C_6$ selectivity for the oxidation reaction. The same reduction heat treatment that has been utilised for previously reported modified impregnation catalysts, 500 °C for 4 hours 5% $H_2$/Ar, have also been investigated, Figure 5.19.

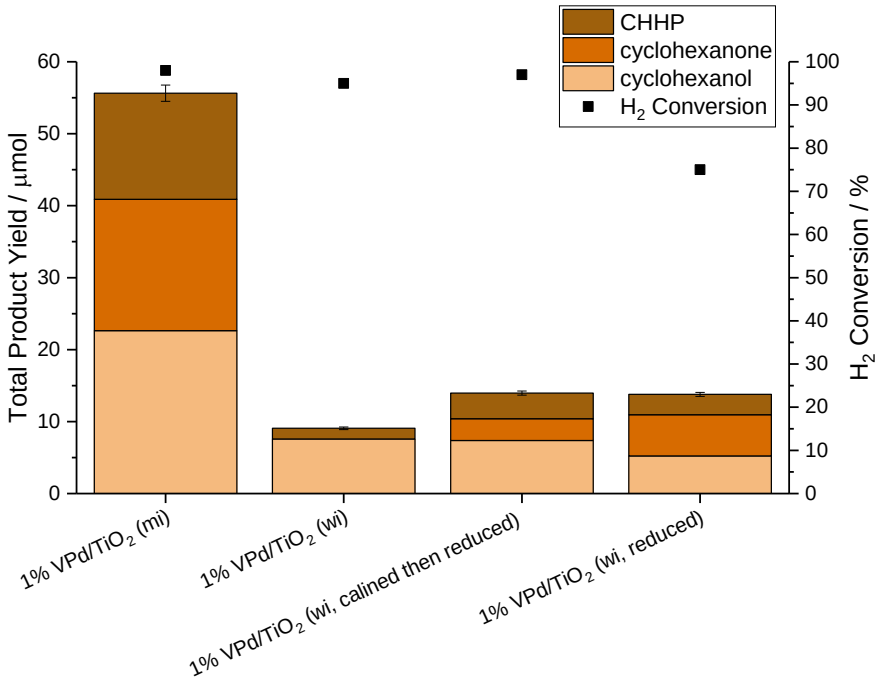


***Figure 5.19.*** *The activity of 1 % VPd/$TiO_2$ prepared by modified (mi) and wet impregnation (wi) towards the oxidation of cyclohexane.* ***Reaction conditions;*** *80 °C, 17 hours, 0.05 g catalyst, 6.37 g t-BuOH, 2.13 g (25 mmol) cyclohexane, 29 bar 5 % $H_2$ / $N_2$ and 11 bar 25 % $O_2$ / $N_2$, 1200 RPM.*

All these new vanadia promoted catalysts have not shown an enhanced activity or selectivity over the 1% VPd/$TiO_2$ catalyst prepared by modified impregnation. For the bimetallic catalysts, the addition of a reductive heat treatment has shown an improvement on the calcined sample increasing selectivity to $C_6$ products, Table 5.14, which could indicate the importance of Pd reduction on activity.

***Table 5.14.*** *$H_2$ conversion and selectivity to $C_6$ products during oxidation of cyclohexane.*

| Catalyst | $H_2$ Conversion / % | Total Product Yield / % | Selectivity to all $C_6$* products based on $H_2$ / % |
|---|---|---|---|
| 1% VPd/$TiO_2$ (modified impregnation) | 98 | 0.22 | 2.3 |
| 1% VPd/$TiO_2$ (wet impregnation) | 95 | 0.04 | 0.4 |
| 1% VPd/$TiO_2$ (wet impregnation, calcined then reduced) | 97 | 0.06 | 0.6 |
| 1% VPd/$TiO_2$ (wet impregnation, reduced) | 75 | 0.05 | 0.7 |

***Reaction conditions;*** *80 °C, 17 hours, 0.05 g catalyst, 6.37 g t-BuOH, 2.13 g cyclohexane, 29 bar 5 % $H_2$ / $N_2$ and 11 bar 25 % $O_2$ / $N_2$, 1200 RPM. *$C_6$ products; cyclohexanol, cyclohexanone and CHHP.*

XPS analysis, Table 5.15, has shown an increase in $Pd^0$ content when a reductive heat treatment has been used.

***Table 5.15*** *XPS analysis of 1% VPd/$TiO_2$ catalysts prepared by wet impregnation and different heat treatments. Where; wi indicates wet impregnation and mi indicates modified impregnation.*

| Catalyst | $Pd^0$:$Pd^{2+}$ | Pd:V |
|---|---|---|
| 1% VPd/$TiO_2$ (modified impregnation) | 3.3 | 0.19 |
| 1% VPd/$TiO_2$ (modified impregnation) used | 3.8 | 0.18 |
| 1% VPd/$TiO_2$ (wet impregnation, calcined) | 1.1 | 0.23 |
| 1% VPd/$TiO_2$ (wet impregnation, calcined) used | 0.18 | 0.25 |
| 1% VPd/$TiO_2$ (wet impregnation, calcined then reduced) | 3 | 0.22 |
| 1% VPd/$TiO_2$ (wet impregnation, calcined then reduced) used | 1 | 0.28 |
| 1% VPd/$TiO_2$ (wet impregnation, reduced) | All $Pd^0$ | 0.25 |
| 1% VPd/$TiO_2$ (wet impregnation, reduced) used | All $Pd^0$ | 0.17 |

Comparing the modified and wet impregnation prepared catalysts has shown the initial oxidation state of Pd may have not been the leading factor in activity. The wet impregnation catalysts which have undergone reductive heat treatments showed similar or higher $Pd^0$ content than the modified impregnation catalysts. However, the modified impregnation catalyst has maintained its $Pd^0$:$Pd^{2+}$ showing the stability of the Pd oxidation/ electronic state during the catalytic reaction. Conversely the wet impregnation catalysts have shown changes in the ratio and hence the Pd-PdO interfaces which are important for $H_2O_2$ activity[65] and the Pd stability is maintained. Analysis by ICP-MS has shown that the catalysts prepared by wet impregnation have limited stability with even greater V leaching than the modified impregnation catalyst.

Garcia *et al.* have reported that for the co impregnation of V and Pd onto $TiO_2$ via the preparation method described here produces large Pd particles, 10 – 50 nm, compared to much smaller Pd particles, 5 – 10 nm, observed on the Pd only catalyst.[79] 1% VPd/$TiO_2$ prepared by modified impregnation has shown much smaller Pd particles, which were not measurable by TEM analysis, Figure 5.5. Thus, the decrease in activity for the wet impregnation catalysts, compared to the modified impregnation, could be due to an increase in Pd particle size and hence a decrease in the dispersion of the Pd active sites. This decrease in Pd dispersion would also decrease the interfaces between Pd and V species which could indicate that interaction between Pd and V is important for catalytic activity.

#### 5.4.5.3 Pd/$VO_x$ supported on $TiO_2$.

Leaching of V species has been a problem with all V catalysts. It was postulated the incorporating V into the support prior to impregnation of Pd could increase catalyst

stability. For these catalysts a procedure reported by Barthos *et al.* has been adapted.[80,81] In this series of catalysts $TiO_2$ was impregnated with a solution of decavanadate ions and then calcined at 400 °C for 4 hours under static air. The V impregnated support was then impregnated with a $PdCl_2$ solution and heat treated again (400 °C, 4 hrs).

An initial heat treatment for V impregnated $TiO_2$ prior to Pd impregnation was anticipated to increase the stability of surface V species. This impregnation procedure was found to produce polymeric vanadia species on the support which at low V concentration produces a monolayer, < 6 wt.% $V_2O_5$.[81] When Pd is impregnated and bound on to the surface $Pd/VO_x$ redox pairs are formed with easily reducible V species, it is believed that these redox active V species can then re-oxidise $Pd^{2+}$.[80]

Two different loadings of V were tested, 1% and 3%, and the heat treatments explored were both calcination and reduction, both 400 °C for 4 hours, Figure 5.20.

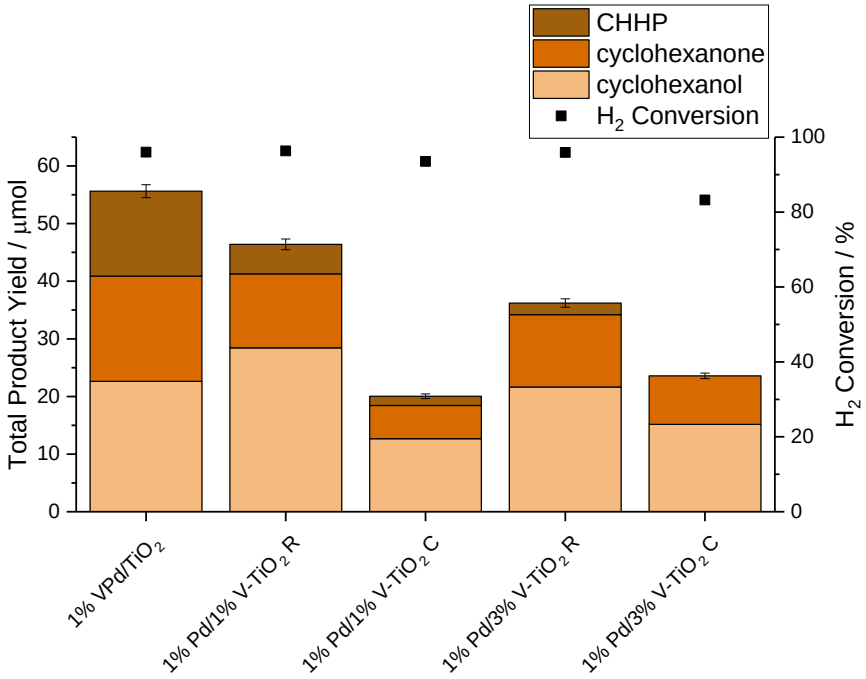


***Figure 5.20.*** *The activity of 1% Pd/ X% V-$TiO_2$ prepared by towards the oxidation of cyclohexane.* ***Reaction conditions;*** *80 °C, 17 hours, 0.05 g catalyst, 6.37 g t-BuOH, 2.13 g (25 mmol) cyclohexane, 29 bar 5 % $H_2$ / $N_2$ and 11 bar 25 % $O_2$ / $N_2$, 1200 RPM. Where C indicates calcination (400 °C, 4 hours, static air) and R indicates reductive heat treatment (400 °C, 4 hours, 5% $H_2$/Ar).*

Comparing calcination and reductive heat treatments for both V loadings we can see that the reductive heat treatment has produced greater activity with greater selectivity based on $H_2$, Table 5.16. The comparison of 1% and 3% V loadings has shown that the lower loaded V has shown greater activity to the higher V loaded catalysts. As previously mentioned monolayer vanadia species have been shown to be more

active[23,24,77] and with these higher loadings of V could have decreased the dispersion of V on the catalyst.

***Table 5.16.*** *$H_2$ conversion and selectivity to $C_6$ products during oxidation of cyclohexane.*

| Catalyst | $H_2$ Conversion / % | Total Product Yield / % | Selectivity to all $C_6^*$ products based on $H_2$ / % |
|---|---|---|---|
| 1% VPd/$TiO_2$ | 98 | 0.22 | 2.3 |
| 1% Pd/1% V-$TiO_2$ (R) | 96 | 0.18 | 1.9 |
| 1% Pd/1% V-$TiO_2$ (C) | 94 | 0.08 | 0.9 |
| 1% Pd/3% V-$TiO_2$ (R) | 96 | 0.14 | 1.5 |
| 1% Pd/3% V-$TiO_2$ (C) | 83 | 0.07 | 1.1 |

***Reaction conditions;*** *80 °C, 17 hours, 0.05 g catalyst, 6.37 g t-BuOH, 2.13 g cyclohexane, 29 bar 5 % $H_2$ / $N_2$ and 11 bar 25 % $O_2$ / $N_2$, 1200 RPM. Where C indicates calcination (400 °C, 4 hours, static air) and R indicates reductive heat treatment (400 °C, 4 hours, 5% $H_2$/Ar). *$C_6$ products; cyclohexanol, cyclohexanone and CHHP.*

It can be observed that $Pd^0$:$Pd^{2+}$ are all much lower that the catalyst prepared by modified impregnation showing a much lower metallic Pd content, Table 5.17. Although the catalysts that have been reduced, show a greater $Pd^0$ content, and a greater activity than the corresponding calcined catalyst this indicates the Pd oxidation state is not the ruling factor on activity. Even the reduced catalysts have still shown a large $Pd^{2+}$ content which has not previously been observed for catalysts undergoing this reductive heat treatment. This could indicate a lower dispersion of Pd on the catalyst surface so less Pd is available on the surface to be reduced during heat treatment. It could also be attributed to the interaction with V which could stabilise the $Pd^{2+}$ oxidation state. The reductive heat treatment has reduced the concentration of Cl on the surface of the catalyst but for both calcined and reduced catalysts though this is still higher than seen for modified impregnation. These high concentrations of Cl could have attributed to the catalytic activity of these catalyst, especially in the synthesis of $H_2O_2$ where it is known that Cl can promote $H_2O_2$ formation.[82]

***Table 5.17.*** *XPS analysis of 1% Pd/ X% V-$TiO_2$ that have been both calcined at reduced.*

| Catalyst | $Pd^0$:$Pd^{2+}$ | Pd:V | Cl |
|---|---|---|---|
| 1% VPd/$TiO_2$ (mi) | 3.3 | 0.19 | 0 |
| 1% Pd/ 1%V-$TiO_2$ (calcined) | 0.08 | 0.30 | 1.48 |
| 1% Pd/ 1%V-$TiO_2$ (reduced) | 0.3 | 0.19 | 0.79 |
| 1% Pd/ 3%V-$TiO_2$ (calcined) | All $Pd^{2+}$ | 0.21 | 1.5 |
| 1% Pd/ 3%V-$TiO_2$ (reduced) | 0.16 | 0.13 | 0.87 |

These catalysts have all shown greater leaching in V than modified impregnation hence the pre-treatment of the V impregnated $TiO_2$ catalysts has not been successful in stabilising the V species and reducing leached V (Appendix Table S5.5). From this

however it can be observed that there is no correlation between product yield and leached V species, Figure 5.21. From this it could be concluded that even if leached V is having a small contribution to catalytic activity there is not a direct activity correlation for the leached V.

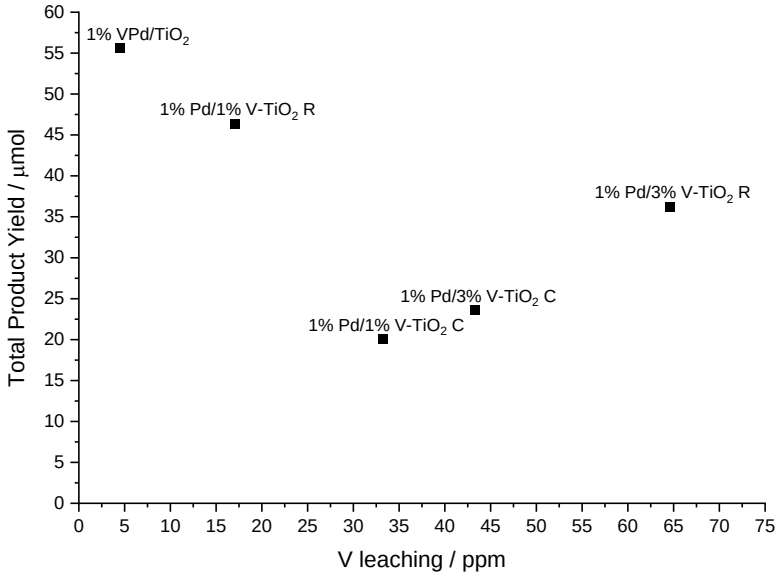


***Figure 5.21.*** *The correlation between the total product yield for cyclohexane oxidation and the concentration of V leaching for Pd/$VO_x$/$TiO_2$ catalysts.* ***Reaction conditions;*** *80 °C, 17 hours, 0.05 g catalyst, 6.37 g t-BuOH, 2.13 g (25 mmol) cyclohexane, 29 bar 5 % $H_2$ / $N_2$ and 11 bar 25 % $O_2$ / $N_2$, 1200 RPM.*

## 5.5 Conclusions.

A range of Pd-based bimetallic catalysts, where Au is replaced with arrange of secondary metals have been studied. All 1% XPd/$TiO_2$ catalysts, except 1% CuPd/$TiO_2$, have shown appreciable $H_2O_2$ synthesis activity (between 20 to 40 $mol_{H_2O_2}$ $kg_{cat}^{-1}$ $hr^{-1}$) compared to 68 $mol_{H_2O_2}$ $kg_{cat}^{-1}$ $hr^{-1}$ for the previous studied 1% AuPd/$TiO_2$. Furthermore, the newly prepared 1% XPd/$TiO_2$ catalysts degrade $H_2O_2$ to a much lesser extent than 1% AuPd/$TiO_2$. By alloying Pd with a secondary non-noble metal (V, Co, Mn, Fe) a similar enhancement in $H_2O_2$ synthesis activity to that previously reported upon Au incorporation[27] is observed.

All bimetallic 1 % XPd/$TiO_2$ have been tested for the oxidation of cyclohexane under both *in-situ* and aerobic conditions. All catalysts have performed better under *in-situ* conditions showing the significance of the presence of $H_2$ in the reaction.

1 % VPd/$TiO_2$ has shown superior activity to all other catalysts, Table 5.18, with a much-increased yield of 56 µmol of cyclohexanol and cyclohexanone compared to the

19 µmol produced by the AuPd catalyst. It is postulated that the coupling of V and Pd has enhanced catalytic activity by combining sites for $H_2O_2$ synthesis, Pd, in close contact with dispersed V species which are active for cyclohexane oxidation.

***Table 5.18.*** *A comparison of key results from the oxidation of cyclohexane via the in-situ utilisation of $H_2O_2$.*

| Catalyst | Yield of cyclohexanol / µmol | Yield of cyclohexanone / µmol | Yield of CHHP/ µmol |
|---|---|---|---|
| 1% AuPd/$TiO_2$ (wi) | 5.96 | 3.93 | 2.94 |
| 1% AuPd/$TiO_2$ (mi) | 12.48 | 6.30 | 5.43 |
| 1% VPd/$TiO_2$ (mi) | 35.01 | 20.79 | 12.37 |

Extended studies on this superior VPd catalyst have focused on attempting to elucidate the reasons behind this activity and further catalyst design to reduce leaching of V into solution and to increase catalyst stability. Despite attempts to reduce the leaching of V none have been successful, however no correlation between leaching and activity has been observed. A range of studies have focussed on determining the role of leached V and efforts have been made to inhibit leaching.

Stabilising V on the catalyst has thus far been unsuccessful and hence future work would focus on stabilising V while still maintaining the high activity. To stabilise the V, future work would focus on incorporating the V into the $TiO_2$ support to form a mixed Ti-V oxide. Another option would be to incorporate V into other support materials such as a zeolite. In the literature several successful incorporations of ionic V into zeolitic frameworks have be reported and utilised for oxidation catalysis.[83–85] In these zeolites the V replaces Ti sites and can be incorporated either in an octahedral environment, with $V^{4+}$, or in tetrahedral sites, with $V^{5+}$. This shows that V can be present in multiple oxidation states while also having the catalytic selectivity advantages of zeolite frameworks.[84] The incorporation of V into the support structure would hopefully decrease the leaching of V.

## 5.6 References.

1. M. Sankar, Q. He, M. Morad, J. Pritchard, S. J. Freakley, J. K. Edwards, S. H. Taylor, D. J. Morgan, A. F. Carley, D. W. Knight, C. J. Kiely and G. J. Hutchings, *ACS Nano*, 2012, **6**, 6600–6613.
2. P. Paalanen, B. M. Weckhuysen and M. Sankar, *Catal. Sci. Technol.*, 2013, **3**, 2869–2880.
3. M. Conte, X. Liu, D. M. Murphy, K. Whiston and G. J. Hutchings, *Phys. Chem. Chem. Phys.*, 2012, **14**, 16279–16285.

4. B. Modén, B.-Z. Zhan, J. Dakka, J. G. Santiesteban and E. Iglesia, *J. Catal.*, 2006, **239**, 390–401.
5. V. Van-Dúnem, A. P. Carvalho, L. M. D. R. S. Martins and A. Martins, *ChemCatChem*, 2018, **10**, 4058–4066.
6. Denicourt-Nowicki, A. Lebedeva, C. Bellini and A. Roucoux, *ChemCatChem*, 2016, **8**, 357–362.
7. Hermans, J. Peeters and P. A. Jacobs, *J. Phys. Chem. A*, 2008, **112**, 1747–1753.
8. Hermans, P. A. Jacobs and J. Peeters, *Chem. Eur. J.*, 2006, **12**, 4229–4240.
9. Walling, *Acc. Chem. Res.*, 1975, **8**, 125–131.
10. Walling and S. Kato, *J. Am. Chem. Soc.*, 1971, **93**, 4275–4281.
11. S. Navalon, M. Alvaro and H. Garcia, *Appl. Catal. B Environ.*, 2010, **99**, 1–26.
12. S. Contreras, M. S. Yalfani, F. Medina and J. E. Sueiras, *Water Sci. Technol.*, 2011, **63**, 2017–2024.
13. R. C. C. Costa, M. F. F. Lelis, L. C. A. Oliveira, J. D. Fabris, J. D. Ardisson, R. R. V. A. Rios, C. N. Silva and R. M. Lago, *J. Hazard. Mater.*, 2006, **129**, 171–178.
14. Santos, R. J. Lewis, G. Malta, A. G. R. Howe, D. J. Morgan, E. Hampton, P. Gaskin and G. J. Hutchings, *Ind. Eng. Chem. Res.*, 2019, **58**, 12623–12631.
15. M. H. A. Rahim, R. D. Armstrong, C. Hammond, N. Dimitratos, S. J. Freakley, M. M. Forde, D. J. Morgan, G. Lalev, R. L. Jenkins, J. A. Lopez-Sanchez, S. H. Taylor and G. J. Hutchings, *Catal. Sci. Technol.*, 2016, **6**, 3410–3418.
16. M. Joshi, W. N. Delgass and K. T. Thomson, *J. Phys. Chem. C*, 2007, **111**, 7384–7395.
17. S. J. Freakley, Q. He, J. H. Harrhy, L. Lu, D. A. Crole, D. J. Morgan, E. N. Ntainjua, J. K. Edwards, A. F. Carley, A. Y. Borisevich, C. J. Kiely and G. J. Hutchings, *Science*, 2016, **351**, 965–968.
18. D. A. Crole, R. Underhill, J. K. Edwards, G. Shaw, S. J. Freakley, G. J. Hutchings and R. J. Lewis, *Philos. Trans. R. Soc. Math. Phys. Eng. Sci.*, 2020, **378**, 20200062.
19. S. E. Dapurkar, A. Sakthivel and P. Selvam, *J. Mol. Catal. Chem.*, 2004, **223**, 241–250.
20. C. Santra, S. Shah, A. Mondal, J. K. Pandey, A. B. Panda, S. Maity and B. Chowdhury, *Microporous Mesoporous Mater.*, 2016, **223**, 121–128.
21. S. H. Nouri and H. Hosseini-Monfared, *Appl. Organomet. Chem.*, 2017, **31**, e3649.
22. X. Lyu, H. Mao, K. Zhu, Y. Kong and M. Kobayashi, *Microporous Mesoporous Mater.*, 2017, **252**, 1–9.
23. T. Garcia, B. Solsona, D. M. Murphy, K. L. Antcliff and S. H. Taylor, *J. Catal.*, 2005, **229**, 1–11.
24. T. Garcia, B. Solsona, D. Cazorla-Amorós, Á. Linares-Solano and S. H. Taylor, *Appl. Catal. B Environ.*, 2006, **62**, 66–76.
25. K. Edwards, J. Pritchard, M. Piccinini, G. Shaw, Q. He, A. F. Carley, C. J. Kiely and G. J. Hutchings, *J. Catal.*, 2012, **292**, 227–238.
26. D. Gudarzi, W. Ratchananusorn, I. Turunen, M. Heinonen and T. Salmi, *Catal. Today*, 2015, **248**, 58–68.
27. Y.-F. Han, Z. Zhong, K. Ramesh, F. Chen, L. Chen, T. White, Q. Tay, S. N. Yaakub and Z. Wang, *J. Phys. Chem. C*, 2007, **111**, 8410–8413.

28. D. Wang, A. Villa, F. Porta, L. Prati and D. Su, *J. Phys. Chem. C*, 2008, **112**, 8617–8622.
29. D. P. Dissanayake and J. H. Lunsford, *J. Catal.*, 2003, **214**, 113–120.
30. E. A. Buvaylo, V. N. Kokozay, O. Yu. Vassilyeva, B. W. Skelton, O. V. Nesterova and A. J. L. Pombeiro, *Inorg. Chem. Commun.*, 2017, **78**, 85–90.
31. M. D. R. S. Martins, A. P. C. Ribeiro and A. J. L. Pombeiro, *Lett. Org. Chem.*, *2017*, **14**, 517 – 574.
32. A. Alshaheri, M. I. M. Tahir, M. B. A. Rahman, T. B. S. A. Ravoof and T. A. Saleh, *Chem. Eng. J.*, 2017, **327**, 423–430.
33. G. S. Mishra, T. F. S. Silva, L. M. D. R. S. Martins and A. J. L. Pombeiro, *Pure Appl. Chem.*, 2009, **81**, 1217–1227.
34. F. Vailati, R. D. Huelsmann, E. Martendal, A. J. Bortoluzzi, F. R. Xavier and R. A. Peralta, *New J. Chem.*, 2020, **44**, 2514–2526.
35. Garcia-Bosch and M. A. Siegler, *Angew. Chem. Int. Ed.*, 2016, **55**, 12873–12876.
36. Balkus and A. Gabrielov, US005830429A, 1998.
37. Qu, J. He, W. Jiang, M. Lin, Y. Yang, X. Shu and Wang, CN102757303 (A), 2012.
38. H. L. Cates, J. O. Pundersom and R. W. Wheatcroft, 2851496, 1958.
39. D Loder, 2223494, 1940.
40. X. Lui, H. Wang, L. Song, K. Qiao and L. Wang, CN109248699 (A), 2019.
41. Triki, S. Contreras and F. Medina, *J. Sol-Gel Sci. Technol.*, 2014, **71**, 96–101.
42. Y. Qin, M. Sun, H. Liu and J. Qu, *Electrochimica Acta*, 2015, **186**, 328–336.
43. S. Yalfani, A. Georgi, S. Contreras, F. Medina and F.-D. Kopinke, *Appl. Catal. B Environ.*, 2011, **104**, 161–168.
44. R. Underhill, R. J. Lewis, S. J. Freakley, M. Douthwaite, P. J. Miedziak, O. Akdim, J. K. Edwards and G. J. Hutchings, *Johns. Matthey Technol. Rev.*, 2018, **62**, 417–425.
45. Rios-Enriquez, N. Shahin, C. Durán-de-Bazúa, J. Lang, E. Oliveros, S. H. Bossmann and A. M. Braun, *Sol. Energy*, 2004, **77**, 491–501.
46. S. Zha, Y. Cheng, Y. Gao, Z. Chen, M. Megharaj and R. Naidu, *Chem. Eng. J.*, 2014, **255**, 141–148.
47. C. Lindhorst, S. Haslinger and F. E. Kühn, *Chem. Commun.*, 2015, **51**, 17193–17212.
48. Retcher, J. S. Costa, J. Tang, R. Hage, P. Gamez and J. Reedijk, *J. Mol. Catal. Chem.*, 2008, **286**, 1–5.
49. Y. Saleh, I. E. Wachs, S. Chan and C. Chersich, *J. Catal.*, 1986, **98**, 102–114.
50. E. Wachs and B. M. Weckhuysen, *Appl. Catal. Gen.*, 1997, **157**, 67–90.
51. G. Chen, W.-T. Chou and C. Yeh, *Appl. Catal.*, 1983, **8**, 389–397.
52. Chen, D. Kumar, C.-W. Yi and D. W. Goodman, *Science*, 2005, **310**, 291–293.
53. Seoane, P. Boutry and R. Montarnal, *J. Catal.*, 1980, **63**, 191–200.
54. R. S. G. Ferreira, P. G. P. de Oliveira and F. B. Noronha, *Appl. Catal. B Environ.*, 2004, **50**, 243–249.
55. T. Garcia, B. Solsona and S. H. Taylor, *Catal. Lett.*, 2004, **97**, 99–103.
56. Bellifa, D. Lahcene, Y. N. Tchenar, A. Choukchou-Braham, R. Bachir, S. Bedrane and C. Kappenstein, *Appl. Catal. Gen.*, 2006, **305**, 1–6.
57. Rezaei, A. Najafi Chermahini and H. A. Dabbagh, *Chem. Eng. J.*, 2017, **314**, 515–525.
58. Abon, J. M. Herrmann and J. C. Volta, *Catal. Today*, 2001, **71**, 121–128.

59. Jian, K. You, X. Duan, H. Gao, Q. Luo, R. Deng, P. Liu, Q. Ai and H. Luo, *Chem. Commun.*, 2016, **52**, 3320–3323.
60. Y. N. Kozlov, G. V. Nizova and G. B. Shul'pin, *J. Mol. Catal. Chem.*, 2005, **227**, 247–253.
61. E. F. Aboelfetoh and R. Pietschnig, *Catal. Lett.*, 2009, **127**, 83–94.
62. E. F. Aboelfetoh, M. Fechtelkord and R. Pietschnig, *J. Mol. Catal. Chem.*, 2010, **318**, 51–59.
63. G. B. Shul'pin and G. Süss-Fink, *J. Chem. Soc. Perkin Trans. 2*, 1995, **0**, 1459–1463.
64. G. Süss-Fink, S. Stanislas, G. B. Shul'pin, G. V. Nizova, H. Stoeckli-Evans, A. Neels, C. Bobillier and S. Claude, *J. Chem. Soc. Dalton Trans.*, 1999, **0**, 3169–3175.
65. Ouyang, P. Tian, G. Da, X.-C. Xu, C. Ao, T. Chen, R. Si, J. Xu and Y.-F. Han, *J. Catal.*, 2015, **321**, 70–80.
66. R. D. Armstrong, J. Hirayama, D. W. Knight and G. J. Hutchings, *ACS Catal.*, 2019, **9**, 325–335.
67. K. Edwards, B. Solsona, E. N. N, A. F. Carley, A. A. Herzing, C. J. Kiely and G. J. Hutchings, *Science*, 2009, **323**, 1037–1041.
68. H. P. Boehm, G. Mair, T. Stoehr, A. R. De Rincón and B. Tereczki, *Fuel*, 1984, **63**, 1061–1063.
69. E. Lam and J. H. T. Luong, *ACS Catal.*, 2014, **4**, 3393–3410.
70. R. J. Lewis, Jennifer. K. Edwards, S. J. Freakley and G. J. Hutchings, *Ind. Eng. Chem. Res.*, 2017, **56**, 13287–13293.
71. E. N. Ndifor, T. Garcia and S. H. Taylor, *Catal. Lett.*, 2006, **110**, 125–128.
72. H. Ehrich, H. Berndt, M.-M. Pohl, K. Jähnisch and M. Baerns, *Appl. Catal. Gen.*, 2002, **230**, 271–280.
73. S. Wuyts, J. Wahlen, P. A. Jacobs and D. E. D. Vos, *Green Chem.*, 2007, **9**, 1104–1108.
74. Haber, *Catal. Today*, 2009, **142**, 100–113.
75. B. M. Weckhuysen and D. E. Keller, *Catal. Today*, 2003, **78**, 25–46.
76. J. K. Edwards, B. E. Solsona, P. Landon, A. F. Carley, A. Herzing, C. J. Kiely and G. J. Hutchings, *J. Catal.*, 2005, **236**, 69–79.
77. O. Guerrero-Pérez, *Catal. Today*, 2017, **285**, 226–233.
78. Y. Hong, D. Sun and Y. Fang, *Chem. Cent. J.*, 2018, **12**, 36.
79. T. Garcia, W. Weng, B. Solsona, E. Carter, A. F. Carley, C. J. Kiely and S. H. Taylor, *Catal. Sci. Technol.*, 2011, **1**, 1367–1375.
80. R. Barthos, G. Novodárszki and J. Valyon, *React. Kinet. Mech. Catal.*, 2017, **121**, 17–29.
81. R. Barthos, A. Hegyessy, G. Novodárszki, Z. Pászti and J. Valyon, *Appl. Catal. Gen.*, 2017, **531**, 96–105.
82. E. Ntainjua N., M. Piccinini, J. C. Pritchard, J. K. Edwards, A. F. Carley, J. A. Moulijn and G. J. Hutchings, *ChemSusChem*, 2009, **2**, 575–580.
83. S. Dzwigaj, P. Massiani, A. Davidson and M. Che, *J. Mol. Catal. Chem.*, 2000, **155**, 169–182.
84. T. Sen, V. Ramaswamy, S. Ganapathy, P. R. Rajamohanan and S. Sivasanker, *J. Phys. Chem.*, 1996, **100**, 3809–3817.
85. E. Z. Hegazy, S. A. Kosa, I. H. A. El Maksod and D. F. Baamer, *Silicon*, 2019.

# Appendix.

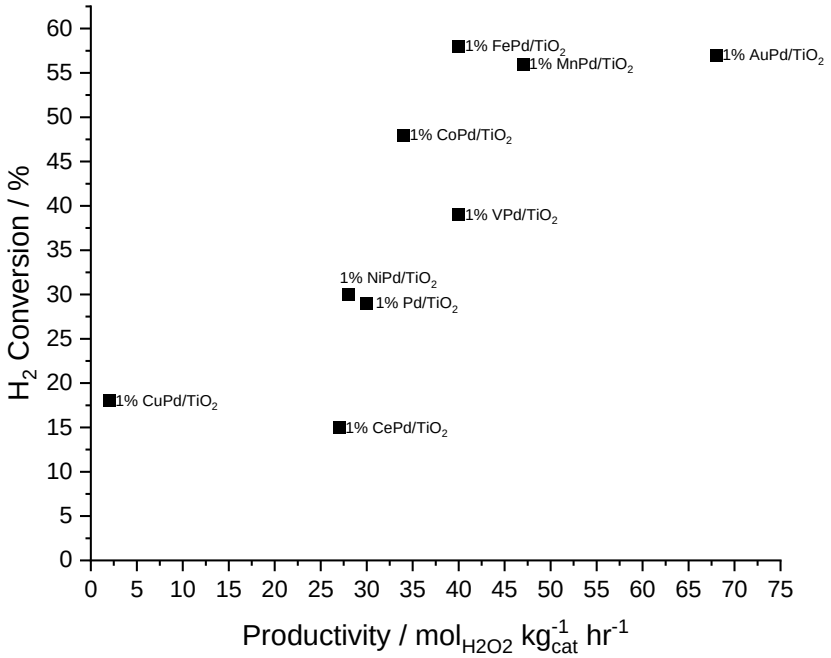


***Figure S5.1.*** *The correlation between productivity towards $H_2O_2$ synthesis and $H_2$ conversion for the series of 1% XPd/TiO₂.* ***Reaction conditions;*** *0.01 g catalyst, 2.9 g water, 5.6 g methanol, 29 bar 5 % $H_2/CO_2$ and 11 bar 25 % $O_2/CO_2$, 1200 RPM, 30 minutes, 25 °C.*

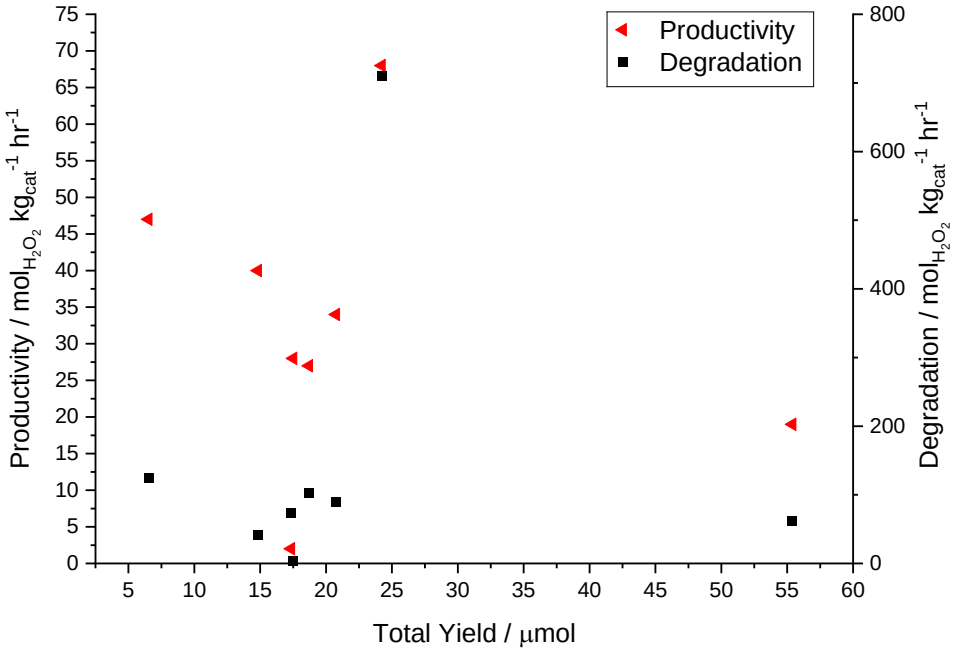


***Figure S5.2.*** *The correlation between productivity and degradation towards $H_2O_2$ synthesis and the yield of oxidation products from the oxidation of cyclohexane via the in-situ production of $H_2O_2$ for the series of 1% XPd/TiO₂.*

***Table S5.1.*** *Surface composition of Pd and X determined by XPS of 1 % XPd/$TiO_2$ catalysts fresh and after use in the cyclohexane oxidation via in-situ $H_2O_2$ synthesis.*

| Catalyst | Binding Energy of X / eV | Atomic concentration / % | | |
|---|---|---|---|---|
| | | X | $Pd^{2+}$ | $Pd^0$ |
| 1 % VPd/$TiO_2$ | 516.38 | 1.32 | 0.06 | 0.2 |
| 1 % VPd/$TiO_2$ used | 516.07 | 1.31 | 0.05 | 0.19 |
| 1 % MnPd/ $TiO_2$ | 640.75 | 0.7 | 0.08 | 0.16 |
| 1 % MnPd/ $TiO_2$ used | 641.19 | 0.68 | 0.06 | 0.17 |
| 1 % FePd/ $TiO_2$ | 709.50 | 0.78 | 0.05 | 0.16 |
| 1 % FePd/ $TiO_2$ used | 709.60 | 0.7 | 0.02 | 0.27 |
| 1 % CoPd/ $TiO_2$ | 780.78 | 0.84 | 0.01 | 0.17 |
| 1 % CoPd/ $TiO_2$ used | 780.59 | 0.85 | 0.05 | 0.16 |
| 1 % NiPd/$TiO_2$ | 855.27 | 0.12 | 0.02 | 0.08 |
| 1 % NiPd/$TiO_2$ used | 855.34 | 0.11 | 0.03 | 0.06 |
| 1 % CuPd/ $TiO_2$ | 932.31 | 1.23 | 0.02 | 0.32 |
| 1 % CuPd/ $TiO_2$ used | 932.80 | 1.08 | 0.07 | 0.34 |
| 1 % AuPd/ $TiO_2$ | 82.76 | 0.11 | 0 | 0.25 |
| 1 % AuPd/ $TiO_2$ used | 82.76 | 0.03 | 0.03 | 0.3 |
| 1 % CePd/ $TiO_2$ | 885.18 | 0.46 | 0 | 0.05 |
| 1 % CePd/ $TiO_2$ used | 885.91 | 0.36 | 0 | 0.03 |

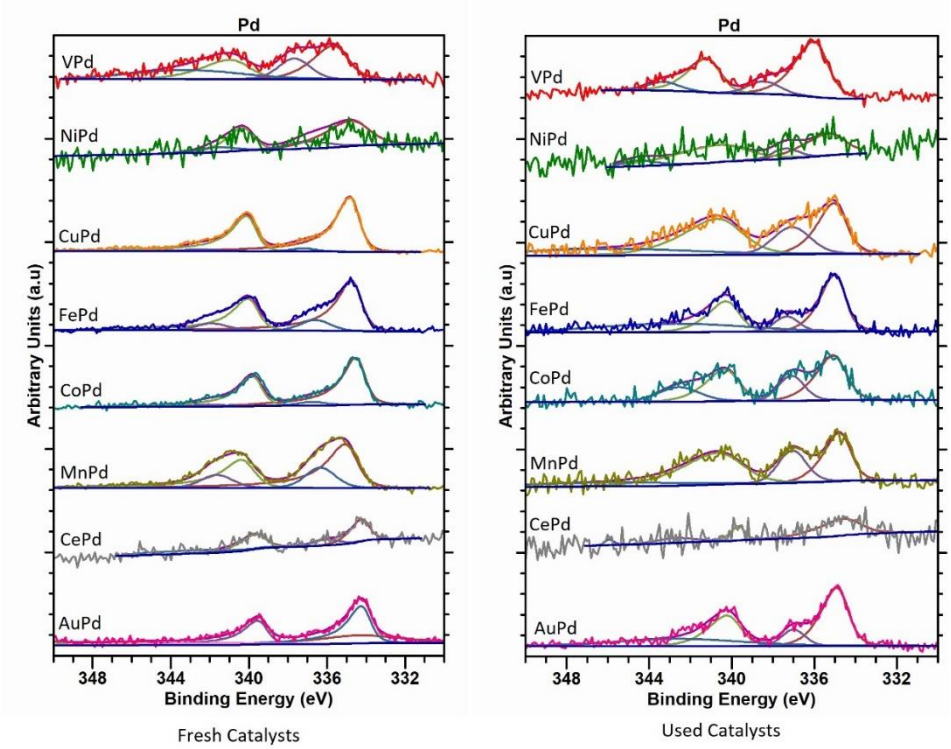


***Figure S5.3.*** *XPS spectra and fitting of Pd d region for series of 1% XPd/$TiO_2$ both fresh and after use in the oxidation of cyclohexane via the in-situ production of $H_2O_2$.*

***Table S5.2.*** *Surface composition of Pd and V determined by XPS of 1 % VPd/$TiO_2$ catalysts, with varying V:Pd, fresh and after use in the cyclohexane oxidation via in-situ $H_2O_2$ synthesis.*

| Catalyst | Atomic concentration / % | | |
|---|---|---|---|
| | V | $Pd^{2+}$ | $Pd^0$ |
| 1% Pd/$TiO_2$ | - | 0 | 0.14 |
| 0.25% V 0.75% Pd/$TiO_2$ | 0.37 | 0.03 | 0.1 |
| 0.5% V 0.5% Pd/$TiO_2$ | 1.32 | 0.06 | 0.2 |
| 0.75% V 0.25% Pd/$TiO_2$ | 1.61 | 0.06 | 0.05 |
| 1% V/$TiO_2$ | 1.86 | - | - |

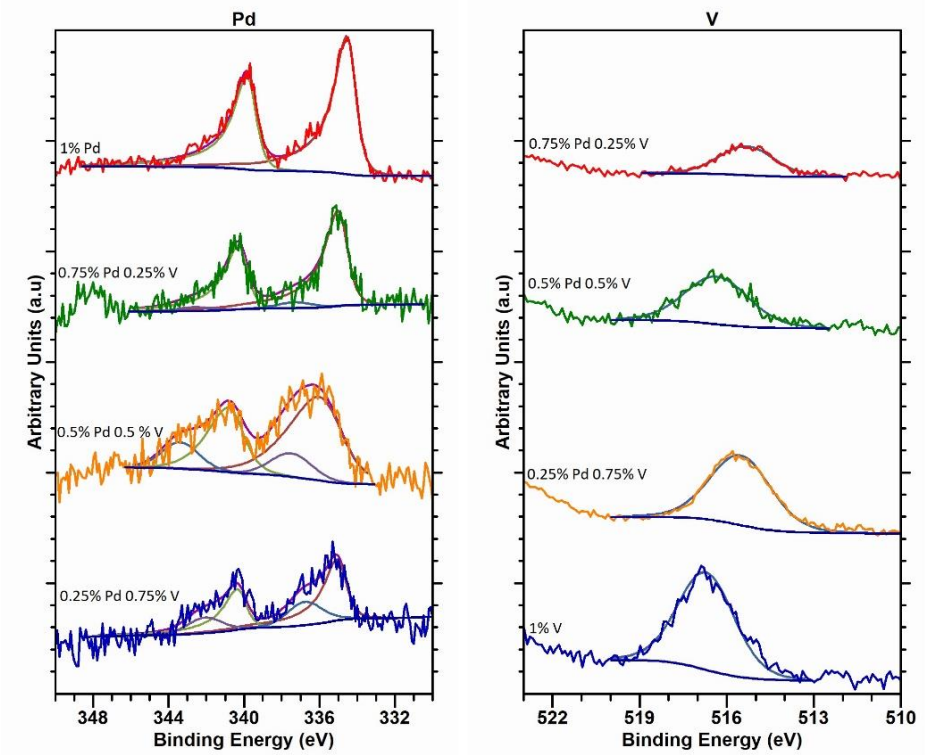


***Figure S5.4.*** *XPS spectra and fitting in Pd 3d and V 2p regions for fresh 1% VPd/$TiO_2$ catalysts with varying V:Pd.*

***Table S5.3*** *Surface composition of Pd and V determined by XPS of 1% VPd/$TiO_2$ catalysts prepared by wet impregnation and different heat treatments. Where; wi indicates wet impregnation and mi indicates modified impregnation.*

| Catalyst | Atomic concentration / % | | |
|---|---|---|---|
| | V | $Pd^{2+}$ | $Pd^0$ |
| 1% VPd/$TiO_2$ (modified impregnation) | 1.32 | 0.06 | 0.2 |
| 1% VPd/$TiO_2$ (modified impregnation) used | 1.31 | 0.05 | 0.19 |
| 1% VPd/$TiO_2$ (wet impregnation, calcined) | 0.92 | 0.1 | 0.11 |
| 1% VPd/$TiO_2$ (wet impregnation, calcined) used | 0.79 | 0.17 | 0.03 |
| 1% VPd/$TiO_2$ (wet impregnation, calcined then reduced) | 0.91 | 0.05 | 0.15 |
| 1% VPd/$TiO_2$ (wet impregnation, calcined then reduced) used | 0.72 | 0.1 | 0.1 |
| 1% VPd/$TiO_2$ (wet impregnation, reduced) | 0.32 | 0 | 0.08 |
| 1% VPd/$TiO_2$ (wet impregnation, reduced) used | 0.42 | 0 | 0.07 |

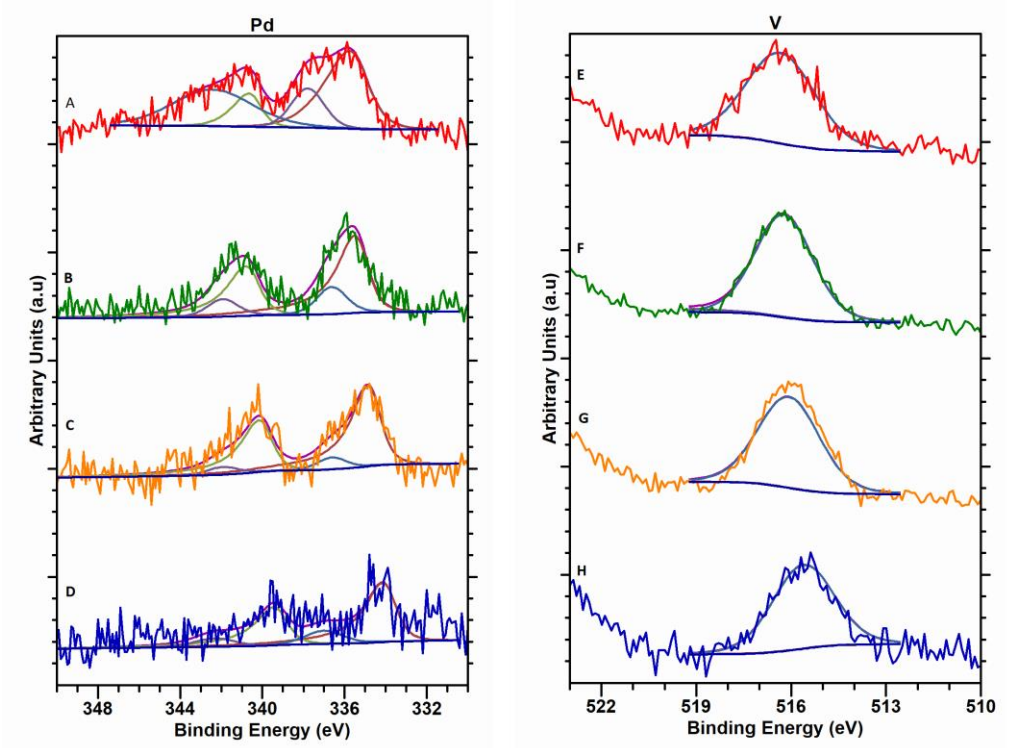


***Figure S5.5.*** *XPS spectra and fitting in the Pd 3d and V 2p regions for 1% VPd/$TiO_2$ catalyst prepared by different methods and heat treatments as prepared.* ***A*** *and* ***E*** *modified impregnation,* ***B*** *and* ***F*** *wet impregnation calcined,* ***C*** *and* ***G*** *wet impregnation calcined and then reduced,* ***D*** *and* ***H*** *wet impregnation reduced.*

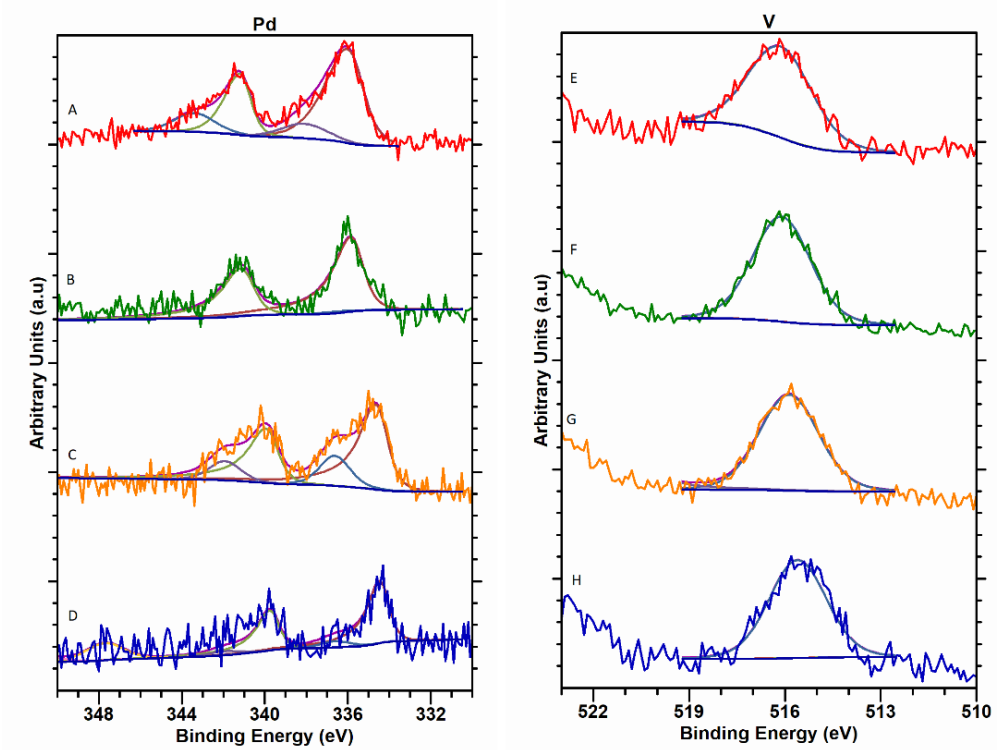


***Figure S5.6.*** *XPS spectra and fitting in the Pd 3d and V 2p regions for 1% VPd/$TiO_2$ catalyst prepared by different methods and heat treatments after use in the oxidation of cyclohexane via the in-situ production of $H_2O_2$.* ***A*** *and* ***E*** *modified impregnation,* ***B*** *and* ***F*** *wet impregnation calcined,* ***C*** *and* ***G*** *wet impregnation calcined and then reduced,* ***D*** *and* ***H*** *wet impregnation reduced.*

***Table S5.4.*** *Surface composition of Pd and V determined by XPS of 1% Pd/ X% V-$TiO_2$ that have been both calcined at reduced.*

| Catalyst | Atomic concentration / % | | |
|---|---|---|---|
| | V | $Pd^{2+}$ | $Pd^0$ |
| 1% Pd/ 1%V-$TiO_2$ (calcined) | 3.73 | 1.05 | 0.08 |
| 1% Pd/ 1%V-$TiO_2$ (reduced) | 2.71 | 0.4 | 0.12 |
| 1% Pd/ 3%V-$TiO_2$ (calcined) | 5.43 | 1.16 | 0 |
| 1% Pd/ 3%V-$TiO_2$ (reduced) | 4.32 | 0.5 | 0.08 |

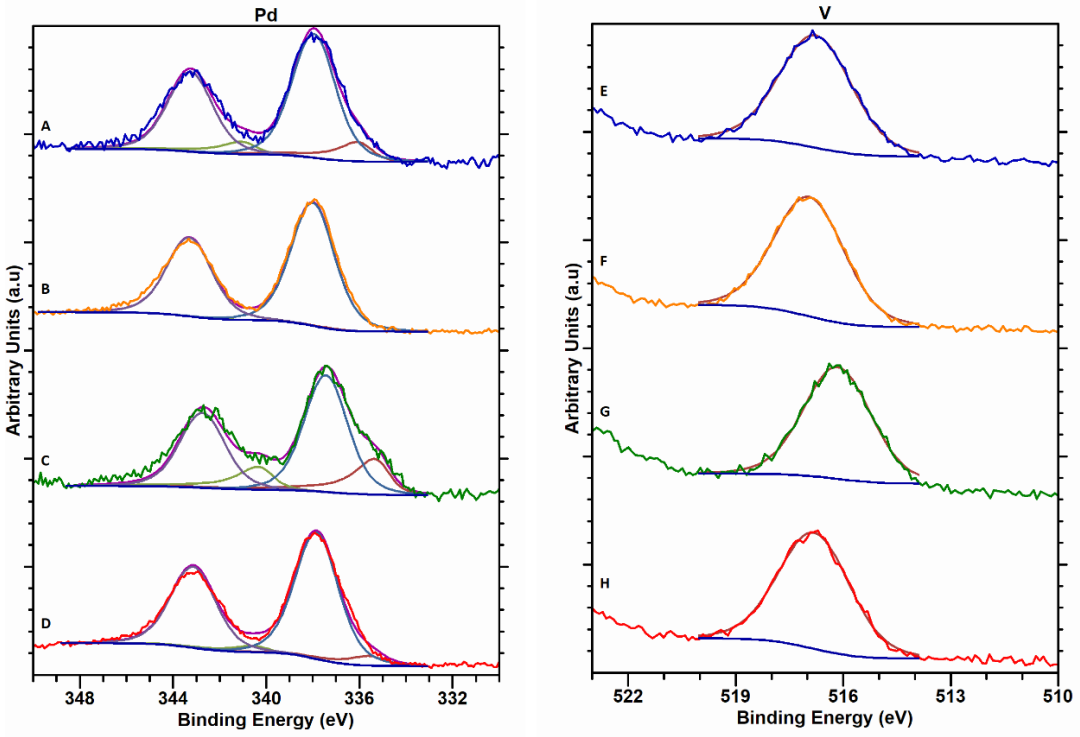


***Figure S5.7.*** *XPS spectra and fitting of the Pd 3d and V 2p regions for 1% Pd/ X% V-$TiO_2$ which have been under different heat treatments, as prepared.* ***A*** *and* ***E*** *1% Pd/1% V-$TiO_2$ calcined,* ***B*** *and* ***F*** *1% Pd/ 1% V-$TiO_2$ reduced,* ***C*** *and* ***G*** *1% Pd/ 3% V-$TiO_2$ calcined, D and H 1% Pd/ 3% V-$TiO_2$ reduced.*

***Table S5.5.*** *ICP-MS analysis of post reaction solutions of 1 % Xpedx/$TiO_2$ used in the oxidation of cyclohexane, indicating the percentage of the metal leached.*

| Catalyst | Pd leached / ppb | X leached / ppm |
|---|---|---|
| 1% Pd/ 1%V-$TiO_2$ (calcined) | 13.3 | 33.3 |
| 1% Pd/ 1%V-$TiO_2$ (reduced) | 42.5 | 17.0 |
| 1% Pd/ 3%V-$TiO_2$ (calcined) | 32.3 | 43.3 |
| 1% Pd/ 3%V-$TiO_2$ (reduced) | 25.6 | 64.6 |

# 6. Oxidation of benzyl alcohol via the *in-situ* production of $H_2O_2$.

## 6.1 Introduction.

As discussed in Chapter 1 Santonastaso *et al.* have previously investigated the oxidation of benzyl alcohol via the *in-situ* production of $H_2O_2$ over 5% AuPd catalysts.[1] They investigated a range of reaction conditions to couple the production of $H_2O_2$, which is performed at sub-ambient temperatures, and the high temperature oxidation of benzyl alcohol. The oxidation of benzyl alcohol is believed to proceed via a radical process involving a hydroperoxy intermediate, Scheme 6.1,[2,3] where normally high temperatures are utilised to produce these intermediates and hence this work focussed on using mixtures of $H_2$ and $O_2$ to produce these radicals *in-situ*. It was demonstrated that through the production of reactive oxygen species, including $H_2O_2$, formed over a 5 % AuPd/$TiO_2$ catalyst, reaction temperatures significantly lower than that in the literature could be utilised, with good selectivity to benzaldehyde observed.[1]

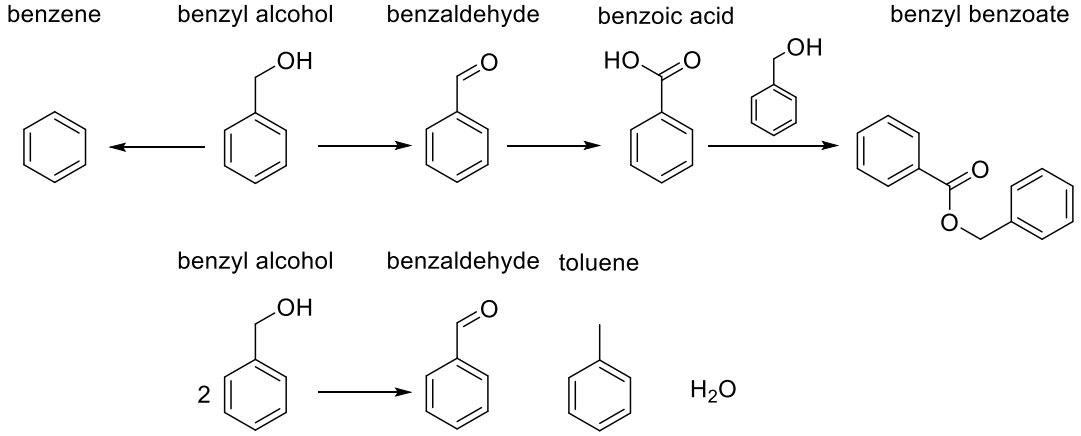


***Scheme 6.1.*** *A reaction scheme for the oxidation of benzyl alcohol.*

These reaction conditions developed by Santonastaso *et al.*[1] have been utilised to test novel catalysts, prepared by modified impregnation, for the oxidation of benzyl alcohol via the *in-situ* production of $H_2O_2$.

## 6.2 Initial studies for benzyl alcohol oxidation via the *in-situ* production of $H_2O_2$.

Firstly, the comparison between $H_2$, $O_2$ and $H_2$ and $O_2$ gas mixtures under standard reaction conditions were investigated. For 1% Pd/$TiO_2$ it can be observed that the greatest activity has been observed when both $H_2$ and $O_2$ are present, Figure 6.1, with

the highest selectivity to benzaldehyde. This illustrates the importance of both $H_2$ and $O_2$ and the $H_2O_2$ (or reactive oxygen species that originate from it) in the oxidation reaction under these mild conditions.

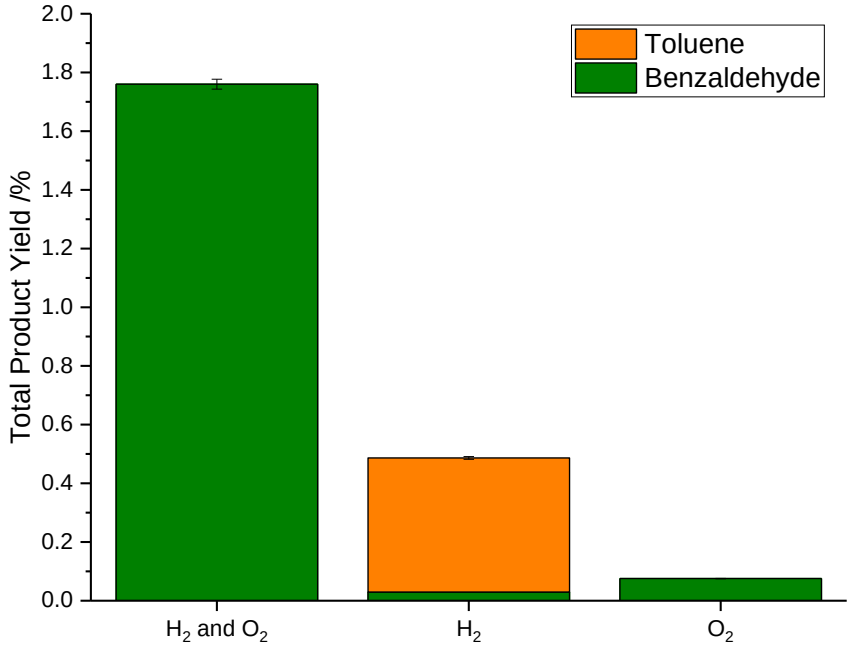


***Figure 6.1*** *The comparison of the activity of $H_2$, $O_2$ and $H_2$ and $O_2$ gas mixture on the oxidation of benzyl alcohol using 1% $Pd/TiO_2$.* ***Reaction conditions;*** *0.01 g catalyst, 1.04 g (9.6 mmol) benzyl alcohol, 7.1 g methanol, 29 bar 5 % $H_2/CO_2$, 11 bar 25 % $O_2/CO_2$, 1200 RPM, 30 minutes, 50 °C.*

When only $O_2$ is present limited catalytic activity has been observed showing the importance of the addition of $H_2$. These standard conditions are much milder than usually implanted for aerobic oxidation of benzyl alcohol, 120 °C.[4] It has been previously noted in the literature that with increasing reaction temperature the selectivity to benzaldehyde is reduced and the selectivity to toluene is increased.[5] The greater selectivity towards benzaldehyde hence could be attributed to milder reaction temperatures reducing toluene formation. When $H_2$ only is present a switch in selectivity towards toluene has been observed showing that the reduction of benzyl alcohol pathway is more prevalent here.

The *ex-situ* addition of commercial $H_2O_2$ has illustrated the increased efficiency of the *in-situ* production of $H_2O_2$ for the oxidation of benzyl alcohol under these mild conditions, Figure 6.2. Assuming 100% conversion and selectivity of $H_2$ into $H_2O_2$ the maximum amount of $H_2O_2$ that could be produced is 2.51 mmol and hence this amount of $H_2O_2$ has been used as a comparison to the *in-situ* conditions, using both $H_2$ and $O_2$ gases.

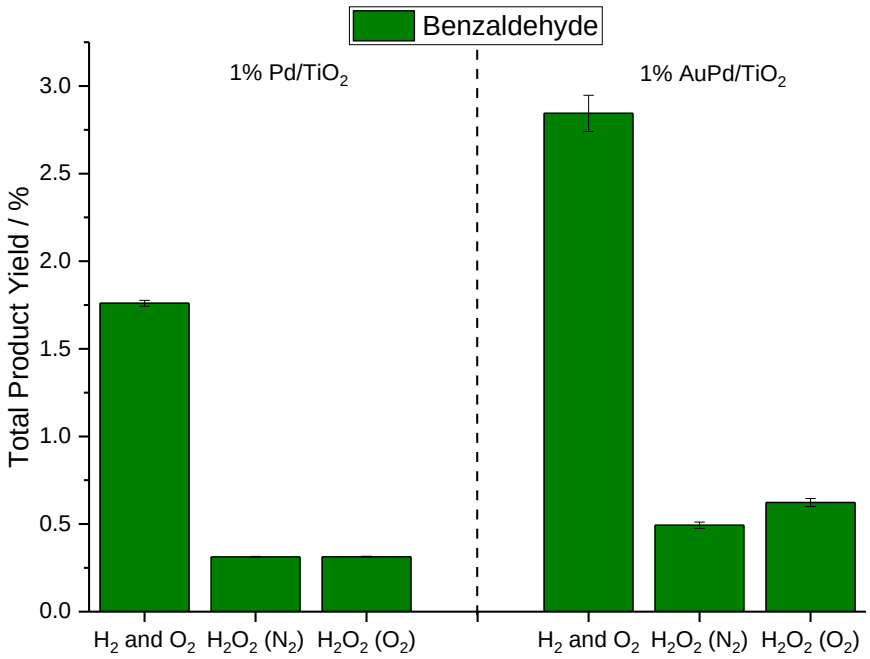


***Figure 6.2.*** *The comparison of the activity in-situ and ex-situ addition of $H_2O_2$ on the oxidation of benzyl alcohol using 1% Pd/$TiO_2$ and 1% AuPd/$TiO_2$.* ***Reaction conditions;*** *0.01 g catalyst, 1.04 g (9.6 mmol) benzyl alcohol, 7.1 g methanol, 29 bar 5 % $H_2$/$CO_2$ and 11 bar 25 % $O_2$/$CO_2$ or 40 bar $N_2$ or 29 bar $N_2$ and 11 bar 25% $O_2$/$CO_2$, 1200 RPM, 30 minutes, 50 °C.*

For both 1% Pd/$TiO_2$ and 1% AuPd/$TiO_2$ a greater catalytic activity has been observed when both $H_2$ and $O_2$ gases have been used compared to the *ex-situ* addition of commercial $H_2O_2$. With *ex-situ* addition of $H_2O_2$ degradation of the $H_2O_2$ can occur both during the heating up of the reaction as well as during the reaction reducing the $H_2O_2$ available for oxidation and limiting the activity. Within the literature $H_2O_2$ is often utilised in molar excess, 2:1, to benzyl alcohol to overcome this loss in degradation.[6–8] This has shown the effectiveness of *in-situ* $H_2O_2$ production which can be synthesised and utilised for oxidation immediately without the use of large excesses of $H_2O_2$.

## 6.3 Bimetallic Pd based catalysts for the oxidation of benzyl alcohol via the *in-situ* production of $H_2O_2$.

All bimetallic 1 % XPd/$TiO_2$ catalysts, previously investigated for $H_2O_2$ synthesis and the oxidation of cyclohexane in Chapter 5, have also been tested for the oxidation of benzyl alcohol via the *in-situ* production of $H_2O_2$, Figure 6.3.

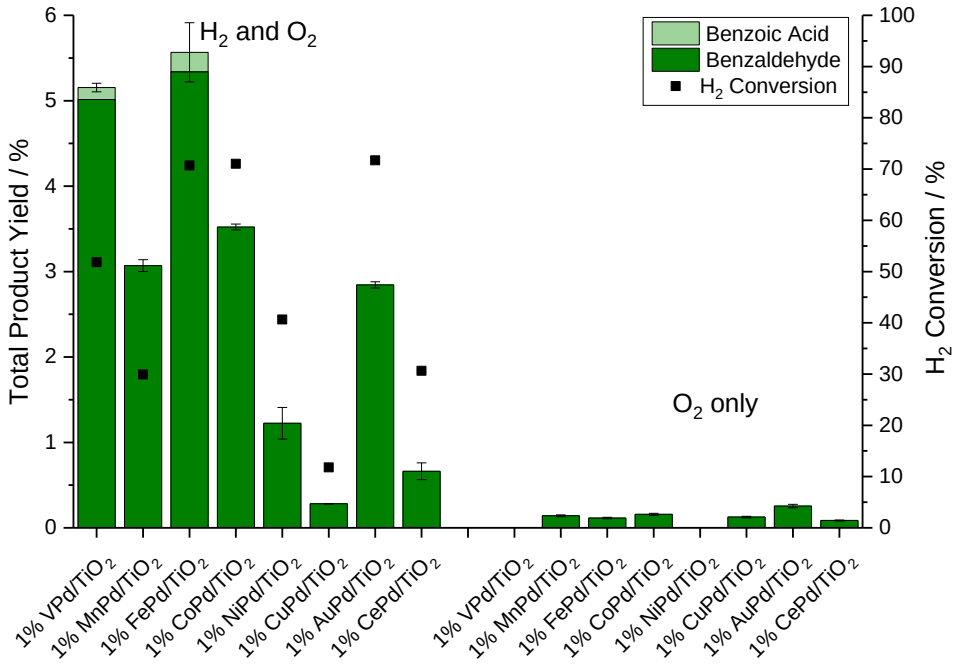


***Figure 6.3*** *The activity of 1 % XPd/TiO₂ catalysts towards benzyl alcohol oxidation.* ***Reaction conditions;*** *0.01 g catalyst, 1.04 g (9.6 mmol) benzyl alcohol, 7.1 g methanol, 29 bar 5 % H₂/CO₂ and 11 bar 25 % O₂/CO₂ (only 11 bar 25 % O₂/CO₂ present under O₂ only conditions), 1200 RPM, 30 minutes, 50 °C.*

Regardless of catalyst composition, activity towards benzyl alcohol oxidation is limited under purely aerobic conditions compared to when both $H_2$ and $O_2$ are present, highlighting the greater efficacy of $H_2O_2$ compared to $O_2$, under these mild conditions. Typically, in the literature aerobic oxidation of benzyl alcohol is investigated at 120 °C and under continuous pressures of $O_2$, 3 bar.[4,9–11]

Moreno *et al.* observed similar findings when testing 5% AuPd/TS-1 catalysts at 30 ºC in a water/methanol solvent mixture. They showed that the introduction of $H_2$ diluted in $CO_2$ gave 5 times greater yield of benzaldehyde compared to $O_2$ alone.[12] This was attributed to the production of hydroperoxyl species *in-situ*, of which TS-1 is known to well facilitate.[13] When TS-1 is mixed with $H_2O_2$ the Ti(IV) sites coordinate with $H_2O_2$ forming a Ti- hydroperoxyl species (Ti-OOH). These Ti-OOH species are known to have strong oxidising potential.[13]

Upon introduction of $H_2$ all catalysts have shown high selectivity towards benzaldehyde, > 96%, with benzoic acid only having been observed for 1 % VPd/$TiO_2$ and 1 % FePd/$TiO_2$ catalysts, at yields of 0.14% and 0.15 % respectively. No toluene formation, and hence disproportionation products, have been detected, under these reaction conditions. Sankar *et al.* have previously reported that the over oxidation of benzaldehyde to benzoic acid is limited under benzyl alcohol aerobic conditions.[14]

They investigated that even small concentrations of benzyl alcohol, >10%, can eliminate the oxidation of benzaldehyde to benzoic acid. Benzyl alcohol inhibits benzaldehyde oxidation by removing, by H atom transfer, the benzoylperoxy radical which is a key intermediate for benzoic acid formation.[14]

The first row transition metal-Pd bimetallic catalysts 1 % VPd/$TiO_2$, 1 % MnPd/$TiO_2$, 1 % FePd/$TiO_2$ and 1 % CoPd/$TiO_2$ have all shown a greater activity than 1 % AuPd/$TiO_2$. This can be attributed to these catalysts showing lower activity for the degradation of $H_2O_2$ compared to 1 % AuPd/$TiO_2$ as previously discussed in Chapter 5 Section 5.2.1. These catalysts have also shown, higher or similar, selectivity towards oxidation products, Table 6.1.

***Table 6.1*** *$H_2$ conversion, selectivity towards oxidation products based on $H_2$ conversion and residual $H_2O_2$ for a series of 1 % XPd/$TiO_2$ catalysts.*

| Catalyst | Benzyl Alcohol Conversion / % | $H_2$ Conversion / % | Selectivity* based on $H_2$ / % | Residual $H_2O_2$ / µmol |
|---|---|---|---|---|
| 1% VPd/$TiO_2$ | 5.2 | 52 | 38 | 35 |
| 1% MnPd/$TiO_2$ | 3.1 | 30 | 39 | 67 |
| 1% FePd/$TiO_2$ | 5.3 | 71 | 33 | 25 |
| 1% CoPd/$TiO_2$ | 3.5 | 71 | 19 | 82 |
| 1% NiPd/$TiO_2$ | 1.2 | 40 | 13 | 30 |
| 1% CuPd/$TiO_2$ | 0.3 | 12 | 9 | 13 |
| 1% AuPd/$TiO_2$ | 2.8 | 72 | 11 | 94 |
| 1% CePd/$TiO_2$ | 0.7 | 31 | 11 | 65 |

***Reaction conditions;*** *0.01 g catalyst, 1.04 g (9.6 mmol) benzyl alcohol, 7.1 g methanol, 29 bar 5 % $H_2/CO_2$ and 11 bar 25 % $O_2/CO_2$, 1200 RPM, 30 minutes, 50 °C.* Selectivity towards all oxidation products based on $H_2$ consumption.*

A correlation between the yield of oxidation products and the selectivity based on $H_2$ consumption has been observed, Figure 6.4, displaying that the most catalytically active catalysts, 1% FePd/$TiO_2$ and 1% VPd/$TiO_2$, are also the most selective based on $H_2$ consumption. This could also be partly explained by looking at the residual $H_2O_2$ measured after the oxidation reaction. Those catalysts showing higher activity and selectivity, compared to 1% AuPd/$TiO_2$, have also shown lower concentrations of $H_2O_2$ post reaction despite similar $H_2$ conversions. This means a greater proportion $H_2O_2$ is being utilised in the reaction effectively.

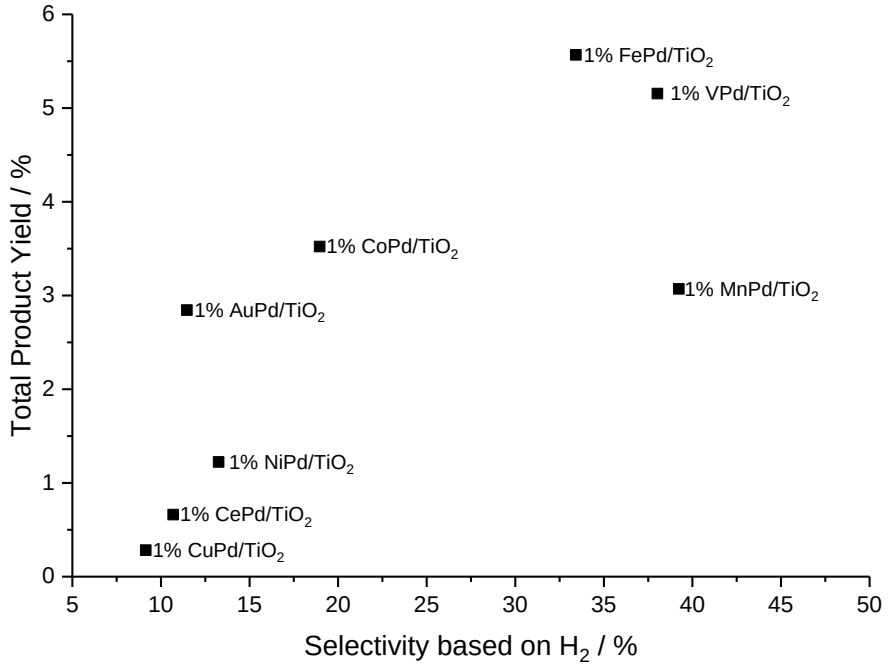


***Figure 6.4.*** *The correlation between the yield of oxidation products against the selectivity towards oxidation products based on $H_2$ consumption.* ***Reaction conditions;*** *0.01 g catalyst, 1.04 g (9.6 mmol) benzyl alcohol, 7.1 g methanol, 29 bar 5 % $H_2/CO_2$ and 11 bar 25 % $O_2/CO_2$, 1200 RPM, 30 minutes, 50 °C.*

It can be observed that 1% VPd/$TiO_2$ and 1% FePd/$TiO_2$ have given the greatest activity towards the oxidation of benzyl alcohol as well as showing the greatest selectivity. Catalysts consisting of alloyed Fe and Pd are known to have high activity towards Fenton reactions[15–18] and should lead to increased radical production from $H_2O_2$. Hence the trend observed could be correlated with the radical production activity of the catalysts. The increased activity could also be attributed to more disperse Pd active centres on the surface, as will be discussed later in Section 6.3.2.

A slight correlation has also been observed between the catalytic activity towards $H_2O_2$ production and the yield of oxidation products. This trend was most prominently observed for the first row transition metal-Pd catalysts, Figure 6.5. However, it should be noted the difficultly in comparing the two reactions, $H_2O_2$ synthesis and benzyl alcohol oxidation, as they are conducted under very different conditions. The catalysts $H_2O_2$ synthesis activity will depend on temperature as although the kinetics can be increased the formation of $H_2O$, either directly or by $H_2O_2$ degradation, is greater at higher temperatures.[19]

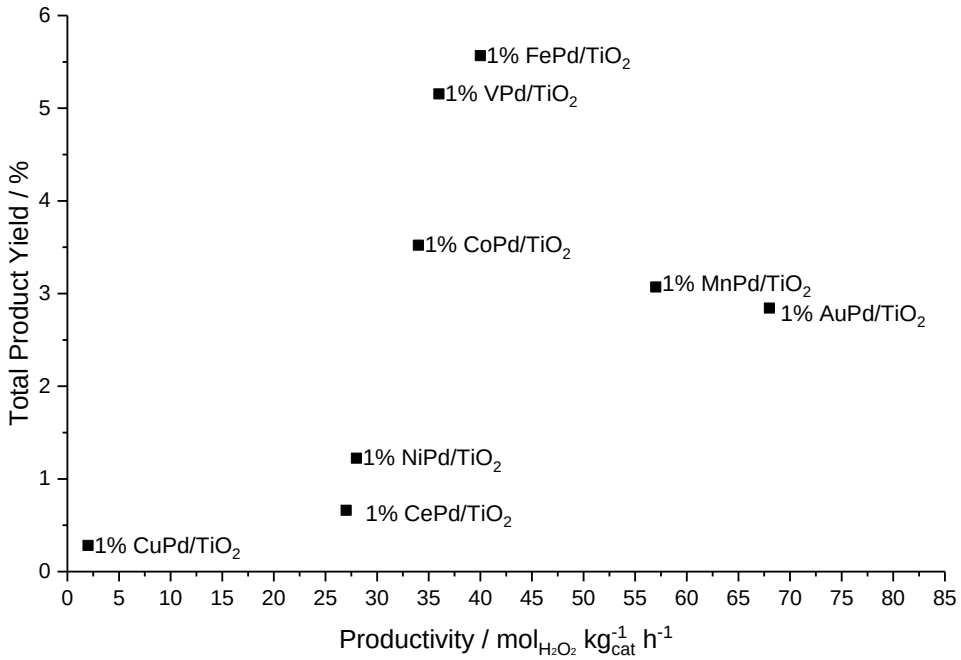


***Figure 6.5.*** *The trend observed between the yield of oxidation products against the productivity observed for 1 % XPd/TiO$_2$ catalysts for H$_2$O$_2$ production under ambient temperatures.*

No correlation could be observed between the degradation of $H_2O_2$ and the product yield for benzyl alcohol oxidation. However, it should be noted that all new XPd catalysts degraded $H_2O_2$ to a much lesser extent than 1% AuPd/TiO$_2$ and hence this decrease in the $H_2O_2$ degradation could explain the increased selectivity, based on $H_2$, observed for especially 1% FePd/TiO$_2$ and 1% VPd/TiO$_2$ as previously mentioned.

All post reaction solutions from the oxidation of benzyl alcohol oxidation were submitted for ICP-MS analysis to determine any leaching of metals from the catalysts during the benzyl alcohol oxidation reaction, Table 6.2. These show limited Pd leaching from all catalysts. Leaching of the second X metal was observed for all catalysts except 1 % AuPd/TiO$_2$ and 1 % CePd/TiO$_2$. The most significant leaching was observed for 1 % CoPd/TiO$_2$, 1 % NiPd/TiO$_2$ and 1 % FePd/TiO$_2$.

***Table 6.2.*** *ICP-MS analysis of post reaction solutions using 1 % XPd/TiO$_2$ catalysts for the oxidation of benzyl alcohol.*

| Catalyst | % Pd leached (ppb) | % X leached (ppb) |
|---|---|---|
| 1 % VPd/TiO2 | 0.30 (14) | 7.5 (357) |
| 1 % MnPd/TiO$_2$ | 0.58 (28) | 39.6 (1887) |
| 1 % FePd/TiO$_2$ | 0.15 (7) | 12.5 (593) |
| 1 % CoPd/TiO$_2$ | 0.86 (41) | 60.1 (2862) |
| 1 % NiPd/TiO$_2$ | 0.22 (10) | 29.4 (1398) |
| 1 % CuPd/TiO$_2$ | 0.14 (7) | 2.1 (101) |
| 1 % AuPd/TiO$_2$ | 0.23 (11) | BDL* |
| 1 % CePd/TiO$_2$ | 0.20 (9) | BDL* |

* Below detection limit.

The leaching of Fe species from the 1 % $FePd/TiO_2$ bimetallic catalyst could be contributing to the high catalytic activity observed. It was previously reported for phenol oxidation via the *in-situ* production of $H_2O_2$ that a correlation between the extent of Fe leaching and catalytic activity could be observed.[18] In this study Underhill *et al.* showed that by changing the weight loading of Fe on the FePd catalyst, from 0.5% to 2.5%, an increase in leaching of Fe was observed. From this the increase in phenol conversion was attributed to an increasing concentration of Fe in solution.[18] Further investigations into the efficacy of solution Fe species is discussed in Section 6.4.3.1.

### 6.3.1 Catalyst re-use

The re-use of the best catalysts; 1% $AuPd/TiO_2$, 1% $VPd/TiO_2$, 1% $MnPd/TiO_2$, 1% $FePd/TiO_2$ and 1% $CoPd/TiO_2$, has been evaluated, Figure 6.6. For these experiments 0.05g of catalyst was used in the reaction and the catalyst were separated from the reaction solution by filtration. The catalysts were then washed with methanol prior to drying in air at room temperature. The catalysts were dried at room temperature to reduce the coalescence of metal nanoparticles, at higher temperatures.

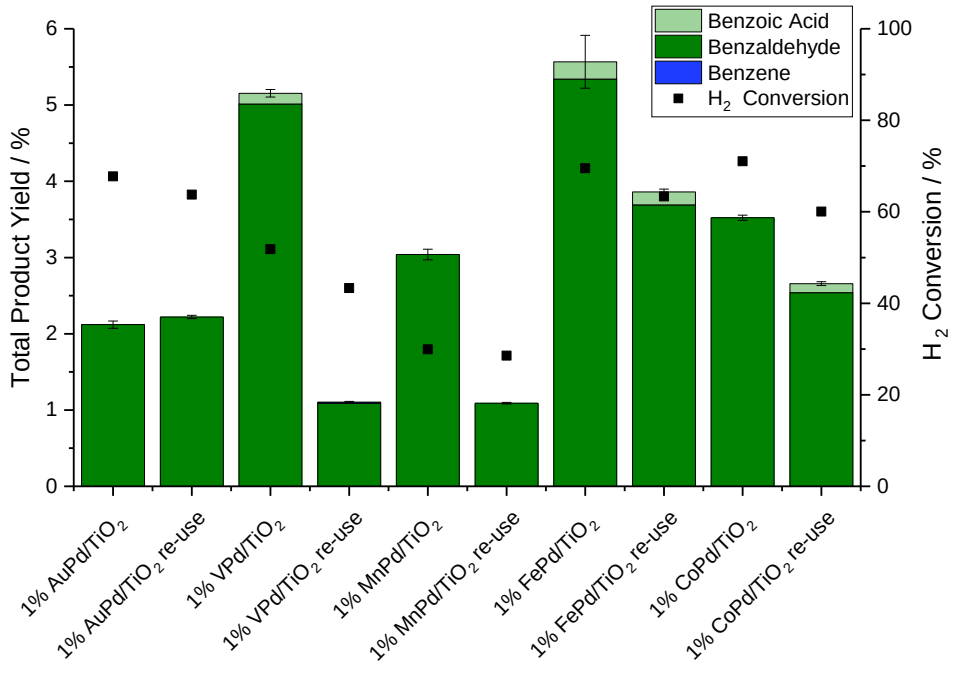


***Figure 6.6*** *The re-use activity of 1 % $XPd/TiO_2$ catalysts towards benzyl alcohol oxidation.* ***Reaction conditions;*** *0.01 g catalyst, 1.04 g (9.6 mmol) benzyl alcohol, 7.1 g methanol, 29 bar 5 % $H_2/CO_2$ and 11 bar 25 % $O_2/CO_2$, 1200 RPM, 30 minutes, 50 °C.*

It can be observed that all bimetallic catalysts, with the exception of 1% $AuPd/TiO_2$, show a decrease in activity upon second use. This can be attributed to the leaching of

catalysts shown by ICP-MS. However, a direct correlation between the amount of metal leached and reduction on activity cannot be made. With re-use of the catalysts a decrease in $H_2$ conversion is also observed indicating that the loss of activity is also related to a loss in $H_2O_2$ activity. It is possible that upon reuse an agglomeration of the metals has occurred, as observed previously for 1% AuPd/$TiO_2$ in Chapter 3 Section 3.3.9. An increase in particle sizes could decrease the number of available surface active sites and hence a decrease in activity would be observed.

It should also be noted that despite a loss of activity upon re-use 1% FePd/$TiO_2$ and 1% CoPd/$TiO_2$ have still shown a greater activity than 1% AuPd/$TiO_2$ upon re-use.

### 6.3.2 Catalyst characterisation.

These 1% XPd/$TiO_2$ catalysts have been characterised by XPS, Table 6.3, both fresh, as previously discussed in Chapter 5 - Section 5.3.1.1, and used. Again, all Pd is present most prominently in its metallic state while the second metal is present in a non-metallic oxidation state.

***Table 6.3.*** *XPS analysis 1 % XPd/$TiO_2$ catalysts both fresh and after use for benzyl alcohol oxidation.*

| Catalyst | $Pd^0$:$Pd^{2+}$ | Pd:X | X oxidation state |
|---|---|---|---|
| 1 % VPd/ $TiO_2$ | 3.3 | 0.19 | +4/+5 |
| 1 % VPd/ $TiO_2$ used | 3 | 0.35 | |
| 1 % MnPd/ $TiO_2$ | 2 | 0.34 | +2 |
| 1 % MnPd/ $TiO_2$ used | 3.8 | 1.5 | |
| 1 % FePd/ $TiO_2$ | 3.2 | 0.27 | +2 |
| 1 % FePd/ $TiO_2$ used | 2.38 | 0.51 | |
| 1 % CoPd/ $TiO_2$ | 17 | 0.21 | +2 |
| 1 % CoPd/ $TiO_2$ used | 1.67 | 1.09 | |
| 1 % NiPd/ $TiO_2$ | 4 | 0.83 | +2 |
| 1 % NiPd/ $TiO_2$ used | 3 | 0.24 | |
| 1 % CuPd/ $TiO_2$ | 16 | 0.28 | 0/+1 |
| 1 % CuPd/ $TiO_2$ used | 2.6 | 0.27 | |
| 1 % AuPd/ $TiO_2$ | All $Pd^0$ | 2.27 | 0 |
| 1 % AuPd/ $TiO_2$ used | 5.5 | 2.17 | |
| 1 % CePd/ $TiO_2$ | All $Pd^0$ | 0.11 | +3 |
| 1 % CePd/ $TiO_2$ used | 2.33 | 0.23 | |

In the fresh catalysts, it can be observed that the most active 1% VPd/$TiO_2$ and 1% FePd/$TiO_2$ have the lowest $Pd^0$:$Pd^{2+}$ ratios. Meher and Rana have reported the importance of Pd-PdO interface for the aerobic oxidation of benzyl alcohol. They showed the mixed Pd-PdO nanoparticles gave higher activity and selectivity towards benzaldehyde compared to the individual Pd species.[20] When both Pd and PdO are

present the activation of $O_2$ is promoted, which is an important initial step both for the aerobic oxidation reaction but also for the production of reactive oxygen species when both $H_2$ and $O_2$ are present.[20] For 1% FePd/$TiO_2$ and 1% VPd/$TiO_2$ there is a lower $Pd^0$:$Pd^{2+}$ and hence there is a greater mixture of these mixed phases of Pd, compared to the other catalysts, which could lead to greater activity.

After use $Pd^0$ content on the catalyst surface decreases for all catalysts except 1% VPd/$TiO_2$ and 1% MnPd/$TiO_2$. This indicates that the $Pd^0$ present on the catalyst surface have been oxidised under the reaction conditions. Pd:X has remained constant for 1% AuPd/$TiO_2$ and 1% VPd/$TiO_2$ but an increase is observed for 1% MnPd/$TiO_2$, 1% FePd/$TiO_2$ and 1% CoPd/$TiO_2$ which is in correlation with leaching of X from the catalysts during the reaction. 1% AuPd/$TiO_2$ has maintained the highest $Pd^0$ content and hence this could explain why no loss in activity is seen for this catalyst.

## 6.4 Further investigations into reaction parameters.

### 6.4.1 1 % Pd/$TiO_2$.

Monometallic 1% Pd/$TiO_2$ has been further investigated for comparison to the bimetallic catalysts, 1% AuPd/$TiO_2$ and 1% FePd/$TiO_2$.

This monometallic catalyst showed 100% selectivity towards benzaldehyde with a yield of 1.8 %, Figure 6.1, under standard reactions conditions (50 ºC, 30 minutes). At 30 minutes a $H_2$ conversion of 72 % was observed leading to a selectivity towards oxidation products, based on $H_2$, at 9 %.

High-angle annular dark-field scanning transmission electron microscopy (HAADF-STEM) imaging, conducted by Xi Lui at Shanghai Jiao Tong University, has revealed small nanoparticles with the existence of some smaller sub-nanometre clusters, Figure 6.7. An average particle size of 4.1 ± 1.7 nm has been determined from bright field transmission electron micrographs such as those presented in Figure 6.7.

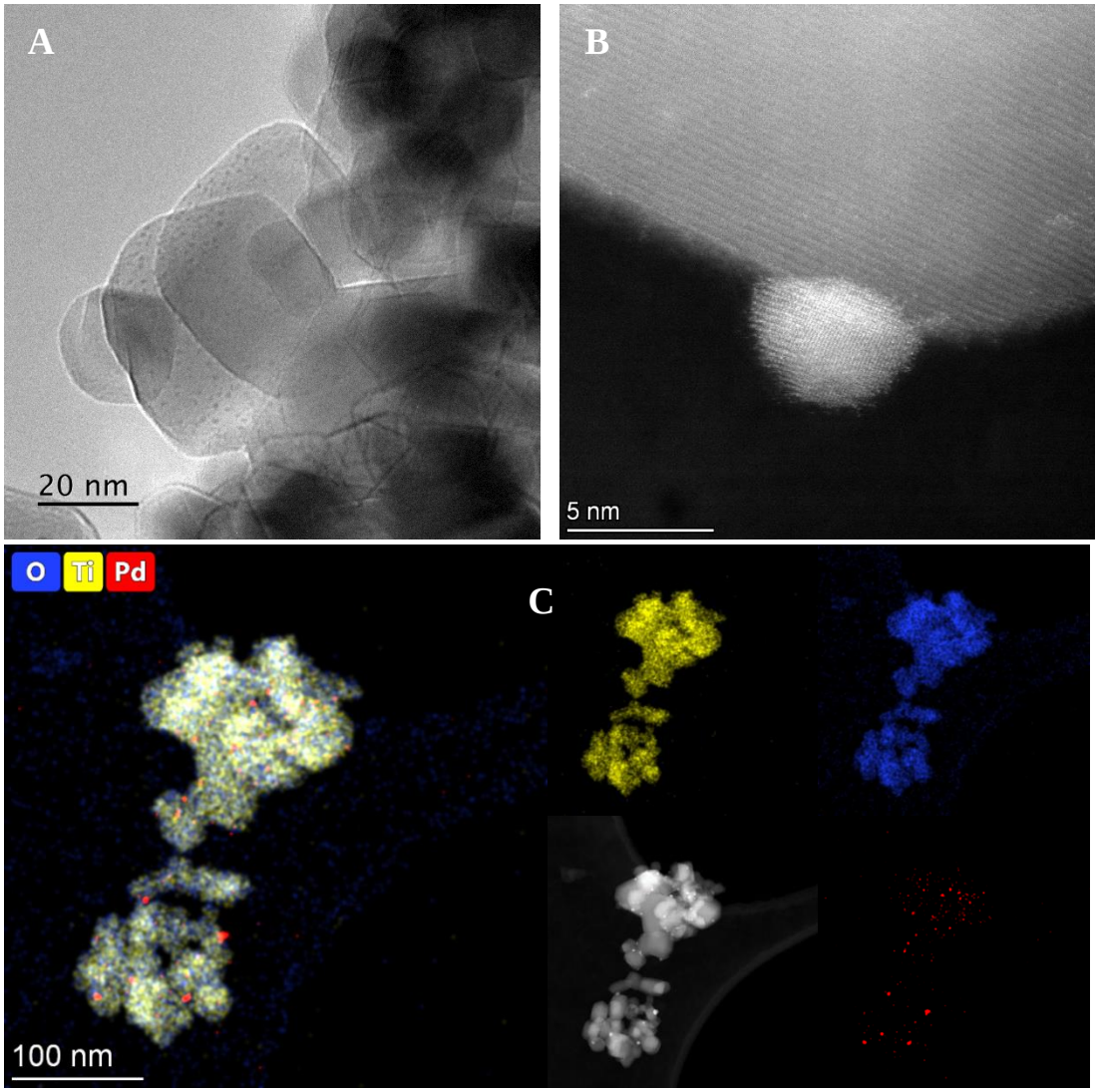


***Figure 6.7*** *TEM images (A) and HAADF- STEM (B) with EDS mapping (C) of 1% Pd/ $TiO_2$.*

It has been reported for both $H_2O_2$ synthesis and benzyl alcohol oxidation that the size of Pd nanoparticles can have a significant effect on catalytic activity.[21–23] It has been reported that small Pd particles are active for the synthesis of $H_2O_2$ but are also very active for the subsequent degradation of $H_2O_2$.[21] It has also been shown that increasing particle size can decrease the exposure of sites for the formation of water and hence an increase in $H_2O_2$ productivity is observed.[22] For aerobic benzyl alcohol oxidation Zhang *et al.* have reported that an average particle size of 4 nm is optimum.[23] From TEM analysis many sub-nanometer Pd particles can be observed which could be more active for the formation of water and hence decrease the selectivity towards $H_2O_2$ and hence decrease the selectivity towards oxidation products, based on $H_2$. It can also be seen that the average particle size is below that which has been deemed optimum for aerobic oxidation of benzyl alcohol and this could partially explain the reduced activity, especially under $O_2$ only conditions where no activity was observed.

### 6.4.1.1 Extended reaction times.

Time on line studies have been investigated to determine whether over oxidation and/or disproportionation products can be produced, but are limited by the relatively low benzyl alcohol conversion rates observed under these mild conditions. Reaction times of 5 to 120 minutes have been explored for 1% $Pd/TiO_2$, Figure 6.8.

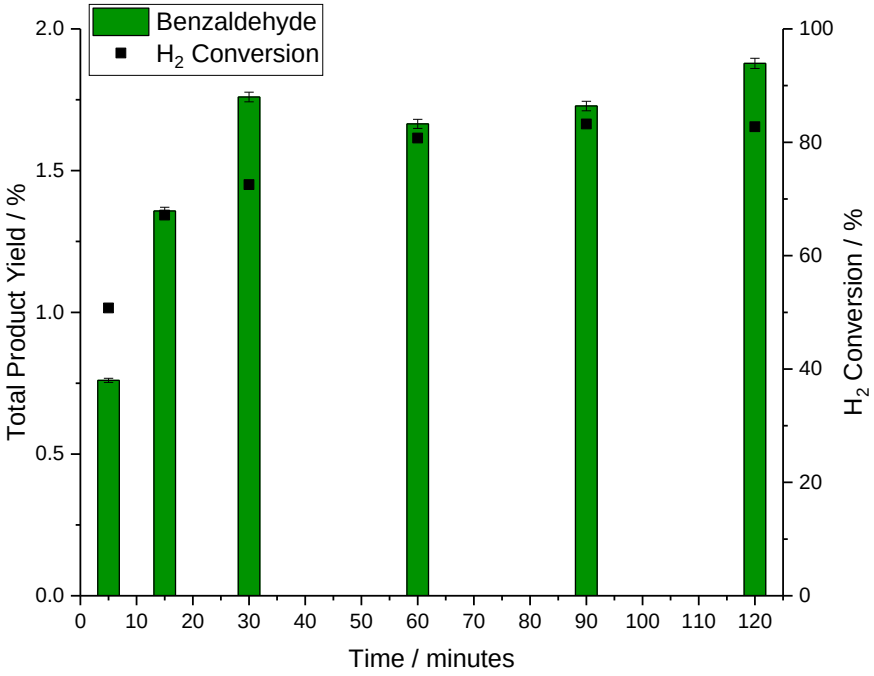


***Figure 6.8*** *The activity of 1 % $Pd/TiO_2$ catalysts towards benzyl alcohol oxidation at different reaction times.* ***Reaction conditions;*** *0.01 g catalyst, 1.04 g (9.6 mmol) benzyl alcohol, 7.1 g methanol, 29 bar 5 % $H_2/CO_2$ and 11 bar 25 % $O_2/CO_2$, 1200 RPM, 5 - 120 minutes, 50 °C.*

Benzaldehyde has been observed as the only oxidation product under all reaction times. An increase in product yield is seen with increasing reaction time with $H_2$ conversion increasing up to 60 minutes to 81 % at which a plateau is reached, Table 6.4. This trend is coupled with a decrease in residual $H_2O_2$ with increasing reaction time indicating that $H_2O_2$ is produced at high concentrations initially which is consumed throughout the oxidation reaction. The greatest drop in residual $H_2O_2$ can be observed between 30 and 60 minutes it is also here that the $H_2$ conversion plateaus and hence we could surmise at this point that no more $H_2O_2$ can be produced and hence is utilised quickly limiting further oxidation. Upon this point when all $H_2$ has been utilised to produced $H_2O_2$ and all $H_2O_2$ has reacted there is also a slowing in the increase of product yield and a maximum product yield of 1.9 % observed. It should also be noted that some $H_2$ will be consumed via the hydrogenation of $H_2O_2$ which will decrease $H_2O_2$ concentration and hence decrease the oxidation products.

***Table 6.4.*** *$H_2$ and $O_2$ conversion, selectivity based on $H_2$ conversion and residual $H_2O_2$ concentration observed at all reaction times for 1 % $Pd/TiO_2$.*

| Time / minutes | Benzyl Alcohol Conversion / % | $H_2$ Conversion / % | Selectivity based on $H_2$ / % | $O_2$ Conversion / % | Residual $H_2O_2$ / µmol |
|---|---|---|---|---|---|
| 5 | 0.8 | 51 | 7 | 34 | 130 |
| 15 | 1.4 | 67 | 8 | 37 | 122 |
| 30 | 1.8 | 73 | 9 | 40 | 110 |
| 60 | 1.7 | 81 | 8 | 54 | 55 |
| 90 | 1.7 | 83 | 9 | 40 | 47 |
| 120 | 1.9 | 83 | 9 | 63 | 49 |

***Reaction conditions;*** *0.01 g catalyst, 1.04 g (9.6 mmol) benzyl alcohol, 7.1 g methanol, 29 bar 5 % $H_2/CO_2$ and 11 bar 25 % $O_2/CO_2$, 1200 RPM, 5 to 120 minutes, 50 °C.*

XPS analysis of the catalyst fresh and after different reaction times has shown only metallic Pd present on the surface, Appendix Table 6S.2. The metallic Pd is maintained on the catalyst after all reaction times.

As mentioned in Section 6.3.2 the interfaces between Pd and PdO can determine benzyl alcohol oxidation. The interface between Pd-PdO have also been investigated for $H_2O_2$ synthesis where Ouyang *et al.* suggested that the interface of Pd-PdO is where $H_2O_2$ formation occurs.[24] Hence by tuning this interface an increase in activity for $H_2O_2$ production can be observed. Ouyang *et al.* also observed that by varying the metal loading of $Pd/TiO_2$ catalysts from 1% to 5% that lower loaded 1% $Pd/TiO_2$ produced the greatest Pd-PdO interfaces, with increasing metal loading increasing the $Pd^0$ content.[24] Hence the plateauing in benzyl alcohol activity could be attributed to a decrease in these Pd-PdO interfaces and a decrease in $H_2O_2$ activity which decreases the *in-situ* oxidation activity. Increased $Pd^0$ nature can also lead to an increase in unwanted $H_2O$ formation over $H_2O_2$ synthesis catalysts [25] and hence at extended reaction times a decrease in selectivity based on $H_2$ could be attributed to the decreased selectivity in $H_2O_2$ formation.

#### 6.4.1.2 Sequential Reactions.

Sequential reactions have been conducted to see whether coupling extended reaction times with increasing amounts of $H_2$ will increase catalytic activity and again whether other reaction pathways can be probed. For these sequential reactions the gas has been replaced in the reactor every 30 minutes, without removing the solution or catalyst, and another reaction commenced.

Freakley *et al.* have shown sequential reactions for $H_2O_2$ using 3% Pd 2% $Sn/TiO_2$ and observed a linear increase in the concentration of $H_2O_2$. From 1 to 5 sequential

reactions an increase in $H_2O_2$ concentration from 0.11 wt% up to 0.53 wt% was observed. [21] This showed that the reintroduction of $H_2$ into the system can increase the concentration of $H_2O_2$ with a stable catalyst and hence this has also been tested for benzyl alcohol oxidation with 1% $Pd/TiO_2$ to observed whether an increase in $H_2O_2$ concentration can increase product yield, Figure 6.9.

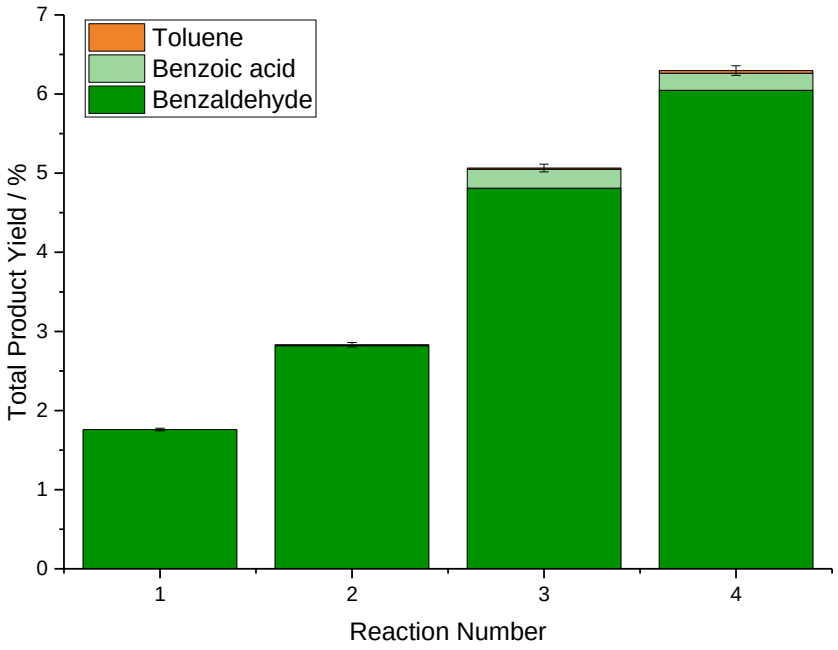


***Figure 6.9*** *The effect of sequential reactions on product yield for benzyl alcohol oxidation using 1 % $Pd/TiO_2$ catalyst.* ***Reaction conditions;*** *0.01 g catalyst, 1.04 g (9.6 mmol) benzyl alcohol, 7.1 g methanol, 29 bar 5 % $H_2$ / $CO_2$ and 11 bar 25 % $O_2$ / $CO_2$, 1200 RPM, 50 °C.*

A much clearer increase in yield with increasing reaction number can be observed compared to equivalent reaction times, with a maximum of 6.3 % at the fourth reaction number (Figure 6.9) compared to 1.9 % for the equivalent 120 minute reaction time (Figure 6.8). The further oxidation to benzoic acid has been observed for both the 3rd and 4th reaction number. Increasing yields of toluene has also been observed for 2nd, 3rd and 4th at 0.012 %, 0.016 % and 0.033 % respectively.

With each sequential reaction the $H_2$ and $O_2$ conversion have been maintained, Table 6.5, indicating stability of the catalyst and system. This also indicates that $H_2$ is limiting the reaction and with increased available $H_2$ increased product yield can be achieved. This is supported with a stable production of residual $H_2O_2$.

***Table 6.5*** *$H_2$ and $O_2$ conversion, selectivity based on $H_2$ conversion and residual $H_2O_2$ concentration observed at all stages of reaction for 1 % $Pd/TiO_2$ used for the oxidation of benzyl alcohol.*

| Reaction Number | Benzyl Alcohol Conversion / % | $H_2$ Conversion / % | Selectivity based on $H_2$ / % | $O_2$ Conversion / % | Residual $H_2O_2$ / µmol |
|---|---|---|---|---|---|
| 1 | 1.8 | 71 | 10 | 40 | 110 |
| 2 | 2.8 | 76 | 7 | 45 | 94 |
| | | 76 | | 46 | |
| 3 | 5.1 | 72 | 9 | 44 | 101 |
| | | 69 | | 45 | |
| | | 72 | | 42 | |
| 4 | 6.3 | 69 | 9 | 46 | 124 |
| | | 69 | | 46 | |
| | | 66 | | 43 | |
| | | 68 | | 52 | |

***Reaction conditions;*** *0.01 g catalyst, 1.04 g (9.6 mmol) benzyl alcohol, 7.1 g methanol, 29 bar 5 % $H_2/CO_2$ and 11 bar 25 % $O_2/CO_2$, 1200 RPM, 50 °C.*

### 6.4.2 1 % $AuPd/TiO_2$.

Bimetallic 1% $AuPd/TiO_2$ showed an increase activity on the monometallic 1% $Pd/TiO_2$ with a total product yield of 2.8 % with 100 % selectivity to benzaldehyde, under standard reaction conditions. Similar $H_2$ conversions were observed for both 1% $Pd/TiO_2$ and 1% $AuPd/TiO_2$ (72 %) but a greater selectivity towards oxidation products, based on $H_2$, was observed for 1% $AuPd/TiO_2$ at 16 % compare to 9 % for 1% $Pd/TiO_2$. This can be attributed to the increased selectivity for the 1% $AuPd/TiO_2$ catalyst towards $H_2O_2$ synthesis where the degradation of $H_2O_2$ has been reduced upon the addition of Au into Pd.[26]

HAADF-STEM imaging, conducted by Xi Lui at Shanghai Jiao Tong University, has revealed a large particle distribution with a range of small (<5nm) particle along with much larger particles (>10 nm), Figure 6.10. An average particle size of 7.9 ± 5.6 nm has been determined. HADDF-STEM imaging coupled with Energy Dispersive X-Ray Spectroscopy (X-EDS) has shown the nanoparticles to be well mixed random alloys, Figure 6.10C.

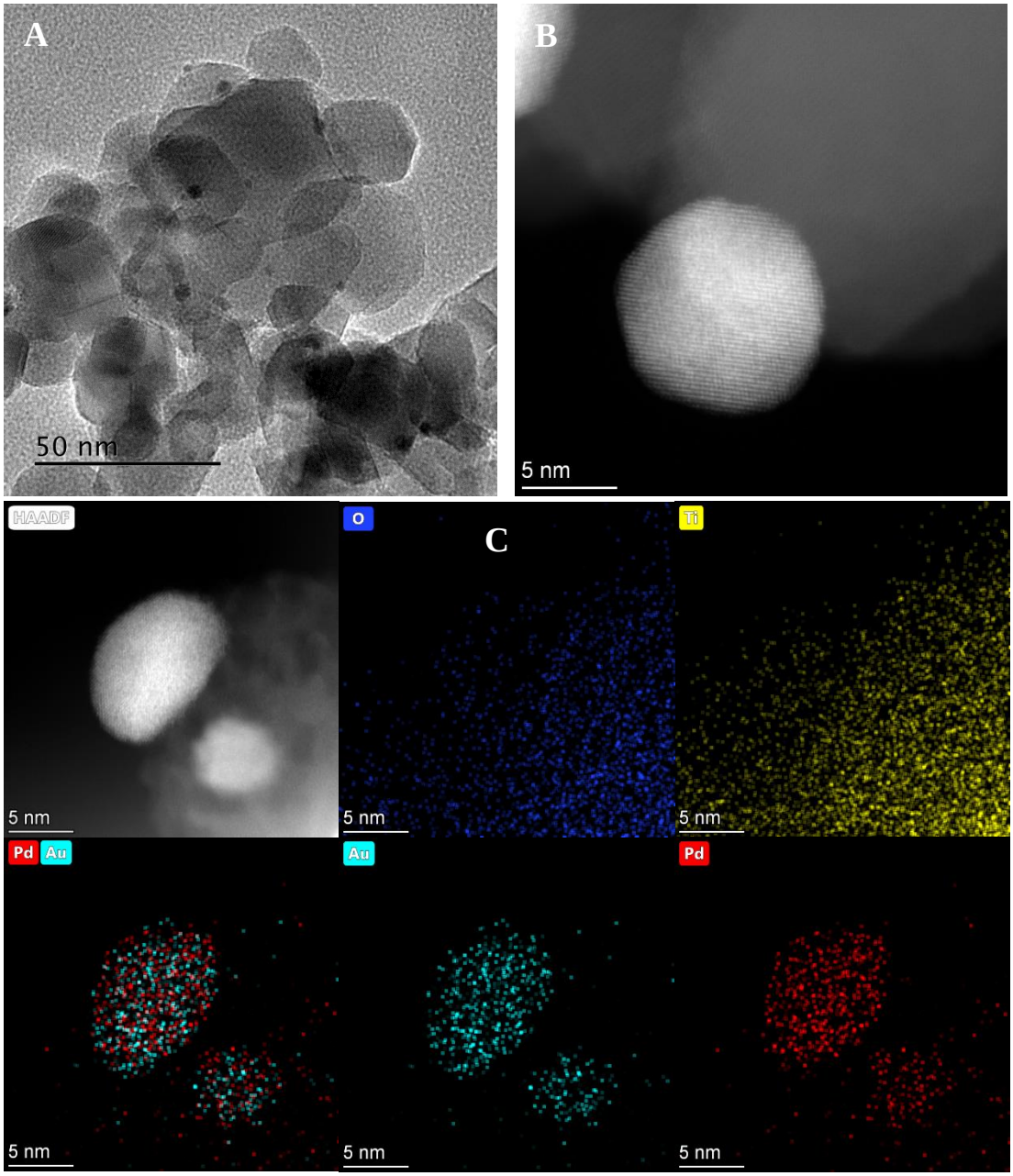


***Figure 6.10*** *TEM images (A) and HAADF- STEM (B) with EDS mapping (C) of 1% AuPd/ $TiO_2$.*

These results support previous findings in the literature by Sankar *et al.* who observed that 1% AuPd/$TiO_2$ catalysts prepared by modified impregnation exhibit bimetallic particles that are random alloy in nature.[27] It has also previously been observed that upon alloying Au and Pd the average particle size can increase compared to Pd alone, when prepared by both wet and modified impregnation.[26,28] This has also been observed here as an increase from 4.1 nm to 7.9 nm was seen for 1% Pd/$TiO_2$ and 1% AuPd/$TiO_2$ respectively.

Fresh 1% Pd/$TiO_2$ has been analysed by TPR and showed a negative peak at 75 ºC, Figure 6.11. This release of $H_2$ is attributed to the decomposition of Pd-H species.[29]

These hydride species are formed from the reduction of PdO in the presence of $H_2$ at ambient temperature and hence occur before spectra are conducted.[30] Addition of Au to Pd has removed this Pd-H peaks and this has been attributed to the stabilisation of these Pd species by the addition of Au. This indicates that upon the alloying of Au and Pd, Au has had an effect on the electronic state of Pd by stabilisation of possible Pd states. This electronic enhancement of Au on Pd upon alloying has previously been suggested in the literature.[31–35]

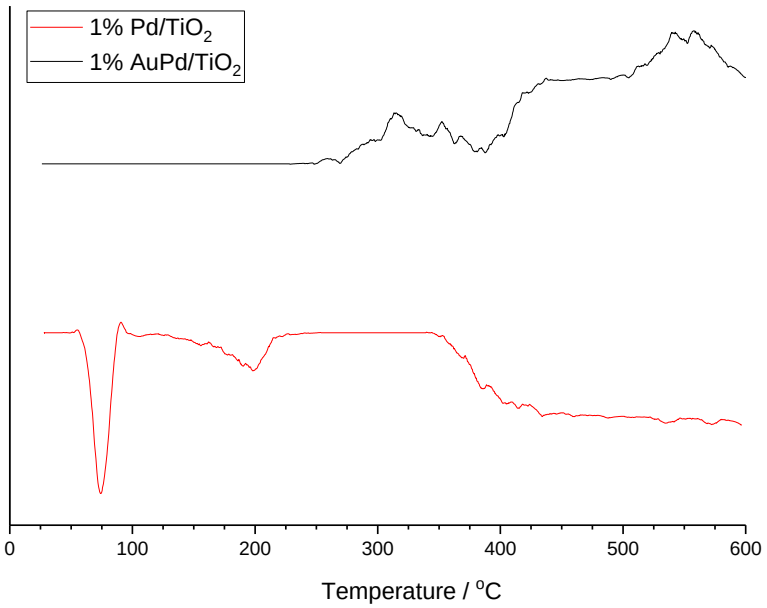


***Figure 6.11.*** *TPR analysis of fresh 1% AuPd/$TiO_2$ and 1% Pd/$TiO_2$.*

As previously discussed, due to an increase in particle size[26] along with electronic enhancement effects,[36] the alloying of Au and Pd has increases the selectivity towards $H_2O_2$ [26,32,33,37,38] which has increased the selectivity towards oxidation products.

### 6.4.2.1 Extended reaction times.

Reaction times of 5 to 120 minutes have also been explored for 1 % AuPd/$TiO_2$, Figure 6.12. Similarly, to 1% Pd/$TiO_2$, only benzaldehyde has been observed at all reaction times. At all reaction times greater activity has been shown for 1 % AuPd/$TiO_2$ compared to 1 % Pd/$TiO_2$ indicating again the greater activity and synergy observed for 1% AuPd/$TiO_2$.

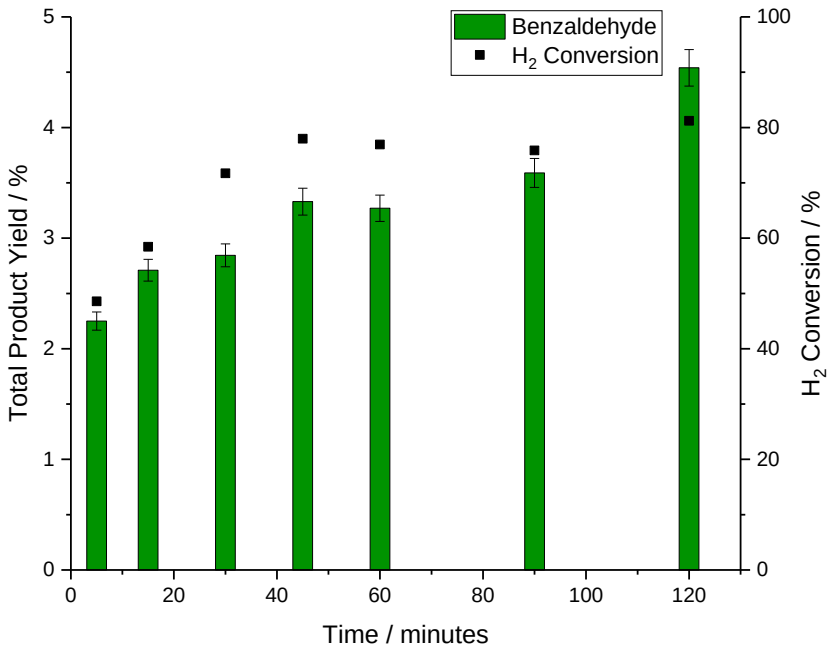


***Figure 6.12.*** *The activity of 1 % AuPd/$TiO_2$ catalysts towards benzyl alcohol oxidation at different reaction times.* ***Reaction conditions;*** *0.01 g catalyst, 1.04 g (9.6 mmol) benzyl alcohol, 7.1 g methanol, 29 bar 5 % $H_2/CO_2$ and 11 bar 25 % $O_2/CO_2$, 1200 RPM, 5 to 120 minutes, 50 °C.*

A general increase in yield with increased reaction time is observed, Figure 6.12. Despite only a small increase in $H_2$ conversion above 30 minutes, Table 6.6, the increase in product yield could be correlated with a decrease in the residual $H_2O_2$ showing that the $H_2O_2$ initially produced is then utilised at these extended reaction times, as was observed for 1% Pd/$TiO_2$.

***Table 6.6*** *$H_2$ and $O_2$ conversion, selectivity based on $H_2$ conversion and residual $H_2O_2$ concentration observed at all reaction times for 1 % AuPd/$TiO_2$.*

| Time / minutes | Benzyl Alcohol Conversion / % | $H_2$ Conversion / % | Selectivity based on $H_2$ / % | $O_2$ Conversion / % | Residual $H_2O_2$ / µmol |
|---|---|---|---|---|---|
| 5 | 2.3 | 49 | 18 | 21 | 188 |
| 15 | 2.7 | 58 | 18 | 14 | 126 |
| 30 | 2.8 | 72 | 11 | 38 | 94 |
| 45 | 3.3 | 78 | 16 | 39 | 61 |
| 60 | 3.3 | 77 | 17 | 34 | 46 |
| 90 | 3.6 | 76 | 19 | 38 | 39 |
| 120 | 4.5 | 81 | 21 | 45 | 32 |

***Reaction conditions;*** *0.01 g catalyst, 1.04 g (9.6 mmol) benzyl alcohol, 7.1 g methanol, 29 bar 5 % $H_2/CO_2$ and 11 bar 25 % $O_2/CO_2$, 1200 RPM, 5 to 120 minutes, 50 °C.*

While investigating 5 % AuPd/$TiO_2$ Santonastaso *et al.* also observed a plateau in the product yield above 30 minutes, however they did not comment on the $H_2$ conversions under these conditions.[1] It can also been noted here that with 5 % AuPd/$TiO_2$ a conversion of 6.9 % was observed with 89 % selectivity towards benzaldehyde after

30 minute reaction.[1] In this work a conversion of 2.8 % has been observed at 100 % selectivity towards benzaldehyde after 30 minutes. Despite the decrease in activity observed by this 1% $AuPd/TiO_2$ the selectivity to aldehyde has been increased at a much lower content of precious metal. This lower selectivity could be attributed to the low conversion but with increasing reaction time an increase in conversion to 4.6 % was observed still at 100% selectivity to benzaldehyde.

XPS has shown that upon use, even after 15 minutes, there is a drop in the $Pd^0$:$Pd^{2+}$ and d:Au ratios, Table 6.7. This can indicate the formation of PdO layers forming on the catalyst surface during the reaction. No significant further change is observed with increasing reaction times. The maintaining of Pd-PdO interfaces in the used catalysts can explain the maintained catalytic activity upon re-use discussed in Section 6.2.1.1. Hence a plateau in activity upon 30 minutes could be attributed to a limit in the available $H_2$ limiting $H_2O_2$ formation.

***Table 6.7.*** *XPS analysis of post reaction solutions using 1 % $AuPd/TiO_2$ catalysts at different reaction times for the oxidation of benzyl alcohol.*

| **Time** | **$Pd^0$: $Pd^{2+}$** | **Pd:Au** |
|---|---|---|
| 0 (fresh) | All $Pd^0$ | 2.3 |
| 5 | 18.5 | 2.8 |
| 15 | 5 | 1.4 |
| 30 | 3.8 | 1.4 |
| 45 | 4.3 | 1.4 |
| 60 | 4.6 | 1.1 |
| 90 | 5.1 | 1.1 |
| 120 | 6.8 | 1.3 |

ICP analysis has been conducted at all reaction times, Appendix Table S6.4. This has shown very minimal leaching for both Au and Pd and hence no significant homogeneous nature can be attributed to catalyst activity.

### 6.4.2.2 Sequential reactions.

Sequential reactions have been conducted to see whether coupling extended reaction times with increasing amounts of $H_2$ will increase catalytic activity and again whether other reaction pathways can be probed. A much clearer increase in yield with increasing reaction number compared to reaction times can be seen, Figure 6.13.

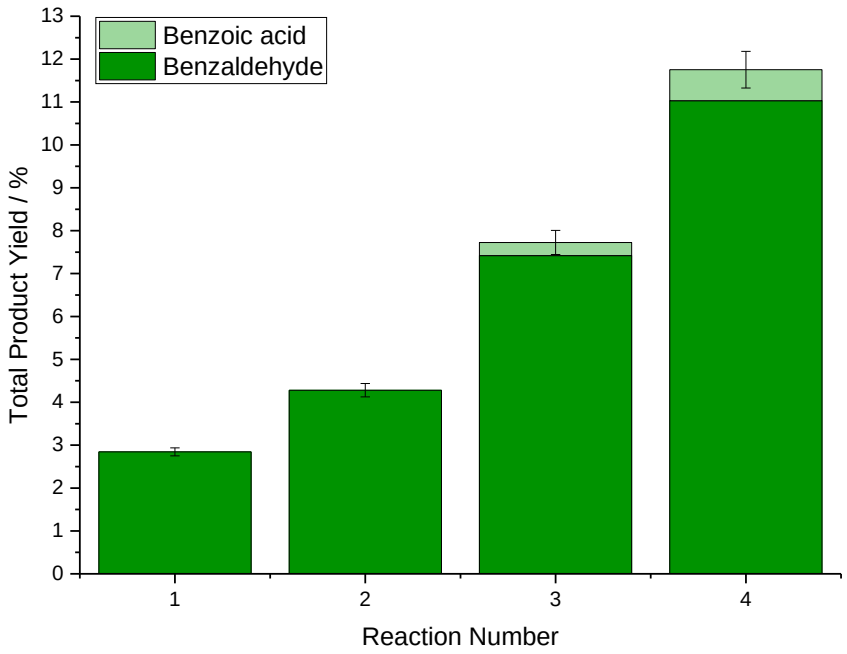


***Figure 6.13.*** *The effect of sequential reactions on product yield from 1 % AuPd/$TiO_2$ catalyst. 0.01 g catalyst, 1.04 g (9.6 mmol) benzyl alcohol, 7.1 g methanol, 29 bar 5 % $H_2$ / $CO_2$ and 11 bar 25 % $O_2$ / $CO_2$, 1200 RPM, 50 °C.*

The further oxidation of benzaldehyde to benzoic acid has been observed, showing this reaction pathway is possible over this catalyst which has not previously been observed under standard reaction conditions over 1% AuPd/$TiO_2$. It can now be postulated that one reason benzoic acid was not previously observed for 1 % AuPd/$TiO_2$ was due to a limit in conversion (< 6 %) and that with sequential reactions have increased the conversion further which has produced higher concentration of benzaldehyde which have been further oxidised.

$H_2$ and $O_2$ conversion are consistent with each top up, Table 6.8, which has helped improve the product yield, compared to time on line where above 30 minutes no increase in either gas conversion could be observed. Consistent $H_2$ and $O_2$ conversions can also indicate catalyst stability. It can also be observed that the residual $H_2O_2$ is greater in the top up reactions compared to the same reaction time without top ups; 95 μmol for 4 sequential reactions compared to 32 μmol for 120 minutes for time on line for example.

***Table 6.8.*** *$H_2$ and $O_2$ conversion, selectivity based on $H_2$ conversion and residual $H_2O_2$ concentration observed at all stages of reaction for 1 % AuPd/$TiO_2$ used for the oxidation of benzyl alcohol.*

| Reaction Number | Benzyl Alcohol Conversion / % | $H_2$ Conversion / % | Selectivity based on $H_2$ / % | $O_2$ Conversion / % | Residual $H_2O_2$ / µmol |
|---|---|---|---|---|---|
| 1 | 2.8 | 72 | 11 | 38 | 94 |
| 2 | 4.3 | 72 | 11 | 45 | 58 |
| | | 72 | | 27 | |
| 3 | 7.7 | 71 | 14 | 37 | 62 |
| | | 69 | | 39 | |
| | | 72 | | 33 | |
| 4 | 11.8 | 69 | 21 | 31 | 95 |
| | | 78 | | 59 | |
| | | 66 | | 33 | |
| | | 66 | | 33 | |

***Reaction conditions;*** *0.01 g catalyst, 1.04 g (9.6 mmol) benzyl alcohol, 7.1 g methanol, 29 bar 5 % $H_2/CO_2$ and 11 bar 25 % $O_2/CO_2$, 1200 RPM, 50 °C.*

### 6.4.2.3 Benzaldehyde as a starting material.

Reactions starting with benzaldehyde were conducted to see if further oxidation to benzoic acid/ benzyl benzoate is possible with 1 % AuPd/$TiO_2$ catalyst under standard reaction conditions, Table 6.9. For the oxidation of benzaldehyde using 1 % AuPd/$TiO_2$ benzoic acid was observed as the only product, compared to when benzyl alcohol is used as the starting material only benzaldehyde is observed.

***Table 6.9.*** *Total yield, $H_2$ and $O_2$ conversion, selectivity based on $H_2$ conversion and residual $H_2O_2$ concentration measured when both benzyl alcohol and benzaldehyde are used as the starting material, using 1 % AuPd/$TiO_2$ catalyst.*

| Starting material | Conversion / % | $H_2$ Conversion / % | Selectivity based on $H_2$ / % | $O_2$ Conversion / % |
|---|---|---|---|---|
| Benzyl alcohol | 2.8 | 72 | 11 | 38 |
| Benzaldehyde | 1.1 | 71 | 6 | 32 |

***Reaction conditions;*** *0.01 g catalyst, 1.04 g (9.6 mmol) benzyl alcohol or 1.04 g benzaldehyde, 7.1 g methanol, 29 bar 5 % $H_2/CO_2$ and 11 bar 25 % $O_2/CO_2$, 1200 RPM, 30 minutes, 50 °C.*

Despite similar $H_2$ and $O_2$ conversion when the starting material is both benzyl alcohol and benzaldehyde the conversions observed was lower for benzaldehyde. However, this does show that under these conditions benzaldehyde can be further oxidised to benzoic acid despite not being observed under the standard conditions for oxidation of benzyl alcohol using this catalyst.

### 6.4.3 1 % FePd/$TiO_2$.

Alloying Fe and Pd has shown a dramatic increase from the monometallic Pd catalysts with an increase in total product yield from 1.8 % to 5.6 % which is coupled with a decrease in benzaldehyde selectivity from 100 % to 96 %, under standard reaction conditions. However, it cannot be determined that 1% FePd/$TiO_2$ is less selective under these reaction conditions, compared to the Pd-only catalyst, as these reactions are not at iso-conversions. Hence if we compare under iso-conversion, at 5.1 % conversion, for 1% Pd/$TiO_2$ a selectivity towards benzaldehyde of 95 % is observed (Section 6.4.1.2) compared to 96% for 1% FePd/$TiO_2$ showing similar selectivity trends for both catalysts but 1% FePd/$TiO_2$ being more active.

This 1% FePd/$TiO_2$ catalyst has shown a similar total product yield to the 5% AuPd/$TiO_2$ reported by Santonastaso *et al.*[1] at a higher selectivity towards benzaldehyde with 10 times lower precious metal content. This shows the obvious financial benefits of this novel catalyst.

TEM conducted in Cardiff University and HAADF-STEM imaging, conducted by Xi Lui at Shanghai Jiao Tong University, has revealed 1% FePd/$TiO_2$ consisting predominately of sub-nanometer particles, Figure 6.14 A and B. Some larger particles of approximately 5 nm in size were also apparent but were very few and sparsely dispersed over the support, Figure 6.14 B. HAADF-STEM imaging and X-EDS mapping, Figure 6.15, has shown these larger particles to consist of intermetallic Fe-Pd alloyed particles. The iron is present on the catalyst in oxide form as supported by previous XPS analysis, Table 6.3. The larger particles are surrounded by smaller islands, Figure 6.14 B, however it is undetermined whether these are Fe or Pd in nature.

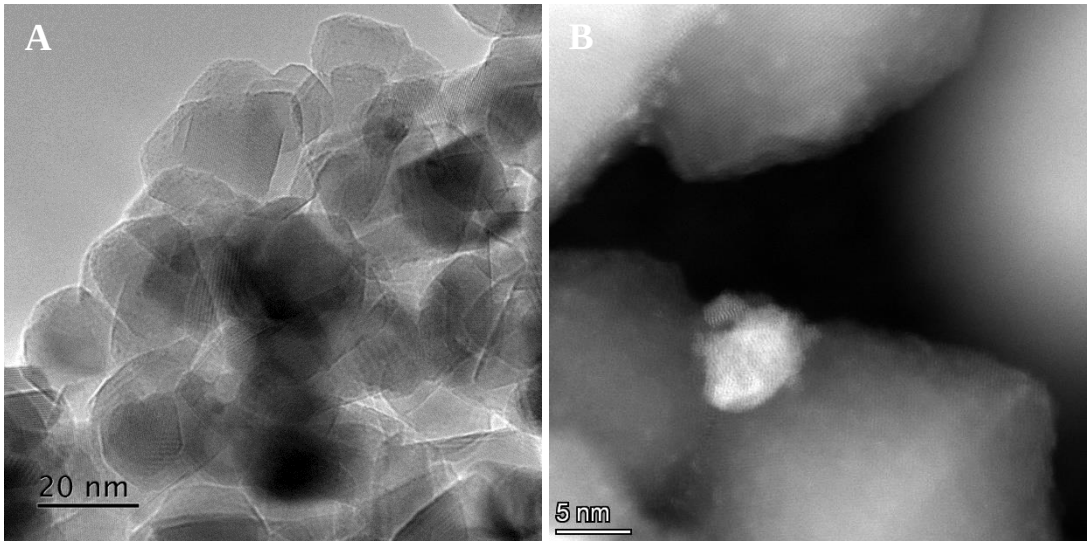


***Figure 6.14.*** *TEM (A) and HAADF-STEM (B) images of 1% FePd/$TiO_2$.*

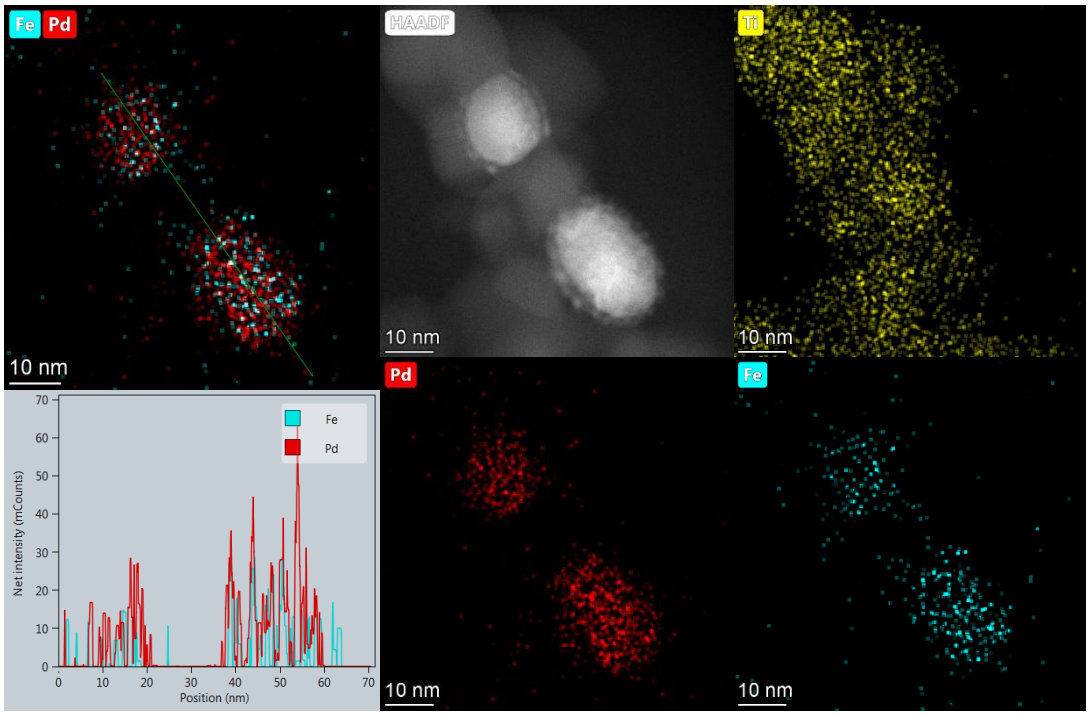


***Figure 6.15*** *HAADF- STEM image with EDS mapping of 1% FePd/ $TiO_2$*

### 6.4.3.1 Efficacy of solution Fe species.

To indicate whether the Fe species which are leached into the reaction solution are contributing to the catalytic activity hot filtration experiments have been conducted where the reaction solution is recovered and separated from the catalyst after 30 minutes and the solution is re-introduced into the reactor, Table 6.10.

***Table 6.10.*** *The re-use of reaction solutions of benzyl alcohol oxidation using 1% $FePd/TiO_2$, comparing both with and without additional 1% $Pd/TiO_2$.*

| Catalyst | Reaction time / minutes | Benzaldehyde yield / % | Benzoic acid yield/ % | $H_2$ Conversion / % | Residual $H_2O_2$ / µmol |
|---|---|---|---|---|---|
| 1% $Pd/TiO_2$ | 30 | 1.8 | 0 | 73 | 110 |
| 1% $FePd/TiO_2$ | 30 | 5.3 | 0.2 | 71 | 29 |
| 1% $FePd/TiO_2$ hot filtration* | 60 | 5.6 | 0.3 | 71, 16 | 0 |
| 1% $FePd/TiO_2$ hot filtration with 1% $Pd/TiO_2$* | 60 | 7.3 | 0.3 | 71, 39 | 132 |

***Reaction conditions;*** *0.01 g catalyst, 1.04 g (9.6 mmol) benzyl alcohol, 7.1 g methanol, 29 bar 5 % $H_2/CO_2$ and 11 bar 25 % $O_2/CO_2$, 1200 RPM, 30 minutes, 50 °C. *total 60 minute reaction time.*

In the absence of the heterogeneous catalyst, limited additional activity was observed. Similar total product yields were observed after this two-part, 60 minute, reaction (5.9 %) compared to a standard 30 minute reaction with 1% $FePd/TiO_2$ catalyst (5.6 %). The small increase in activity has been attributed to the oxidation from residual $H_2O_2$ generated in the initial 30 minute reaction.

Additional experiments have been conducted where after the initial 30 minute reaction with 1% $FePd/TiO_2$ the catalyst was substituted for 1% $Pd/TiO_2$ for the remaining 30 minutes. This was completed to establish whether limited activity was observed for the 1% $FePd/TiO_2$ hot filtration experiments due to homogeneous Fe species being unable to produce $H_2O_2$. The hot filtration experiment with 1% $Pd/TiO_2$ has shown an increase in total product yield (7.6 %). This activity is similar to the summation of 1% $FePd/TiO_2$ (5.6 %) and 1% $Pd/TiO_2$ (1.8 %) activity used independently for a standard 30 minute reaction. Hence from these reactions it is possible to conclude that the activity of leached Fe species can be considered negligible.

To test the efficacy of other homogeneous Fe species $FeCl_3$ solution was introduced into the reactor. For comparison the entire weight of Fe present on 1% $FePd/TiO_2$ (0.05 mg) and the amount of leached Fe in a standard 30 minute reaction (0.01 mg) have been tested as a solution of $FeCl_3$, Figure 6.16.

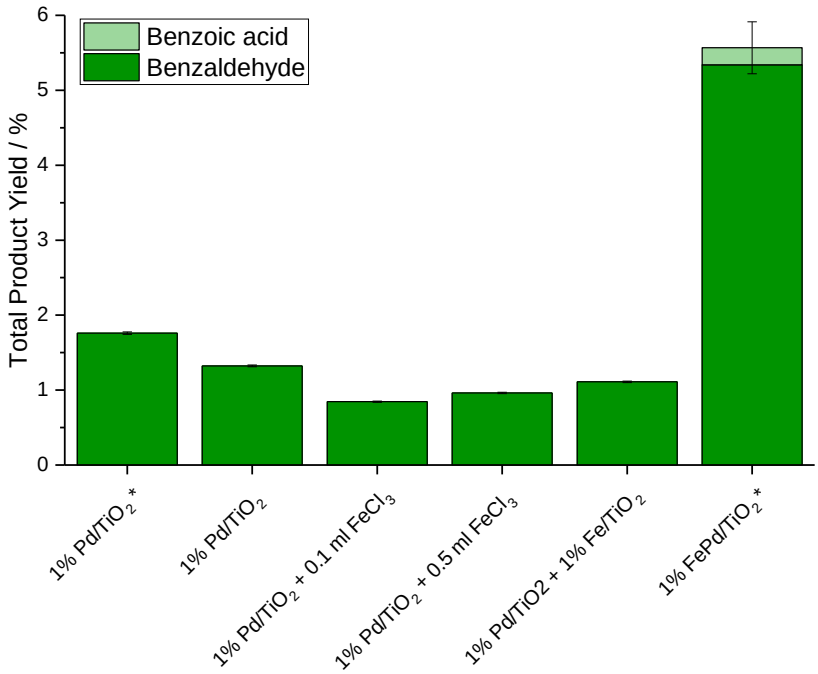


***Figure 6.16*** *A comparison of the catalytic activity towards benzyl alcohol oxidation for 1% Pd/$TiO_2$ and 1% Pd/$TiO_2$ with $FeCl_3$ solution.* ***Reaction conditions;*** *0.005 g catalyst, 0.1 or 0.5 ml 0.1 mg $ml^{-1}$ Fe, 1.04 g (9.6 mmol) benzyl alcohol, 7.1 g methanol, 29 bar 5 % $H_2/CO_2$ and 11 bar 25 % $O_2/CO_2$, 1200 RPM, 30 minutes, 50 °C. *0.01 g catalyst.*

Using a $FeCl_3$ solution with a Fe concentration of 0.1 mg $ml^{-1}$ along with 1% Pd/$TiO_2$ has shown no enhancement in the observed product yield (0.96 %) compared to 1% Pd/$TiO_2$ alone (1.3 %). A decrease in activity has been observed between 1% Pd/$TiO_2$ and 1% Pd/$TiO_2$ with solution Fe which could show that Fe in solution is having a detrimental effect on the catalytic activity. This loss in activity could be attributed to homogeneous Fe decomposing $H_2O_2$ in solution.[39] Solution Fe species are efficient at breaking $H_2O_2$ into radical species however if these are happening in solution and not in close contact with Pd these radicals [39] can be quenched before they can be utilised for the oxidation reaction.

These experiments show not only that solution Fe species are not as active as Pd and FePd heterogenous catalysts but that the Pd and Fe must be in close contact, on the same support, for the enhanced activity to be observed.

### 6.4.3.2 Extended reaction times.

Extended reaction times up to 120 minutes have also been investigated for 1% FePd/$TiO_2$, Figure 6.17.

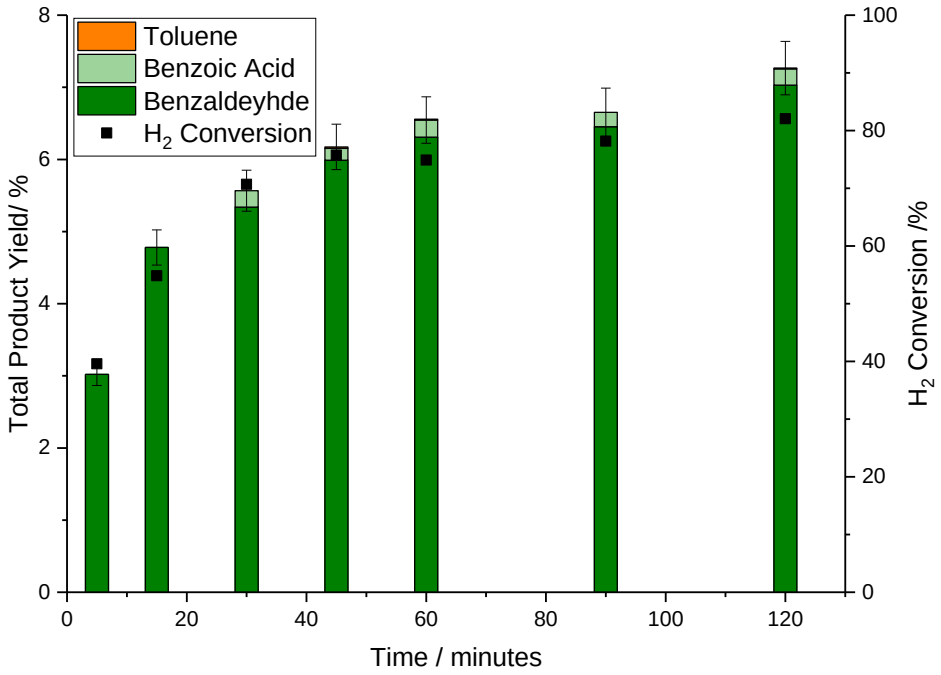


***Figure 6.17.*** *The activity of 1% FePd/$TiO_2$ catalysts towards benzyl alcohol oxidation at different reaction times.* ***Reaction conditions;*** *0.01 g catalyst, 1.04 g (9.6 mmol) benzyl alcohol, 7.1 g methanol, 29 bar 5 % $H_2/CO_2$ and 11 bar 25 % $O_2/CO_2$, 1200 RPM, 30 minutes, 50 °C.*

A general increase in yield with increased reaction time is observed accompanied with increasing $H_2$ conversion up to 45 minutes. Toluene formation is observed after 45 minute reaction time. Residual $H_2O_2$ concentrations are also maintained at all reaction times, Table 6.11. After 120 minutes a total yield of 7.3% has been observed compared to 4.5% for 1% AuPd/$TiO_2$ and 1.8% for 1% Pd/$TiO_2$ despite similar $H_2$ and $O_2$ conversions.

***Table 6.11*** *$H_2$ and $O_2$ conversion, selectivity based on $H_2$ conversion and residual $H_2O_2$ concentration observed at all reaction times for 1% FePd/$TiO_2$.*

| Time / minutes | Benzyl Alcohol Conversion / % | $H_2$ Conversion / % | Selectivity based on $H_2$ / % | $O_2$ Conversion / % | Residual $H_2O_2$ / µmol |
|---|---|---|---|---|---|
| 5 | 3.0 | 40 | 29 | 24 | 29 |
| 15 | 4.8 | 55 | 33 | 28 | 32 |
| 30 | 5.6 | 71 | 33 | 33 | 25 |
| 45 | 6.2 | 76 | 29 | 44 | 26 |
| 60 | 6.5 | 75 | 32 | 45 | 29 |
| 90 | 6.7 | 78 | 42 | 44 | 26 |
| 120 | 7.3 | 82 | 37 | 43 | 32 |

***Reaction conditions;*** *0.01 g catalyst, 1.04 g (9.6 mmol) benzyl alcohol, 7.1 g methanol, 29 bar 5 % $H_2/CO_2$ and 11 bar 25 % $O_2/CO_2$, 1200 RPM, 5 to 120 minutes, 50 °C.*

XPS showed a general increase in metallic Pd is with increasing reaction time, Table 6.12. Pd:Fe is unchanged with time indicating no change in particle morphology.

Satellite peaks in XPS indicate Fe present as $Fe^{2+}$ in all samples, indicating possible FeO formation. The increase in metallic Pd content on the surface of the catalyst could explain the deactivation of the catalyst at longer reaction times. This increase in $Pd^0$ will decrease the interfaces of Pd-PdO which have previously been discussed to be important for both $H_2O_2$ and benzyl alcohol oxidation.[20,24]

***Table 6.12.*** *XPS analysis of post reaction solutions using 1 % FePd/$TiO_2$ catalysts at different reaction times for the oxidation of benzyl alcohol.*

| Time | $Pd^0$: $Pd^{2+}$ | Pd:Fe |
|---|---|---|
| 0 (fresh) | 3.2 | 0.27 |
| 5 | 5.8 | 0.52 |
| 15 | 8.3 | 0.47 |
| 30 | 14 | 0.53 |
| 45 | 30 | 0.39 |
| 60 | 11.5 | 0.35 |
| 90 | 15 | 0.48 |
| 120 | All $Pd^0$ | 0.39 |

ICP-MS showed minimal leaching of Pd is observed at all reaction times, Table 6.13. Fe leaching is observed at all reaction times reaching a maximum of 30 % at 120 minutes. ICP-MS suggests a continual leaching of Fe from the catalyst and these leached species could be contributing to the activity of the 1% FePd/$TiO_2$ catalyst.

***Table 6.13.*** *ICP-MS analysis of post reaction solutions using 1 % FePd/$TiO_2$ catalysts at different reaction times for the oxidation of benzyl alcohol.*

| Time | Pd leached / % (ppb) | Fe leached / % (ppb) |
|---|---|---|
| 5 | 0.14 (7) | 4 (180) |
| 15 | 0.37 (17) | 16 (754) |
| 30 | 0.30 (15) | 19 (904) |
| 45 | 0.33 (19) | 16 (760) |
| 60 | 0.39 (21) | 17 (818) |
| 90 | 0.43 (13) | 30 (1434) |
| 120 | 0.28 (49) | 30 (1413) |

It has previously been reported by Underhill *et al.* for phenol oxidation that an increase in concentration of Fe in solution can lead to an increase in oxidation activity.[18] Hence the increase in catalytic activity with increasing reaction time could be attributed to the increase in homogeneous Fe species in solution, Figure 6.18. However as with the previous Pd and AuPd catalyst we have also seen a time dependence on product yield and although a correlation between Fe leaching and product yield has been observed it cannot be concluded that this is down to solution Fe alone.

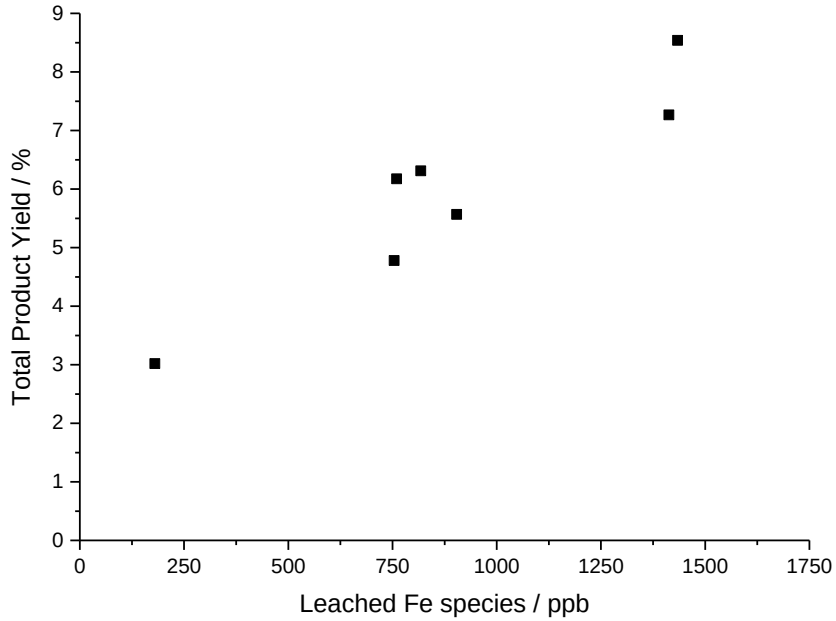


***Figure 6.18*** *Correlation observed between total product yield and the measure concentration of leached Fe species, as observed by ICP-MS.* ***Reaction conditions;*** *0.01 g catalyst, 1.04 g (9.6 mmol) benzyl alcohol, 7.1 g methanol, 29 bar 5 % $H_2/CO_2$ and 11 bar 25 % $O_2/CO_2$, 1200 RPM, 5 to 120 minutes, 50 °C.*

### 6.4.3.3 Sequential reactions.

Sequential reactions have also been investigated for 1% FePd/$TiO_2$, Figure 6.19.

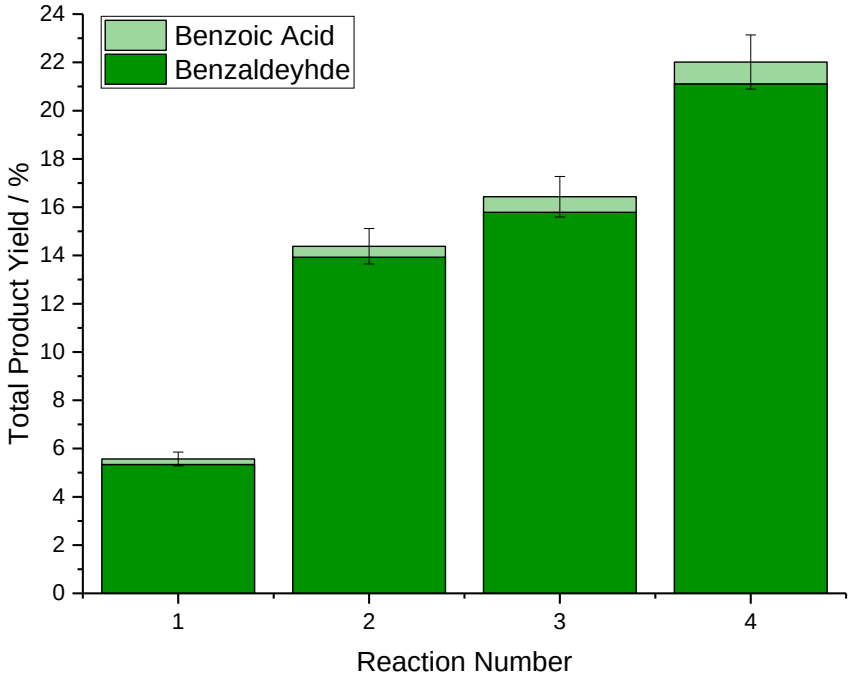


***Figure 6.19.*** *The effect of sequential reaction and reaction time on product yield from 1 % FePd/$TiO_2$ catalyst.* ***Reaction conditions;*** *0.01 g catalyst, 1.04 g (9.6 mmol) benzyl alcohol, 7.1 g methanol, 29 bar 5 % $H_2$ / $CO_2$ and 11 bar 25 % $O_2$ / $CO_2$, 1200 RPM, 50 °C.*

A much greater increase in yield with sequential reactions and reaction times can be seen here. The greatest increase in yield is observed between first and the second reaction. After 4 sequential reactions close to three times greater yield had been

produced than the equivalent reaction time (120 minutes) showing the importance of $H_2$ and production of reactive intermediates ($H_2O_2$). After four sequential reactions a total product yield of 22.0% has been observed for 1% FePd/$TiO_2$ which is doubled that observed for 1% AuPd/$TiO_2$ (11.8 %) and more than 3 times greater than 1% Pd/$TiO_2$ (6.3 %). This has shown that 1% FePd/$TiO_2$ can continue to show enhanced catalytic activity at prolonged testing despite questions on its stability.

With increasing sequential reactions a decrease in $H_2$ and $O_2$ conversion is observed, Table 6.14, which could indicate a slight decrease in catalyst activity. However, an increase in $H_2O_2$ is also observed for increasing top ups indicating that $H_2O_2$ is continually being produced but not utilised for the oxidation, again could be due to catalyst deactivation.

***Table 6.14.*** *$H_2$ and $O_2$ conversion, selectivity based on $H_2$ conversion and residual $H_2O_2$ concentration observed at all stages of reaction for 1 % FePd/$TiO_2$ used for the oxidation of benzyl alcohol.*

| Reaction Number | Benzyl Alcohol Conversion / % | $H_2$ Conversion / % | Selectivity based on $H_2$ / % | $O_2$ Conversion / % | Residual $H_2O_2$ / µmol |
|---|---|---|---|---|---|
| 1 | 5.6 | 71 | 33 | 33 | 25 |
| 2 | 14.4 | 65 | 40 | 60 | 51 |
| | | 74 | | 37 | |
| 3 | 16.4 | 64 | 38 | 36 | 52 |
| | | 58 | | 30 | |
| | | 43 | | 23 | |
| 4 | 22.0 | 69 | 37 | 38 | 83 |
| | | 64 | | 34 | |
| | | 49 | | 47 | |
| | | 45 | | 24 | |

***Reaction conditions;*** *0.01 g catalyst, 1.04 g (9.6 mmol) benzyl alcohol, 7.1 g methanol, 29 bar 5 % $H_2/CO_2$ and 11 bar 25 % $O_2/CO_2$, 1200 RPM, 50 °C.*

#### 6.4.3.4 Effect of solvent.

The effect of different solvents was investigated for 1% FePd/$TiO_2$ to try and elucidate whether solvent effects were observed or if increasing the solubility of gases could improve catalytic activity.

Similar total yields of around 3% was observed for all solvents except methanol, Table 6.15. A change in selectivity of benzaldehyde is observed from 100 % for methanol to 65 % in ethanol which could indicate the disproportionation reaction being more favourable here.

***Table 6.15.*** *The activity of 1% FePd/$TiO_2$ towards the oxidation of benzyl alcohol in different solvents.*

| Solvent | Total product yield / % | Selectivity to benzaldehyde / % | Selectivity to benzoic acid / % | Selectivity to toluene / % |
|---|---|---|---|---|
| Methanol | 5.6 | 96 | 4 | 0 |
| Ethanol | 3.0 | 66 | 0 | 34 |
| t-butanol | 3.1 | 100 | 0 | 0 |
| Water | 3.1 | 100 | 0 | 0 |

***Reaction conditions;*** *0.01 g catalyst, 1.04 g (9.6 mmol) benzyl alcohol, 9 ml solvent, 29 bar 5 % $H_2/CO_2$ and 11 bar 25 % $O_2/CO_2$, 1200 RPM, 50 °C.*

Santonastaso *et al.* also investigated the activity of 5% AuPd/$TiO_2$ in both methanol and water-methanol solvents and a solvent free system. They also observed an increase activity in pure methanol compared to water-methanol from 2.3 % to 9.5% and limited activity of 0.7% conversion under solvent free conditions.[1] From the solubility data shown in Table 6.16 it can be observed that no correlation between the solubility of $H_2$ and catalytic activity can be made. With increasing alcohol chain length an increase in $H_2$ solubility is observed.

***Table 6.16*** *$H_2$ solubility data for different solvents at 298 K and 1 atm.*[40]

| Solvent | $H_2$ Solubility as mol fraction / $10^{-4}$ |
|---|---|
| Methanol | 1.61 |
| Ethanol | 2.06 |
| t-butanol | 33.4 |
| Water | 0.175 |

Lunsford and co-workers investigated the dependence of $H_2O_2$ formation on both $H_2$ and $O_2$ pressure and showed that activity was first order dependant on $H_2$ and zero effect with respect to $O_2$.[41,42] Hence with increasing $H_2$ solubility and increasing mole fraction of $H_2$ in the liquid phase we can expect an increase in $H_2O_2$ formation. It has previously been observed that $H_2O_2$ synthesis in methanol is much greater than in water.[28,43] This has also been attributed to the increasing solubility of reactant gases in methanol compared to water as well as the decrease in $H_2O_2$ decomposition in methanol.[28]

### 6.4.4 Electron Paramagnetic Resonance (EPR) investigations.

Comparison of 1% Pd/$TiO_2$, 1% AuPd/$TiO_2$ and 1%FePd/$TiO_2$ has shown an increasing activity with addition of Au or Fe into Pd with 1% FePd/$TiO_2$ showing the greatest enhancement even at extended reaction times.

The comparison of activity between 1% Pd/$TiO_2$, 1% AuPd/$TiO_2$ and 1% FePd/$TiO_2$ was investigated by EPR. Using 5,5-dimethyl-1-pyrroline N-oxide (DMPO) as a

radical trap, reactions were run for both 5 minutes and 30 minutes to compare the radicals present for each catalyst, Figure 6.20. All experiments were run and interpreted by Rebekah Taylor and Andrea Folli at Cardiff University.

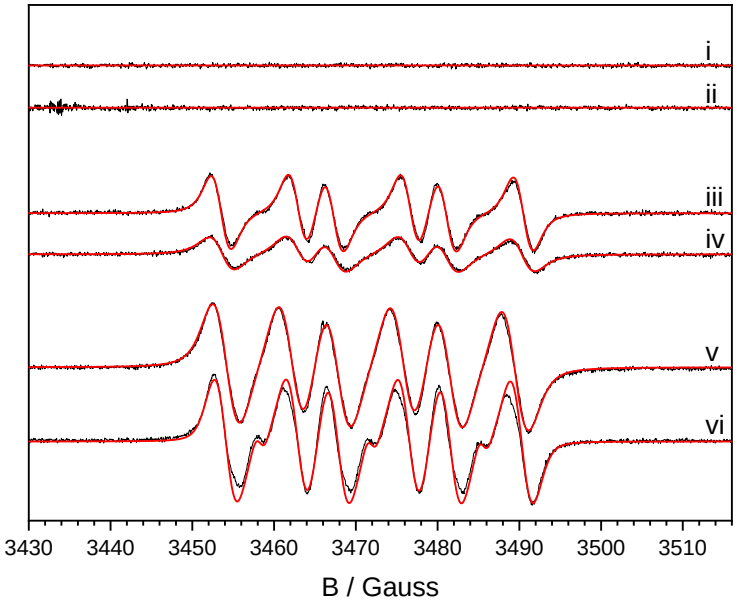


***Figure 6.20.*** *Experimental (black) and simulated (red) EPR spectra of DMPO-radical adducts formed during benzyl alcohol oxidation conducted in methanol at 50 °C, with benzyl alcohol (9.6 mmol), 5 % $H_2/CO_2$ (29 bar, 2.51 mmol $H_2$), 25 % $O_2/CO_2$ (11 bar, 4.77 mmol $O_2$), in the presence of DMPO and* ***i*** *1% $Pd/TiO_2$ 5 min reaction;* ***ii*** *1% $Pd/TiO_2$ 30 min reaction;* ***iii*** *1% $AuPd/TiO_2$ 5 min reaction;* ***iv*** *1% $AuPd/TiO_2$ 30 min reaction;* ***v*** *1% $FePd/TiO_2$ 5 min reaction;* ***vi*** *1% $FePd/TiO_2$ 30 min reaction.*

EPR spectra for 1% $Pd/TiO_2$ at both 5 and 30 minutes showed no obvious spectra and hence it could be concluded that no radical formation is observed over this catalyst. For $H_2O_2$ synthesis in a flow reactor it has previously been observed that no radicals are detected over a monometallic Pd catalyst but with the addition of Au $^{\bullet}OH$ radicals can be detected.[44] It is considered that the addition of Au facilitates the release of radicals from the catalyst surface[45] which increases the $H_2O_2$ activity.

Both spectra for 1% $FePd/TiO_2$ and 1% $AuPd/TiO_2$ at 5 and 30 minutes show the same splitting. This indicates the same radicals are present in both catalytic systems. This peak splitting implies an O centred radical that has reacted with DMPO. The shoulder peaks observed Figure 6.20 iii-vi can be attributed to a degradation, ring opened, product of DMPO characterised by only the one $a^N$ splitting being observed [46], this decomposition has previously been noted in the literature for Fenton's systems.[47] The O centred radical has been attributed to a methoxy radical that has been trapped by DMPO forming the nitroxide radical adduct, DMPO-$OCH_3$. The hyperfine coupling, Table 6.17, is in agreement with methoxy radical adducts reported in the literature.[46] It is thought that $MeO^{\bullet}$ forms in the reaction from the solvent, methanol, scavenging

•OH and •OOH radicals that are formed in the of synthesis $H_2O_2$ from $H_2$ and $O_2$.[44] Methanol is a well-known radical scavenger [48] and hence MeO• is a plausible radical intermediate for this reaction.

***Table 6.17.*** *EPR parameters of DMPO adducts and the radical associated with them.*

| Radical source | *g* | $a^N$ / G | $a^H$ / G |
|---|---|---|---|
| $CH_3O^•$ | 2.00622 ± 0.00006 | 13.73 ± 0.02 | 8.58 ± 0.25 |

Comparison of the intensities of the peaks shows that the concentration of radicals produced from 1% FePd/$TiO_2$ is greater than 1% AuPd/$TiO_2$ at reaction times of both 5 and 30 minutes which correlates with benzaldehyde yields. It can also be observed that the intensity for both catalysts has decreased from 5 minutes to 30 minutes, this decrease in intensity could be attributed to the degradation of DMPO at longer reaction times.

Control experiments were also run to see the signals produced when no reactant gases were present (reaction run under $N_2$), no substrate and no catalyst as shown in Figure 6.21.

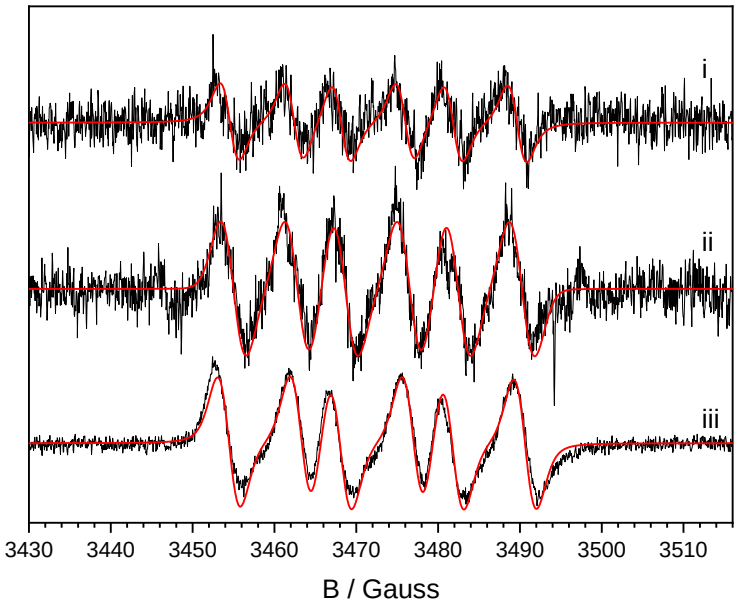


***Figure 6.21.*** *Experimental (black) and simulated (red) EPR spectra of DMPO-radical adducts formed during benzyl alcohol oxidation conducted in methanol at 50 °C with 1% AuPd/$TiO_2$,* ***i*** *no catalyst,* ***ii*** *no reacting gases and* ***iii*** *no substrate.*

All control experiments have shown the same spectral pattern identical to previously seen when the catalysts are present. It can be observed that when no catalyst or reactant gases are present limited signal is produced, indicated by reduced line intensity and an increase signal to noise ratio, signifying a reduced production of radical as expected. As a slight signal is observed for all spectra this could indicate that a small reaction

between DMPO and methanol could also be occurring. When no benzyl alcohol is present a much greater intensity is seen to show that a greater intensity of radical formation. This is in agreement with proposed $H_2O_2$ formation when no gases or catalyst are present no $H_2O_2$ and no subsequent radicals from $H_2O_2$ can be formed.

From these experiments it can be observed that only methoxy radicals were being added to DMPO. As methanol is a well known scavenger it is unknown whether any other radicals were being produced *in-situ* but not detected due to the quick scavenging by methanol. To deduce how large this methanol effect was and to determine the primary radicals produced from $H_2$ and $O_2$ EPR experiments were also conducted in water, Figure 6.22.

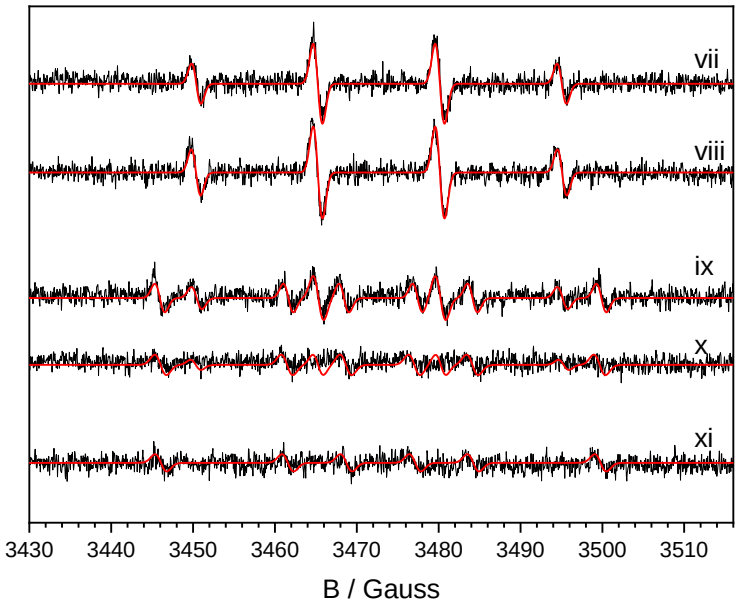


***Figure 6.22.*** *Experimental (black) and simulated (red) EPR spectra of DMPO-radical adducts formed during benzyl alcohol oxidation conducted in water at 50 °C, in the presence of DMPO and* ***vii*** *5 % $H_2/CO_2$ (29 bar, 2.51 mmol H2), 25 % $O_2/CO_2$ (11 bar, 4.77 mmol O2), 1% AuPd/$TiO_2$;* ***viii*** *5 % $H_2/CO_2$ (29 bar, 2.51 mmol $H_2$), 25 % $O_2/CO_2$ (11 bar, 4.77 mmol $O_2$), 1% FePd/$TiO_2$;* ***ix*** *benzyl alcohol (9.6 mmol), 1% AuPd/$TiO_2$;* ***x*** *benzyl alcohol (9.6 mmol), 1% FePd/$TiO_2$;* ***xi*** *benzyl alcohol (9.6 mmol), 5 % $H_2/CO_2$ (29 bar, 2.51 mmol $H_2$), 25 % $O_2/CO_2$ (11 bar, 4.77 mmol $O_2$).*

When both the catalyst and reactant gases were present, Figure 6.22 vii and viii, a clear signal of four peaks equidistant apart with the intensity ratio of 1:2:2:1 has been observed for both 1% AuPd/$TiO_2$ (vii) and 1% FePd/$TiO_2$ (viii). This characteristic peak corresponds to a DMPO-OH adduct, showing equal hyperfine couplings for the $^{14}N$ of the NO$^{\bullet}$ moiety and the beta proton, $a_{iso}(^{14}N)$ = 14.93 G and $a_{iso}(^{1}H_{\beta})$ = 14.93 G. This signal is symptomatic of $^{\bullet}OH$ and/or $^{\bullet}OOH$ trapping. DMPO-OOH adduct has a half-life of 1-4 min and decays into DMPO-OH if unreacted DMPO is present,[49] illustrated in Figure 6.23. Hence from these experiments it is not possible to

distinguish whether •OH and •OOH radicals have been formed form $H_2$ and $O_2$ and whether they have gone via the formation of $H_2O_2$.

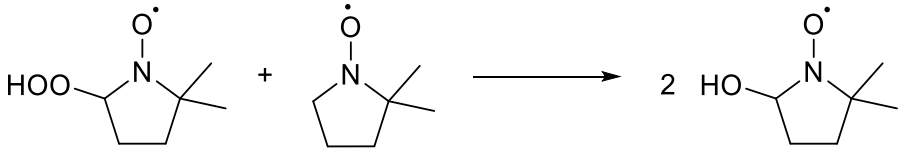


***Figure 6.23.*** *Th reaction of DMPO-OOH adduct with DMPO to produce DMPO-OH.*

When no reactant gases are present, Figure 6.22 ix and x, the concentration of the DMPO-OH adduct has been significantly decreased as expected. Interestingly, a new signal characterised by $a_{iso}(^{14}N)$ = 15.59 G and $a_{iso}(^{1}H_{\beta})$ = 22.60 G has been observed and these hyperfine couplings are consistent with a DMPO-trapped C-centred PhCH•(OH) radical. This radical is consistent with the first step in the benzyl alcohol reaction mechanism[1,3] where it is believed the first step is the abstraction of the H from the carbon adjacent to OH, Figure 6.24. This also indicates that the catalyst itself without $H_2$ and $O_2$ might be responsible for some limited activity in the oxidation reaction. When no gases were present the amount of radicals trapped when using 1% $AuPd/TiO_2$ was actually higher than when using 1% $FePd/TiO_2$.

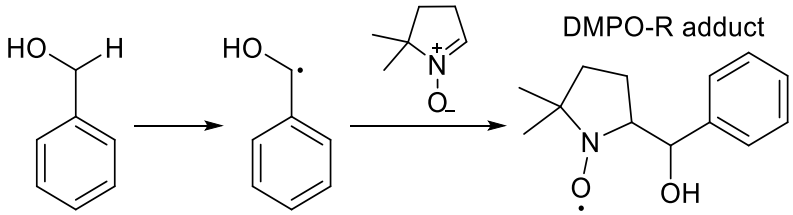


***Figure 6.24.*** *The proposed formation of carbon based radical in the oxidation of benzyl alcohol and its consequent reaction with DMPO.*

When the reaction was run in the absence of a catalyst, Figure 6.22 xi, no radical reactive oxygen species (ROS) have been observed. This agrees with the results suggested above and indicates that radical ROS formation is a catalytic process. Though, the spectrum shows a small contribution of trapped PhCH•(OH) radicals. This is consistent with a small equilibrium amount of $H_2O_2$ forming from $H_2$ and $O_2$ without the presence of a catalyst which could have then oxidised some of the benzyl alcohol present.

From these EPR experiments it can be observed that by comparison of 1% $Pd/TiO_2$, 1% $AuPd/TiO_2$ and 1% $FePd/TiO_2$ that a correlation of radical formation and catalyst oxidation activity can be made. With methanol as the solvent only methoxy radicals can be observed, however it is believed this is due to the scavenging of other radicals present (•OH and/or •OOH). When water is used as a solvent it can be seen that when

the catalysts, 1% $AuPd/TiO_2$ and 1% $FePd/TiO_2$, and reactant gases are present $^{\bullet}OH$ radicals are formed and hence it can be deduced that these catalytic systems can produce reactive oxygen species via the formation of $H_2O_2$.

## 6.5 Conclusions.

All bimetallic 1 % $XPd/TiO_2$ have been tested for the oxidation of benzyl alcohol under both *in-situ* and $O_2$ only conditions. All catalysts have performed better under *in-situ* conditions showing the significance of $H_2$ in the reaction under these mild conditions.

All catalysts have shown extremely high selectivity towards benzaldehyde, >96 %, and benzoic acid being the only other oxidation product observed. The bimetallic 1 % $VPd/TiO_2$, 1 % $MnPd/TiO_2$, 1 % $FePd/TiO_2$ and 1 % $CoPd/TiO_2$ have shown improved activity upon 1 % $AuPd/TiO_2$. However, leaching of 7.5 %, 39.6 %, 12.5 % and 60.1 % of X metal have been observed for these catalysts respectively.

In depth comparison studies have focused on the difference in activity between 1% $Pd/TiO_2$, 1 % $AuPd/TiO_2$ and 1% $FePd/TiO_2$, Table 6.18. Addition of Au and Fe to 1% $Pd/TiO_2$ has shown an enhancement in activity with the greatest seen for 1% $FePd/TiO_2$. This has been observed in the initial rates of reaction, extended reaction times and sequential reactions.

***Table 6.18.*** *Comparison of initial rates of benzyl alcohol oxidation over supported Pd-based catalysts.*

| Catalyst | Initial rate of reaction* / μmol $s^{-1}$ | Benzaldehyde Selectivity /% | Benzyl Alcohol Conversion / % | Selectivity based on $H_2$ / % |
|---|---|---|---|---|
| 1% $Pd/TiO_2$ | 0.24 | 100 | 1.8 | 9 |
| 1% $AuPd/TiO_2$ | 0.72 | 100 | 2.8 | 16 |
| 1% $FePd/TiO_2$ | 0.97 | 96 | 5.6 | 33 |

***Reaction conditions;*** *0.01g catalyst, 1.04 g (9.6 mmol) benzyl alcohol, 7.1 g methanol, 29 bar 5 % $H_2/CO_2$ and 11 bar 25 % $O_2/CO_2$, 1200 RPM, 50 °C.*calculated from 5 minute reaction.*

A maximum yield of benzaldehyde of 21.2% after 4 sequential reactions has been observed, with high selectivity maintained at 96%, using 1% $FePd/TiO_2$ catalyst. The enhanced activity of 1% $FePd/TiO_2$ has been attributed to the greater influx of oxygen-based radicals, as seen by EPR. It has been proposed that the oxygen based radical have originated from Fe initiated Fenton's pathway breaking $H_2O_2$ into $^{\bullet}OH$ and $^{\bullet}OOH$ radicals which have been quenched by methanol and detected by EPR.

## 6.6 References.


1. M. Santonastaso, S. J. Freakley, P. J. Miedziak, G. L. Brett, J. K. Edwards and G. J. Hutchings, *Org. Process Res. Dev.*, 2014, **18**, 1455–1460.
2. E. Nowicka, J. P. Hofmann, S. F. Parker, M. Sankar, G. M. Lari, S. A. Kondrat, D. W. Knight, D. Bethell, B. M. Weckhuysen and G. J. Hutchings, *Phys. Chem. Chem. Phys.*, 2013, **15**, 12147–12155.
3. F. Galvanin, M. Sankar, S. Cattaneo, D. Bethell, V. Dua, G. J. Hutchings and A. Gavriilidis, *Chem. Eng. J.*, 2018, **342**, 196–210.
4. M. Morad, M. Sankar, E. Cao, E. Nowicka, T. E. Davies, P. J. Miedziak, D. J. Morgan, D. W. Knight, D. Bethell, A. Gavriilidis and G. J. Hutchings, *Catal. Sci. Technol.*, 2014, **4**, 3120–3128.
5. Savara, C. E. Chan-Thaw, I. Rossetti, A. Villa and L. Prati, *ChemCatChem*, 2014, **6**, 3464–3473.
6. M. P. Chaudhari and S. B. Sawant, *Chem. Eng. J.*, 2005, **106**, 111–118.
7. C. Hammond, I. Hermans and N. Dimitratos, *ChemCatChem*, 2015, **7**, 434–440.
8. Y. Yu, B. Lu, X. Wang, J. Zhao, X. Wang and Q. Cai, *Chem. Eng. J.*, 2010, **162**, 738–742.
9. Q. He, P. J. Miedziak, L. Kesavan, N. Dimitratos, M. Sankar, J. A. Lopez-Sanchez, M. M. Forde, J. K. Edwards, D. W. Knight, S. H. Taylor, C. J. Kiely and G. J. Hutchings, *Faraday Discuss.*, 2013, **162**, 365–378.
10. F. Li, Q. Zhang and Y. Wang, *Appl. Catal. Gen.*, 2008, **334**, 217–226.
11. E. Nowicka, S. Althahban, T. D. Leah, G. Shaw, D. Morgan, C. J. Kiely, A. Roldan and G. J. Hutchings, *Sci. Technol. Adv. Mater.*, 2019, **20**, 367–378.
12. Moreno, N. F. Dummer, J. K. Edwards, M. Alhumaimess, M. Sankar, R. Sanz, P. Pizarro, D. P. Serrano and G. J. Hutchings, *Catal. Sci. Technol.*, 2013, **3**, 2425–2434.
13. F. Bonino, A. Damin, G. Ricchiardi, M. Ricci, G. Spanò, R. D'Aloisio, A. Zecchina, C. Lamberti, C. Prestipino and S. Bordiga, *J. Phys. Chem. B*, 2004, **108**, 3573–3583.
14. M. Sankar, E. Nowicka, E. Carter, D. M. Murphy, D. W. Knight, D. Bethell and G. J. Hutchings, *Nat. Commun.*, 2014, **5**, 3332.
15. M. Triki, S. Contreras and F. Medina, *J. Sol-Gel Sci. Technol.*, 2014, **71**, 96–101.
16. M. S. Yalfani, S. Contreras, J. Llorca, M. Dominguez, J. E. Sueiras and F. Medina, *Phys. Chem. Chem. Phys.*, 2010, **12**, 14673–14676.
17. Georgi, M. Velasco Polo, K. Crincoli, K. Mackenzie and F.-D. Kopinke, *Environ. Sci. Technol.*, 2016, **50**, 5882–5891.
18. R. Underhill, R. J. Lewis, S. J. Freakley, M. Douthwaite, P. J. Miedziak, O. Akdim, J. K. Edwards and G. J. Hutchings, *Johns. Matthey Technol. Rev.*, 2018, **62**, 417–425.
19. M. Piccinini, E. N. N, J. K. Edwards, A. F. Carley, J. A. Moulijn and G. J. Hutchings, *Phys. Chem. Chem. Phys.*, 2010, **12**, 2488–2492.
20. S. Meher and R. K. Rana, *Green Chem.*, 2019, **21**, 2494–2503.
21. S. J. Freakley, Q. He, J. H. Harrhy, L. Lu, D. A. Crole, D. J. Morgan, E. N. Ntainjua, J. K. Edwards, A. F. Carley, A. Y. Borisevich, C. J. Kiely and G. J. Hutchings, *Science*, 2016, **351**, 965–968.
22. S. Kim, D.-W. Lee, K.-Y. Lee and E. A. Cho, *Catal. Lett.*, 2014, **144**, 905–911.

23. Q. Zhang, W. Deng and Y. Wang, *Chem. Commun.*, 2011, **47**, 9275–9292.
24. L. Ouyang, P. Tian, G. Da, X.-C. Xu, C. Ao, T. Chen, R. Si, J. Xu and Y.-F. Han, *J. Catal.*, 2015, **321**, 70–80.
25. F. Wang, C. Xia, S. P. de Visser and Y. Wang, *J. Am. Chem. Soc.*, 2019, **141**, 901–910.
26. K. Edwards and G. J. Hutchings, *Angew. Chem. Int. Ed.*, 2008, **47**, 9192–9198.
27. M. Sankar, Q. He, M. Morad, J. Pritchard, S. J. Freakley, J. K. Edwards, S. H. Taylor, D. J. Morgan, A. F. Carley, D. W. Knight, C. J. Kiely and G. J. Hutchings, *ACS Nano*, 2012, **6**, 6600–6613.
28. Santos, R. J. Lewis, G. Malta, A. G. R. Howe, D. J. Morgan, E. Hampton, P. Gaskin and G. J. Hutchings, *Ind. Eng. Chem. Res.*, 2019, **58**, 12623–12631.
29. G. Chen, W.-T. Chou and C. Yeh, *Appl. Catal.*, 1983, **8**, 389–397.
30. C.-B. Wang, H.-K. Lin and C.-M. Ho, *J. Mol. Catal. Chem.*, 2002, **180**, 285–291.
31. M. Chen, D. Kumar, C.-W. Yi and D. W. Goodman, *Science*, 2005, **310**, 291–293.
32. Y.-F. Han, Z. Zhong, K. Ramesh, F. Chen, L. Chen, T. White, Q. Tay, S. N. Yaakub and Z. Wang, *J. Phys. Chem. C*, 2007, **111**, 8410–8413.
33. D. Gudarzi, W. Ratchananusorn, I. Turunen, M. Heinonen and T. Salmi, *Catal. Today*, 2015, **248**, 58–68.
34. S. Han and C. B. Mullins, *ACS Catal.*, 2018, **8**, 3641–3649.
35. P. A. P. Nascente, S. G. C. de Castro, R. Landers and G. G. Kleiman, *Phys. Rev. B*, 1991, **43**, 4659–4666.
36. D. I. Enache, J. K. Edwards, P. Landon, B. Solsona-Espriu, A. F. Carley, A. A. Herzing, M. Watanabe, C. J. Kiely, D. W. Knight and G. J. Hutchings, *Science*, 2006, **311**, 362–365.
37. H. Xu, D. Cheng and Y. Gao, *ACS Catal.*, 2017, **7**, 2164–2170.
38. N. M. Wilson, P. Priyadarshini, S. Kunz and D. W. Flaherty, *J. Catal.*, 2018, **357**, 163–175.
39. De Laat and H. Gallard, *Environ. Sci. Technol.*, 1999, **33**, 2726–2732.
40. C. L. Young, Ed., *Hydrogen and deuterium*, Pergamon Press, Oxford ; New York, 1st ed., 1981.
41. Q. Liu and J. H. Lunsford, *Appl. Catal. Gen.*, 2006, **314**, 94–100.
42. Q. Liu, J. C. Bauer, R. E. Schaak and J. H. Lunsford, *Appl. Catal. Gen.*, 2008, **339**, 130–136.
43. S. J. Freakley, M. Piccinini, J. K. Edwards, E. N. Ntainjua, J. A. Moulijn and G. J. Hutchings, *ACS Catal.*, 2013, **3**, 487–501.
44. T. Richards *et al*., unpublished.
45. I. bin Saiman, G. L. Brett, R. Tiruvalam, M. M. Forde, K. Sharples, A. Thetford, R. L. Jenkins, N. Dimitratos, J. A. Lopez-Sanchez, D. M. Murphy, D. Bethell, D. J. Willock, S. H. Taylor, D. W. Knight, C. J. Kiely and G. J. Hutchings, *Angew. Chem. Int. Ed.*, 2012, **51**, 5981–5985.
46. G. R. Buettner, *Free Radic. Biol. Med.*, 1987, **3**, 259–303.
47. K. Makino, T. Hagiwara, A. Hagi, M. Nishi and A. Murakami, *Biochem. Biophys. Res. Commun.*, 1990, **172**, 1073–1080.
48. F. Vailati, R. D. Huelsmann, E. Martendal, A. J. Bortoluzzi, F. R. Xavier and R. A. Peralta, *New J. Chem.*, 2020, **44**, 2514–2526.
49. E. Finkelstein, G. M. Rosen, E. J. Rauckman and J. Paxton, *Mol. Pharmacol.*, 1979, **16**, 676–685.

# Appendix.

***Table S6.1.*** *Surface composition of Pd and X determined by XPS of 1 % XPd/$TiO_2$ catalysts after use for benzyl alcohol oxidation.*

| Catalyst | Atomic concentration / % | | |
|---|---|---|---|
| | X | $Pd^0$ | $Pd^{2+}$ |
| 1 % VPd/ $TiO_2$ used | 0.69 | 0.18 | 0.06 |
| 1 % MnPd/ $TiO_2$ used | 0.16 | 0.19 | 0.05 |
| 1 % FePd/ $TiO_2$ used | 0.53 | 0.19 | 0.08 |
| 1 % CoPd/ $TiO_2$ used | 0.22 | 0.15 | 0.09 |
| 1 % NiPd/ $TiO_2$ used | 0.34 | 0.06 | 0.02 |
| 1 % CuPd/ $TiO_2$ used | 1.31 | 0.26 | 0.10 |
| 1 % AuPd/ $TiO_2$ used | 0.12 | 0.22 | 0.04 |
| 1 % CePd/ $TiO_2$ used | 0.43 | 0.07 | 0.03 |

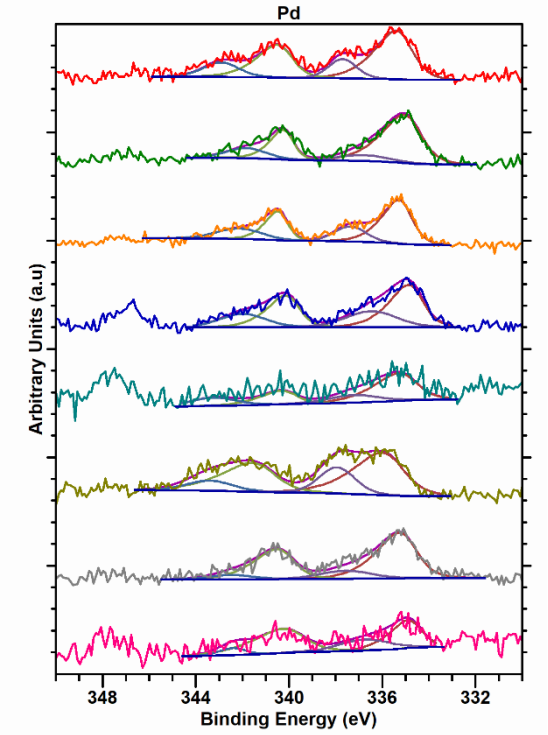


***Figure S6.1.*** *XPS spectra and fitting in the Pd 3d region for 1% XPd/$TiO_2$ catalysts after used in the oxidation of cyclohexane via the in-situ production of $H_2O_2$.*

***Table S6.2.*** *Surface composition of Pd determined by XPS of 1% Pd/$TiO_2$ used at varying reaction times.*

| Reaction time / minutes | Atomic concentration / % | |
|---|---|---|
| | $Pd^0$ | $Pd^{2+}$ |
| 0 (fresh) | 0.33 | 0 |
| 5 | 0.29 | 0 |
| 15 | 0.27 | 0 |
| 30 | 0.28 | 0 |
| 60 | 0.33 | 0 |
| 90 | 0.29 | 0 |
| 120 | 0.30 | 0 |

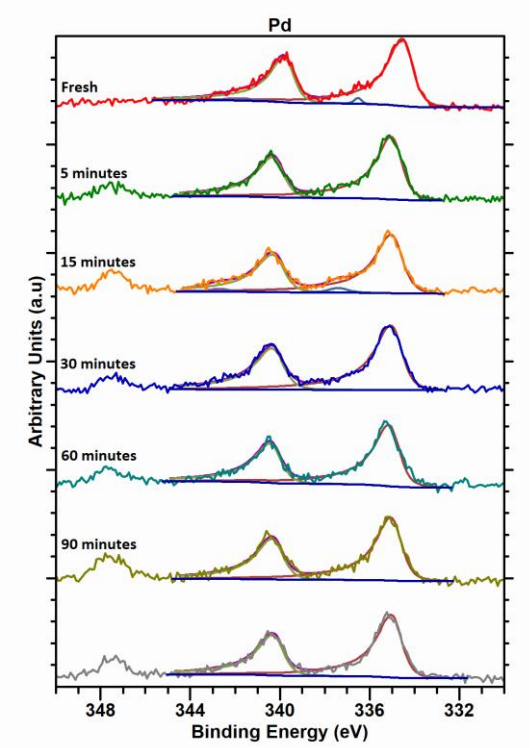


***Figure S6.25**. XPS spectra and fitting for Pd 3d region for 1% Pd/$TiO_2$ catalyst used at varying reactions times for the oxidation of benzyl alcohol via the in-situ production of $H_2O_2$.*

***Table S6.3.** Surface composition of Pd and Au determined by XPS of 1 % AuPd/$TiO_2$ catalysts at different reaction times for the oxidation of benzyl alcohol via the in-situ production of $H_2O_2$l.*

| Time / minutes | Atomic concentration / % | | |
|---|---|---|---|
| | Au | $Pd^0$ | $Pd^{2+}$ |
| 0 (fresh) | 0.11 | 0.25 | 0 |
| 5 | 0.14 | 0.37 | 0.02 |
| 15 | 0.35 | 0.4 | 0.08 |
| 30 | 0.35 | 0.38 | 0.1 |
| 45 | 0.35 | 0.39 | 0.09 |
| 60 | 0.35 | 0.32 | 0.07 |
| 90 | 0.35 | 0.36 | 0.07 |
| 120 | 0.35 | 0.41 | 0.06 |

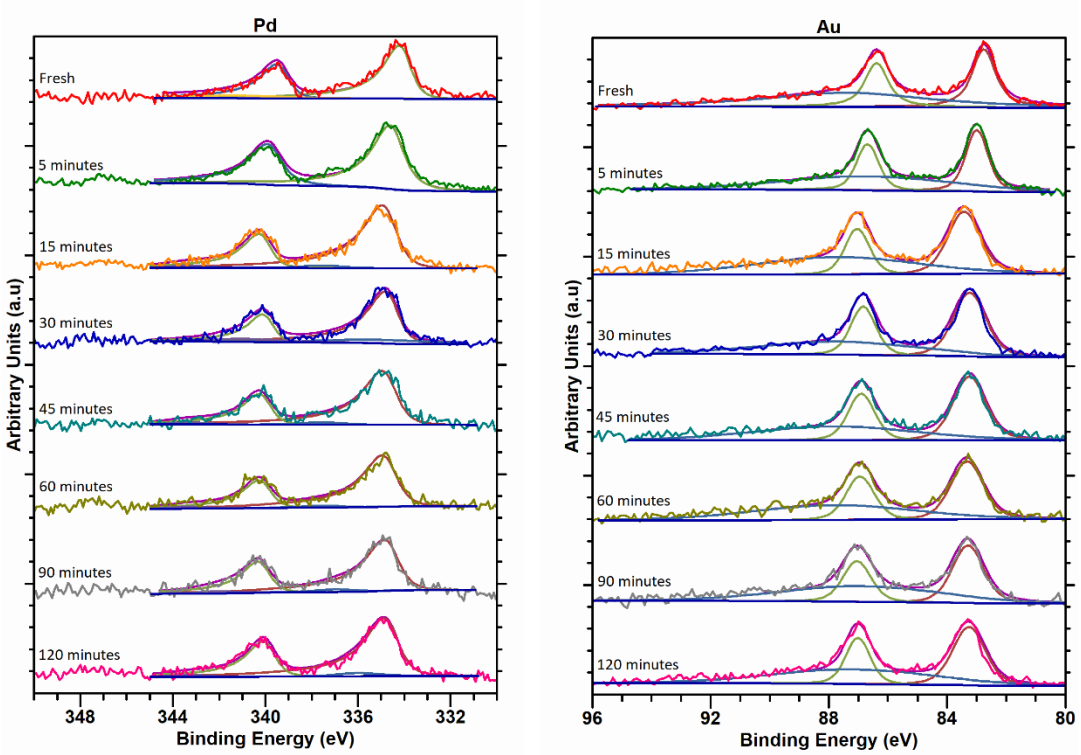


***Figure S6.3.*** *XPS spectra and fitting for Pd 3d and Au 4f regions for 1% AuPd/$TiO_2$ catalyst used a varying reaction times for the oxidation of benzyl alcohol via the in-situ production of $H_2O_2$.*

***Table S6.4.*** *ICP-MS analysis of post reaction solutions using 1 % AuPd/$TiO_2$ catalysts at different reaction times for the oxidation of benzyl alcohol via the in-situ production of $H_2O_2$.*

| Time / minutes | Pd leached / % (ppb) | Au leached / % (ppb) |
|---|---|---|
| 15 | 0.20 (10) | 0.01 (0.6) |
| 30 | 0.10 (5) | 0.01 (0.5) |
| 45 | 0.10 (5) | 0.01 (0.3) |
| 60 | 0.08 (4) | 0.00 (0.2) |
| 90 | 0.07 (3) | 0.00 (0.1) |
| 120 | 0.12 (6) | 0.01 (0.4) |

On the fresh 1% AuPd/$TiO_2$ there is a total of 4762 ppb of each metal present.

***Table S6.5.*** *Surface composition of Pd and Fe determined by XPS of 1 % FePd/$TiO_2$ catalysts at different reaction times for the oxidation of benzyl alcohol via the in-situ production of $H_2O_2$.*

| Time / minutes | Atomic concentration / % | | |
|---|---|---|---|
| | Fe | $Pd^0$ | $Pd^{2+}$ |
| 0 (fresh) | 0.78 | 0.05 | 0.16 |
| 5 | 0.65 | 0.29 | 0.05 |
| 15 | 0.6 | 0.25 | 0.03 |
| 30 | 0.58 | 0.3 | 0.01 |
| 45 | 0.54 | 0.18 | 0.03 |
| 60 | 0.72 | 0.23 | 0.02 |
| 90 | 0.67 | 0.3 | 0.02 |
| 120 | 0.8 | 0.31 | 0 |

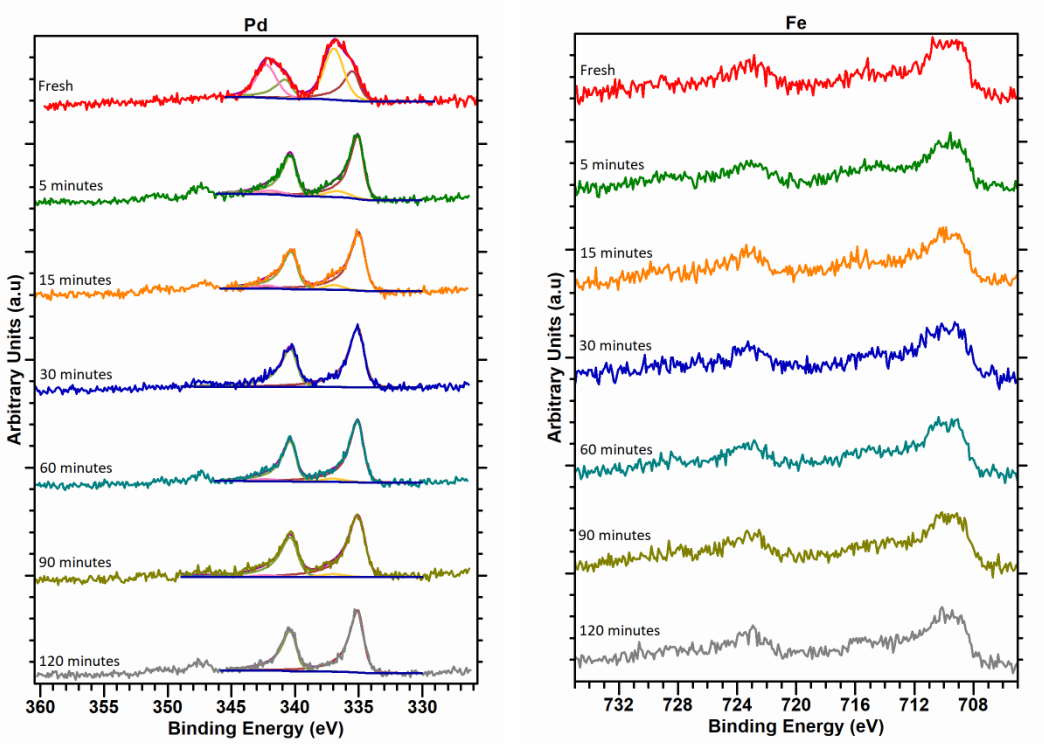


***Figure S6.4.*** *XPS spectra and fitting for Pd 3d and Fe 2p regions for 1% FePd/$TiO_2$ catalysts used at varying reaction times in the oxidation of benzyl alcohol via the in-situ production of $H_2O_2$.*

# 7 Conclusions and future work.

## 7.1 The direct synthesis of $H_2O_2$.

As detailed in Chapter 1 the current production of $H_2O_2$ is via the anthraquinone process (AO) which although has been optimised to give high selectivity towards $H_2O_2$ it still has its disadvantages. The degradation of anthraquinone throughout the process requires the continual addition, and recovery, of the anthraquinone molecule. There is also the obvious energy intensive drawbacks of continual distillation of $H_2O_2$ solution to a high concentration for transportation and distribution. Again, the transportation of these high concentrations of $H_2O_2$ has many safety issues. Hence the direct synthesis of $H_2O_2$ with heterogeneous catalysts does show it advantages. Small batch synthesis of $H_2O_2$ could be used at need of use at low concentrations for immediate use, removing concerns around transport, storage and dilution. The continuous production of $H_2O_2$ at low concentrations also has the potential to be used as an *in-situ* oxidant again avoiding the need for high concentrations of $H_2O_2$ to be stored.

As discussed in the literature and within this work catalyst design for $H_2O_2$ synthesis is focussed on increasing the selectivity of $H_2O_2$ by avoiding the subsequent degradation of $H_2O_2$. Although many ways have been utilised to stabilise $H_2O_2$ such as the use of acid[1–3] and halide[4–6] additives or low temperatures[7–9] these may not be industrially practical. Acid and halide additives can have detrimental effect on reactors including corrosion as well as the concerns associated with having additives in product steams which typically require removal prior to shipping. The use of low temperatures does decrease the decomposition of $H_2O_2$ however it is an energy intensive process and hence the use of ambient temperature while still maintaining high $H_2O_2$ selectivity has its benefits.

Catalysts design for $H_2O_2$ synthesis within this work has focused on both the preparation method of the catalyst (Chapter 4) and utilising non-precious metals, alloyed with Pd, within the catalyst (Chapter 5). The effect of the support on $H_2O_2$ synthesis has previously been explored by Hutchings and co-workers at sub-ambient temperatures (2 °C) using 5% AuPd catalyst.[10,11] By comparison, in this work AuPd catalysts, with a fifth of the precious metal content, have been investigated at ambient temperature. Both the reduction in metal content and the use of ambient temperature is clearly preferential for industrial application. Although increasing the reaction

temperature to 25 °C has led to a decreased $H_2$ selectivity, compared to 2 °C, through increased rates of $H_2O_2$ degradation similar yields of $H_2O_2$ have been produced to that reported in the literature, Table 7.1.

***Table 7.1.*** *Comparison of $H_2O_2$ activity and selectivity of the catalysts and conditions used in literature and reported in this work.*

| Catalyst | Conditions | Productivity / $mol_{H_2O_2}kg_{cat}^{-1}hr^{-1}$ | $H_2O_2$ Selectivity / % |
|---|---|---|---|
| 2.5% Au 2.5% Pd/$TiO_2$ (wet impregnation)[10] | 2 °C, water/methanol | 64 | 70 |
| 2.5% Au 2.5% Pd /$TiO_2$ (wet impregnation)[12] | 20 °C, water/methanol | 50 | n.d* |
| 0.5% Au 0.5% Pd /$TiO_2$ (modified impregnation) [7] | 25 °C, water/methanol | 75 | 14 |
| 0.5% Au 0.5% Pd Pd/$TiO_2$ (wet impregnation) | 25 °C, water/methanol | 55 | 30 |

* Not determined.

For catalysts produced via a wet impregnation procedure it has previously been reported that catalysts supported on materials of higher isoelectric point (IEP) result in improved activity towards $H_2O_2$ synthesis.[11] In keeping with these results it is reported that the catalysts prepared by wet impregnation tested at 25 °C also follow this trend, Table 7.2. However, these trends have not been observed for the other preparation methods, modified impregnation and sol immobilisation. Both modified impregnation and sol immobilisation use acids during catalyst preparation and hence as all catalysts are acidified during preparation the acidity of the support becomes less important in catalyst activity.

Comparing preparation methods it has been observed that $TiO_2$ supported catalysts prepared via modified impregnation leads to higher $H_2O_2$ activity, while also improving selectivity as has previously been observed by Sankar *et al* at 2 °C.[13] However these trends have not been observed for other supports and could indicate that the promotional effects that occur on $TiO_2$ can not be presumed for other supports. Modified impregnation utilises an acidic Pd precursor and the effect of acid in catalyst preparation can depend on the support used. From catalyst characterisation (Chapter 3) it could be observed for the high IEP support MgO that the use of acid, both in modified impregnation and sol immobilisation, disrupted the catalyst support eliminating MgOH. Hence it could be suggested that acidic promotion of catalyst is best when the support utilised is neutral or a moderate IEP.

***Table 7.2.*** *Synthesis and degradation of $H_2O_2$ of supported 1 % AuPd catalysts, comparison between catalyst preparation and support.*

| Preparation method | Support | Productivity / $mol_{H_2O_2} kg_{cat}^{-1} hr^{-1}$ | Degradation / $mol_{H_2O_2}$ $kg^{-1}$ $hr^{-1}$ |
|---|---|---|---|
| Wet impregnation | $SiO_2$ | 72 | 73 |
| | $TiO_2$ | 55 | 212 |
| | $CeO_2$ | 51 | 163 |
| | MgO | 14 | 217 |
| | C | 35 | 78 |
| Modified impregnation | $SiO_2$ | 20 | 711 |
| | $TiO_2$ | 68 | 612 |
| | $CeO_2$ | 30 | 673 |
| | MgO | 5 | 1263 |
| | C | 33 | 380 |
| Sol immobilisation | $SiO_2$ | 3 | 1237 |
| | $TiO_2$ | 48 | 488 |
| | $CeO_2$ | 7 | 162 |
| | MgO | 2 | 389 |
| | C | 29 | 431 |

***Reaction conditions;*** *0.01 g catalyst, 2.9 g water, 5.6 g methanol, 29 bar 5 % $H_2/CO_2$ and 11 bar 25 % $O_2/CO_2$, 1200 RPM, 30 minutes, 25 °C.*

In an attempt to improve catalytic performance, as has been recently reported in the literature, a range of non-precious metals were introduced into a supported Pd catalysts prepared by modified impregnation. This illustrated that non-precious metals could be utilised at low metals loadings and although the productivity was not as high as previously observed for 1% $AuPd/TiO_2$ (68 $mol_{H_2O_2}$ $kg^{-1}$ $hr^{-1}$) the degradation of these novel catalysts, Table 7.3, is much reduced.

***Table 7.3.*** *Synthesis and degradation of $H_2O_2$ by 1% $XPd/TiO_2$ as reported in this thesis.*

| Catalyst | Productivity / $mol_{H_2O_2}$ $kg^{-1}$ $hr^{-1}$ | Degradation / $mol_{H_2O_2}$ $kg^{-1}$ $hr^{-1}$ |
|---|---|---|
| 1 % $AuPd/TiO_2$ | 68 | 711 |
| 1 % $VPd/TiO_2$ | 40 | 62 |
| 1 % $MnPd/TiO_2$ | 47 | 147 |
| 1 % $FePd/TiO_2$ | 40 | 41 |
| 1 % $CoPd/TiO_2$ | 34 | 89 |
| 1 % $NiPd/TiO_2$ | 28 | 4 |
| 1 % $CuPd/TiO_2$ | 2 | 73 |
| 1 % $CePd/TiO_2$ | 27 | 103 |

***Reaction conditions;*** *0.01 g catalyst, 2.9 g water, 5.6 g methanol, 29 bar 5 % $H_2/CO_2$ and 11 bar 25 % $O_2/CO_2$, 1200 RPM, 30 minutes, 25 °C. [a] Selectivity based on $H_2$ consumption.*

### 7.1.1 Future Work.

These investigations into $H_2O_2$ have begun to explore the use of non-precious metals and Pd combinations to reduce the degradation of $H_2O_2$ under more industrial relevant

conditions while still maintaining appreciable $H_2O_2$ activity. However, there are still improvements to be made. Further investigations into all the catalysts produced in this study would be beneficial to attempt to increase concentrations of $H_2O_2$. Extended reaction times and gas replacement reactions are efficient ways to increase the yield of $H_2O_2$. As previously reported by Lunsford and co-workers $H_2O_2$ synthesis is first order with respect to $H_2$ and zero order with respect to $O_2$.[14] This indicates that $H_2O_2$ formation is limited by available $H_2$ and from this we could assume that increasing amounts $H_2$ would increase concentrations of $H_2O_2$. However, as increasing amounts of $H_2$ can also increase the hydrogenation of $H_2O_2$ the case is not so simple. Hence to increase $H_2$ contact with the catalyst without contact with the $H_2O_2$ a flow reactor system would be a good alternative to increase $H_2O_2$ concentrations and to allow for lifetime studies of the catalyst.

As will be discussed later the temperatures explored in this work for the oxidation reactions are higher than normally explored for $H_2O_2$ synthesis. Trapping experiments to indicate which species are present at elevated temperature would be useful to understand the mechanisms occurring. *In-situ* spectroscopy studies would also be beneficial to see what surfaces and oxidation states are important in $H_2O_2$ synthesis to design future catalysts.

## 7.2 The oxidation of cyclohexane via the *in-situ* production of $H_2O_2$.

Industrial oxidation of cyclohexane is conducted under high temperatures (140 °C) and high pressures of $O_2$ (10 – 12 bar) using homogeneous Co catalysts.[15,16] However more recent patents have been filed to include the use of heterogeneous catalysts which show increased stability and ease of recovery.[17–19] To avoid the over oxidation of the products and maintain selectivity to KA oil the conversion of these processes are always kept low, below 10%. Academic research has focussed on the use of alternative oxidants such as; $H_2O_2$[20–22] and t-BHP[23–25], which require lower reaction temperatures and shorted reaction times compared to conventional procedures.

Initial studies for the oxidation of cyclohexane via the *in-situ* production of $H_2O_2$ focussed on establishing standard reaction conditions for the new approach. These studies primarily investigated whether dilute mixtures of $H_2$ and $O_2$ could be utilised to oxidise cyclohexane. Using a catalyst, it was shown that these gas mixtures were efficient at oxidising cyclohexane under temperatures at which cyclohexane could not

be oxidised by $O_2$ alone. From these experiments standard reaction conditions for the oxidation of cyclohexane via the *in-situ* production of $H_2O_2$ have now been defined as; 50 mg catalyst, 80°C, 17 hours, 29 bar 5% $H_2/N_2$, 11 bar 25% $O_2/N_2$, 1200RPM, and it is these conditions which have been used for further studies. These conditions were utilised as it was observed that at this temperature cyclohexane could not be oxidised by $O_2$ alone and it was below the autoxidation and hence the influence of the addition of $H_2$ could truly be observed. Although the yields and activity observed under these mild conditions are not as high as previously reported in the literature for the aerobic oxidation this is an interesting and novel approach to show the scope of *in-situ* generated $H_2O_2$ in oxidation reactions where elevated temperatures are often required.

Initial studies utilised a 1% AuPd/$TiO_2$ catalyst prepared by wet impregnation. Re-use studies showed that catalyst activity improved on successive re-use due to an increase in the $Pd^0$ species present on the surface of the catalysts after use, Table 7.4, coupled with a re-structuring of the metal nanoparticles surface, enhancing the Pd-core Au-shell structure. These observations along with the testing of the catalyst prepared by different preparation methods, which showed the modified impregnation catalysts giving the greatest activity, suggests that reduced $Pd^0$ species were more active than $Pd^{2+}$ species, for cyclohexane oxidation via the *in-situ* production of $H_2O_2$, Table 7.4. Further studies focused on modified impregnation catalysts using different metals and replacing Au in 1% AuPd/$TiO_2$ with non-precious metals. These studies showed that 1% VPd/$TiO_2$ could produce the greatest activity, doubling the activity of 1% AuPd/$TiO_2$, Table 7.4. Extended studies were conducted to elucidate the reasons behind this activity and further catalyst design to reduce leaching of V into solution and to increase catalyst stability.

***Table 7.4.*** *The key catalysts used for the cyclohexane oxidation via the in-situ production of $H_2O_2$, the activity they showed and the $Pd^{2+}$: $Pd^0$ of these catalysts as determined by XPS.*

| Catalyst | Yield of KA oil / µmol | $Pd^{2+}$:$Pd^0$ |
|---|---|---|
| 1% AuPd/$TiO_2$ (wi) | 6 | All $Pd^{2+}$ |
| 1% AuPd/$TiO_2$ used (wi) | 9 | 6.7 |
| 1% Pd/$TiO_2$ (mi) | 2 | All $Pd^0$ |
| 1% AuPd/$TiO_2$ (mi) | 19 | 0.28 |
| 1% VPd/$TiO_2$ (mi) | 41 | 0.30 |

***Reaction conditions;*** *80 °C, 17 hours, 0.05g catalyst, 6.37 g t-BuOH, 2.13 g cyclohexane, 29 bar 5 % $H_2$ / $N_2$ and 11 bar 25 % $O_2$ / $N_2$, 1200 RPM. Where wi and mi denote wet impregnation and modified impregnation preparation methods respectively.*

### 7.2.1 Future Work.

For all the catalysts tested for the oxidation of cyclohexane no correlations between $H_2O_2$ synthesis activity and oxidation activity have been observed. Correlations between $H_2O_2$ selectivity and oxidation activity were also not observed. The conditions under which $H_2O_2$ activity and cyclohexane activity are determined are very different and hence it may not be a surprise that different activities are observed. It has been shown that the addition of $H_2$ has dramatically increased catalytic cyclohexane oxidation activity and hence it is not just simply aerobic oxidation occurring. Further investigations are needed to investigate whether $H_2O_2$ is produced and utilised during the oxidation reaction or whether other reactive oxygen species (ROS) are produced prior or via $H_2O_2$. EPR studies would be interesting to detect whether $^{\bullet}OH$ and $^{\bullet}OOH$ species, which have previously been shown during $H_2O_2$ synthesis, are present during the cyclohexane oxidation. EPR could also indicate which C based species are present during cyclohexane oxidation and would help elucidate the reaction mechanism of oxidation. It would show whether the same mechanism of autoxidation is occurring and how the addition of the catalyst changes the abundance and nature of the radical species present. These investigations into the key radical intermediates in the catalytic system would give insights into the types of catalysts needed and better improve catalyst design.

Further investigations into the superior 1% VPd/$TiO_2$ catalyst were unsuccessful in stabilising the V on the catalyst and hence leached V species were detected in post reaction solutions. Although this leaching didn't have a detrimental effect on the re-use of the catalyst further studies are required to determine the long term stability of the catalyst. Future work would have to focus on stabilising this active catalyst to minimise the V leaching to maintain the catalytic activity. Work began on trying to pre-impregnate $TiO_2$ with V prior to impregnation of Pd to form mix oxide support, however this was unsuccessful. The production of mixed metal oxides from metal precursors has previously shown to be successful with V and Ti to produce mixed phases of $TiO_2$ and $V_2O_5$ with some solid $V^{4+}$ in $TiO_2$.[26] Mixed metal oxides have been widely used in the literature as inexpensive catalysts for a variety of catalytic transformations; fine chemical synthesis, biofuel production and transformation and oxidation reactions.[27–29] Hence other mixed metal oxides could also be investigated. V mixed oxides have been produced with other transition metals such as Ce and V

mixed oxides which have been shown to be good oxidation catalysts.[30] This shows that V can be mixed with other metals which were also shown to be active for cyclohexane oxidation, such as Fe, Co and Mn (Chapter 5). However, these mixed metal oxides are not known to synthesis $H_2O_2$ and hence the oxides could be used as supports onto which Pd could be impregnated or as physical mixtures with known $H_2O_2$ synthesising catalysts such as 1% $Pd/TiO_2$, as was shown for 1% $Pd/TiO_2$ and $V_2O_4$ and $V_2O_5$ mixtures (Chapter 5).

It has also been shown that after the formation of V and Ti mixed oxides the type of V species present can be determined by extraction with ammonium sulphate ($NH_2SO_4$). This leaves weakly interacting V species in solution and strongly interacting V species in the solid.[31] This technique could also be used to remove the weakly bound V species prior to catalytic use to reduce the concentration of V into the reaction solution.

Another way of stabilising redox available V species would be to incorporate them into zeolitic frameworks. In the literature successful incorporation of V into several zeolitic frameworks have be reported.[32–36] Some have been reported and utilised for oxidation catalysis.[32–34] In these zeolites the V replaces Ti sites and can be incorporated either in an octahedral environment, with $V^{4+}$, or in tetrahedral sites, with $V^{5+}$.[33] The vanadium in the zeolite frameworks can be in multiple oxidation states showing that it can still maintain the redox properties which it's high oxidation properties are often attributed to. Again, these zeolites could be used as supports for Pd impregnation. Zeolites such as TS-1,[37] ZSM5 and Zeolite Y[38] have previously been reported in the literature as good supports for AuPd catalysts for the direct synthesis of $H_2O_2$ so these are promising support material for the oxidation of cyclohexane via the *in-situ* production of $H_2O_2$.

It was previously reported (Chapter 5) that the addition of carbon extrudates increased the activity of the active 1% $VPd/TiO_2$ catalyst, from 41 to 95 µmol of KA oil. Hence further exploration into this phenomenon is needed. Further characterisation into the carbon extrudates used would indicate which functional groups are present and how these can interact with the reactants and products. C additives have previously been shown to increase $H_2O_2$ productivity[3] as was also shown for 1% $AuPd/TiO_2$ in this work (Chapter 5). With the addition of carbon extrudates a decrease in the intermediate

CHHP was observed increasing the selectivity to KA oil this could indicate that the extrudates were helping in determining product selectivity. The functional groups present on the surface of the carbon extrudate could interact with the reactants and productive and hence investigations to see if the extrudates have affect the mechanism or the formation and quantity of intermediates.

One feature of all the cyclohexane oxidation reactions was high $H_2$ conversions when $H_2$ and $O_2$ were present. It is assumed that some $H_2$ is utilised in the synthesis and degradation of $H_2O_2$ at temperatures where the oxidation of cyclohexane is thermodynamically unfavoured. Hence investigations into better utilisation of $H_2$ is needed. One way is to introduce $H_2$ later into the reaction, this would decrease the $H_2$ that is converted during the heating up of the reactor and could leave more available for the oxidation reactions. The use of flow or a semi-continuous process could be useful in decreasing $H_2$ waste. This would introduce continuous levels of $H_2$ and reduce the contact of $H_2$ with the catalyst and $H_2O_2$ which would hopefully decrease $H_2O_2$ degradation. This continual addition of $H_2$ would also be beneficial as it was previously observed, in a batch system, that KA oil yield increased with increasing $H_2$ concentration. It would also be attractive to use low concentrations of $H_2$ in air as this would still provide continuous $H_2$ flow but decrease $H_2$ waste and a more economical and safe use. Any unreacted gas could also be circulated back into the reactor to reduce waste.

## 7.3 The oxidation of benzyl alcohol via the *in-situ* production of $H_2O_2$.

The oxidation of benzyl alcohol via the *in-situ* production of $H_2O_2$ has previously been reported by Santonastaso *et al.*[39] and Moreno *et al.*[40] Both of these studies used much milder conditions than are often utilised for the aerobic oxidation of benzyl alcohol, 120 °C. They observed the importance of $H_2$ under these mild conditions with limited conversion with $O_2$ alone and an increase in activity when both $H_2$ and $O_2$ are present. These increases in activity with $H_2$ and $O_2$ have been attributed to the formation of peroxide species.

In this work a series of 1% XPd/$TiO_2$ catalysts have been explored which again have shown the presence of $H_2$ imperative for higher activity. Investigations have then focussed on the comparison of monometallic 1% Pd/$TiO_2$ and bimetallic 1%

AuPd/$TiO_2$ and 1% FePd/$TiO_2$ catalysts. Firstly, the comparison of reaction times indicated the bimetallic catalysts were more active with 1% FePd/$TiO_2$ showing the greatest activity at all reaction times with increased initial rates, Figure 7.1.

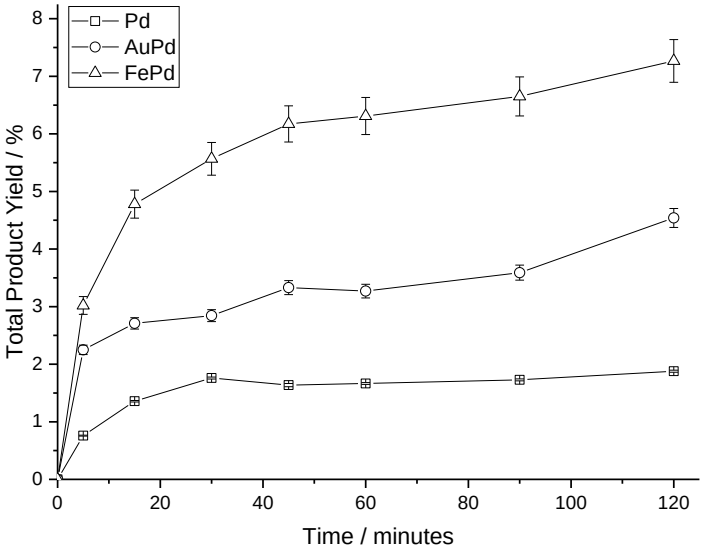


***Figure 7.1.*** *Comparison of the catalytic activity of 1% Pd/$TiO_2$, 1% AuPd/$TiO_2$, 1% FePd/$TiO_2$ towards the selective oxidation of benzyl alcohol as a function of reaction time.* ***Reaction conditions;*** *0.01 g catalyst, 1.04 g benzyl alcohol, 7.1 g methanol, 29 bar 5 % $H_2$ / $CO_2$ and 11 bar 25 % $O_2$ / $CO_2$, 1200 RPM, 50 °C.*

Further investigations used sequential reactions to increase the product yield further, Figure 7.2. Using 1% FePd/$TiO_2$ increased the product yield to 22% after 4 sequential reactions at 95 % selectivity towards benzaldehyde. These investigations showed that appreciable yields of benzaldehyde could be produced under mild conditions where aerobic oxidation does not occur.

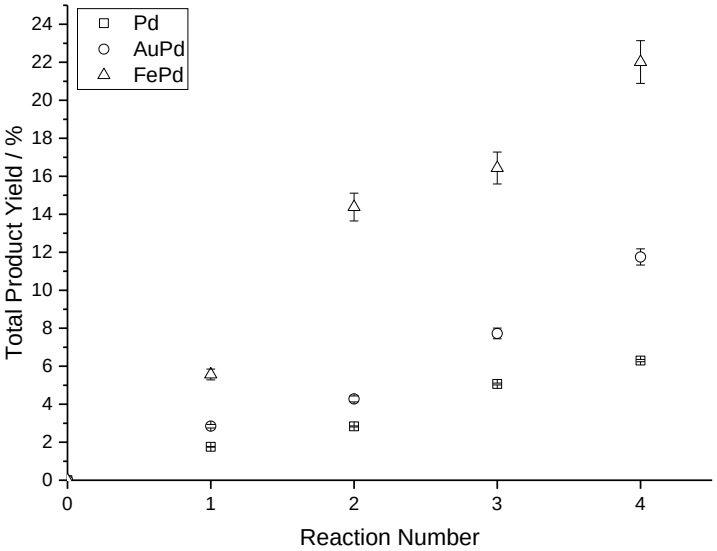


***Figure 7.2.*** *Comparison of the catalytic activity of 1% Pd/$TiO_2$, 1% AuPd/$TiO_2$, 1% FePd/$TiO_2$ towards the selective oxidation of benzyl alcohol as a function of reaction number.* ***Reaction conditions;*** *0.01 g catalyst, 1.04 g benzyl alcohol, 7.1 g methanol, 29 bar 5 % $H_2$ / $CO_2$ and 11 bar 25 % $O_2$ / $CO_2$, 1200 RPM, 50 °C.*

Santonastaso *et al.* utilised radical quenchers to illustrate the oxidation reaction proceeded via a radical mechanism under identical conditions to those used in this work. This suggested that peroxy based species produced when $H_2$ and $O_2$ are utilised.[39] This work has further investigated this using EPR spectroscopy to determine which radicals were present during the reaction and how the different catalysts effected the distribution of the radicals. A larger concentration of oxygen-based radical was observed for 1% FePd/$TiO_2$ compared to 1% AuPd/$TiO_2$ and no radical formation observed over 1% Pd/$TiO_2$ with a methanol solvent. Hence a correlation between radical concentration and oxidation activity could be made. The oxygen-based radicals observed were proposed to be methoxy from the scavenging of radicals by methanol. Further investigations using water as the solvent showed that $^{\bullet}OH$ radicals were formed over 1% AuPd/$TiO_2$ and 1% FePd/$TiO_2$ catalysts. Hence it was suggested that the methoxy radicals detected under standard reaction conditions have originated from breaking $H_2O_2$ into $^{\bullet}OH$ and $^{\bullet}OOH$ radicals which have been quenched by methanol and detected by EPR.

### 7.3.1 Future Work.

These studies have shown the promise of 1% FePd/$TiO_2$ for the oxidation of benzyl alcohol via *in-situ* production of $H_2O_2$. However, this catalyst has shown leaching of Fe (13%) into the reaction solution and this has had a detrimental effect on the re-use of the catalyst. Both solution Fe species as well as supported Fe catalysts are known to be efficient Fenton reagents.[41,42] Hence future work would initially identify these solution Fe species and what their impact is on catalytic activity. Combinations of stable solid Fe species, such as iron oxides, and $H_2O_2$ synthesis catalysts, such as 1% Pd/$TiO_2$, would indicate whether other Fe species in combination with $H_2O_2$ are still active but with prolonged catalyst stability.

Further investigations into 1% FePd/$TiO_2$ would be to further enhance the catalytic activity. Investigations into changing the ratio of Fe:Pd to find the optimum ratio would indicate how much Fe is needed to catalyse the Fenton's reaction. Under the current reaction conditions residual $H_2O_2$ was observed post reaction which indicates that not all $H_2O_2$ has been utilised for the oxidation reaction. With increasing Fe content it could be possible to enhance the activation of $H_2O_2$ into reactive oxygen species and increase the observed catalytic activity. With changing the Fe content it would be interesting to observe whether the Fe leaching could be decreased.

Zeolites which have been ion exchanged to incorporate Fe into the zeolite framework have been reported in the literature.[43–45] Hammond *et al.* have shown the use of FeZSM5 for the oxidation of methane to methanol using commercial $H_2O_2$.[45,46] This illustrated that FeZSM5 could be utilised as an efficient Fenton catalyst with $H_2O_2$. This shows the potential of FeZSM5 as a heterogenous catalyst for benzyl alcohol oxidation via the *in-situ* production of $H_2O_2$. FeZSM5 could either be utilised as a physical mixture with 1% $Pd/TiO_2$, a $H_2O_2$ synthesising catalyst, or as a support for impregnating Pd proving a bifunctional catalyst.

Sequential reactions have indicated that 1% $FePd/TiO_2$ can maintain activity if the $H_2$ available for the reaction is increased. This gives indication that changes in reactor set up could improve catalytic activity. As selectivity of $H_2$ is low and we have already observed that all $H_2O_2$ is not utilised under standard reaction conditions efficiently using a flow or semi-continuous set up could be a good possibility if low concentrations of $H_2$ are used. This would hopefully provide a continual feed of $H_2$ which can increase oxidation yield but low concentrations of $H_2$ to avoid the waste of $H_2$.

## 7.4 References.


1. E. Ntainjua N., M. Piccinini, J. C. Pritchard, J. K. Edwards, A. F. Carley, J. A. Moulijn and G. J. Hutchings, *ChemSusChem*, 2009, **2**, 575–580.
2. G. Blanco-Brieva, M. Montiel-Argaiz, F. Desmedt, P. Miquel, J. M. Campos-Martin and J. L. G. Fierro, *Top. Catal.*, 2017, **60**, 1151–1155.
3. R. J. Lewis, Jennifer. K. Edwards, S. J. Freakley and G. J. Hutchings, *Ind. Eng. Chem. Res.*, 2017, **56**, 13287–13293.
4. E. Ntainjua N., M. Piccinini, J. C. Pritchard, Q. He, J. K. Edwards, A. F. Carley, J. A. Moulijn, C. J. Kiely and G. J. Hutchings, *ChemCatChem*, 2009, **1**, 479–484.
5. V. R. Choudhary and C. Samanta, *J. Catal.*, 2006, **238**, 28–38.
6. Y.-F. Han and J. H. Lunsford, *J. Catal.*, 2005, **230**, 313–316.
7. Santos, R. J. Lewis, G. Malta, A. G. R. Howe, D. J. Morgan, E. Hampton, P. Gaskin and G. J. Hutchings, *Ind. Eng. Chem. Res.*, 2019, **58**, 12623–12631.
8. S. J. Freakley, M. Piccinini, J. K. Edwards, E. N. Ntainjua, J. A. Moulijn and G. J. Hutchings, *ACS Catal.*, 2013, **3**, 487–501.
9. M. Piccinini, E. N. N, J. K. Edwards, A. F. Carley, J. A. Moulijn and G. J. Hutchings, *Phys. Chem. Chem. Phys.*, 2010, **12**, 2488–2492.
10. J. K. Edwards, A. Thomas, B. E. Solsona, P. Landon, A. F. Carley and G. J. Hutchings, *Catal. Today*, 2007, **122**, 397–402.
11. E. Ntainjua, J. K. Edwards, A. F. Carley, J. A. Lopez-Sanchez, J. A. Moulijn, A. A. Herzing, C. J. Kiely and G. J. Hutchings, *Green Chem.*, 2008, **10**, 1162–1169.

12. D. A. Crole, S. J. Freakley, J. K. Edwards and G. J. Hutchings, *Proc R Soc A*, 2016, **472**, 20160156.
13. M. Sankar, Q. He, M. Morad, J. Pritchard, S. J. Freakley, J. K. Edwards, S. H. Taylor, D. J. Morgan, A. F. Carley, D. W. Knight, C. J. Kiely and G. J. Hutchings, *ACS Nano*, 2012, **6**, 6600–6613.
14. S. Chinta and J. H. Lunsford, *J. Catal.*, 2004, **225**, 249–255.
15. D. J Loder, US2223494, 1940.
16. H. J. Cates, J. O. Punderson and R. W. Wheatcroft, 2851496, 1958.
17. X. Liu, H. Wang, L. Song, K. Qiao and L. Wang, CN109248699 (A), 2019.
18. S. Saleh M. Abdalla and K. Khairou, WO2016116776 (A1), 2016.
19. K. Whiston, X. Liu and G. Hutchings, WO2013114330 (A1), 2013.
20. T. F. S. Silva, A. J. Silvestre, B. G. M. Rocha, M. R. Nunes, O. C. Monteiro and L. M. D. R. S. Martins, *Catal. Commun.*, 2017, **96**, 19–22.
21. R. Raja and P. Ratnasamy, *Catal. Lett.*, 1997, **48**, 1–10.
22. V. J. Mayani, S. V. Mayani and S. W. Kim, *Chem. Eng. Commun.*, 2016, **203**, 539–547.
23. T. Maschmeyer, R. D. Oldroyd, G. Sankar, J. M. Thomas, I. J. Shannon, C. R. A. Catlow, J. A. Klepetko, A. F. Masters and J. K. Beattie, *Angew. Chem. Int. Ed. Engl.*, 1997, **36**, 1639–1642.
24. N. Pal, M. Pramanik, A. Bhaumik and M. Ali, *J. Mol. Catal. Chem.*, 2014, **392**, 299–307.
25. J. Wang, H. Zhao, X. Zhang, R. Liu and Y. Hu, *Chin. J. Chem. Eng.*, 2008, **16**, 373–375.
26. W. E. Slink and P. B. DeGroot, *J. Catal.*, 1981, **68**, 423–432.
27. J. Védrine, *Catalysts*, 2017, **7**, 341.
28. *Metal Oxide Catalysis*, John Wiley & Sons, Ltd, 1st edn., 2008.
29. J. C. Védrine, *ChemSusChem*, 2019, **12**, 577–588.
30. S. Yasyerli, G. Dogu and T. Dogu, *Catal. Today*, 2006, **117**, 271–278.
31. F. Trifirò, *Catal. Today*, 1998, **41**, 21–35.
32. S. Dzwigaj, P. Massiani, A. Davidson and M. Che, *J. Mol. Catal. Chem.*, 2000, **155**, 169–182.
33. T. Sen, V. Ramaswamy, S. Ganapathy, P. R. Rajamohanan and S. Sivasanker, *J. Phys. Chem.*, 1996, **100**, 3809–3817.
34. E. Z. Hegazy, S. A. Kosa, I. H. A. El Maksod and D. F. Baamer, *Silicon*, 2017.
35. S. Dzwigaj, M. J. Peltre, P. Massiani, A. Davidson, M. Che, S. Dzwigaj, P. Massiani, T. Sen and S. Sivasanker, *Chem. Commun.*, 1998, **0**, 87–88.
36. K. J. Chao, C. N. Wu, H. Chang, L. J. Lee and S. Hu, *J. Phys. Chem. B*, 1997, **101**, 6341–6349.
37. R. J. Lewis, K. Ueura, Y. Fukuta, S. J. Freakley, L. Kang, R. Wang, Q. He, Jennifer. K. Edwards, D. J. Morgan, Y. Yamamoto and G. J. Hutchings, *ChemCatChem*, 2019, **11**, 1673–1680.
38. G. Li, J. Edwards, A. F. Carley and G. J. Hutchings, *Catal. Today*, 2007, **122**, 361–364.
39. M. Santonastaso, S. J. Freakley, P. J. Miedziak, G. L. Brett, J. K. Edwards and G. J. Hutchings, *Org. Process Res. Dev.*, 2014, **18**, 1455–1460.
40. Moreno, N. F. Dummer, J. K. Edwards, M. Alhumaimess, M. Sankar, R. Sanz, P. Pizarro, D. P. Serrano and G. J. Hutchings, *Catal. Sci. Technol.*, 2013, **3**, 2425–2434.

41. W. G. Barb, J. H. Baxendale, P. George and K. R. Hargrave, *Nature*, 1949, **163**, 692–694.
42. S. Navalon, M. Alvaro and H. Garcia, *Appl. Catal. B Environ.*, 2010, **99**, 1–26.
43. E. V. Starokon, K. A. Dubkov, L. V. Pirutko and G. I. Panov, *Top. Catal.*, 2003, **23**, 137–143.
44. B. E. R. Snyder, M. L. Bols, R. A. Schoonheydt, B. F. Sels and E. I. Solomon, *Chem. Rev.*, 2018, **118**, 2718–2768.
45. C. Hammond, M. M. Forde, M. H. Ab Rahim, A. Thetford, Q. He, R. L. Jenkins, N. Dimitratos, J. A. Lopez-Sanchez, N. F. Dummer, D. M. Murphy, A. F. Carley, S. H. Taylor, D. J. Willock, E. E. Stangland, J. Kang, H. Hagen, C. J. Kiely and G. J. Hutchings, *Angew. Chem. Int. Ed.*, 2012, **51**, 5129–5133.
46. C. Hammond, I. Hermans and N. Dimitratos, *ChemCatChem*, 2015, **7**, 434–440.